B. KURTMAN

# A DETAILED ANALYSIS FOR EVALUATION OF THE DEGRADATION CHARACTERISTICS OF SIMPLE STRUCTURAL SYSTEMS

BURAK KURTMAN

APRIL 2007

METU 2007

# A DETAILED ANALYSIS FOR EVALUATION OF THE DEGRADATION CHARACTERISTICS OF SIMPLE STRUCTURAL SYSTEMS

A THESIS SUBMITTED TO
THE GRADUATE SCHOOL OF NATURAL AND APPLIED SCIENCES
OF
MIDDLE EAST TECHNICAL UNIVERSITY

BY

BURAK KURTMAN

IN PARTIAL FULFILLMENT OF THE REQUIREMENTS
FOR
THE DEGREE OF MASTER OF SCIENCE
IN
CIVIL ENGINEERING

APRIL 2007

Approval of the Graduate School of Natural and Applied Sciences

Prof. Dr. Canan Özgen
Director

I certify that this thesis satisfies all the requirements as a thesis for the degree of Master of Science.

Prof. Dr. Güney Özcebe
Head of Department

This is to certify that we have read this thesis and that in our opinion it is fully adequate, in scope and quality, as a thesis for the degree of Master of Science.

Asst. Prof. Dr. M.Altuğ Erberik
Supervisor

**Examining Committee Members**

Prof. Dr. Haluk Sucuoğlu (METU,CE) _____

Asst. Prof. Dr. M.Altuğ Erberik (METU,CE) _____

Asst. Prof. Dr. Erdem Canbay (METU,CE) _____

Asst. Prof. Dr. Burcu B. Canbolat (METU,CE) _____

Asst. Prof. Dr. M.Tolga Yılmaz (METU,ES) _____

**I hereby declare that all information in this document has been obtained and presented in accordance with academic rules and ethical conduct. I also declare that, as required by these rules and conduct, I have fully cited and referenced all material and results that are not original to this work.**

Name, Last name : Burak Kurtman

Signature :

# ABSTRACT

A DETAILED ANALYSIS FOR EVALUATION OF THE DEGRADATION CHARACTERISTICS OF SIMPLE STRUCTURAL SYSTEMS

Kurtman, Burak

M.S., Department of Civil Engineering

Supervisor: Asst. Prof. Dr. M. Altuğ Erberik

April 2007, 188 pages

Deterioration in the mechanical properties of concrete, masonry and steel structures are usually observed under repeated cyclic loading in the inelastic response range. Therefore such a behavior becomes critical when these types of structures are subjected to ground motions with specific characteristics. The objective of this study is to address the influence of degrading behavior on simple systems. The Structural Performance Database on the PEER web site, which contains the results of cyclic, lateral-load tests of reinforced concrete columns, are employed to quantify the degradation characteristics of simple systems by calibrating the selected degrading model parameters for unloading stiffness, strength and pinching of a previously developed hysteresis model. The obtained values of parameters from cyclic test results are compared with the recommended values in literature.

In the last part of the study, response of SDOF systems with various degradation characteristics are investigated using a set of seismic excitations recorded during some major earthquakes. The results indicate that when all the degradation components are combined in a structural system, the effect of degradation on response values becomes much more pronounced.

Keywords: Hysteresis models, unloading stiffness degradation, strength degradation, pinching, cyclic test, reinforced concrete column

# ÖZ


BASİT YAPISAL SİSTEMLERİN AZALIM ÖZELLİKLERİNİN BELİRLENMESİ İÇİN DETAYLI BİR ANALİZ

Kurtman, Burak

Yüksek Lisans, İnşaat Mühendisliği Bölümü

Tez Yöneticisi: Asst. Prof. Dr. M. Altuğ Erberik

Nisan 2007, 188 sayfa

Tekrarlanan ve tersinir yüklemeler altında elastik ötesi davranış gösteren beton, çelik ve yığma yapıların mekanik özelliklerinde azalmalar gözlemlenmektedir. Bu yüzden belirli karakteristik özelliklere sahip kuvvetli yer hareketlerine maruz kalan bu tip yapıların davranışlarının detaylı bir biçimde incelenmesi gerekir. Bu çalışmanın amacı, azalım davranışının basit yapısal sistemlerdeki etkisini incelemektir. Çalışmada kullanılan PEER (Pasifik Deprem Mühendisliği Araştırma Merkezi) web sitesindeki yapısal performans veri tabanı, çok sayıda betonarme kolon deney elemanının tersinir yatay yük testlerinin sonuçlarını içermektedir. Deneysel veriler kullanılarak önceden geliştirilmiş histeresiz (çevrimsel davranış) modelindeki yük boşalımı anındaki rijitlik azalımı, kapasite azalımı ve çevrimlerde daralma parametreleri kalibre edilmiş ve bu parametreler, diğer araştırmacıların önerdiği değerlerle karşılaştırılmıştır.

Çalışmanın son kısmında ise, çeşitli azalım özelliklerine sahip tek serbestlik derecesine sahip sistemlerin deprem yüklemeleri altındaki davranışları incelenmiştir. Elde edilen sonuçlara göre, bütün azalım özelliklerinin mevcut olması halinde, sismik davranış değerleri dikkate değer şekilde etkilenmektedir.

Anahtar Kelimeler: Histeresiz Modeller, yük boşalımı anındaki rijitlik azalımı, kapasite azalımı, çevrimlerde daralma, tersinir yükleme deneyi, betonarme kolon

## TABLE OF CONTENTS

## LIST OF SYMBOLS

| | |
|---|---|
| $a$ | Unloading stiffness degradation parameter (Ductility-based rule) |
| $A$ | Strength degradation parameter (severe-to-gradual, exponential case) |
| $A_g$ | Cross-sectional area of column |
| $A_0$ | Cross-sectional area of transverse reinforcement |
| $B$ | Strength degradation parameter (severe-to-gradual, exponential case) |
| $B_k$ | Width of core concrete |
| $c$ | Clear cover |
| $C$ | Strength degradation parameter (linear case) |
| $d$ | Column depth |
| $d_l$ | Diameter of longitudinal reinforcement bars |
| $d_t$ | Diameter of transverse reinforcement bars |
| $E_h$ | Cumulative dissipated energy |
| $E_{h,i}$ | Energy dissipated at the $i^{th}$ half-cycle |
| $f_c$ | Compressive strength of concrete |
| $f_{su}$ | Ultimate strength of longitudinal reinforcement |
| $f_{su,t}$ | Ultimate strength of transverse reinforcement |
| $f_{yl}$ | Yield strength of longitudinal reinforcement |
| $f_{yt}$ | Yield strength of transverse reinforcement |
| $F_c$ | Strength capacity at capping point |
| $F_i$ | Strength capacity of the $i^{th}$ half-cycle |
| $F_r$ | Residual strength |
| $F_y$ | Yield strength |
| $H_k$ | Height of core concrete |
| $i$ | Radius of gyration |
| $I_{BL}$ | Energy-based index for bilinear model |
| $I_{SD}$ | Energy-based index for stiffness degrading model |

| | |
|---|---|
| $K$ | Strength degradation parameter (gradual-to-severe, exponential case) |
| $K_{un}$ | Unloading stiffness |
| $K_0$ | Initial elastic stiffness |
| $L$ | Length of equivalent cantilever |
| $L_B$ | Length of transverse reinforcement in the direction of the width of column section |
| $L_H$ | Length of transverse reinforcement in the direction of the height of column section |
| $L_{splice}$ | Splice length of longitudinal reinforcement bars |
| $L_t$ | Total length of transverse reinforcement in the cross-section |
| $M_{fl}$ | Calculated flexural moment capacity |
| $M_m$ | Observed flexural moment capacity |
| $n_b$ | Number of longitudinal reinforcement bars |
| $N$ | Number of half-cycles |
| $N_v$ | Number of transverse shear bars in cross-section |
| $P$ | Axial load on column section |
| $s$ | Spacing of longitudinal reinforcement |
| $S$ | Strength degradation parameter (gradual-to-severe, exponential case) |
| $T$ | Fundamental period |
| $u_c$ | Displacement value of capping point |
| $u_m$ | Maximum displacement |
| $u_r$ | Displacement value of residual strength point |
| $u_s$ | Displacement value of crack closure point |
| $u_y$ | Yield displacement |
| $V_{core}$ | Volume of core concrete bounded by ‘s’ |
| $V_{max}$ | Maximum shear force |
| $V_{trans}$ | Volume of transverse reinforcement over a height ‘s’ |
| $\alpha$ | Unloading stiffness degradation parameter (Focus-based rule) |
| $\alpha_1$ | Post-yield stiffness ratio |

| | |
|---|---|
| $\alpha_2$ | Post-capping stiffness ratio |
| $\alpha_p$ | Pinching parameter for Roufaiel & Meyer's rule |
| $\eta$ | Strength level |
| $\gamma$ | Pinching parameter for Park et al.'s rule |
| $\gamma_{actual}$ | Calibrated pinching parameter for Park et al.'s rule |
| $\lambda$ | Slenderness ratio |
| $\rho_l$ | Longitudinal reinforcement ratio |
| $\rho_t$ | Volumetric transverse reinforcement ratio |
| $\rho_w$ | Shear reinforcement ratio in the direction of loading |
| $\xi$ | Viscous damping ratio |

# CHAPTER 1

# INTRODUCTION

## 1.1 General

Structures usually exhibit inelastic behavior under severe cyclic loads associated with strong ground motions. The load-deformation curve plotted under this inelastic action shows itself as in the form of hysteresis loops. The hysteresis term refers to the memory nature of the inelastic system, meaning that the restoring force depends not only the current deformation but also on the past deformations. Each hysteresis loop is a measure of the energy dissipated under cyclic loading as a result of internal friction within the structure or yielding of the structural members.

The performance-based design approach enables engineers to achieve more realistic and economical earthquake resistance design. The philosophy behind this approach is to determine the damage level of the structure, in other words, the deformation of the structure. Therefore, the information about the structural behavior and the characteristics of hysteresis loops are very important. However, under repeated cyclic loading in the inelastic response range, deterioration in the mechanical properties of concrete, masonry and steel structures are usually observed. Such deterioration should be taken into account in the seismic design.

Several hysteresis models with stiffness and strength degradation and pinching characteristics have been developed by different researchers. These can be mainly classified into two types; Polygonal Hysteretic Models (PHM) and Smooth Hysteretic Models (SHM). The purpose of this study is to calibrate the parameters

used for the generation of well known PHM models and to investigate the degradation characteristics of reinforced concrete members under repeated cyclic loads.

## 1.2 Types of Hysteresis Models

Hysteresis models are mainly divided into two groups: polygonal hysteresis models and smooth hysteresis models. Polygonal hysteresis models (PHM) are also called multi-linear models. The polygonal models are composed of linear branches and governed by rules that fix distinct points and dictate the transitions between various stages. Smooth hysteresis models are derived from the theory of viscoplasticity and use of differential equations. The branches of the models are curved and the transitions between the branches are smooth.

Hysteresis models can also be classified according to degradation implementation. The hysteresis models which do not have degradation in stiffness or strength are called “non-degrading” hysteresis models. The implementation of stiffness and strength degradation or pinching characteristics of reinforced concrete makes the model “degrading” hysteresis model. In the next section well-known polygonal hysteresis models in the literature are introduced.

## 1.3 Literature Survey on Hysteresis Models

Non-degrading hysteresis models:

The most basic model for non-degrading models is the elasto-plastic model (see Figure 1.1.a). The unloading and reloading stiffness branches are equal to the initial stiffness. The post-yield stiffness is zero meaning there is no strength loss or gain. It is very simple and easy to implement, but the experimental behavior of reinforced concrete is very different from elasto-plastic behavior. The hysteretic energy dissipation is overestimated by this model.

Bilinear hysteresis model is very similar to elasto-plastic model but a finite post-yield stiffness ratio is introduced as a percentage of initial stiffness (Figure 1.1.b). Post-yield slope does not have a significant effect on dynamic analysis but has an effect on residual deformations (Kawashima et. al., 1998).

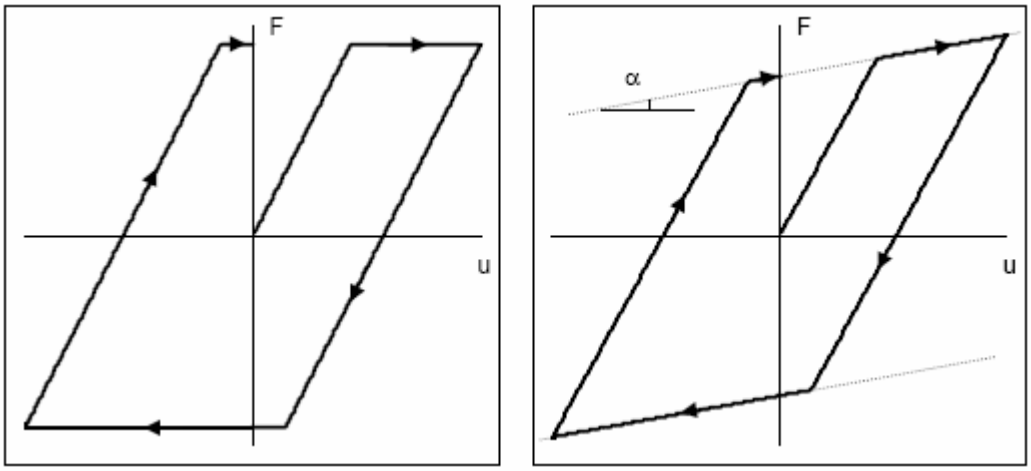


**Figure 1.1** Non-degrading models a) elasto-plastic model, b) bilinear model

Stiffness degrading hysteresis models:

In 1970, a modified version of bilinear model was proposed by Nielsen and Imbeault introducing a reduction factor to unloading stiffness branch. The unloading stiffness $K_{un}$ is defined as

$$K_{un} = K_0 \left( \frac{u_y}{u_m} \right)^a \tag{1.1}$$

where $K_0$ is the initial stiffness, $u_m$ is the previous maximum displacement, $u_y$ is the yield displacement and $a$ is the unloading stiffness degradation parameter which takes values between 0 and 1.

Clough and Johnston (1966) proposed a stiffness degrading model which is an enhanced version of bilinear model. The model considers degradation in reloading stiffness. The reloading branch aims at the previous maximum response point in the direction of loading. On the other hand, there is no degradation in unloading stiffness and it is equal to the initial stiffness (Figure 1.2).

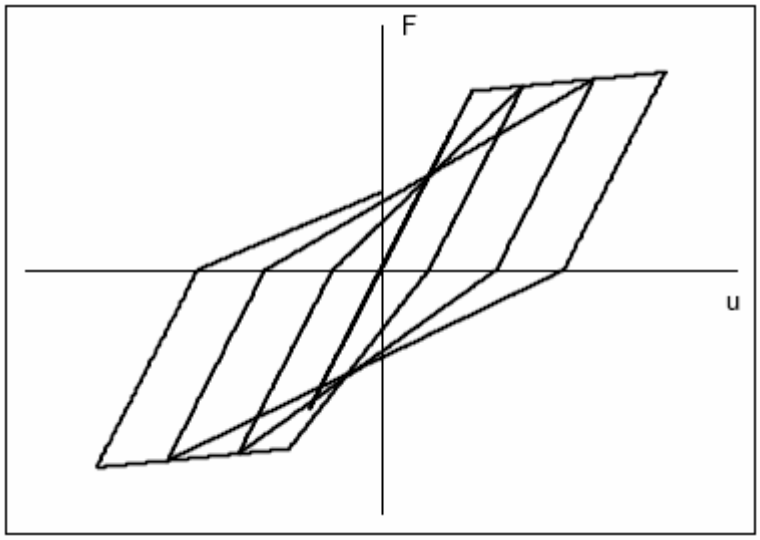


**Figure 1.2** Clough and Johnston's stiffness degrading model

Mahin and Bertero (1976) proposed that the reloading path be directed to the maximum displacement of the last cycle instead of maximum displacement of all former cycles if the former path results in a larger reloading stiffness.

Takeda et. al (1970) developed a well-known hysteresis model by studying the experimental force-displacement relations of reinforced concrete members (Figure 1.3.a). The model has a trilinear backbone curve with cracking and yield points. It has 16 rules for the transitions of the model. Unloading stiffness is determined from Eq. (1.1) with '*a*' is equal to 0.4. Reloading stiffness branch aims

at the previous maximum response point. In 1979, Saiidi and Sozen developed a simpler model (Q-Hyst model) compared to Takeda's model by implementing the unloading rule of Takeda's model to the Clough's model. The value of parameter '*a*' is recommended as 0.5 (Figure 1.3.b).

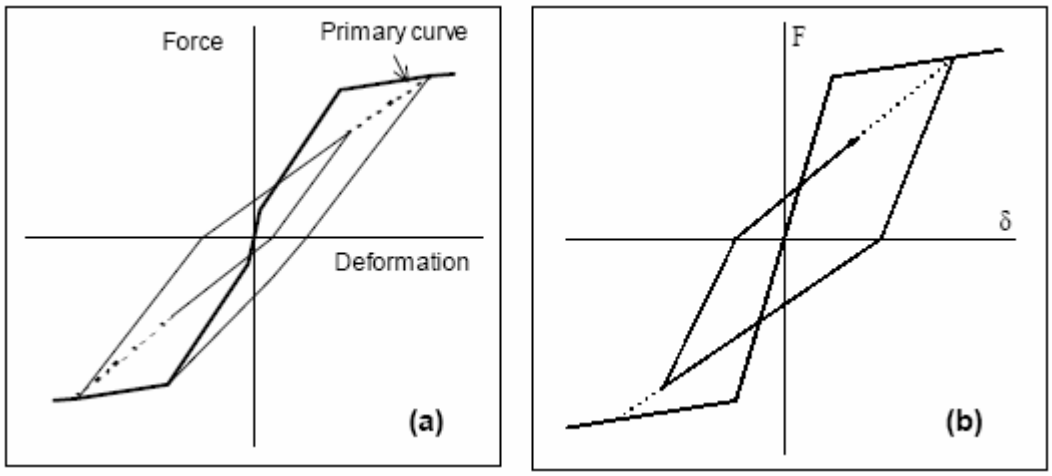


**Figure 1.3** a) Takeda model, b) Q-Hyst model

Stiffness and strength degrading hysteresis models:

IDARC hysteresis model developed by Park et. al (1987) can simulate stiffness and strength degradation as well as pinching behavior. The unloading branches aim at an imaginary point which is located at a distance of $\alpha F_y$ on the extension of the elastic branch on the opposite side. As a result, unloading stiffness degrades with increasing ductility levels. Strength degradation is determined as a function of incremental energy dissipated at each cycle (Figure 1.4).

In 1987, Roufaiel and Meyer proposed a strength degradation formula based on the exceedance of a certain critical strain level. Chung et. al. (1989) developed another

strength degradation formulation with the parameters of monotonic moment-curvature relationship.

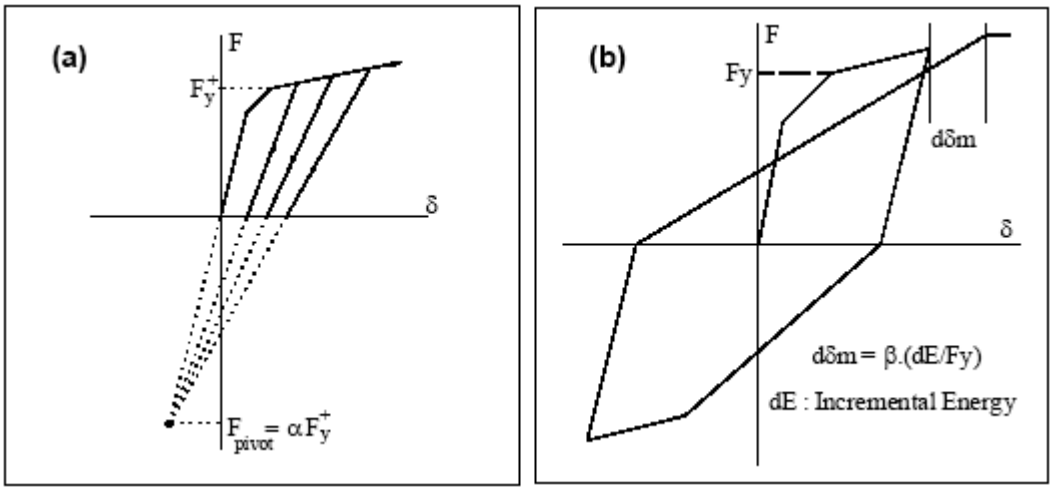


**Figure 1.4** IDARC model a) unloading degradation, b) strength degradation

There are many other hysteresis models in the literature and the aforementioned models are well-known and widely used models.

### 1.4 Objective and Scope

The main objective of the study is to calibrate the selected degrading model parameters by using the available cyclic test data from PEER database. Also, the effect of degradation types and levels on the seismic behavior of RC members is discussed. Actual behavior of RC structural members under seismic excitation can be estimated within a certain degree of accuracy by employing structural models with degradation characteristics such as stiffness/strength degradation and pinching behavior. The enhanced models for the performance based design enables engineers to obtain more reliable results.

The study is composed of seven chapters. First chapter gives a general overview of the study and brief information about the hysteresis models used in the literature.

Chapter 2 presents the properties and statistics of the cyclic tests of PEER database. In this chapter the classification of test results is performed in order to investigate the degradation characteristics of the considered RC members more specifically rather than considering the complete database.

The unloading stiffness degradation rules are investigated and the degradation parameters are calibrated by using the available cyclic test data in Chapter 3.

In Chapter 4, strength degradation behavior of RC members during hysteretic response is investigated in two parts: cyclic (cinematic) strength degradation and in-cycle (post-capping) strength degradation. The parameters of cyclic strength degradation are calibrated using cyclic test data.

Pinching rules of two widely used hysteresis models are investigated in Chapter 5. The effect of pinching parameters on the energy dissipation capacity of RC members is discussed as well.

In Chapter 6, the response of SDOF systems with various degradation characteristics is investigated using a set of seismic excitations recorded during some major earthquakes. This chapter is identified as a part of a future research project and complementary to the study conducted in previous chapters.

Finally, Chapter 7 is devoted to summary and conclusions. Future research recommendations are also given in this chapter.

# CHAPTER 2

# PACIFIC EARTHQUAKE ENGINEERING RESEARCH CENTER STRUCTURAL PERFORMANCE DATABASE

## 2.1 General

Pacific Earthquake Engineering Research Center (PEER) Structural Performance Database contains results of uni-axial, cyclic, lateral load tests of reinforced concrete columns. The purpose of the database is to enable researchers to study and develop more realistic seismic performance or structural damage models. The improved quality of the seismic performance models results in more reliable predictions of the behavior of the structures during and after an earthquake.

The original study for the Structural Performance Database was conducted by National Institute of Standards and Technology (NIST). The database consisted of 107 test results of rectangular reinforced concrete (RC) columns and 92 test results of spiral reinforced concrete columns. The data was available from two reports and digitized force-displacement values (Taylor and Stone 1993, Taylor et al. 1997). In January 2004, University of Washington added new test results to the database with the support from the Pacific Earthquake Engineering Research Center. Today the PEER Structural Performance database provides 253 rectangular RC columns and 163 spiral RC columns lateral load test results, test setup information, geometrical and material properties of the specimens.

The PEER Structural Performance database is accessible by the world wide websites; **http://www.ce.washington.edu/~peera1/** (last accessed date: *04.03.2006*) and **http://nisee.berkeley.edu/spd/** (last accessed date:

04.03.2006). The latter website provides a search option which enables researchers to find the test results with specified attributes.

## 2.2 Properties of RC Columns in the PEER Database

The PEER Structural Performance Database provides all geometrical and key material properties of the test specimens. In addition, the test configurations of the specimens and the transverse reinforcement details are provided. The failure modes of the columns are also reported by the researchers and are available in the database. There are three modes of column failure as; flexure-critical, flexure-shear-critical and shear-critical. The classification of the failure modes is determined as follows: If no shear damage is observed then the test is classified as flexure-critical regardless of column strength. If shear damage is present, the observed flexural moment capacity ($M_m$) is compared with the calculated flexural moment capacity ($M_{fl}$) according to the procedures of the American Concrete Institute's Building Code Requirements for Structural Concrete (ACI 318-02). If $M_m \leq 0.85\ M_{fl}$, the test is classified as shear-critical. On the other hand, if $M_m > 0.85\ M_{fl,}$ the test is classified as flexure-shear-critical. In this study, the test results of rectangular reinforced concrete columns with flexure failure mode were used. Additional geometrical properties of the columns were also calculated from the available data when necessary.

### 2.2.1 Material Properties of Columns

The material properties provided for each column specimen in the database are listed as follows with their notations: characteristic compressive strength of concrete ($f_c$), yield strength of longitudinal reinforcement ($f_{yl}$), ultimate strength of longitudinal reinforcement ($f_{su}$), yield strength of transverse reinforcement ($f_{yt}$) and ultimate strength of transverse reinforcement ($f_{su,t}$). The parameters $f_{yl}$ and $f_{su}$ are reported both for corner bars and intermediate bars separately.

### 2.2.2 Geometrical Properties of Columns

The definitions of the geometrical properties of the test columns are presented in this section. The dimensions of the cross-section, bar diameters/spacing and the reinforcement ratios are the main geometrical properties.

In terms of overall column dimensions, the following parameters are reported: column height as the dimension in the direction of loading ($H$), column width ($B$), cross-sectional area of column ($A_g$) and length of equivalent cantilever ($L$). The term equivalent cantilever is explained in Section 2.2.4.

In terms of longitudinal reinforcement, the following parameters are reported: number of longitudinal reinforcement bars ($n_b$), diameter of longitudinal reinforcement bars ($d_l$), splice length of longitudinal reinforcement ($L_{splice}$) and longitudinal reinforcement ratio ($\rho_l$).

In terms of transverse reinforcement, the following parameters are reported: diameter of transverse reinforcement ($d_t$), spacing of transverse reinforcement ($s$), number of transverse shear bars in cross section ($N_v$), clear cover ($c$), which is defined as the distance from outer surface of column to outer edge of transverse reinforcement, and volumetric transverse reinforcement ratio ($\rho_t$).

In the PEER Structural Performance database, the volumetric transverse reinforcement ratio values of the columns are obtained from researchers who conducted the tests. However the reported transverse reinforcement ratios differ in definition, so there is an inconsistency with these values. In order to eliminate this problem, the volumetric transverse reinforcement ratios were calculated from the available geometrical data by using the definition given below which has been taken from the Kent & Park (1971) confined concrete material model.

The volumetric transverse ratio is defined as the ratio of the volume of transverse reinforcement steel over a height of '*s*' to the volume of core concrete bounded by '*s*'

$$\rho_t = \frac{V_{trans}}{V_{core}} \tag{2.1}$$

The volume of transverse reinforcement is equal to total length of transverse steel in the cross section multiplied by the cross sectional area of the bars.

$$V_{trans} = A_0 \, L_t \tag{2.2}$$

The volume of core concrete is calculated by the following equation,

$$V_{core} = B_k \, H_k \, s \tag{2.3}$$

where

$$A_0 = \frac{\pi \, d_t^2}{4} \tag{2.4}$$

$$L_t = N_v \, L_H + N_v \, L_B \tag{2.5}$$

$$B_k = B - 2c \tag{2.6}$$

$$H_k = H - 2c \tag{2.7}$$

$$L_H = H - 2c - d_t \tag{2.8}$$

$$L_B = B - 2c - d_t \tag{2.9}$$

Substituting Eq. (2.8) and Eq. (2.9) into Eq. (2.5) and rearranging,

$$L_t = N_v (H + B - 4c - 2d_t) \tag{2.10}$$

Substituting Eq. (2.3), Eq. (2.4) and Eq. (2.10) into Eq. (2.1) and rearranging,

$$\rho_t = \frac{\pi d_t^2 N_v (H + B - 4c - 2d_t)}{4 B_k H_k s} \tag{2.11}$$

Figure 2.1 shows the legend for the above calculations.

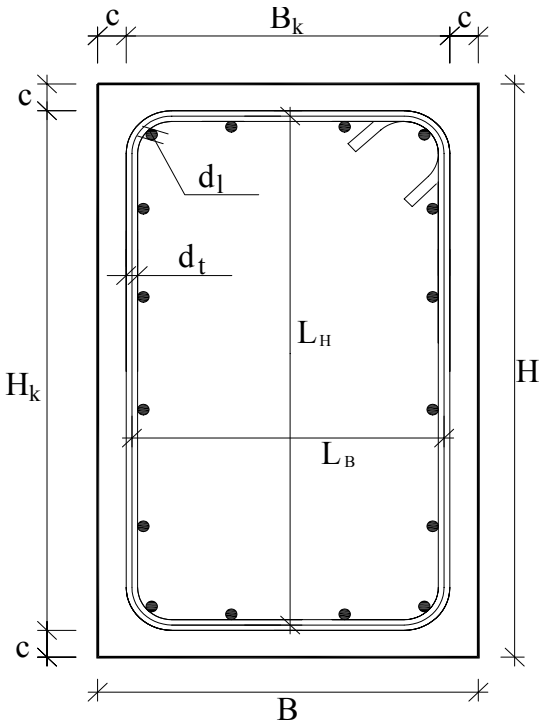


**Figure 2.1** Sketch showing the legend for calculation of volumetric transverse reinforcement ratio

In addition to the geometrical properties present in the PEER Structural Performance database, the following properties are calculated using the available data:

$$\text{Axial load ratio} = \frac{P}{f_c \, A_g} \tag{2.12}$$

where '$P$' is the axial load on column section. Shear reinforcement ratio in the direction of loading is given as

$$\rho_w = \frac{N_v \, \pi \, d_t^2 / 4}{B \, s} \tag{2.13}$$

for which all the parameters have been defined previously.

$$\text{Slenderness ratio, } \lambda = \frac{k \, L}{i} \tag{2.14}$$

where $k$ = 2.0 for all columns and '$i$' is the radius of gyration.

$$\text{Shear ratio} = \frac{V_{\max}}{B \, d \, \sqrt{f_c}} \tag{2.15}$$

where '$V_{max}$' is the maximum shear force and '$d$' is the column depth.

$$\text{Shear span /depth ratio} = \frac{a}{d} \tag{2.16}$$

where shear span '$a$' is equal to equivalent cantilever length '$L$'.

### 2.2.3 Confinement Details of Columns

The test columns in the PEER database have different configurations of transverse reinforcement. There are mainly nine categories of configurations and these are defined below in Table 2.1 and illustrated in Figure 2.2.

**Table 2.1** Definition of confinement types in the PEER database

| Confinement Type | Confinement Code |
|---|---|
| Interlocking ties | 1 |
| Rectangular ties | 2 |
| Rectangular and Diagonal ties | 3 |
| Rectangular and Interlocking ties | 4 |
| Rectangular and Interlocking ties with J-hooks | 5 |
| Rectangular ties and cross-ties | 6 |
| Rectangular and Octagonal ties | 7 |
| Rectangular ties and U-bars | 8 |
| U-bars with cross-ties | 9 |

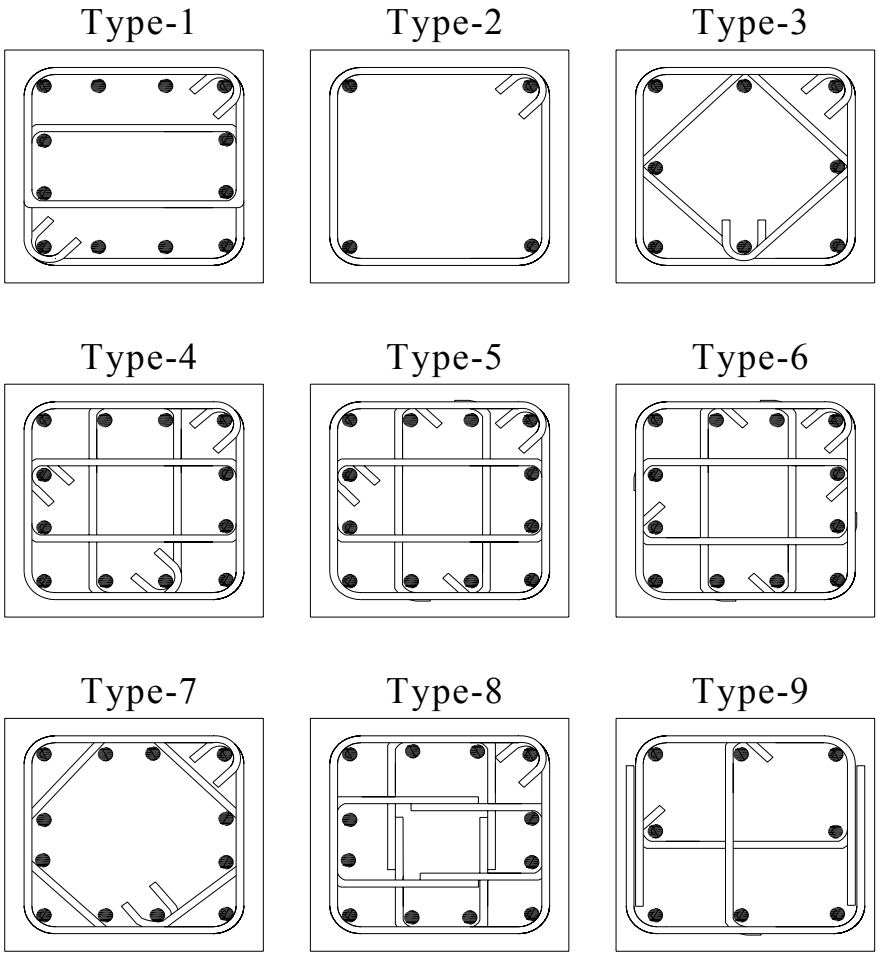


**Figure 2.2** Confinement types in the PEER database

### 2.2.4 Test Configuration of Columns

Many researchers contributed to the PEER column database and as a result, there are different test configurations which can be seen in Figure 2.3. To compare the test results more consistently, the lateral force-deflection relationships should be modified as if the column is a cantilever as shown in Figure 2.3.a. Hence the equivalent cantilever length '*L*' was used for the transformation.

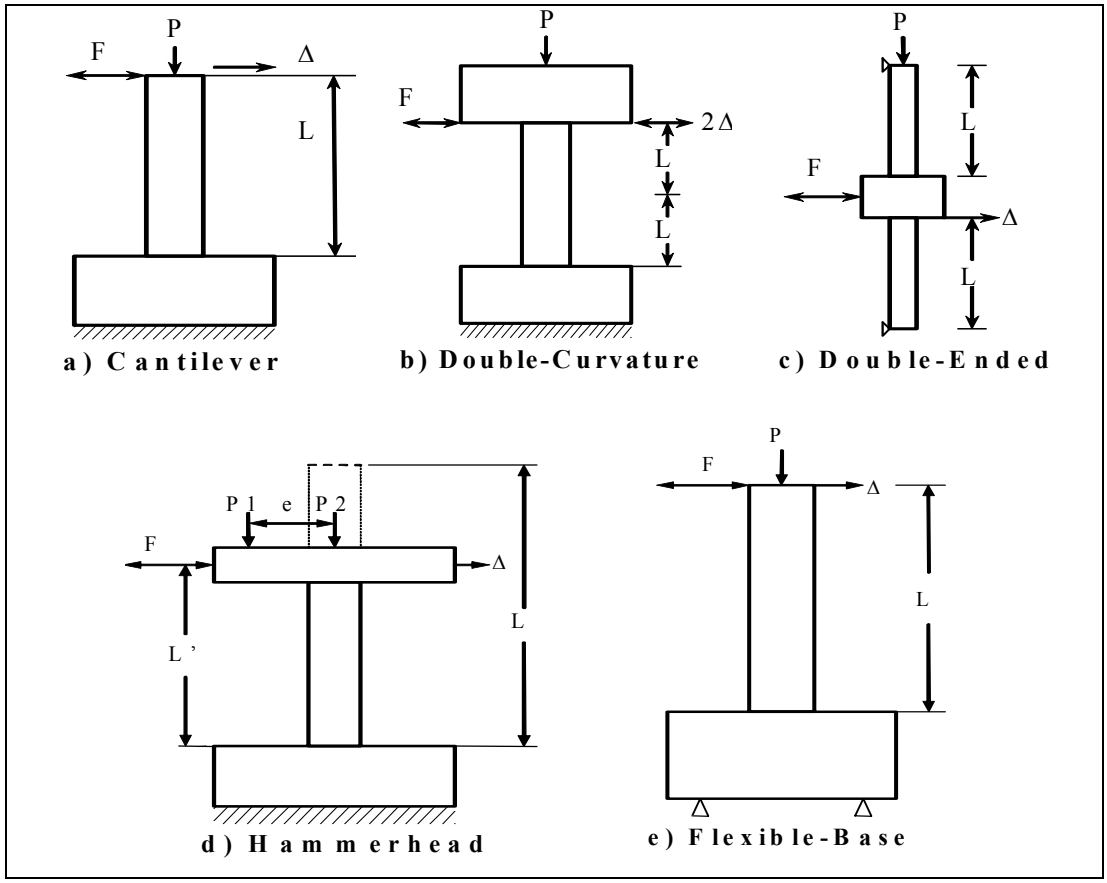


**Figure 2.3** Column test setup configurations (taken from PEER structural performance database user's manual, version 1.0)

## 2.3 Loading Characteristics of Column Tests

Loading histories that have been used for column tests are also important in terms of structural behavior. Column tests in PEER database that are considered in this study were conducted by quasi-static cyclic load application. A loading history in a quasi-static test is basically described as a set of lateral displacements imposed to the test specimen. Taylor et al. (1997) investigated a variety of loading histories and concluded that the type and level of damage is dependent to the order and pattern of applied displacements, if the loading causes inelastic behavior of the member.

The load paths or loading histories used in the testing of the PEER Structural Performance database columns can be separated into three groups;

- Standard Amplitude Loading History, (SA)
- Constant Amplitude Loading History, (CA)
- Variable Amplitude Loading History, (VA)

The most used type of loading history in the cyclic lateral load tests is the standard amplitude loading history that has a pattern with a series of stepwise increasing loading cycles (Figure 2.4.a). This type of loading is generally preferred if only a few specimens are available, the monotonic load-deformation response can be predicted with good confidence, the rate of strength degradation is slow and cumulative damage modeling is not part of the investigation (Krawinkler, 1996). In constant amplitude cyclic tests, the displacement amplitude is kept constant throughout the test (Figure 2.4.b). This type of loading is employed if a cumulative damage model is being developed or low-cycle fatigue behavior is being investigated. The variable amplitude loading histories are used for investigation of column behavior in a more realistic manner because of the similarity with the random loading nature of the earthquakes (Figure 2.4.c).

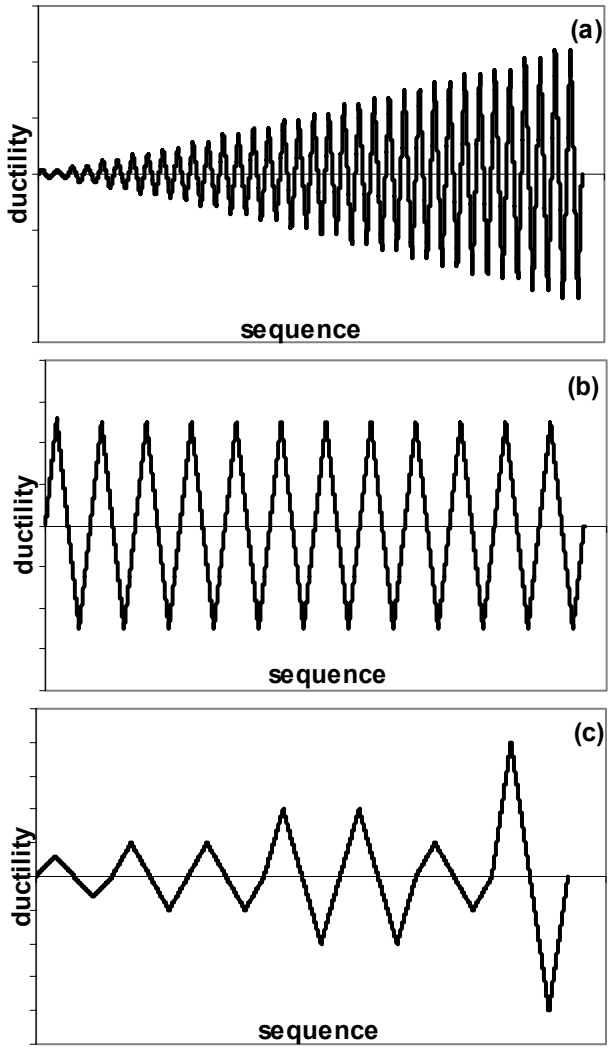


**Figure 2.4** Types of loading patterns: a) standard amplitude b) constant amplitude c) variable amplitude

## 2.4 Statistics of Major Parameters in Column Tests

The PEER Structural Performance database has a variety of columns that have different attributes. There are mainly 213 results of uni-axial, cyclic, lateral load tests of reinforced concrete rectangular columns which have flexure failure mode in the PEER database. In addition to that, the test results from Erberik & Sucuoglu (2001) were included to the data which add up to a total number of 225 tests. The

number of the column test data then reduced to its final value of 196. The reason for this reduction is the elimination of the cyclic tests which have missing force-displacement data, missing key properties or irregular shapes of force-displacement relationship. General information regarding the considered properties of RC column tests in PEER database are given in Table A.1 in Appendix A. The statistical distributions of the major column properties are given in Figure 2.5. The purpose of this study is to identify the general characteristics of the database for a better assessment of the results that will be observed from the studies using the PEER column database.

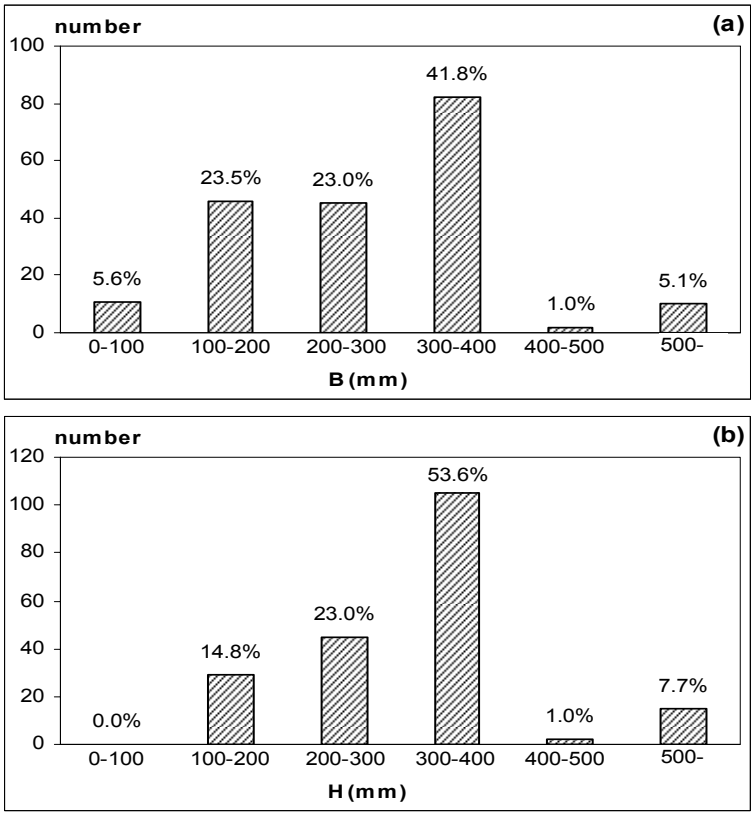


**Figure 2.5** Statistical distributions of the major column properties

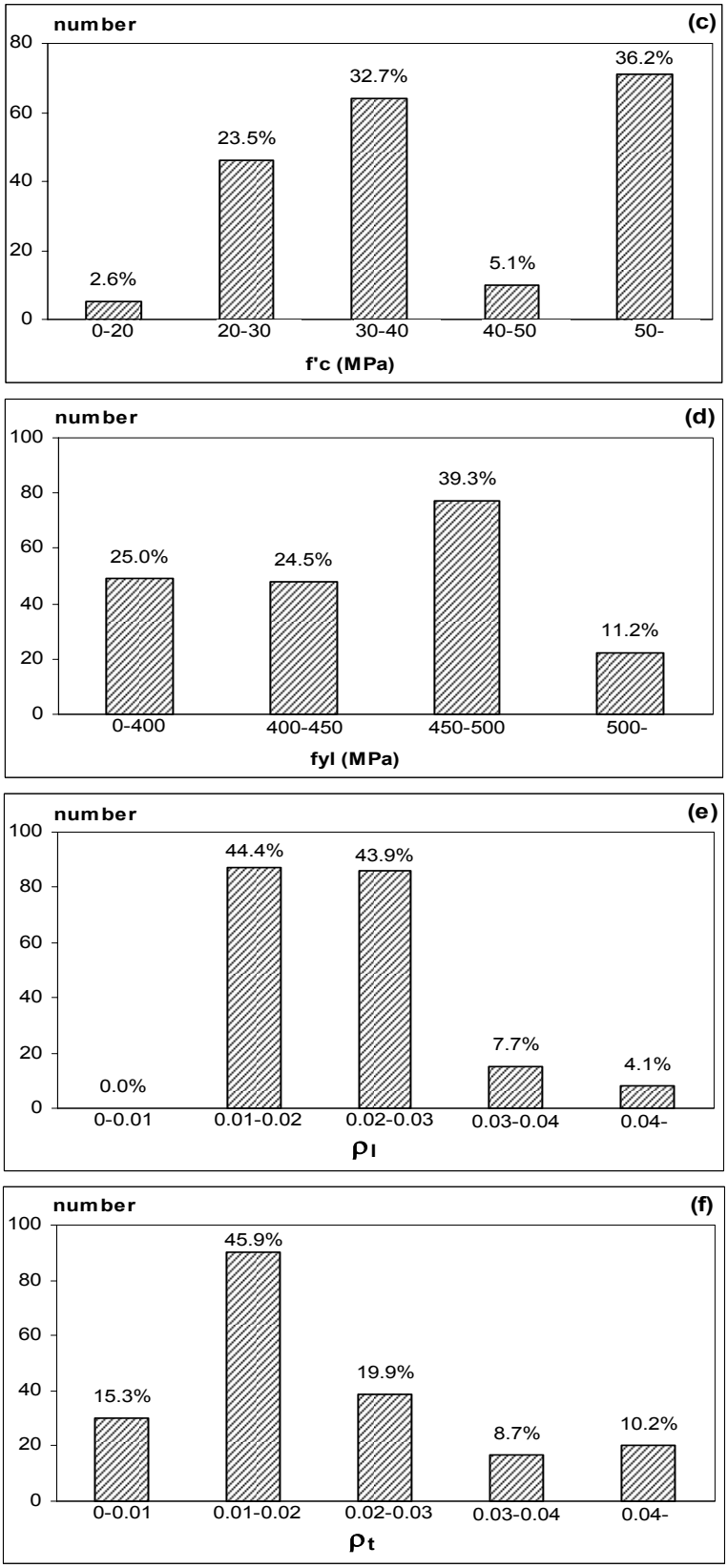


**Figure 2.5** (cont'd)

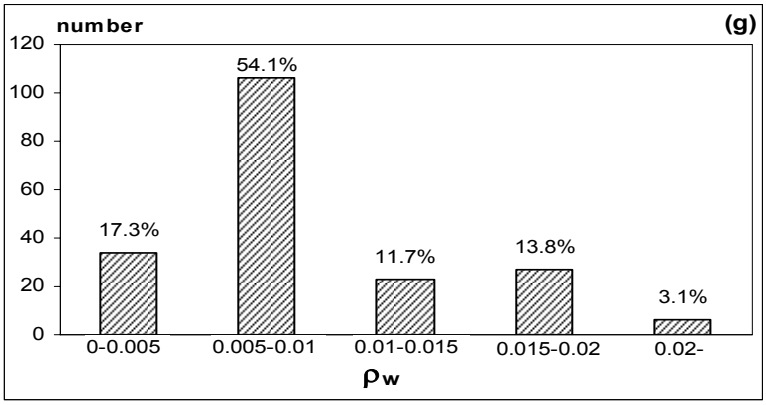


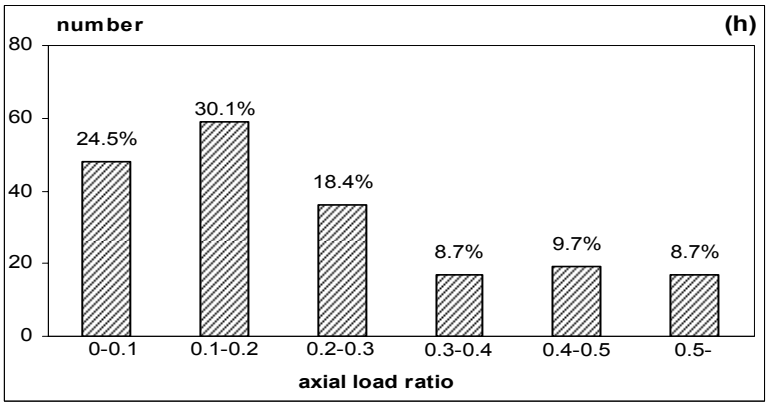


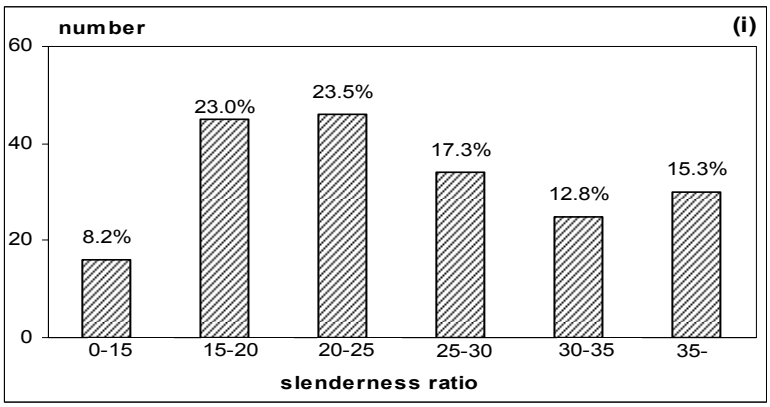


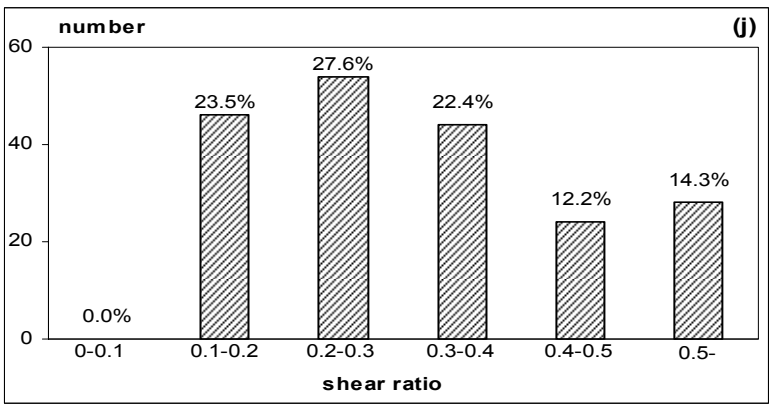


**Figure 2.5** (cont'd)

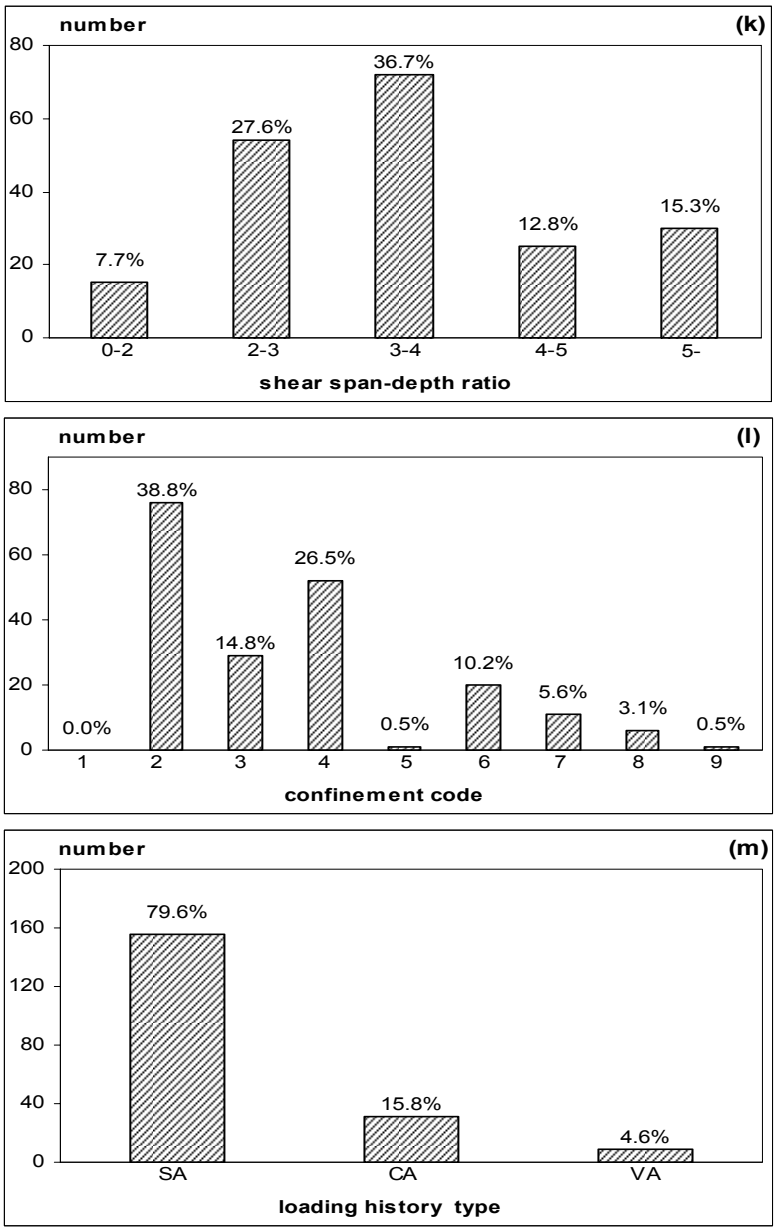


**Figure 2.5** (cont'd)

As it can be observed from Figure 2.5, approximately 60 % of the columns have compressive concrete strength less than 40 MPa and the remaining 40 % of the columns have high strength concrete. This indicates that the database columns represent a wide range in concrete strength. The longitudinal reinforcement steel yield strength is mostly between 400 and 500 MPa confirming with the common

practice of the longitudinal steel grade used in the structural members. The longitudinal reinforcement ratio and the volumetric transverse reinforcement ratio are observed to be generally in the range of 1 % - 3 %. More than half of the columns have axial load ratio below 0.2. Another observation is that in majority of the cyclic tests, standard amplitude loading history has been employed. The number of constant amplitude cyclic tests is small in percentage (~16 %). That is why the research concerning the low-cycle fatigue characteristics of RC members is rather limited. When it comes to variable amplitude cyclic loading, the percentage even falls down to nearly 5 % due to issues in the selection and application of variable load histories to RC specimens.

## 2.5 Cyclic Loading Test Data

The lateral force – displacement data of the columns tested under cyclic loading is available in the PEER structural performance database. The data is provided in text format so that it can be imported into a spreadsheet program easily. First column of the text file is the lateral displacement values in millimeters and the second column is the lateral force values in kN. Figure 2.6 shows a sample plot for lateral force – displacement data.

As it can be observed from the Figure 2.6, cyclic loading applied to the column causes deformations beyond elastic limit and in turn the test specimen exhibits a hysteretic response. Such repeated cyclic loading in the inelastic response range can cause deterioration in the mechanical properties of concrete. Therefore, a closer examination of the degradation characteristics of the columns in the PEER database can assist to improve the estimations of structural performance under cyclic loading.

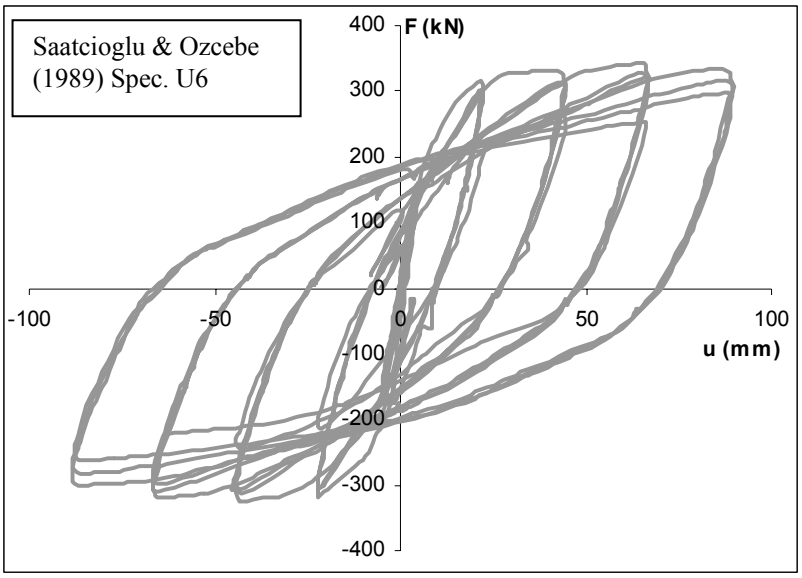


**Figure 2.6** Sample plot for lateral force – displacement data available in the PEER database.

Degradation of mechanical properties for RC members can be examined under three headings: stiffness degradation, strength degradation and pinching. Samples from the cyclic test results of RC members that experienced different types of degradation are presented in Figure 2.7.

## 2.6 Classification of Test Results

This section focuses on the classification of the cyclic load tests. The purpose of the classification of the cyclic tests is to study and investigate the degradation characteristics of the considered RC members more specifically rather than considering the complete database with various material and geometrical parameters as well as different loading histories.

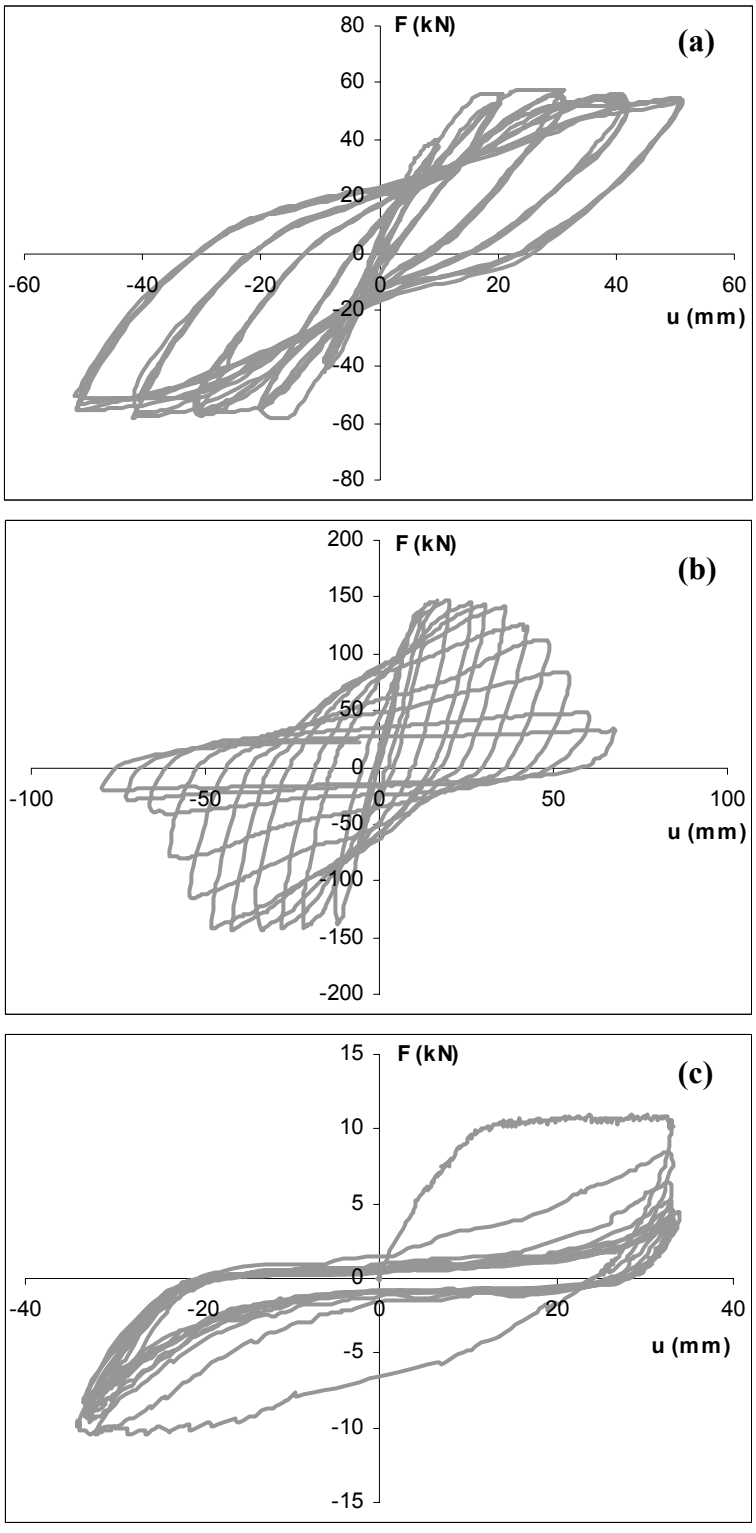


**Figure 2.7** Samples from degradations observed in the columns under cyclic loads: a) Stiffness degradation b) Strength degradation c) Pinching

The classification is conducted in terms of hysteretic energy dissipation characteristics of RC column specimens since energy is a scalar functional of vectorial quantities, such as forces, displacements and deformations and hence is more appropriate for the quantification of a scalar output, such as damage. Furthermore, dissipated energy is an enhanced parameter which implicitly includes the influence of many structural parameters on the cyclic behavior of RC structural members. In other words, the structural parameters which have an effect on the force-displacement relationship have an effect also on the dissipated energy.

The hysteretic energy dissipation as a numerical quantity is meaningless because of the differences in the yield strength, lateral stiffness, ductility characteristics, degradation characteristics and loading histories of the columns. The solution for this problem is to normalize the experimental dissipated energy values with respect to a reference value. For this purpose, dissipated energy values obtained from two general and well known hysteresis models (bilinear and stiffness degrading hysteresis models) in the literature are employed. Hence the ratio of experimental to theoretical cumulative dissipated energy, which can be considered as an "energy-based index", is employed as a non-dimensional measure for the classification of cyclic test results of RC columns in the database. The details are given in Section 2.6.2. However, the considered unit cycle definition should be introduced first because the index values are obtained by using this definition.

### 2.6.1 Unit Cycle Definition

The dissipated energy is the total area enclosed by the force-displacement curve. The force-displacement relationship is composed of a series of unit cycles depending on the applied loading history. The unit cycle definition is important since the dissipated energy values, and in turn the energy-based index is calculated according to this definition. In the literature there are two different definitions of unit cycle. First one is the displacement-based unit cycle which is composed of two half cycles and each half cycle is bounded by two zero displacement points

(Figure 2.8.a). On the other hand, force-based unit cycle is composed of two half cycles which are bounded by two zero force points as shown in Figure 2.8.b. From the two different unit cycle definitions, the force-based unit cycle definition is used in this study. The reason for this choice is the fact that, displacement-based unit cycle is found to be incapable of interpreting the half cycles under variable amplitude loading when displacement cycles oscillate around a non-zero axis (Erberik, 2001). Throughout the rest of study, the word "half cycle" is used instead of "forced-based half cycle".

Force-based unit cycle definition is composed of one positive half cycle and one negative half cycle (Figure 2.8.b). In the positive half cycle part, all the force values are greater than zero and the displacement values are both positive and negative. The force values are all negative in the negative half cycle. The energy dissipated for a cycle is the summation of dissipated energy values of two half cycles. The total energy dissipation is found by adding all dissipated energy values of the unit cycles that form the entire force-displacement relationship.

### 2.6.2 Energy-based Indices

In this section, two energy-based indices are introduced and the procedure for determination of these indices is explained. The index values obtained for each cyclic column test in the PEER database are presented in tabulated format at the end of this section.

Energy-based index is defined as the ratio of the cumulative experimental dissipated energy value obtained at the end of the cyclic test to the cumulative analytical dissipated energy value obtained from the analytical simulation of the same cyclic test by employing a theoretical hysteresis model. Two different hysteresis models can be employed for the analytical simulation of cyclic tests: bilinear model and stiffness degrading model. The detailed information about the models is presented in the first chapter. There are two reasons for selecting these

hysteresis models in the calculation of energy-based index. First, these models are simple to implement and practical to use. Second, they generally represent non-degrading and stable behavior for structural members, which make them good candidates to be used as reference models.

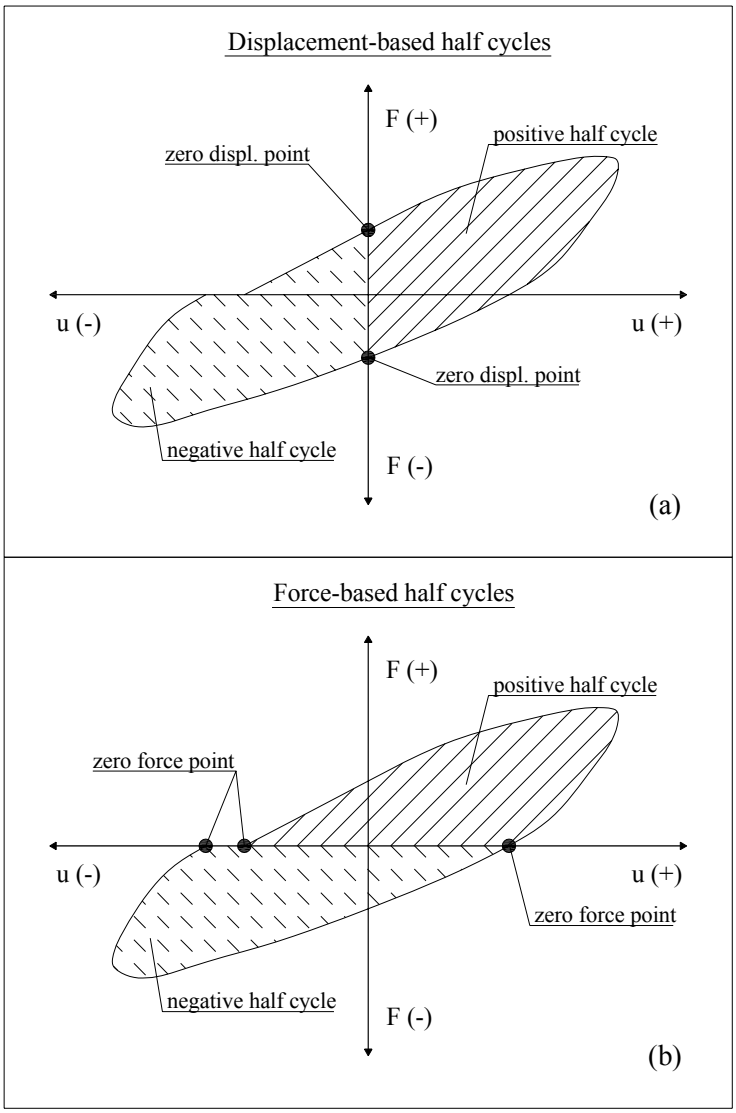


**Figure 2.8** Half cycle definitions: a) displacement-based b) forced-based

The first version of the energy-based index is denoted as $I_{BL}$ where the subscript '*BL*' refers to bilinear hysteresis model as the reference model. The index $I_{BL}$ is defined as the ratio of the cumulative experimental dissipated energy to the cumulative dissipated energy obtained from the bilinear hysteresis model.

$$I_{BL} = \frac{\sum_{i=1}^{m} E_{h,i(EXP)}}{\sum_{i=1}^{m} E_{h,i(BL)}} \tag{2.17}$$

where $m$ is the total number of half cycles and $E_{h,i(EXP)}$ is the experimental dissipated energy at the $i^{th}$ half cycle whereas $E_{h,i(BL)}$ is the analytical dissipated energy at the $i^{th}$ half cycle.

The second version of the index is denoted as $I_{SD}$ where the subscript '*SD*' refers to stiffness degrading model as the reference model. The index $I_{SD}$ is defined as the ratio of the cumulative experimental dissipated energy to the cumulative analytical dissipated energy obtained from the stiffness degrading hysteresis model proposed by Clough and Johnston (1966).

$$I_{SD} = \frac{\sum_{i=1}^{m} E_{h,i(EXP)}}{\sum_{i=1}^{m} E_{h,i(SD)}} \tag{2.18}$$

where $m$ is the total number of half cycles and $E_{h,i(SD)}$ is the analytical dissipated energy at the $i^{th}$ half cycle.

The bilinear hysteresis model exhibits neither deterioration in strength or stiffness nor pinching behavior. Hence it is not appropriate to use the index $I_{BL}$ for the classification of RC column specimens subjected to cyclic loading. In this study the index $I_{BL}$ is used to examine the validity and reliability of bilinear model in the estimation of inelastic response for RC members. On the other hand, the stiffness

degrading model can simulate the behavior of code confirming RC members with an acceptable level of accuracy. Furthermore the rules of the hysteresis model are simple and easy to apply. Hence as stiffness degrading model being a suitable reference model for RC member behavior, the index $I_{SD}$ can be used for the classification of the RC column specimens regarding the cyclic test results.

First step for the determination of the indices $I_{BL}$ and $I_{SD}$ is to calculate the cumulative experimental and analytical dissipated energies from the force-displacement data. The total dissipated energy is equal to the total area enclosed by force-displacement relationship. As mentioned in Section 2.6.1, the total dissipated energy is obtained by summing up the dissipated energy values of all half cycles.

The area under each half cycle of force-displacement relationship is calculated using simple numerical integration method; the trapezoidal rule. Figure 2.9 shows a single half cycle which is on the positive side of the force-displacement relationship. An incremental area, $A_j$, is calculated as,

$$A_j = \overline{F_j}\,\Delta u_j \tag{2.19}$$

where

$$\overline{F_j} = \frac{F_j + F_{j+1}}{2} \tag{2.20}$$

and

$$\Delta u_j = u_{j+1} - u_j \tag{2.21}$$

The incremental area $A_j$ is equal to the incremental dissipated energy $\Delta E_{h,j}$

$$\Delta E_{h,j} = A_j \tag{2.22}$$

and the dissipated energy of the $i^{th}$ half cycle is obtained as

$$E_{h,i} = \sum_{j=1}^{n-1} \Delta E_{h,j} \tag{2.23}$$

The cumulative dissipated energy is obtained by summing up the energies of all cycles

$$E_h = \sum_{i=1}^{m} E_{h,i} \tag{2.24}$$

where *m* is the total number of half cycles (positive and negative).

Hence considering Equations 2.19 - 2.24, the following formulation can be obtained

$$E_h = \sum_{i=1}^{m} \sum_{j=1}^{n-1} \left( \frac{F_{j+1} + F_j}{2} \right) \left( u_{j+1} - u_j \right) \tag{2.25}$$

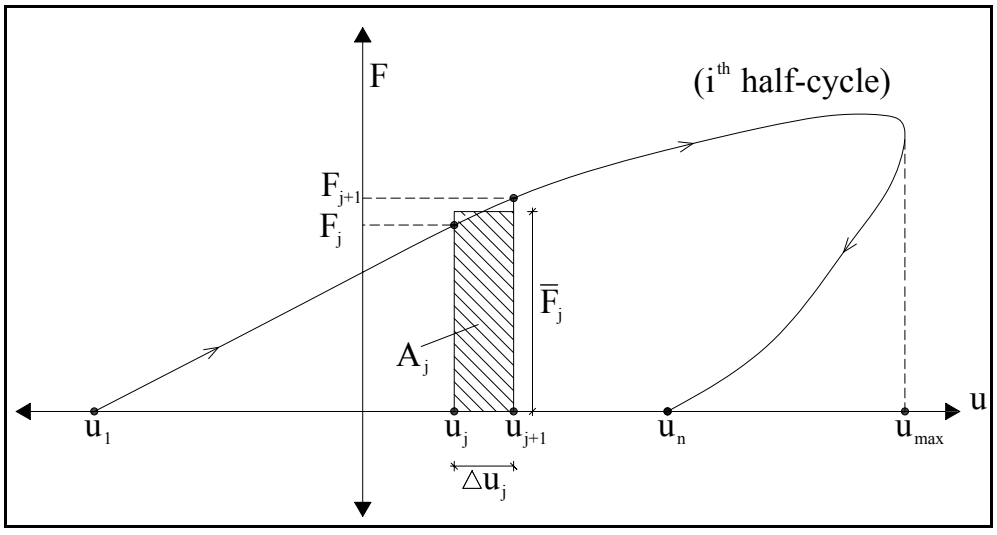


**Figure 2.9** Calculation of dissipated energy for the i$^{th}$ half-cycle

The cumulative experimental and analytical dissipated energies are calculated by using the same approach as explained above. For the calculation of analytical dissipated energy values from bilinear and stiffness degrading models, the computer program INSPEC written in FORTRAN language by Erberik (2001) is employed. The program is capable of simulating the degradation characteristics such as strength degradation, stiffness degradation and pinching. The program generates the force-displacement relationship for a RC column specimen under cyclic loading with the specified hysteresis rules.

The analytical force-displacement relationships of a typical cyclic column test are presented in Figure 2.10 with the corresponding experimental data. The dissipated energy values required for the calculation of the indices $I_{BL}$ and $I_{SD}$ for each half cycle are given in Table 2.2. Hence the index values obtained for this specific cyclic test are

$$I_{BL} = \frac{73308}{147405} = 0.497 \tag{2.26}$$

$$I_{SD} = \frac{73308}{86862} = 0.844 \tag{2.27}$$

**Table 2.2** Dissipated energy values of each half cycle for the sample cyclic test

| Half cycle no | $E_{h,i\,(EXP)}$ (Nm) | $E_{h,i\,(BL)}$ (Nm) | $E_{h,i\,(SD)}$ (Nm) |
|---|---|---|---|
| 1 | 377 | 0 | 0 |
| 2 | 422 | 0 | 0 |
| 3 | 1690 | 0 | 0 |
| 4 | 1561 | 596 | 450 |
| 5 | 1169 | 412 | 207 |
| 6 | 1195 | 398 | 219 |
| 7 | 6289 | 7023 | 6657 |
| 8 | 7098 | 12932 | 9572 |
| 9 | 5004 | 12916 | 6378 |
| 10 | 5740 | 13671 | 7308 |
| 11 | 10408 | 20416 | 13362 |
| 12 | 11566 | 26368 | 16367 |
| 13 | 10391 | 26305 | 12994 |
| 14 | 10398 | 26368 | 13347 |
| $\sum E_{h,i}$ | **73308** | **147405** | **86862** |

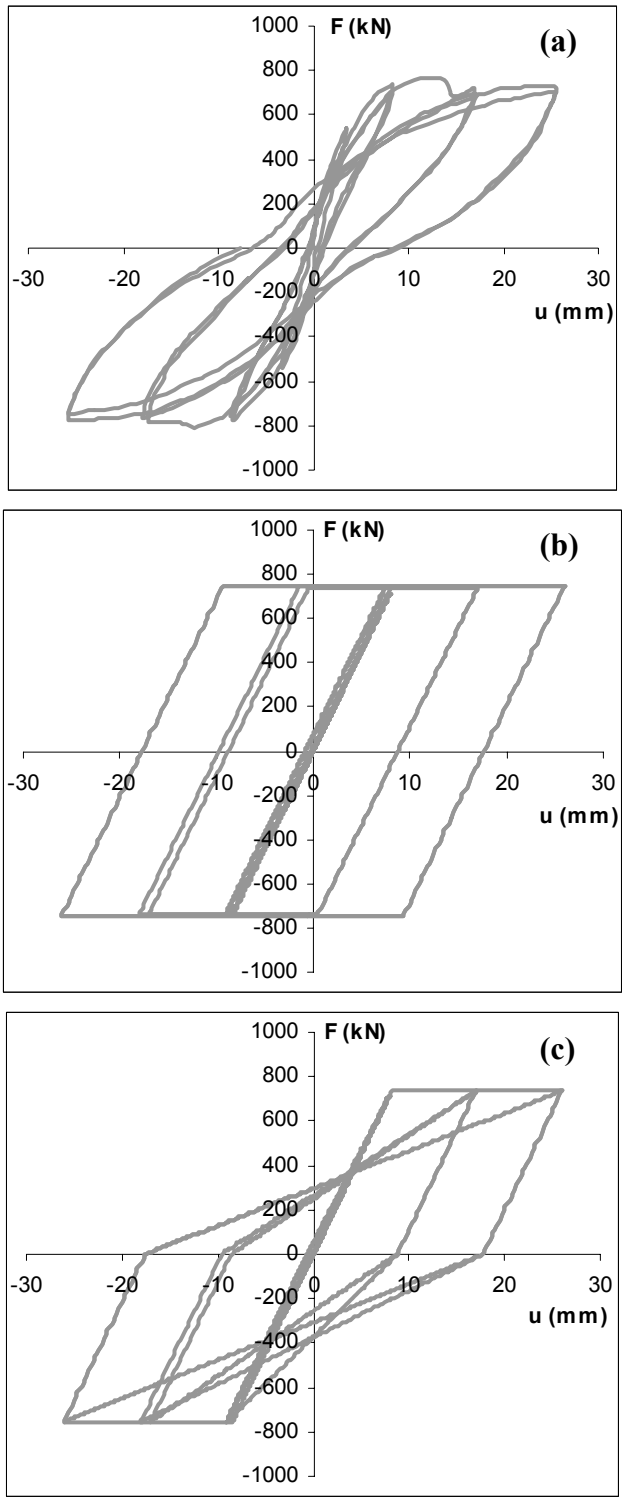


**Figure 2.10** Force-displacement data for a sample cyclic column test;
a) experimental b) analytical (bilinear model)
c) analytical (stiffness degrading model)

The values of the indices $I_{BL}$ and $I_{SD}$ for all the considered cyclic tests in the database are listed in Table 2.3.

**Table 2.3** The indices $I_{BL}$ and $I_{SD}$ of the database cyclic column tests

| No. | Test Specimen ID | $I_{BL}$ | $I_{SD}$ | No. | Test Specimen ID | $I_{BL}$ | $I_{SD}$ |
|---|---|---|---|---|---|---|---|
| **1** | Gill et al. 1979, No. 1 | 0.595 | 1.001 | **42** | Sakai et al. 1990, B4 | 0.526 | 0.880 |
| **2** | Gill et al. 1979, No. 2 | 0.497 | 0.844 | **43** | Atalay and Penzien 1975,1 | 0.372 | 0.706 |
| **3** | Gill et al. 1979, No. 3 | 0.560 | 0.981 | **44** | Atalay and Penzien 1975,2 | 0.384 | 0.753 |
| **4** | Gill et al. 1979, No. 4 | 0.534 | 0.953 | **45** | Atalay and Penzien 1975, 3 | 0.401 | 0.770 |
| **5** | Ang et al. 1981, No. 3 | 0.446 | 0.834 | **46** | Atalay and Penzien 1975,4 | 0.508 | 0.922 |
| **6** | Ang et al. 1981, No. 4 | 0.430 | 0.814 | **47** | Atalay and Penzien 1975,5 | 0.359 | 0.677 |
| **7** | Soesianawati et al. 1986, No. 1 | 0.468 | 0.895 | **48** | Atalay and Penzien 1975,6 | 0.331 | 0.638 |
| **8** | Soesianawati et al. 1986, No. 2 | 0.401 | 0.769 | **49** | Atalay and Penzien 1975,9 | 0.431 | 0.821 |
| **9** | Soesianawati et al. 1986, No. 3 | 0.398 | 0.711 | **50** | Atalay and Penzien 1975,10 | 0.434 | 0.826 |
| **10** | Soesianawati et al. 1986, No. 4 | 0.398 | 0.727 | **51** | Atalay and Penzien 1975,11 | 0.522 | 0.969 |
| **11** | Zahn et al. 1986, No. 7 | 0.423 | 0.769 | **52** | Atalay and Penzien 1975, 12 | 0.318 | 0.605 |
| **12** | Zahn et al. 1986, No. 8 | 0.462 | 0.776 | **53** | Azizinamini et al. 1988, NC-2 | 0.408 | 0.784 |
| **13** | Watson and Park 1989, No. 5 | 0.461 | 0.857 | **54** | Azizinamini et al. 1988, NC-4 | 0.360 | 0.654 |
| **14** | Watson and Park 1989, No. 6 | 0.426 | 0.751 | **55** | Saatcioglu and Ozcebe 1989, U1 | 0.218 | 0.433 |
| **15** | Watson and Park 1989, No. 7 | 0.564 | 1.010 | **56** | Saatcioglu and Ozcebe 1989, U3 | 0.519 | 0.928 |
| **16** | Watson and Park 1989, No. 8 | 0.545 | 0.972 | **57** | Saatcioglu and Ozcebe 1989, U4 | 0.520 | 1.007 |
| **17** | Watson and Park 1989, No. 9 | 0.534 | 1.031 | **58** | Saatcioglu and Ozcebe 1989, U6 | 0.646 | 1.243 |
| **18** | Tanaka and Park 1990, No. 1 | 0.478 | 0.879 | **59** | Saatcioglu and Ozcebe 1989, U7 | 0.554 | 1.081 |
| **19** | Tanaka and Park 1990, No. 2 | 0.447 | 0.839 | **60** | Galeota et al. 1996, AA4 | 0.259 | 0.496 |
| **20** | Tanaka and Park 1990, No. 3 | 0.469 | 0.834 | **61** | Galeota et al. 1996, BA1 | 0.317 | 0.569 |
| **21** | Tanaka and Park 1990, No. 4 | 0.438 | 0.834 | **62** | Galeota et al. 1996, BA4 | 0.336 | 0.613 |
| **22** | Tanaka and Park 1990, No. 5 | 0.447 | 0.798 | **63** | Galeota et al. 1996, CA1 | 0.327 | 0.602 |
| **23** | Tanaka and Park 1990, No. 6 | 0.433 | 0.799 | **64** | Galeota et al. 1996, CA2 | 0.394 | 0.740 |
| **24** | Tanaka and Park 1990, No. 7 | 0.358 | 0.642 | **65** | Galeota et al. 1996, CA3 | 0.391 | 0.694 |
| **25** | Tanaka and Park 1990, No. 8 | 0.361 | 0.639 | **66** | Galeota et al. 1996, CA4 | 0.403 | 0.717 |
| **26** | Park and Paulay 1990, No. 9 | 0.526 | 0.938 | **67** | Galeota et al. 1996, BB | 0.543 | 0.982 |
| **27** | Ohno and Nishioka 1984, L2 | 0.599 | 1.091 | **68** | Galeota et al. 1996, BB1 | 0.450 | 0.788 |
| **28** | Ohno and Nishioka 1984, L3 | 0.459 | 0.849 | **69** | Galeota et al. 1996, BB4 | 0.536 | 0.967 |
| **29** | Zhou et al. 1987, No. 214-08 | 0.488 | 0.804 | **70** | Galeota et al. 1996, BB4B | 0.495 | 0.906 |
| **30** | Kanda et al. 1988, 85STC-1 | 0.393 | 0.728 | **71** | Galeota et al. 1996, CB1 | 0.541 | 0.954 |
| **31** | Kanda et al. 1988, 85STC-2 | 0.374 | 0.726 | **72** | Galeota et al. 1996, CB2 | 0.510 | 0.897 |
| **32** | Kanda et al. 1988, 85STC-3 | 0.393 | 0.728 | **73** | Galeota et al. 1996, CB3 | 0.528 | 0.978 |
| **33** | Muguruma et al. 1989, AH-1 | 0.356 | 0.668 | **74** | Galeota et al. 1996, CB4 | 0.532 | 0.950 |
| **34** | Muguruma et al. 1989, AL-2 | 0.543 | 0.909 | **75** | Wehbe et al. 1998, A1 | 0.437 | 0.801 |
| **35** | Mugumura et al. 1989, AH-2 | 0.443 | 0.823 | **76** | Wehbe et al. 1998, A2 | 0.352 | 0.662 |
| **36** | Muguruma et al. 1989, BL-1 | 0.404 | 0.713 | **77** | Wehbe et al. 1998, B1 | 0.449 | 0.833 |
| **37** | Muguruma et al. 1989, BH-1 | 0.351 | 0.646 | **78** | Wehbe et al. 1998, B2 | 0.423 | 0.787 |
| **38** | Muguruma et al. 1989, BH-2 | 0.368 | 0.675 | **79** | Xiao and Martir.1998, 8L19-0.1P | 0.426 | 0.816 |
| **39** | Sakai et al. 1990, B1 | 0.423 | 0.751 | **80** | Xiao and Martir.1998, 8L19-0.2P | 0.404 | 0.772 |
| **40** | Sakai et al. 1990, B2 | 0.442 | 0.733 | **81** | Xiao and Martir.1998, -8L16-0.1P | 0.391 | 0.766 |
| **41** | Sakai et al. 1990, B3 | 0.450 | 0.735 | **82** | Xiao and Martir.1998, 8L16-0.2P | 0.382 | 0.712 |

**Table 2.3** (cont'd)

| No. | Test Specimen ID | $I_{BL}$ | $I_{SD}$ | No. | Test Specimen ID | $I_{BL}$ | $I_{SD}$ |
|---|---|---|---|---|---|---|---|
| **83** | Sugano 1996, UC10H | 0.512 | 0.880 | **132** | Thomsen and Wallace 1994, C1 | 0.720 | 1.254 |
| **84** | Sugano 1996, UC15H | 0.504 | 0.899 | **133** | Thomsen and Wallace 1994, C2 | 0.567 | 0.994 |
| **85** | Sugano 1996, UC20H | 0.414 | 0.757 | **134** | Thomsen and Wallace 1994, C3 | 0.424 | 0.763 |
| **86** | Sugano 1996, UC15L | 0.284 | 0.530 | **135** | Thomsen and Wallace 1994, D1 | 0.514 | 0.936 |
| **87** | Sugano 1996, UC20L | 0.261 | 0.494 | **136** | Thomsen and Wallace 1994, D2 | 0.511 | 0.928 |
| **88** | Bayrak and Sheikh 1996, ES-1HT | 0.391 | 0.664 | **137** | Thomsen and Wallace 1994, D3 | 0.508 | 0.939 |
| **89** | Bayrak and Sheikh 1996, AS-2HT | 0.358 | 0.698 | **138** | Paultre and Legeron,No. 1006015 | 0.398 | 0.759 |
| **90** | Bayrak and Sheikh 1996, AS-3HT | 0.418 | 0.725 | **139** | Paultre and Legeron,No. 1006025 | 0.359 | 0.677 |
| **91** | Bayrak and Sheikh 1996, AS-4HT | 0.407 | 0.739 | **140** | Paultre and Legeron, No.1006040 | 0.391 | 0.666 |
| **92** | Bayrak and Sheikh 1996, AS-5HT | 0.346 | 0.588 | **141** | Paultre and Legeron,No.10013015 | 0.387 | 0.710 |
| **93** | Bayrak and Sheikh 1996, AS-6HT | 0.387 | 0.689 | **142** | Paultre and Legeron,No.10013025 | 0.292 | 0.522 |
| **94** | Bayrak and Sheikh 1996, AS-7HT | 0.468 | 0.723 | **143** | Paultre and Legeron,No.10013040 | 0.320 | 0.564 |
| **95** | Bayrak and Sheikh 1996, ES-8HT | 0.399 | 0.667 | **144** | Paultre et al., 2001, No. 806040 | 0.338 | 0.646 |
| **96** | Saatcioglu and Grira 1999, BG-1 | 0.491 | 0.857 | **145** | Paultre et al., 2001, No. 1206040 | 0.346 | 0.653 |
| **97** | Saatcioglu and Grira 1999, BG-2 | 0.419 | 0.790 | **146** | Paultre et al., 2001, No. 1005540 | 0.351 | 0.663 |
| **98** | Saatcioglu and Grira 1999, BG-3 | 0.382 | 0.782 | **147** | Paultre et al., 2001, No. 1008040 | 0.404 | 0.678 |
| **99** | Saatcioglu and Grira 1999, BG-4 | 0.407 | 0.773 | **148** | Paultre et al., 2001, No. 1005552 | 0.475 | 0.813 |
| **100** | Saatcioglu and Grira 1999, BG-5 | 0.415 | 0.760 | **149** | Paultre et al., 2001, No. 1006052 | 0.427 | 0.755 |
| **101** | Saatcioglu and Grira 1999, BG-6 | 0.389 | 0.767 | **150** | Pujol 2002, No. 10-2-3N | 0.307 | 0.591 |
| **102** | Saatcioglu and Grira 1999, BG-7 | 0.424 | 0.820 | **151** | Pujol 2002, No. 10-2-3S | 0.322 | 0.629 |
| **103** | Saatcioglu and Grira 1999, BG-8 | 0.376 | 0.734 | **152** | Pujol 2002, No. 10-3-1.5N | 0.387 | 0.772 |
| **104** | Saatcioglu and Grira 1999, BG-9 | 0.361 | 0.718 | **153** | Pujol 2002, No. 10-3-1.5S | 0.402 | 0.797 |
| **105** | Saatcioglu and Grira 1999, BG-10 | 0.446 | 0.829 | **154** | Pujol 2002, No. 10-3-3N | 0.317 | 0.608 |
| **106** | Matamoros et al. 1999,C10-05N | 0.354 | 0.682 | **155** | Pujol 2002, No. 10-3-3S | 0.310 | 0.611 |
| **107** | Matamoros et al. 1999,C10-05S | 0.363 | 0.687 | **156** | Pujol 2002, No. 10-3-2.25N | 0.317 | 0.622 |
| **108** | Matamoros et al. 1999,C10-10N | 0.395 | 0.757 | **157** | Pujol 2002, No. 10-3-2.25S | 0.307 | 0.608 |
| **109** | Matamoros et al. 1999,C10-10S | 0.406 | 0.769 | **158** | Pujol 2002, No. 20-3-3N | 0.366 | 0.712 |
| **110** | Matamoros et al. 1999,C10-20N | 0.308 | 0.581 | **159** | Pujol 2002, No. 20-3-3S | 0.370 | 0.720 |
| **111** | Matamoros et al. 1999,C10-20S | 0.317 | 0.588 | **160** | Pujol 2002, No. 10-2-2.25N | 0.274 | 0.543 |
| **112** | Matamoros et al. 1999,C5-00N | 0.362 | 0.689 | **161** | Pujol 2002, No. 10-2-2.25S | 0.287 | 0.582 |
| **113** | Matamoros et al. 1999,C5-00S | 0.363 | 0.686 | **162** | Pujol 2002, No. 10-1-2.25N | 0.324 | 0.648 |
| **114** | Matamoros et al. 1999,C5-20N | 0.300 | 0.553 | **163** | Pujol 2002, No. 10-1-2.25S | 0.335 | 0.664 |
| **115** | Matamoros et al. 1999,C5-20S | 0.290 | 0.541 | **164** | Bechtoula 2002, D1N30 | 0.401 | 0.758 |
| **116** | Matamoros et al. 1999,C5-40N | 0.336 | 0.597 | **165** | Bechtoula 2002, D1N60 | 0.600 | 1.071 |
| **117** | Matamoros et al. 1999,C5-40S | 0.328 | 0.590 | **166** | Bechtoula 2002, L1N60 | 0.483 | 0.908 |
| **118** | Mo and Wang 2000,C1-1 | 0.352 | 0.684 | **167** | Bechtoula 2002, L1N6B | 0.523 | 0.966 |
| **119** | Mo and Wang 2000,C1-2 | 0.382 | 0.747 | **168** | Takemura and Kawas, 1997, Test 1 | 0.235 | 0.481 |
| **120** | Mo and Wang 2000,C1-3 | 0.300 | 0.587 | **169** | Takemura and Kawas, 1997, Test 2 | 0.341 | 0.650 |
| **121** | Mo and Wang 2000,C2-1 | 0.362 | 0.714 | **170** | Takemura and Kawas, 1997, Test 3 | 0.461 | 0.783 |
| **122** | Mo and Wang 2000,C2-2 | 0.360 | 0.687 | **171** | Takemura and Kawas, 1997, Test 4 | 0.260 | 0.608 |
| **123** | Mo and Wang 2000,C2-3 | 0.299 | 0.587 | **172** | Wight and Sozen,No. 40.033ae | 0.451 | 0.774 |
| **124** | Mo and Wang 2000,C3-1 | 0.407 | 0.782 | **173** | Wight and Sozen No. 40.033aw | 0.421 | 0.726 |
| **125** | Mo and Wang 2000,C3-2 | 0.405 | 0.764 | **174** | Wight and Sozen No. 40.048e | 0.328 | 0.619 |
| **126** | Mo and Wang 2000,C3-3 | 0.332 | 0.653 | **175** | Wight and SozenNo. 40.048w | 0.326 | 0.622 |
| **127** | Thomsen and Wallace 1994, A1 | 0.509 | 0.918 | **176** | Wight and SozenNo. 40.033e | 0.435 | 0.735 |
| **128** | Thomsen and Wallace 1994, A3 | 0.406 | 0.829 | **177** | Wight and Sozen No. 40.033w | 0.444 | 0.761 |
| **129** | Thomsen and Wallace 1994, B1 | 0.685 | 1.139 | **178** | Wight and Sozen No. 25.033e | 0.316 | 0.587 |
| **130** | Thomsen and Wallace 1994, B2 | 0.572 | 1.000 | **179** | Wight and Sozen No. 25.033w | 0.354 | 0.657 |
| **131** | Thomsen and Wallace 1994, B3 | 0.439 | 0.821 | **180** | Wight and SozenNo. 40.067e | 0.525 | 0.920 |

**Table 2.3** (cont'd)

| No. | Test Specimen ID | $I_{BL}$ | $I_{SD}$ | No. | Test Specimen ID | $I_{BL}$ | $I_{SD}$ |
|---|---|---|---|---|---|---|---|
| **181** | Wight and Sozen No. 40.067w | 0.422 | 0.768 | **189** | Erberik and Sucuoglu , CAH-4 | 0.214 | 0.396 |
| **182** | Wight and SozenNo. 40.147e | 0.435 | 0.828 | **190** | Erberik and Sucuoglu , CAH-5 | 0.238 | 0.464 |
| **183** | Wight and Sozen No. 40.147w | 0.452 | 0.817 | **191** | Erberik and Sucuoglu , CAH-6 | 0.221 | 0.425 |
| **184** | Wight and Sozen No. 40.092e | 0.476 | 0.846 | **192** | Erberik and Sucuoglu , CAL-8 | 0.232 | 0.434 |
| **185** | Wight and Sozen No. 40.092w | 0.470 | 0.839 | **193** | Erberik and Sucuoglu, CAL-9 | 0.225 | 0.435 |
| **186** | Erberik and Sucuoglu , CAH-1 | 0.305 | 0.551 | **194** | Erberik and Sucuoglu , CAL-10 | 0.248 | 0.481 |
| **187** | Erberik and Sucuoglu , CAH-2 | 0.270 | 0.535 | **195** | Erberik and Sucuoglu , CALU-11 | 0.163 | 0.317 |
| **188** | Erberik and Sucuoglu , CAH-3 | 0.188 | 0.357 | **196** | Erberik and Sucuoglu , CAL-12 | 0.234 | 0.440 |

## 2.7 Classification of the Cyclic Column Tests

A general classification of the test results according to the calculated indices is proposed and explained in this section. Basic statistical characteristics of the indices are discussed.

Table 2.4 shows the basic statistical properties and Figure 2.11 plots the normal probability distributions of the indices. The mean values of the indices $I_{BL}$ and $I_{SD}$ are 0.405 and 0.746 respectively. This result reveals that, the bilinear hysteresis model used for the calculation of $I_{BL}$ is not a good model for the estimation of the dissipated energy for RC members. The mean value of the $I_{BL}$ indicates that, for a general observation, the actual energy dissipation of the column is nearly 40 % of the energy dissipated for the simulated bilinear model for that column. However, this percentage is about 75 % for the stiffness degrading model used for the calculation of $I_{SD}$. This comparison underlines the fact that, the bilinear model is not a convenient model for the reinforced concrete members subjected to cyclic loads that cause inelastic deformations. The degradation characteristic of the reinforced concrete is the main reason for this conclusion. The stiffness degrading model (Clough and Johnston, 1966) gives more reasonable results in terms of energy dissipation. This is due to fact that, a code confirming reinforced concrete member with average material properties can exhibit a force-displacement

relationship very close to stiffness degrading model. As a result, it is more convenient to make a classification of the test results by considering only the values of the index $I_{SD}$.

Table 2.5 shows the classification of the database columns according to index $I_{SD}$. The columns having an $I_{SD}$ value of 0.85 or greater are assumed to be contained in "Group A", meaning that the column specimens are mostly code confirming and can be modeled with an acceptable degree of accuracy with stiffness degrading model. Generally, there are no or slight deterioration observed in the Group A columns. None of column specimens in this group experienced pinching behavior.

The specimens which have $I_{SD}$ values between 0.85 and 0.70 are contained in "Group B". In general, these specimens exhibit moderate and severe degradation characteristics, especially strength and stiffness degradation but there are a few cases that they exhibit also pinching behavior.

The specimens having $I_{SD}$ values smaller than 0.7 are classified as "Group C". Most of the specimens in Group C have experienced moderate and severe degradation. Also pinching behavior is observed in approximately 30 % of the specimens in this group.

The main consideration in the determination of the $I_{SD}$ limits is to reflect the general distribution of code confirming columns as opposed to poorly designed columns in actual structures. As can be seen from Table 2.5, nearly 20 % of the columns are in Group A and the rest of the column classes nearly get the same share with 40 % each. The index values selected for the boundaries of the intervals are considered as convenient in terms of the energy dissipation and degradation characteristics of the reinforced concrete columns.

**Table 2.4** Statistics of the energy-based indices (total 196 specimens)

| Index | Mean | Standard Deviation | Min.-Max. values |
|---|---|---|---|
| $I_{BL}$ | 0.405 | 0.094 | 0.163-0.720 |
| $I_{SD}$ | 0.746 | 0.158 | 0.317-1.254 |

**Table 2.5** Classification of column specimens according to index $I_{SD}$

| Group | $I_{SD}$ | Number | % |
|---|---|---|---|
| **A** | ≥ 0.85 | 41 | 20.9 |
| **B** | 0.85 > … ≥ 0.70 | 81 | 41.3 |
| **C** | < 0.70 | 74 | 37.8 |
| | **Total** | **196** | **100 %** |

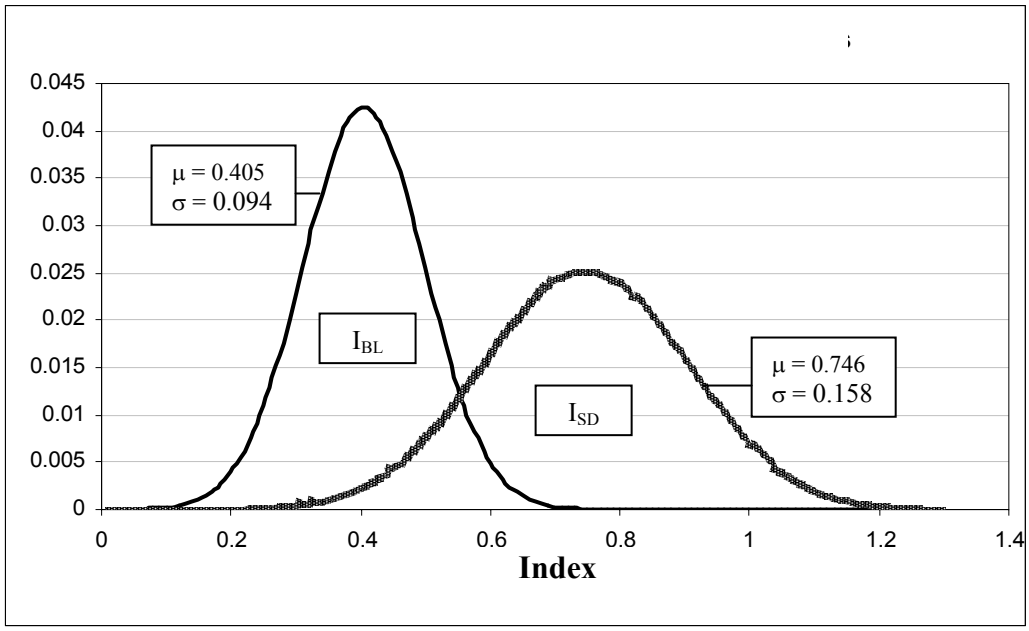


**Figure 2.11** Normal probability distributions for the energy–based indices

Maximum, minimum and average values of the major structural properties of the test specimens for each member group are presented in Table 2.6.

**Table 2.6** Range of major structural properties for each member group

| | **GROUP-A** | | | **GROUP-B** | | | **GROUP-C** | | |
|---|---|---|---|---|---|---|---|---|---|
| | **Max.** | **Min.** | **Avg.** | **Max.** | **Min.** | **Avg.** | **Max.** | **Min.** | **Avg.** |
| $f_c$ (Mpa) | 118.0 | 21.4 | 57.6 | 118.0 | 21.1 | 49.6 | 118.0 | 13.0 | 52.1 |
| $f_{yl}$ (Mpa) | 517.1 | 362.0 | 435.0 | 573.3 | 341.0 | 449.0 | 587.1 | 330.0 | 446.0 |
| $\rho_l$ | 0.060 | 0.014 | 0.028 | 0.060 | 0.013 | 0.022 | 0.038 | 0.013 | 0.020 |
| $\rho_t$ | 0.045 | 0.007 | 0.020 | 0.046 | 0.005 | 0.019 | 0.060 | 0.005 | 0.020 |
| Axial load ratio | 0.70 | 0.00 | 0.30 | 0.80 | 0.03 | 0.24 | 0.50 | 0.00 | 0.18 |
| Shear ratio | 0.706 | 0.112 | 0.370 | 0.750 | 0.106 | 0.337 | 0.708 | 0.142 | 0.311 |
| $\lambda$ | 38.03 | 13.84 | 24.63 | 45.38 | 13.84 | 25.86 | 45.38 | 13.84 | 25.87 |

# CHAPTER 3

# UNLOADING STIFFNESS DEGRADATION

## 3.1 General

Reinforced concrete members which are subjected to repeated cyclic loads generally show degradation in stiffness. The initial or elastic stiffness of the member deteriorates during the load cycles due to the cracking of concrete. This degradation is observed both in the unloading branch and the reloading branch of a hysteresis loop for a reinforced concrete member. Therefore, it is important to be able to incorporate stiffness degradation characteristics into the hysteresis models. There are many hysteresis models that include the stiffness degradation behavior in the literature. The degradation of the reloading branch is generally adopted by reducing the slope by targeting the reloading branch towards the previous maximum displacement point experienced in the direction of loading. On the other hand, the degradation in the unloading branch is modeled in different ways.

This chapter focuses on the unloading stiffness degradation behavior only. The test results from the PEER column database are used to calibrate the unloading stiffness rule parameters available in the literature and then compare the calculated values with the recommended values. The variety of the structural properties of the column specimens in the database enables the examination of the unloading stiffness rule parameters in the whole range.

Two well-known unloading stiffness degradation rules in the literature are introduced and a detailed comparison is conducted in terms of a parametric study. Also, correlations between the calculated unloading parameters are presented and discussed at the end of this chapter.

## 3.2 Unloading Stiffness Degradation Rules in Literature

There are two well-known and widely used approaches for the unloading stiffness degradation in the literature: ductility-based rule and focus-based rule. The basic idea underlying both rules is that the unloading stiffness degradation increases with increasing displacement ductility. Such a behavior in reinforced concrete members has usually been observed from experiments.

The ductility-based approach is based on a simple rule suggesting that the unloading stiffness $K_{un}$ can be determined as a function of initial stiffness $K_0$ and a ductility term.

$$K_{un} = K_0 \left[ \frac{u_y}{u_m} \right]^a \tag{3.1}$$

where $u_m$ is the maximum displacement and $u_y$ is the yield displacement in the direction of loading. The term '$a$' is referred as the ductility-based parameter which takes values between zero and one (Nielsen and Imbeault, 1970). If '$a$' is equal to zero, then the unloading stiffness is simply equal to the initial stiffness. Figure 3.1 illustrates the ductility-based rule for the unloading branch of a typical force-displacement relationship.

Several researchers recommended different values for parameter '$a$' based on experimental studies and implemented Eq. (3.1) into their proposed hysteresis models in order to simulate the degradation in unloading stiffness branches. Takeda et al. (1970) proposed a hysteresis model with a trilinear backbone curve which incorporates the ductility-based rule for unloading stiffness degradation. Takeda et al. recommended the value 0.4 for the parameter '$a$'. The initial stiffness is considered as the line connecting the yield point to the cracking point of concrete. In 1979, Saiidi and Sozen developed a modified version of Takeda model and proposed the value of 0.5 for parameter '$a$'. In 1996,

Stojadinovic and Thewalt proposed and implemented two energy balanced hysteresis models based on the amount of dissipated hysteretic energy and the rate of stiffness degradation. They compared the proposed hysteresis models with the experimentally obtained data. They analyzed the test data and concluded that the ductility-based parameter '*a*' can be selected as 0.3. However, Stojadinovic and Thewalt pointed out that the recommended coefficient is a representative of a well-detailed square column and further study is necessary for different structural systems.

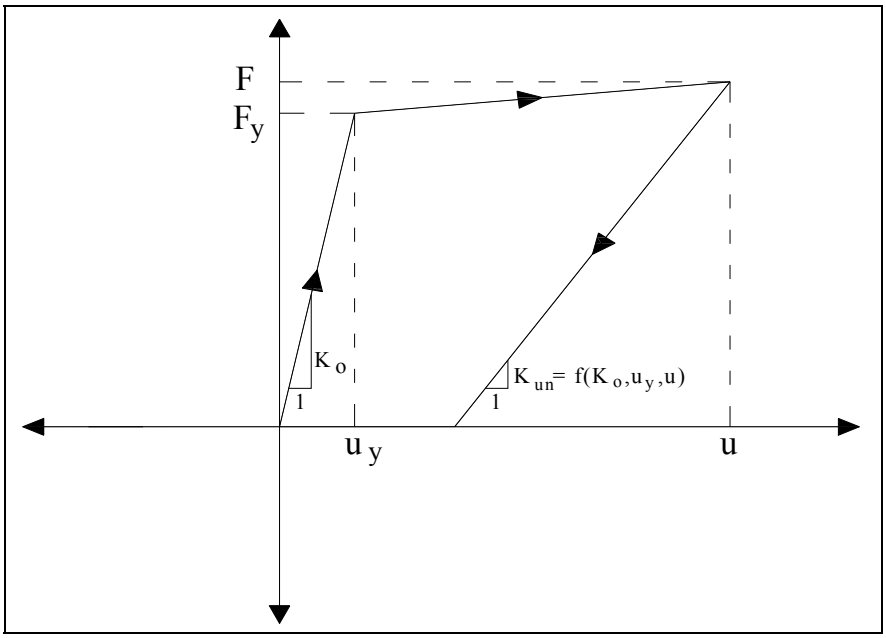


**Figure 3.1** Ductility-based unloading stiffness degradation rule

Another widely used hysteresis rule to simulate degradation in the unloading stiffness branch is the focus-based rule or pivot rule. The unloading branches aim at an imaginary and stationary point which is located at a distance of $\alpha F_y$ on the extension of the elastic branch on the opposite side. As a result, the unloading stiffness decreases with the increasing displacement ductility. Unloading stiffness can be calculated as

$$K_{un} = \frac{F + \alpha F_y}{u + \alpha u_y} \tag{3.2}$$

where ($u$ , $F$) is the load reversal point, $u_y$ is the yield displacement, $F_y$ is the yield force and '$\alpha$' is the focus-based parameter. The definition of the focus-based rule can be seen in Figure 3.2.

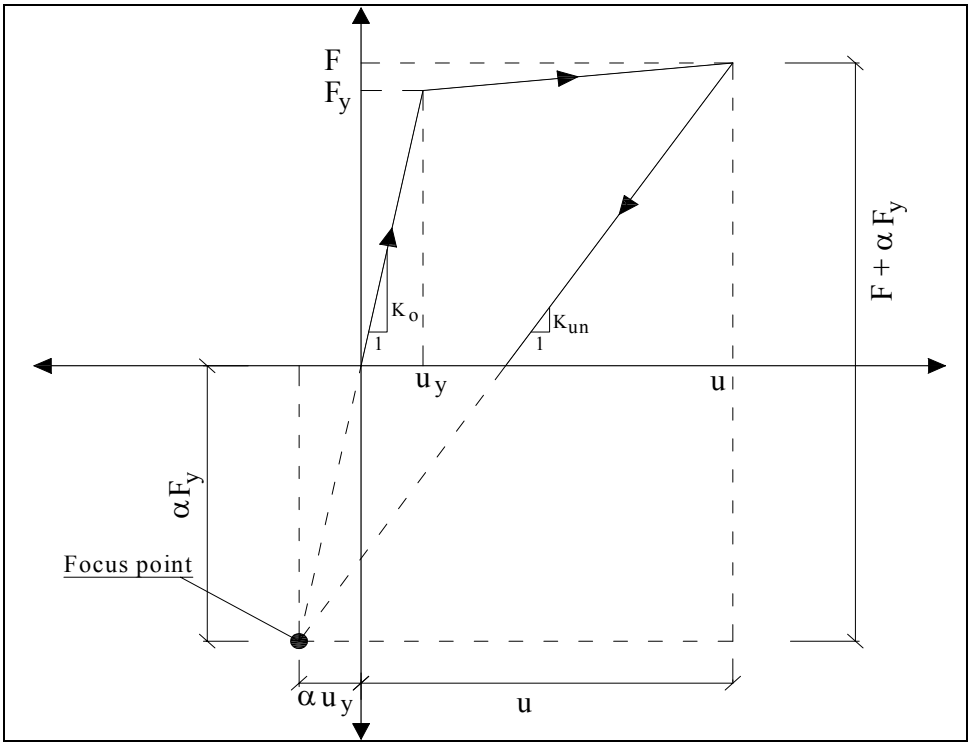


**Figure 3.2** Focus-based unloading stiffness degradation rule

The focus-based rule is first used by the hysteresis model developed for the computer program IDARC (Park et al., 1987). Typical range of values recommended by IDARC for the focus-based stiffness degrading parameter $\alpha$ is as follows: For non-degrading behavior; $\alpha$=200, for mild degrading behavior; $\alpha$=15, for moderate degrading behavior; $\alpha$=10 and for severe degrading behavior; $\alpha$=4.0.

### 3.3 Parametric Study for the Comparison of Unloading Rules

In this study, three rules are considered in order to simulate unloading stiffness degradation. These are unloading with no-degradation (with initial stiffness), unloading with ductility-based rule and unloading with focus-based (pivot point) rule. The detailed explanation for the last two rules was given in the previous section.

The aim of this part of the study is to make a comparison between these three rules related with the unloading branch of hysteresis model in terms of total dissipated energy and the amount of deviation from the initial stiffness per half-cycle. The variables used for the comparison are the parameter '*a*' for the ductility-based rule and the parameter '$\alpha$' for the focus-based rule. Yield level, initial stiffness value and loading history are the parameters that are kept constant. Strength degradation and pinching are not considered in this comparison.

The hysteresis model proposed by Clough and Johnston (1966) is used for the non-degrading unloading stiffness model with post-yield stiffness ratio equal to zero. The unloading rule of the original Clough model is modified for the ductility-based and focus-based approaches. The displacement loading history is arbitrarily selected as variable loading with ductility levels of 1, 2, 3, 4 and 5 to observe the variation of unloading stiffness under different displacement amplitudes. Figure 3.3 shows the loading history used for the generation of hysteresis models. The computer program INSPEC (Erberik, 2001) is employed for the generation of the load-displacement relationships and for the calculation of dissipated energy values.

The original Clough model for the non-degrading unloading stiffness can be seen in Figure 3.4. The generated hysteresis models with ductility-based unloading approach are presented through Figures 3.5.a - 3.5.i. In addition, Figures 3.6.a - 3.6.i present the generated hysteresis models with focus-based unloading rule.

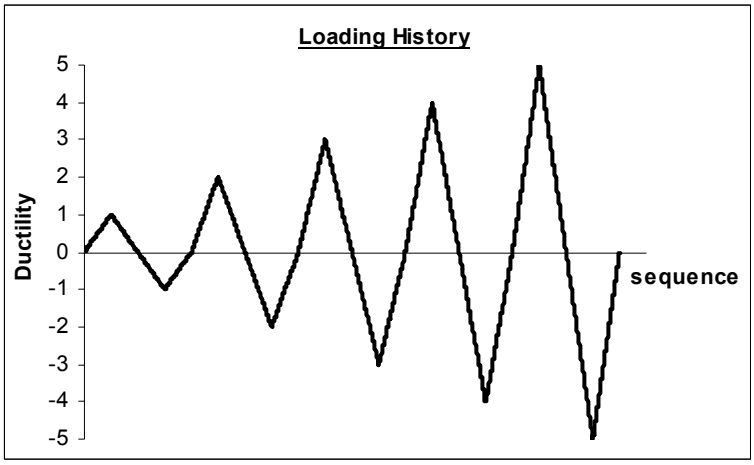


**Figure 3.3** Displacement loading history for the generation of hysteresis curves

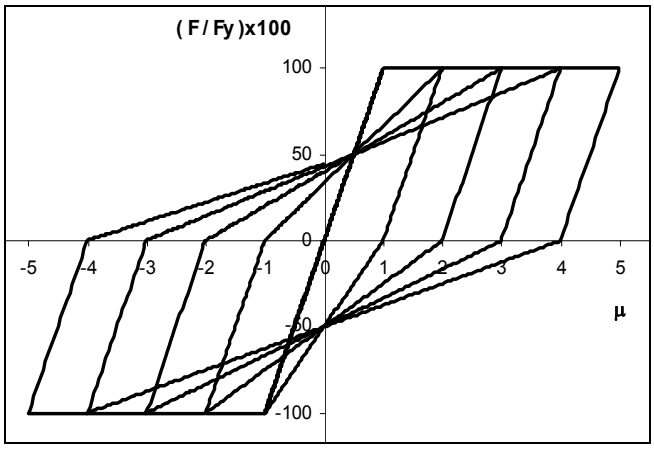


**Figure 3.4** Hysteresis model for non-degrading unloading stiffness

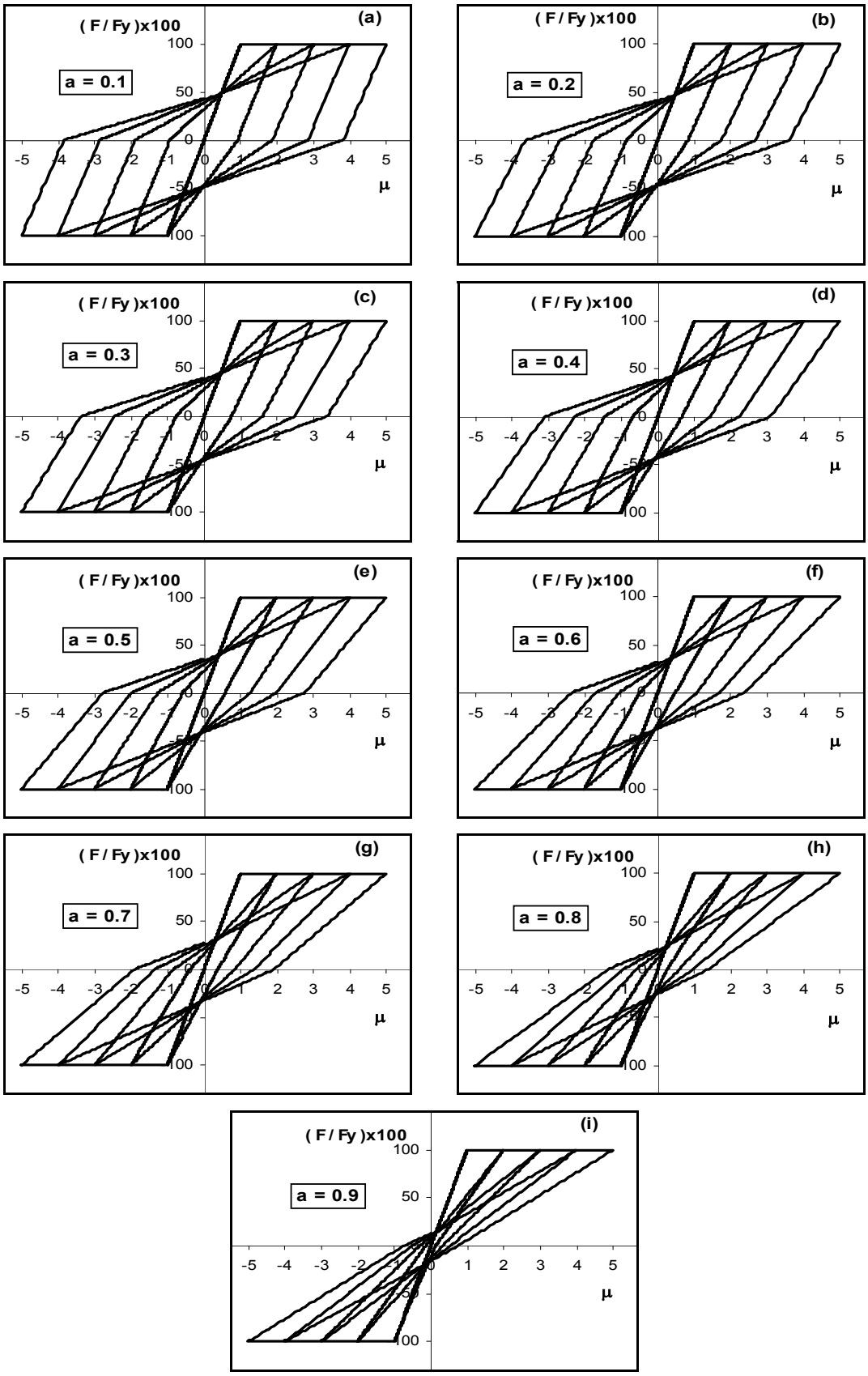


**Figure 3.5** Hysteresis models for ductility-based unloading stiffness rule

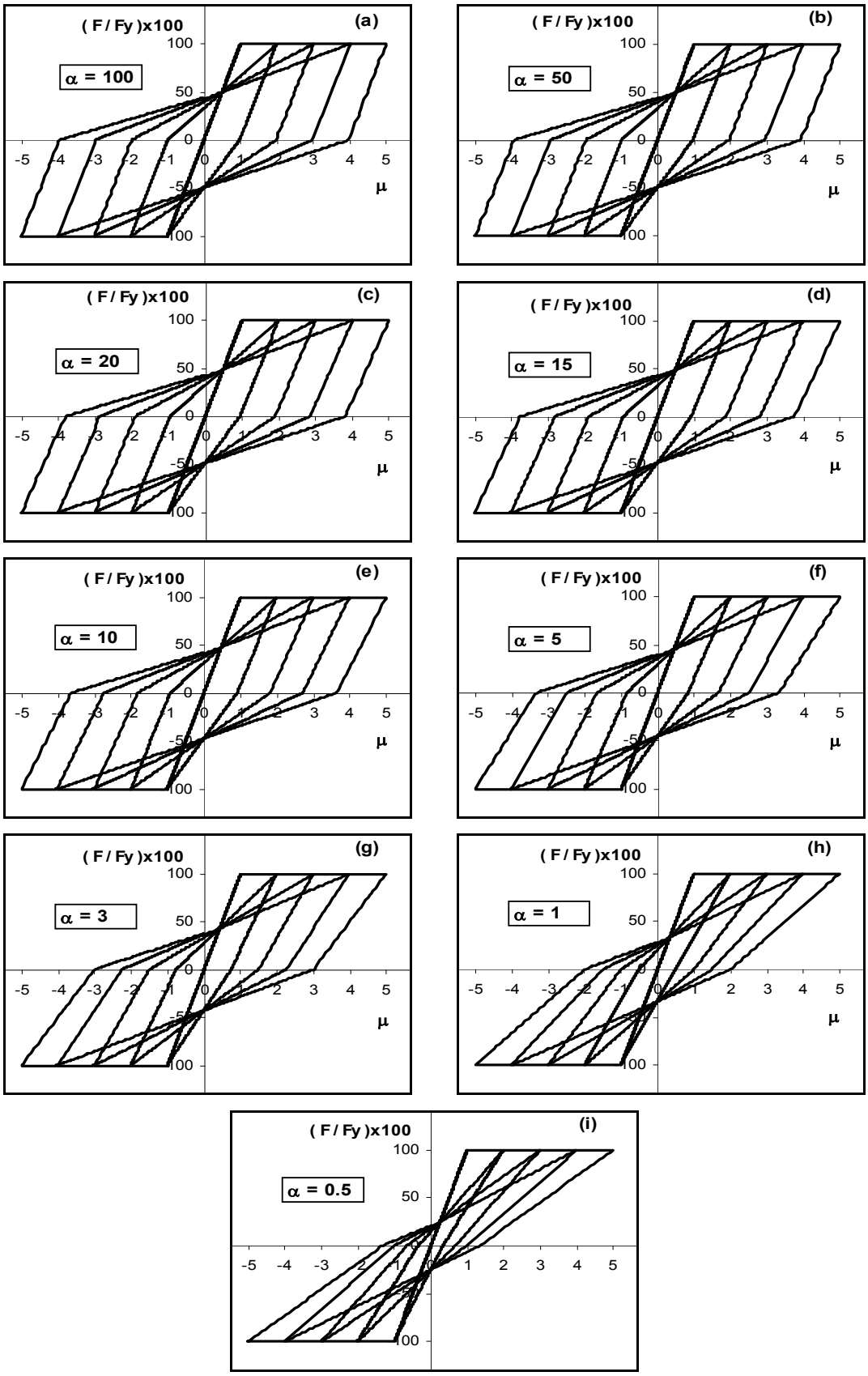


**Figure 3.6** Hysteresis models for focus-based unloading stiffness rule

The unloading stiffness decreases with increasing '$a$' for the ductility-based rule whereas decreases with decreasing '$\alpha$' for the focus-based rule. Nine values of the parameter '$a$' between 0.1 and 0.9 are selected for the ductility-based rule. For the focus-based rule, nine values of the parameter '$\alpha$' are selected for this study ranging from 0.5 to 100.

The dissipated energy per half-cycle and the cumulative dissipated energy values are tabulated for each force-displacement plot and can be seen in Tables 3.1 and Table 3.2. The dissipated energy values are unitless in this parametric study. The cumulative dissipated energy values (normalized by the corresponding dissipated energy value of the non-degrading model) are presented in Table 3.3. Similarities between the ductility-based and the focus based rules can be observed in Table 3.3. For example the ductility-based rule with $a$=0.8 is very similar to the focus-based model with $\alpha$=0.5 in terms of total dissipated energy and the slopes of unloading branches.

The values of the unloading stiffness and the deviation from the initial stiffness are presented in Tables 3.4 and 3.5. $K_0$ represents the initial stiffness value and $K_{un,1}$ to $K_{un,4}$ represent the unloading stiffness values of the hysteresis models in the positive direction. The deviation from the initial stiffness is calculated as follows;

$$Deviation \ \ (\%) = \frac{\left| K_{un} - K_0 \right|}{K_0} \times 100 \tag{3.3}$$

**Table 3.1** Dissipated energy per half-cycle and cumulative dissipated energy values for ductility-based rule

| **Half -cycle #** | **Dissipated energy per half-cycle** | | | | | | | | | |
|---|---|---|---|---|---|---|---|---|---|---|
| | **No degr.** | ***a*=0.1** | ***a*=0.2** | ***a*=0.3** | ***a*=0.4** | ***a*=0.5** | ***a*=0.6** | ***a*=0.7** | ***a*=0.8** | ***a*=0.9** |
| **1** | 0.0 | 0.0 | 0.0 | 0.0 | 0.0 | 0.0 | 0.0 | 0.0 | 0.0 | 0.0 |
| **2** | 0.0 | 0.0 | 0.0 | 0.0 | 0.0 | 0.0 | 0.0 | 0.0 | 0.0 | 0.0 |
| **3** | 100.0 | 96.0 | 92.1 | 88.0 | 83.6 | 78.8 | 73.7 | 68.3 | 62.5 | 56.2 |
| **4** | 150.0 | 142.9 | 135.2 | 127.0 | 118.1 | 108.7 | 98.5 | 87.6 | 75.9 | 63.4 |
| **5** | 200.0 | 190.7 | 180.4 | 169.0 | 156.5 | 142.7 | 127.6 | 110.9 | 92.5 | 72.3 |
| **6** | 250.0 | 238.5 | 225.5 | 211.1 | 194.9 | 176.9 | 156.8 | 134.3 | 109.2 | 81.2 |
| **7** | 300.0 | 286.9 | 271.9 | 254.8 | 235.4 | 213.5 | 188.5 | 160.2 | 128.1 | 91.5 |
| **8** | 350.0 | 335.3 | 318.2 | 298.6 | 276.0 | 250.1 | 220.4 | 186.2 | 146.9 | 101.8 |
| **9** | 400.0 | 384.0 | 365.2 | 343.3 | 317.9 | 288.3 | 253.9 | 213.9 | 167.3 | 113.1 |
| **10** | 450.0 | 432.7 | 412.2 | 388.1 | 359.7 | 326.5 | 287.5 | 241.6 | 187.7 | 124.4 |
| **Cumulative diss. energy** | **2200.0** | **2107** | **2000.7** | **1879.9** | **1742.1** | **1585.5** | **1406.9** | **1203.0** | **970.1** | **703.9** |

**Table 3.2** Dissipated energy per half-cycle and cumulative dissipated energy values for focus-based rule

| Half -cycle # | Dissipated energy per half-cycle | | | | | | | | | |
|---|---|---|---|---|---|---|---|---|---|---|
| | **No degr.** | **α=100** | **α=50** | **α=20** | **α=15** | **α=10** | **α=5** | **α=3** | **α=1** | **α=0.5** |
| **1** | 0.0 | 0.0 | 0.0 | 0.0 | 0.0 | 0.0 | 0.0 | 0.0 | 0.0 | 0.0 |
| **2** | 0.0 | 0.0 | 0.0 | 0.0 | 0.0 | 0.0 | 0.0 | 0.0 | 0.0 | 0.0 |
| **3** | 100.0 | 99.2 | 98.7 | 97.3 | 96.5 | 95.1 | 91.3 | 87.1 | 74.6 | 66.2 |
| **4** | 150.0 | 149.1 | 148.2 | 145.3 | 143.8 | 141.0 | 133.4 | 125.1 | 100.1 | 83.4 |
| **5** | 200.0 | 198.7 | 197.2 | 193.0 | 190.7 | 186.5 | 175.1 | 162.6 | 125.0 | 100.0 |
| **6** | 250.0 | 248.2 | 246.2 | 240.6 | 237.6 | 231.9 | 216.8 | 200.1 | 150.1 | 116.7 |
| **7** | 300.0 | 297.7 | 295.2 | 288.2 | 284.5 | 277.4 | 258.4 | 237.6 | 175.1 | 133.4 |
| **8** | 350.0 | 347.2 | 344.2 | 335.8 | 331.4 | 322.9 | 300.1 | 275.1 | 200.1 | 150.0 |
| **9** | 400.0 | 396.7 | 393.3 | 383.5 | 378.3 | 368.3 | 341.8 | 312.6 | 225.1 | 166.7 |
| **10** | 450.0 | 446.2 | 442.3 | 431.1 | 425.2 | 413.7 | 383.4 | 350.1 | 250.1 | 183.4 |
| **Cumulative diss. energy** | **2200.0** | **2183.0** | **2165.3** | **2114.8** | **2088.0** | **2036.8** | **1900.3** | **1750.3** | **1300.2** | **999.8** |

**Table 3.3** Comparison of the normalized cumulative dissipated energy of the hysteresis models

| **Unloading Stiffness Degradation Rule** | | **Normalized Cumulative Dissipated Energy** |
|---|---|---|
| None | | **100** |
| Ductility-based | $a = 0.1$ | 96 |
| Ductility-based | $a = 0.2$ | 91 |
| Ductility-based | $a = 0.3$ | 85 |
| Ductility-based | $a = 0.4$ | 79 |
| Ductility-based | $a = 0.5$ | 72 |
| Ductility-based | $a = 0.6$ | 64 |
| Ductility-based | $a = 0.7$ | 55 |
| Ductility-based | $a = 0.8$ | 44 |
| Ductility-based | $a = 0.9$ | 33 |
| Focus-based | $\alpha = 100$ | 99 |
| Focus-based | $\alpha = 50$ | 98 |
| Focus-based | $\alpha = 20$ | 96 |
| Focus-based | $\alpha = 15$ | 95 |
| Focus-based | $\alpha = 10$ | 93 |
| Focus-based | $\alpha = 5$ | 86 |
| Focus-based | $\alpha = 3$ | 80 |
| Focus-based | $\alpha = 1$ | 59 |
| Focus-based | $\alpha = 0.5$ | 45 |

**Table 3.4** Unloading stiffness values and deviation from the initial stiffness of the hysteresis models with ductility-based rule for positive direction of the loading

| **Unloading with initial stiffness** | | | **Unloading with ductility-based rule** | | |
|---|---|---|---|---|---|
| Unl. Stiff. Value | | Deviation from initial stiffness | ***a* = 0.1** Unl. Stiff. Value | | Deviation from initial stiffness |
| $K_0$ = | 100 | 0% | $K_0$ = | 100 | 0% |
| $K_{un,1}$= | 100 | 0% | $K_{un,1}$= | 88 | 12% |
| $K_{un,2}$= | 100 | 0% | $K_{un,2}$= | 85 | 15% |
| $K_{un,3}$= | 100 | 0% | $K_{un,3}$= | 83 | 17% |
| $K_{un,4}$= | 100 | 0% | $K_{un,4}$= | 79 | 21% |
| **Unloading with ductility-based rule** | | | **Unloading with ductility-based rule** | | |
| ***a* = 0.2** Unl. Stiff. Value | | Deviation from initial stiffness | ***a* = 0.3** Unl. Stiff. Value | | Deviation from initial stiffness |
| $K_0$ = | 100 | 0% | $K_0$ = | 100 | 0% |
| $K_{un,1}$= | 83 | 17% | $K_{un,1}$= | 79 | 21% |
| $K_{un,2}$= | 77 | 23% | $K_{un,2}$= | 69 | 31% |
| $K_{un,3}$= | 73 | 27% | $K_{un,3}$= | 64 | 36% |
| $K_{un,4}$= | 68 | 32% | $K_{un,4}$= | 58 | 42% |
| **Unloading with ductility-based rule** | | | **Unloading with ductility-based rule** | | |
| ***a* = 0.4** Unl. Stiff. Value | | Deviation from initial stiffness | ***a* = 0.5** Unl. Stiff. Value | | Deviation from initial stiffness |
| $K_0$ = | 100 | 0% | $K_0$ = | 100 | 0% |
| $K_{un,1}$= | 73 | 27% | $K_{un,1}$= | 70 | 30% |
| $K_{un,2}$= | 63 | 38% | $K_{un,2}$= | 54 | 46% |
| $K_{un,3}$= | 55 | 45% | $K_{un,3}$= | 49 | 51% |
| $K_{un,4}$= | 51 | 49% | $K_{un,4}$= | 43 | 57% |
| **Unloading with ductility-based rule** | | | **Unloading with ductility-based rule** | | |
| ***a* = 0.6** Unl. Stiff. Value | | Deviation from initial stiffness | ***a* = 0.7** Unl. Stiff. Value | | Deviation from initial stiffness |
| $K_0$ = | 100 | 0% | $K_0$ = | 100 | 0% |
| $K_{un,1}$= | 64 | 36% | $K_{un,1}$= | 59 | 41% |
| $K_{un,2}$= | 50 | 50% | $K_{un,2}$= | 45 | 55% |
| $K_{un,3}$= | 42 | 58% | $K_{un,3}$= | 36 | 64% |
| $K_{un,4}$= | 37 | 63% | $K_{un,4}$= | 31 | 69% |
| **Unloading with ductility-based rule** | | | **Unloading with ductility-based rule** | | |
| ***a* = 0.8** Unl. Stiff. Value | | Deviation from initial stiffness | ***a* = 0.9** Unl. Stiff. Value | | Deviation from initial stiffness |
| $K_0$ = | 100 | 0% | $K_0$ = | 100 | 0% |
| $K_{un,1}$= | 56 | 44% | $K_{un,1}$= | 53 | 47% |
| $K_{un,2}$= | 40 | 60% | $K_{un,2}$= | 36 | 64% |
| $K_{un,3}$= | 32 | 68% | $K_{un,3}$= | 28 | 72% |
| $K_{un,4}$= | 27 | 73% | $K_{un,4}$= | 23 | 77% |

**Table 3.5** Unloading stiffness values and deviation from the initial stiffness of the hysteresis models with focus-based rule for positive direction of the loading

| **Unloading with initial stiffness** | | | **Unloading with focus-based rule** | | |
|---|---|---|---|---|---|
| Unl. Stiff. Value | | Deviation from initial stiffness | **$\alpha$ = 100** Unl. Stiff. Value | | Deviation from initial stiffness |
| $K_0$ = | 100 | 0% | $K_0$ = | 100 | 0% |
| $K_{un,1}$= | 100 | 0% | $K_{un,1}$= | 93 | 7% |
| $K_{un,2}$= | 100 | 0% | $K_{un,2}$= | 89 | 11% |
| $K_{un,3}$= | 100 | 0% | $K_{un,3}$= | 91 | 9% |
| $K_{un,4}$= | 100 | 0% | $K_{un,4}$= | 90 | 10% |
| **Unloading with focus-based rule** | | | **Unloading with focus-based rule** | | |
| **$\alpha$ = 50** Unl. Stiff. Value | | Deviation from initial stiffness | **$\alpha$ = 20** Unl. Stiff. Value | | Deviation from initial stiffness |
| $K_0$ = | 100 | 0% | $K_0$ = | 100 | 0% |
| $K_{un,1}$= | 91 | 9% | $K_{un,1}$= | 90 | 10% |
| $K_{un,2}$= | 87 | 13% | $K_{un,2}$= | 85 | 15% |
| $K_{un,3}$= | 85 | 15% | $K_{un,3}$= | 80 | 20% |
| $K_{un,4}$= | 83 | 17% | $K_{un,4}$= | 79 | 21% |
| **Unloading with focus-based rule** | | | **Unloading with focus-based rule** | | |
| **$\alpha$ = 15** Unl. Stiff. Value | | Deviation from initial stiffness | **$\alpha$ = 10** Unl. Stiff. Value | | Deviation from initial stiffness |
| $K_0$ = | 100 | 0% | $K_0$ = | 100 | 0% |
| $K_{un,1}$= | 87 | 13% | $K_{un,1}$= | 87 | 13% |
| $K_{un,2}$= | 58 | 42% | $K_{un,2}$= | 77 | 23% |
| $K_{un,3}$= | 80 | 20% | $K_{un,3}$= | 75 | 25% |
| $K_{un,4}$= | 74 | 26% | $K_{un,4}$= | 66 | 34% |
| **Unloading with focus-based rule** | | | **Unloading with focus-based rule** | | |
| **$\alpha$ = 5** Unl. Stiff. Value | | Deviation from initial stiffness | **$\alpha$ = 3** Unl. Stiff. Value | | Deviation from initial stiffness |
| $K_0$ = | 100 | 0% | $K_0$ = | 100 | 0% |
| $K_{un,1}$= | 83 | 17% | $K_{un,1}$= | 77 | 23% |
| $K_{un,2}$= | 71 | 29% | $K_{un,2}$= | 65 | 35% |
| $K_{un,3}$= | 65 | 35% | $K_{un,3}$= | 54 | 46% |
| $K_{un,4}$= | 58 | 42% | $K_{un,4}$= | 49 | 51% |
| **Unloading with focus-based rule** | | | **Unloading with focus-based rule** | | |
| **$\alpha$ = 1** Unl. Stiff. Value | | Deviation from initial stiffness | **$\alpha$ = 0.5** Unl. Stiff. Value | | Deviation from initial stiffness |
| $K_0$ = | 100 | 0% | $K_0$ = | 100 | 0% |
| $K_{un,1}$= | 65 | 35% | $K_{un,1}$= | 58 | 42% |
| $K_{un,2}$= | 49 | 51% | $K_{un,2}$= | 41 | 59% |
| $K_{un,3}$= | 38 | 62% | $K_{un,3}$= | 32 | 68% |
| $K_{un,4}$= | 32 | 68% | $K_{un,4}$= | 27 | 73% |

Based on Figures 3.4-3.6 and Tables 3.1-3.5, the following trends are observed in accordance with the selected values for parameters $a$ and $\alpha$:

As it can be observed from the Figures 3.5.a to 3.5.i, noticeable degradation starts when '$a$' is equal to 0.4. The deviation of unloading stiffness from the initial stiffness reaches up to nearly 50 % for the last cycle in this case. Cumulative hysteretic energy dissipated when '$a$' is equal to 0.4 is 79 % of the energy dissipated for the non-degrading case. For the most extreme case when '$a$' is equal to 0.9, the deviation becomes very significant with 77 % in the last cycle and the total energy dissipation is only 33 % of the non-degrading case. As mentioned before, values of 0.4 & 0.5 has generally been used for the ductility-based parameter '$a$' in the literature in order to represent the unloading stiffness characteristics of typical RC structural members.

As it can be observed from the Figures 3.6.a to 3.6.c, the '$\alpha$' values of 100, 50, 20, 15 and 10 is almost identical to the non-degrading case. The noticeable degradation starts when '$\alpha$' is equal to 5 (Figure 3.6.f). The deviation of unloading stiffness is 42 % for the last cycle. Total hysteretic energy dissipated in this case is 86 % of the energy dissipated for the non-degrading case. It should also be noted that IDARC recommended the values of 15, 10 and 4 for mild, moderate and severe degrading behavior of RC members, respectively. However the results obtained from the parametric study reveal that the energy dissipation characteristics of the hysteretic response when $\alpha$=15 and $\alpha$=10 are very close to each other so that it is difficult to make any distinction between mild and moderate behavior. Furthermore when $\alpha$=4, total hysteretic energy dissipated is approximately 83 % of the corresponding dissipated energy for the non-degrading behavior. Hence this value seems to be a poor representative of severe degrading behavior for RC structural members.

### 3.4 The Calibration of Unloading Stiffness Parameters Using Cyclic Test Data

The parameters of the ductility-based and the focus-based unloading stiffness rules are calibrated by using the RC column cyclic test results from PEER database. The procedure for the determination of the parameters is explained in this section. But first of all, the selection of the experimental data, which is to be employed in the calibration study, from the column database is discussed.

There exist 196 cyclic tests which were classified in three groups according to their hysteretic energy dissipation characteristics. However, unloading stiffness characteristics in the hysteretic behavior of the columns are also different from each other in terms of the shape of the unloading branch. There exist experimental data with linear, bilinear and curved unloading stiffness branches as seen in Figure 3.7.

The force-displacement relationships that have a linear type of unloading branch are suitable for the calibration of parameters in the aforementioned unloading rules due to the fact that these rules considers the unloading branches as linear. Bilinear unloading branches which can only be defined by two line segments and the curved unloading branches that can not be modeled by curved lines are not considered in this study. Therefore the columns that have linear unloading stiffness branches are extracted from the complete database. Table 3.6 presents the numbers and percentages of experimental data for each member group, in which the unloading stiffness can be analytically modeled by using linear, bilinear or curved branches. The figures indicate that in majority of the experimental data (70 %), the unloading stiffness can be modeled by using a single line segment. The percentage of experimental data for which it is not accurate to model the unloading branch by line segment(s) is very small (2 %). Hence 20 cyclic tests are selected from each member group, with the potential of fitting a linear unloading branch in order to calibrate the parameters for ductility-based and focus-based rules. This makes a total of 60 cyclic tests to be used in the calibration of the unloading stiffness

parameters for different classes of hysteretic behavior in terms of energy dissipation characteristics.

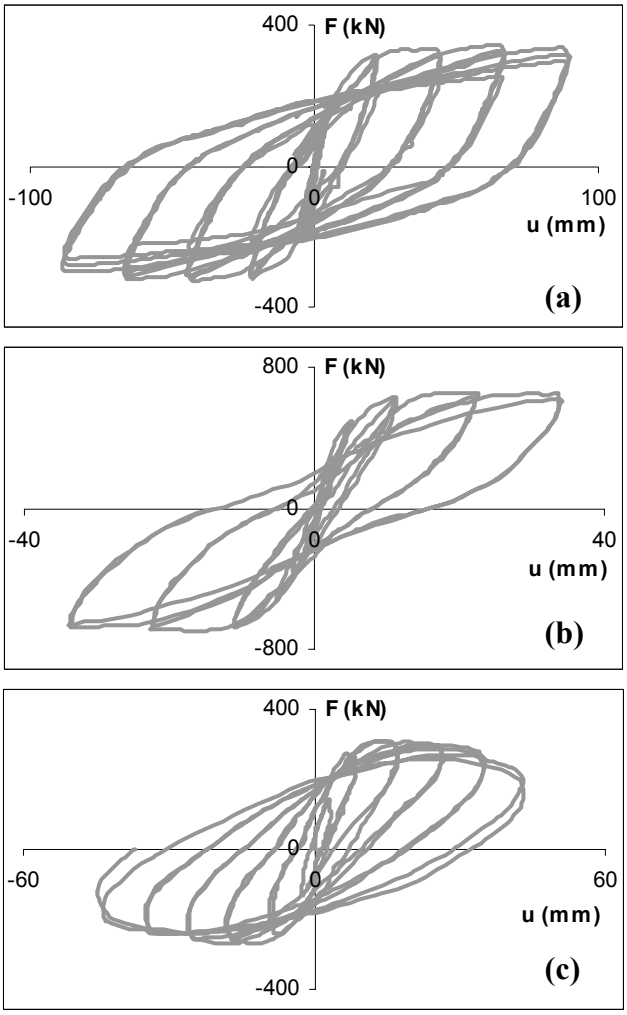


**Figure 3.7** Unloading stiffness types; a) linear b) bilinear c) curved

**Table 3.6** Number and percentage of the experimental data in each group in terms of unloading stiffness branch modeling options

| RC member classification | Total # of cyclic test data | Suitable modeling option for unloading stiffness branch | | |
|---|---|---|---|---|
| | | Linear | Bilinear | Curved |
| Group A | 41 | 27 (*66* %) | 11 (*27* %) | 3 (*7* %) |
| Group B | 81 | 44 (*54* %) | 35 (*43* %) | 2 (*3* %) |
| Group C | 74 | 66 (*89* %) | 8 (*11* %) | - (*0* %) |
| Total | 196 | 137 (*70* %) | 54 (*28* %) | 5 (*2* %) |

After the selection of the cyclic tests that are to be used for the calibration of the parameters for the ductility-based and the focus-based unloading rule, the values of the initial stiffness and unloading stiffness are calculated. For this purpose, imaginary lines are drawn along the unloading branches of the experimental force-displacement data and the slopes of these lines are calculated from simple geometry. Only positive directions (the direction where the first yielding takes place) of the force-displacement relationships are taken into account because the stiffness degradation characteristics of the columns do not differ much in the other direction. After the determination of the unloading slopes, the unloading parameters are calculated. The parameter '*a*' of the ductility-based rule is obtained from

$$a_i = \frac{\ln\left(K_{un,i} / K_0\right)}{\ln\left(u_y / u_{m,i}\right)} \tag{3.4}$$

where

$a_i$: Ductility-based parameter for the $i^{th}$ unloading branch

$K_{un,i}$: Unloading stiffness value of the $i^{th}$ positive half cycle

$K_0$: Initial (elastic) stiffness

$u_y$: Yield displacement in the positive direction

$u_{m,i}$: Top displacement coordinate on the $i^{th}$ unloading line

The parameter '$\alpha$' of the focus-based rule is calculated from

$$\alpha_i = \frac{F_{m,i} - u_{m,i} K_{un,i}}{u_y K_{un,i} - F_y} \tag{3.5}$$

where

$\alpha_i$: Focus-based parameter for the $i^{th}$ unloading branch
$F_{m,i}$: Top force coordinate on the $i^{th}$ unloading line
$F_y$: Yield force in the positive direction

Also, the deviation from the initial stiffness (Eq.3.3) for each unloading branch is calculated.

After the determination of the unloading stiffness parameters and the amount of deviation from initial stiffness for each unloading branch of the force-displacement relationship of the considered column specimen, the statistical properties such as mean, standard deviation and coefficient of variation (COV) are computed. As a result, the obtained mean value of the unloading parameters can be considered as the representative of that cyclic test, but also accounting for the variability in terms of COV. The number of unloading branches which are represented by a single imaginary line for the calculation of the slopes is also taken into consideration when calculating the statistical descriptors.

An example of this procedure is illustrated in Figure 3.8. This is the force-displacement relationship of the cyclic test conducted by Park and Paulay (1990). The dashed lines are the imaginary lines that represent the unloading stiffness branches. Initial stiffness is calculated from the first segment of the continuous line which is the envelope of the force-displacement relationship. In Table 3.7, the calculated initial and unloading stiffness values, the unloading parameters and deviations from initial stiffness for each unloading branch for the same cyclic test is presented. The statistical descriptors are displayed at the bottom

of the table. Considering the eight unloading branches in the positive loading direction, the mean values for the parameters '$a$' and '$\alpha$' that characterize the considered cyclic tests are calculated as 0.47 and 2.8, respectively. The COV values are also tabulated as 0.26 and 0.50. Furthermore, the idealized unloading branches in this cyclic test seem to deviate 46 % on the average from the initial stiffness. Similar tables have been generated for the other cyclic tests considered in Groups A-C and they are presented in Appendix B (Table B.1 - B.60)

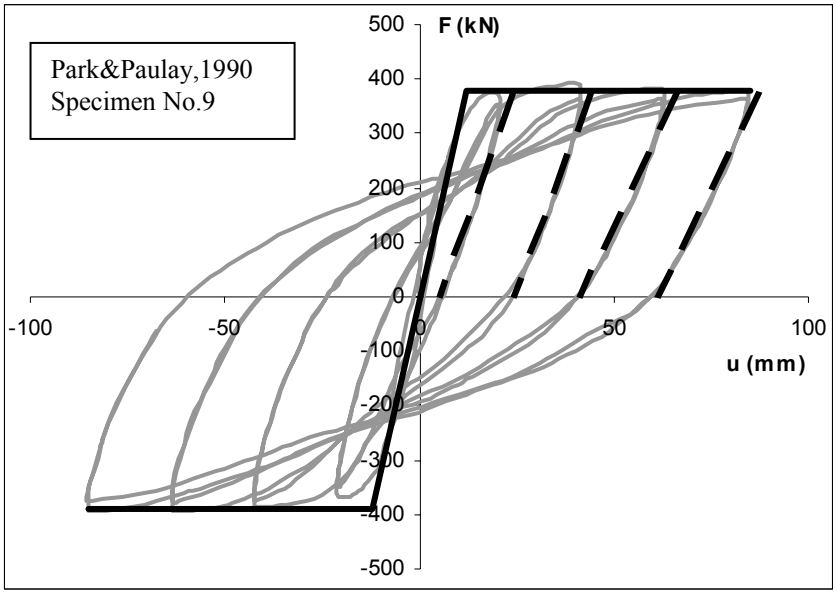


**Figure 3.8** Example plot for the determination of the unloading stiffness parameter values of a cyclic lateral load column test result

The procedure explained above is repeated for the selected 60 cyclic tests and the results are presented in Tables 3.8 - 3.10 for RC member groups A-C, respectively.

**Table 3.7** Unloading stiffness properties of the sample test in Figure 3.8

| **Test ID** | | | **number of occurrence** | **Ductility based** | **Focus based** | **Deviation from initial stiffness (%)** |
|---|---|---|---|---|---|---|
| **Park & Paulay 1990, Specimen 9** | | | | **Parameter '*a*'** | **Parameter 'α'** | |
| Initial | $K_0$ = | 31.67 | - | - | - | - |
| unloading | $K_{un,1}$= | 20.00 | 2 | 0.66 | 0.7 | 36.8 |
| | $K_{un,2}$= | 19.00 | 2 | 0.39 | 3.0 | 40.0 |
| | $K_{un,3}$= | 15.20 | 2 | 0.43 | 3.2 | 52.0 |
| | $K_{un,4}$= | 14.62 | 2 | 0.39 | 4.4 | 53.8 |
| *K* values are in kN/mm. | | | **μ =** | **0.47** | **2.8** | **45.7** |
| | | | **σ =** | 0.12 | 1.4 | 7.9 |
| | | | **cov =** | 0.26 | 0.5 | 0.2 |

**Table 3.8** The result list for unloading stiffness properties (Group-A members)

| **No.** | **Test Specimen ID** | ***a*** | **α** | **Dev. %** |
|---|---|---|---|---|
| **1** | Saatcioglu and Ozcebe 1989, U6 | 0.13 | 14.2 | 11.1 |
| **2** | Ohno and Nishioka 1984, L2 | 0.35 | 4.8 | 44.1 |
| **3** | Galeota et al. 1996, BB | 0.58 | 1.4 | 47.8 |
| **4** | Gill et al. 1979, No. 3 | 0.71 | 1.2 | 49.6 |
| **5** | Galeota et al. 1996, CB3 | 0.52 | 2.9 | 57.8 |
| **6** | Galeota et al. 1996, BB4 | 0.56 | 1.7 | 50.3 |
| **7** | Bechtoula 2002, L1N6B | 0.80 | 0.7 | 53.4 |
| **8** | Galeota et al. 1996, CB1 | 0.48 | 2.5 | 42.1 |
| **9** | Thomsen and Wallace 1994, B1 | 0.20 | 8.7 | 16.4 |
| **10** | Galeota et al. 1996, CB4 | 0.60 | 1.6 | 51.5 |
| **11** | Park and Paulay 1990, No. 9 | 0.47 | 2.8 | 45.7 |
| **12** | Atalay and Penzien 1975, No. 4S1 | 0.37 | 2.7 | 24.2 |
| **13** | Bechtoula 2002, L1N60 | 0.74 | 0.6 | 54.2 |
| **14** | Galeota et al. 1996, BB4B | 0.57 | 1.7 | 49.0 |
| **15** | Sugano 1996, UC15H | 0.65 | 1.0 | 48.2 |
| **16** | Galeota et al. 1996, CB2 | 0.54 | 2.0 | 51.0 |
| **17** | Soesianawati et al. 1986, No. 1 | 0.58 | 2.2 | 58.9 |
| **18** | Sugano 1996, UC10H | 0.62 | 1.1 | 40.2 |
| **19** | Tanaka and Park 1990, No. 1 | 0.63 | 1.6 | 58.9 |
| **20** | Watson and Park 1989, No. 5 | 1.00 | 0.6 | 62.4 |
| | **Mean** | **0.55** | **2.80** | **45.85** |
| | **Standard Deviation** | 0.20 | 3.25 | 13.75 |

**Table 3.9** The result list for unloading stiffness properties (Group-B members)

| No. | Test Specimen ID | *a* | α | Dev. % |
|---|---|---|---|---|
| **1** | Ohno and Nishioka 1984, L3 | 0.43 | 3.0 | 47.3 |
| **2** | Tanaka and Park 1990, No. 2 | 0.67 | 1.4 | 63.8 |
| **3** | Atalay and Penzien 1975, No. 9 | 0.69 | 1.7 | 52.5 |
| **4** | Wight and Sozen No. 40.147w | 0.48 | 2.5 | 52.1 |
| **5** | Ang et al. 1981, No. 4 | 0.73 | 1.2 | 59.2 |
| **6** | Tanaka and Park 1990, No. 6 | 0.60 | 1.8 | 58.5 |
| **7** | Pujol 2002, No. 10-3-1.5S | 0.45 | 2.8 | 47.1 |
| **8** | Wehbe et al. 1998, B2 | 0.88 | 1.2 | 50.4 |
| **9** | Azizinamini et al. 1988, NC-2 | 0.63 | 1.8 | 53.2 |
| **10** | Xiao and Martir. ., .8L19-.0.2P | 0.75 | 1.2 | 60.9 |
| **11** | Atalay and Penzien 1975, No. 3S1 | 0.73 | 0.8 | 50.7 |
| **12** | Zahn et al. 1986, No. 7 | 0.79 | 1.0 | 73.4 |
| **13** | Matamoros et al. 1999,C10-10S | 0.75 | 1.1 | 62.5 |
| **14** | Paultre and Legeron,.No. 1006015 | 0.67 | 1.7 | 69.1 |
| **15** | Atalay and Penzien 1975, No. 2S1 | 0.65 | 1.2 | 41.6 |
| **16** | Watson and Park 1989, No. 6 | 0.86 | 0.5 | 56.5 |
| **17** | Galeota et al. 1996, CA2 | 0.73 | 1.5 | 64.1 |
| **18** | Kanda et al. 1988, 85STC-1 | 0.63 | 1.5 | 61.6 |
| **19** | Pujol 2002, No. 20-3-3N | 0.75 | 1.1 | 59.6 |
| **20** | Atalay and Penzien 1975, No. 1S1 | 0.64 | 1.1 | 36.6 |
| | **Mean** | **0.68** | **1.50** | **56.03** |
| | **Standard Deviation** | 0.12 | 0.63 | 9.07 |

**Table 3.10** The result list for unloading stiffness properties (Group-C members)

| No. | Test Specimen ID | *a* | α | Dev. % |
|---|---|---|---|---|
| **1** | Bayrak and Sheikh 1996, AS-2HT | 0.89 | 0.7 | 82.9 |
| **2** | Bayrak and Sheikh 1996, AS-6HT | 0.83 | 0.9 | 71.3 |
| **3** | Matamoros et al. 1999,C5-00N | 0.42 | 3.1 | 39.2 |
| **4** | Matamoros et al. 1999,C10-05S | 0.67 | 1.5 | 56.6 |
| **5** | Paultre and Legeron. No. 1006025 | 0.78 | 1.4 | 73.7 |
| **6** | Muguruma et al. 1989, BH-2 | 0.78 | 0.8 | 70.6 |
| **7** | Muguruma et al. 1989, AH-1 | 0.79 | 0.8 | 75.7 |
| **8** | Paultre and Legeron. No. 1006040 | 0.81 | 1.0 | 68.7 |
| **9** | Paultre et al., 2001, No. 1005540 | 0.81 | 0.9 | 70.2 |
| **10** | Wehbe et al. 1998, A2 | 0.96 | 0.8 | 62.8 |
| **11** | Azizinamini et al. 1988, NC-4 | 0.75 | 0.9 | 60.2 |
| **12** | Muguruma et al. 1989, BH-1 | 0.83 | 0.6 | 71.2 |

**Table 3.10** (cont'd)

| | | | | |
|---|---|---|---|---|
| **13** | Paultre et al., 2001, No. 806040 | 0.80 | 0.8 | 79.9 |
| **14** | Tanaka and Park 1990, No. 7 | 0.81 | 0.8 | 73.4 |
| **15** | Atalay and Penzien 1975, No. 6S1 | 0.85 | 0.6 | 56.5 |
| **16** | Matamoros et al. 1999,C5-40N | 0.84 | 0.6 | 59.7 |
| **17** | Bayrak and Sheikh 1996, AS-5HT | 0.90 | 0.8 | 73.7 |
| **18** | Matamoros et al. 1999,C10-20N | 0.99 | 0.3 | 70.7 |
| **19** | Bayrak and Sheikh 1996, ES-1HT | 0.82 | 0.6 | 71.1 |
| **20** | Paultre and Legeron,.No.10013025 | 0.98 | 0.6 | 69.2 |
| | **Mean** | **0.82** | **0.92** | **67.87** |
| | **Standard Deviation** | 0.12 | 0.59 | 9.79 |

The mean value of the ductility-based parameter, '*a*' increases shifting from column group A to C. This is an expected trend in terms of the relationship between the unloading stiffness and the energy dissipation characteristics. Increasing '*a*' means decreasing unloading stiffness and the decreasing unloading stiffness leads reduction in the amount of energy dissipation capability of the system. On the other hand, the mean value of the focus-based unloading parameter '$\alpha$' decreases with the deteriorating column behavior. This also confirms with the aforementioned trend because decreasing '$\alpha$' indicates reduction in unloading stiffness. This trend can also be easily observed and verified as the degradation in stiffness becomes more prominent with deteriorating column behavior.

Considering the COV values of parameters '*a*' and '$\alpha$' in Tables B.1 – B.60 (Appendix B), it can be stated that ductility based rule is a better candidate to be used for analytical modeling of unloading stiffness degradation. The COV values for parameter '*a*' are much more smaller when compared to the COV values of parameter '$\alpha$' in most of the cyclic tests.

Another important observation based on the results is that there is a discrepancy between the recommended values of the parameters in the literature and the calculated values of the parameters in each member group. Noting that the values

of 0.4 and 0.5 have been commonly used in the previous studies for parameter '$a$', the mean values of Groups A, B and C are 0.55, 0.68 and 0.82, respectively. The recommended values of parameter '$a$' are only close to the mean value obtained for Group A, that represents RC members with good performance under cyclic loading. This indicates that the values recommended in the literature are generally based on code confirming structural members and higher values of parameter '$a$' should be used when considering RC members which exhibit moderate-to-severe degradation under cyclic loading. The discrepancy is much more pronounced for the focus-based parameter '$\alpha$'. While the recommended value for severe degradation is $\alpha$=4.0, the mean calculated value for RC column group with no or slight degradation (Group A) is 2.80 whereas the mean value for RC column group with severe degradation reduces to 0.92. This reveals the fact that the recommended values are far from representing the actual behavior of RC columns under cyclic loading. The same trend was also observed during the parametric study in Section 3.3.

As a result, if degradation is prominent in the cyclic behavior of a RC member, the recommended values for unloading stiffness degradation parameters are unable to represent the actual behavior and they should be used with great attention. However it should also be pointed out that the results are based on the limited data from 60 different cyclic tests gathered in three groups.

The correlations between parameters are also examined and presented in Figures 3.9-3.12. The parameters of the ductility-based unloading rule and focus-based unloading rule have a good correlation with a coefficient of determination ($R^2$) of 0.90 (Figure 3.9). Figures 3.10 and 3.11 show the relation between the deviation of unloading stiffness from initial stiffness and the unloading parameters '$a$' and '$\alpha$'. It is clearly seen from these figures that, increasing '$a$' results in increasing degradation in unloading stiffness. On the contrary, increasing '$\alpha$' means that the deviation from initial stiffness decreases. These figures indicate that the softening of the structural member in terms of unloading stiffness can be

estimated with a certain degree of uncertainty if the ductility-based or focus-based rules are employed during the analytical simulation of cyclic column tests.

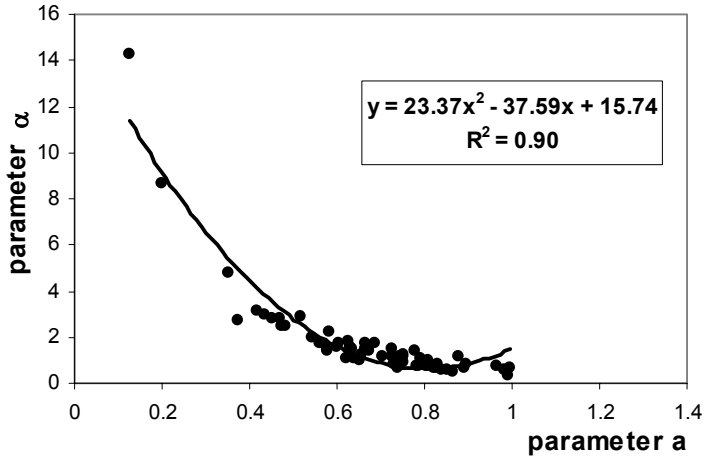


**Figure 3.9** Correlation between ductility-based parameter '*a*' and focus-based parameter '$\alpha$'

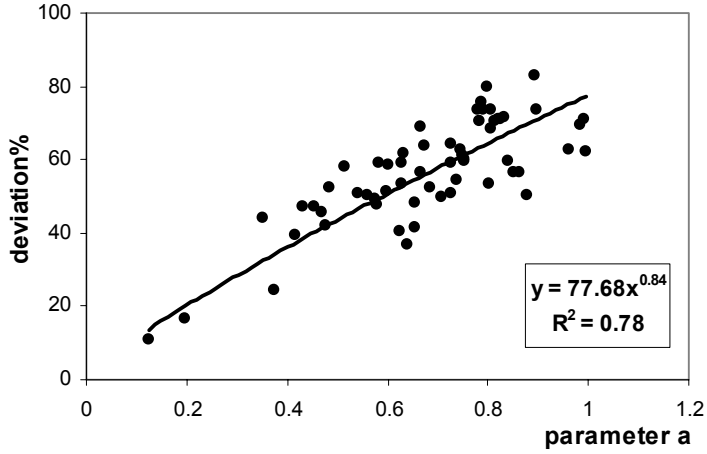


**Figure 3.10** Correlation between ductility-based parameter '*a*' and deviation from initial stiffness

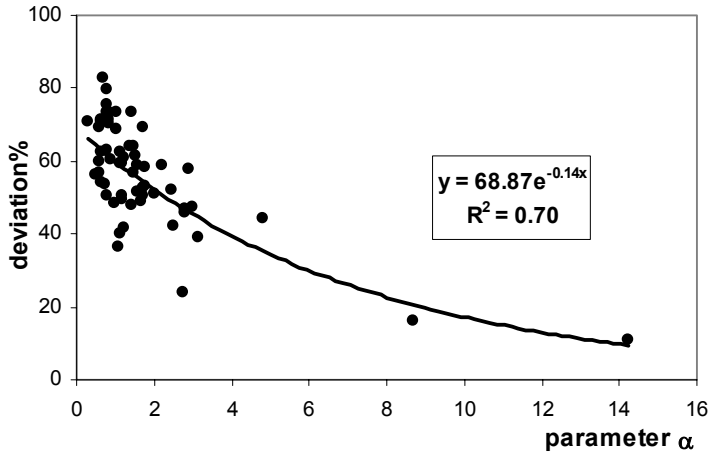


**Figure 3.11** Correlation between focus-based parameter '$\alpha$' and deviation from initial stiffness

In Figure 3.12, trend between the amount of deviation from initial stiffness and displacement ductility can be observed. As mentioned before, the degradation in the stiffness of RC members increases with increasing ductility levels. The cyclic test results verify this trend.

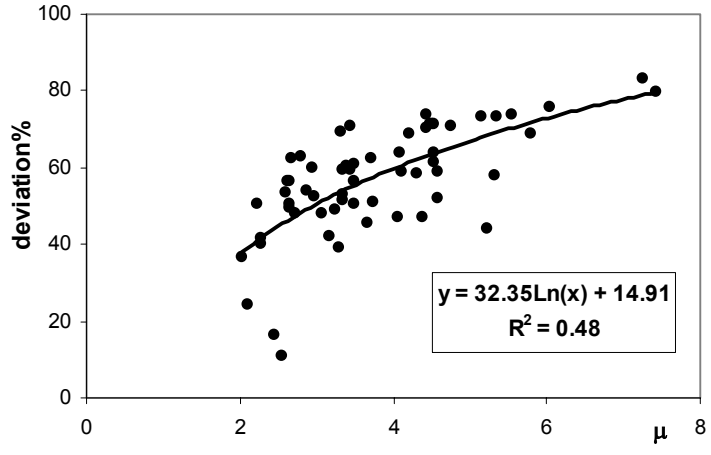


**Figure 3.12** Correlation between ductility level and deviation from initial stiffness

# CHAPTER 4

# STRENGTH DEGRADATION

## 4.1 General

Strength degradation in RC structural members under cyclic loads is a great concern for engineers. The loss of lateral strength can cause instability of the structural system and results in failure. Strength degradation is mainly history dependent and degradation usually increases with increasing number of load cycles. This is an indication of the phenomenon called low-cycle fatigue. Therefore, strength degradation is usually taken into consideration during the development of hysteresis models.

In this chapter, the strength degradation behavior of RC members during hysteretic response is investigated in two parts: cyclic (cinematic) strength degradation and in-cycle (post-capping) strength degradation. Cyclic strength degradation is related with low-cycle fatigue damage of various components in the system. On the other hand, in-cycle strength degradation may occur due to the component damage as deformations increase monotonically (FEMA 440).

PEER column database is used for the investigation of the strength degradation properties of the RC members. First, the parameters of the two strength degradation formulas (linear and exponential) are determined for the selected columns in the database. Second, in-cycle strength degradation properties such as post-yield and post-capping lateral stiffness, deformation level of the capping point and residual strength ratio are investigated for the selected columns in PEER database.

## 4.2 Types of Strength Degradation

The detailed definitions of the strength degradation types and the related parameters are presented in this section.

### 4.2.1 Cyclic Strength Degradation

Cyclic strength degradation is defined by FEMA 440 as the lateral strength loss by the number of load cycles increases. However, the structural member maintains its strength during a load cycle. Figure 4.1 presents a force-displacement relationship example for the cyclic strength degradation. Second half-cycle in the positive direction can not reach the strength capacity of the first half-cycle and a strength loss ($\Delta F$) occurs. The strength degradation at constant displacement amplitude continues with subsequent cycles.

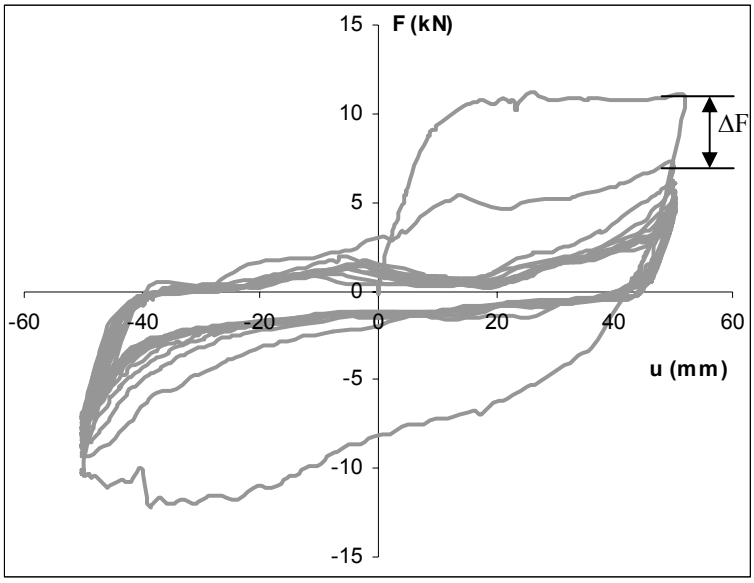


**Figure 4.1** Definition of cyclic strength degradation

Also, it can be observed from Figure 4.1 that, the amount of strength deterioration is different for positive and negative directions of loading for the same member. Therefore, both directions of loading are taken into account while calculating the strength degradation parameters in this study.

Two types of strength degradation approaches are employed for cyclic strength degradation: linear (uniform) and exponential strength degradation. The strength degradation in linear case can be expressed as

$$\Delta F_i = C F_y \left( u_{mi} / u_y \right) N \tag{4.1}$$

where $\Delta F_i$ is the strength degradation of the $i^{th}$ cycle, $C$ is the strength degradation parameter, $F_y$ is the yield strength, $u_{mi}$ is the maximum displacement of the $i^{th}$ cycle, $u_y$ is the yield displacement and $N$ is the number of cycles at the same displacement amplitude. Linear formulation for strength degradation gives same amount of degradation between load cycles if the deformation levels are constant (i.e. $u_m$ is constant).

However, the strength degradation is not usually linear. Experimental results show that in the first few cycles, strength degrades more rapidly and then strength becomes nearly stabilized at a constant level. The positive loading direction of the force-displacement relationship shown in Figure 4.1 is an example for this case. The exponential formulation for the cyclic strength degradation of this type (severe-to-gradual type) is

$$\Delta F_i = A F_y \left( 1 - e^{-B N \left( u_{mi} / u_y \right)} \right) \tag{4.2}$$

where '$A$' and '$B$' are strength degradation parameters. Parameter '$A$' is related with the degree of degradation and parameter '$B$' is related with the rate of

degradation. On the other hand, there are some cases where most of the strength degradation takes place just before the failure of the member. In this case the amount of strength degradation for the first few cycles is small (Figure 4.2). The exponential formula for the cyclic strength degradation of this type (gradual-to-severe type) is

$$\Delta F_i = S\, F_y \left( e^{K\, N \left( u_{mi} / u_y \right)} - 1 \right) \tag{4.3}$$

where '*S*' and '*K*' are strength degradation parameters. Parameter '*S*' is related with the degree of degradation and parameter '*K*' is related with the rate of degradation.

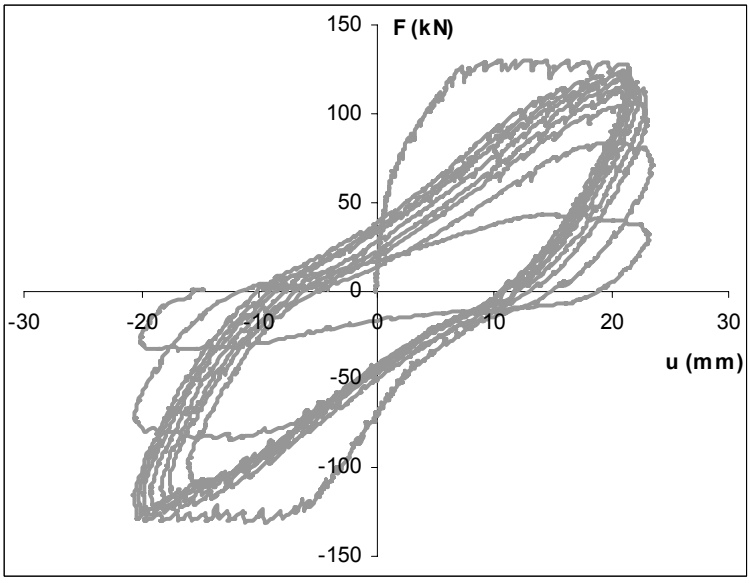


**Figure 4.2** Example plot for cyclic strength degradation (gradual-to-severe type)

#### 4.2.1.1 Parametric Study for Cyclic Strength Degradation

In this part of the study, a set of parameters of cyclic strength degradation formulas are selected and corresponding hysteresis models are generated. The computer program INSPEC (Erberik, 2001) is used for this purpose. The aim of this parametric study is to compare the strength degradation amounts and rates as well as the dissipated hysteretic energy values of various hysteresis models with linear and exponential type of cyclic strength degradation. Degradation in unloading stiffness and pinching behavior is not considered in this parametric study.

The selected strength degradation parameters (parameter *C*) for linear case are 0.0050, 0.0075, 0.0100, 0.0125, 0.0150, 0.0175 and 0.0200. For the exponential cyclic strength degradation, only "severe-to-gradual" type is considered and the selected pair of parameters (parameters *A* and *B*) are (0.25,0.05), (0.25,0.15), (0.25,0.25), (0.50,0.05), (0.50,0.15), (0.50,0.25), (0.75,0.05), (0.75,0.15) and (0.75,0.25). The loading history which is selected as constant amplitude in order to simulate cyclic strength degradation more clearly is composed of 10 cycles with a ductility level of 4.0 (Figure 4.3).

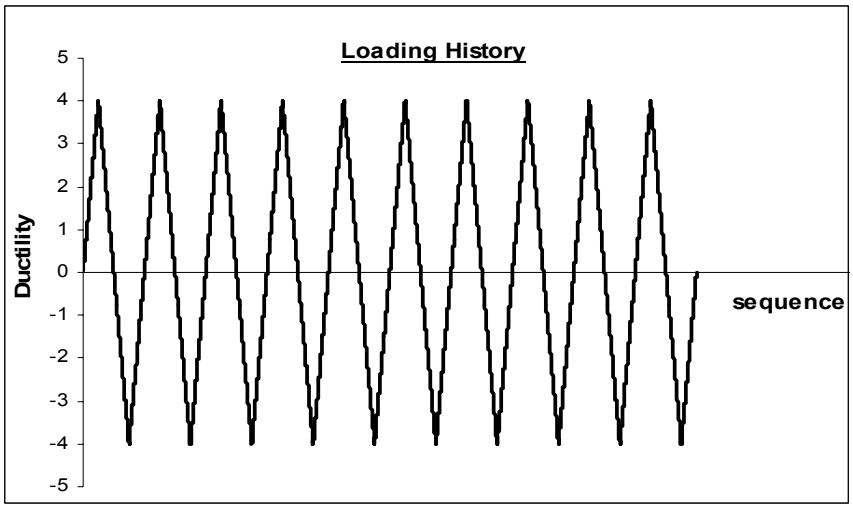


**Figure 4.3** Displacement loading history for the generation of hysteresis curves

The force-displacement relationship for the non-degrading strength case is illustrated in Figure 4.4.

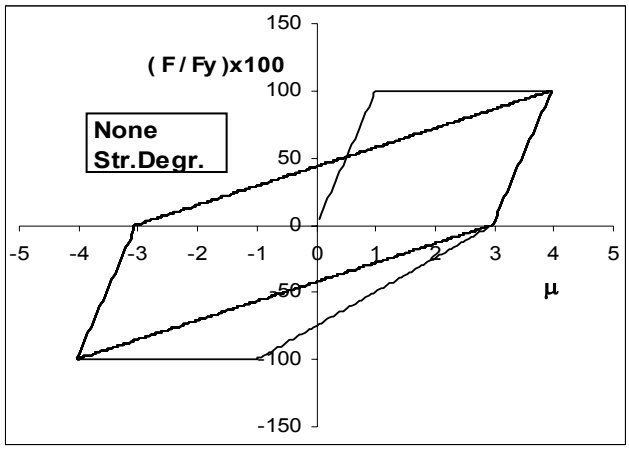


**Figure 4.4** Hysteresis model for non-degrading lateral strength

The generated force-displacement relationships of cyclic strength degradation of linear type and exponential type are presented in Figure 4.5 and Figure 4.6, respectively. The strength capacity values at the end of each cycle (positive direction) of the generated hysteresis models are presented in Tables 4.1 and 4.2.

As it can be observed from Figure 4.5 and Table 4.1, the degradation in strength is uniform and the amount of degradation increases with increasing value of parameter '*C*'. Since the ductility term, $u_m/u_y$, and the yield strength, $F_y$, is constant for this study, '*C*' is the only parameter that affects the amount of strength degradation. For the exponential cyclic strength degradation case, as it can be observed from Figure 4.6 and Table 4.2, parameter '*A*' is related with the degree of degradation and parameter '*B*' is related with the rate of degradation. Hysteresis models having the same value of parameter '*A*' experience almost the same amount of capacity loss at the end of the cyclic loading. However, among these models, the one which has a larger value of parameter '*B*' degrades more rapidly and a few cycles are sufficient for losing all the strength capacity.

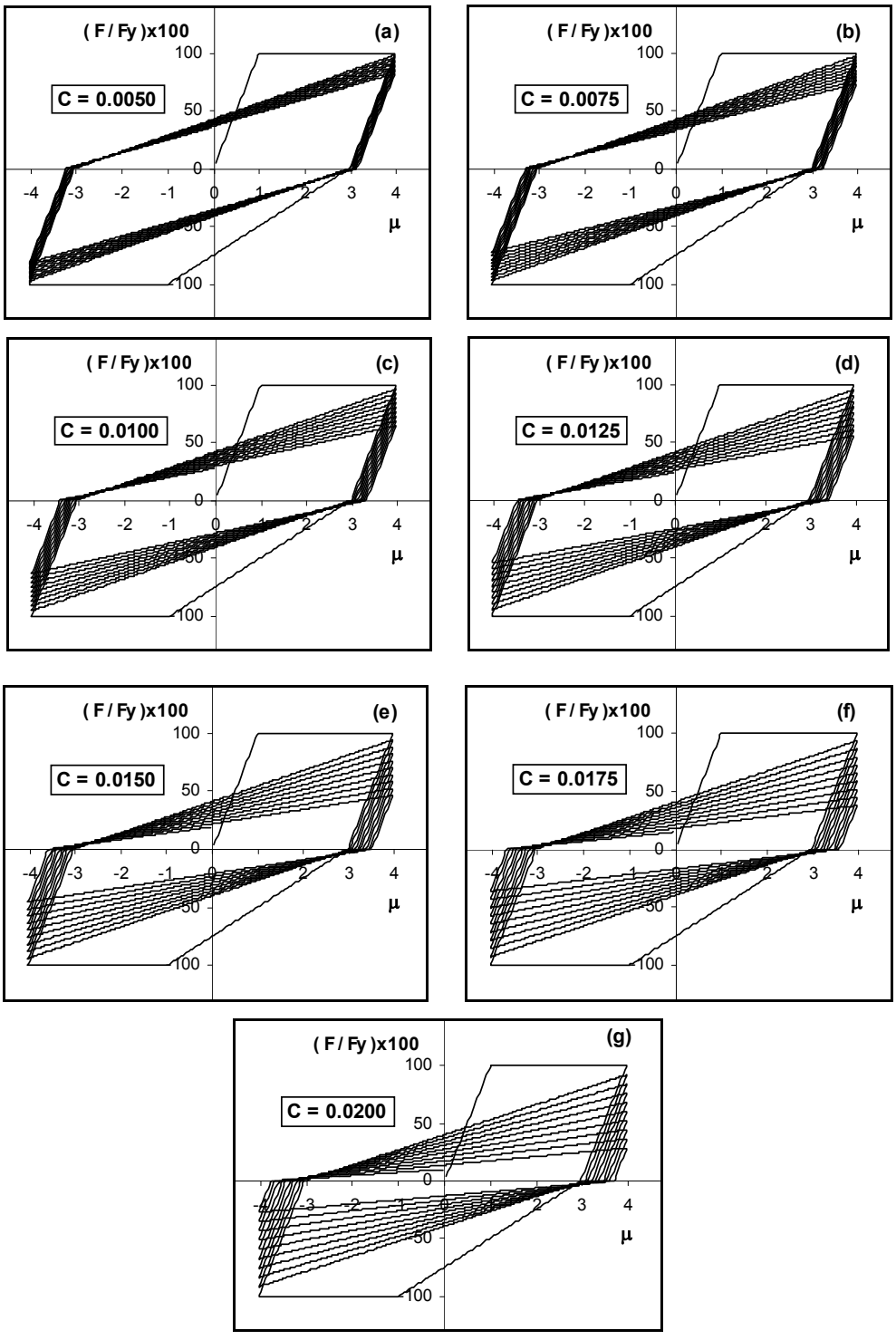


**Figure 4.5** Hysteresis models for linear cyclic strength degradation

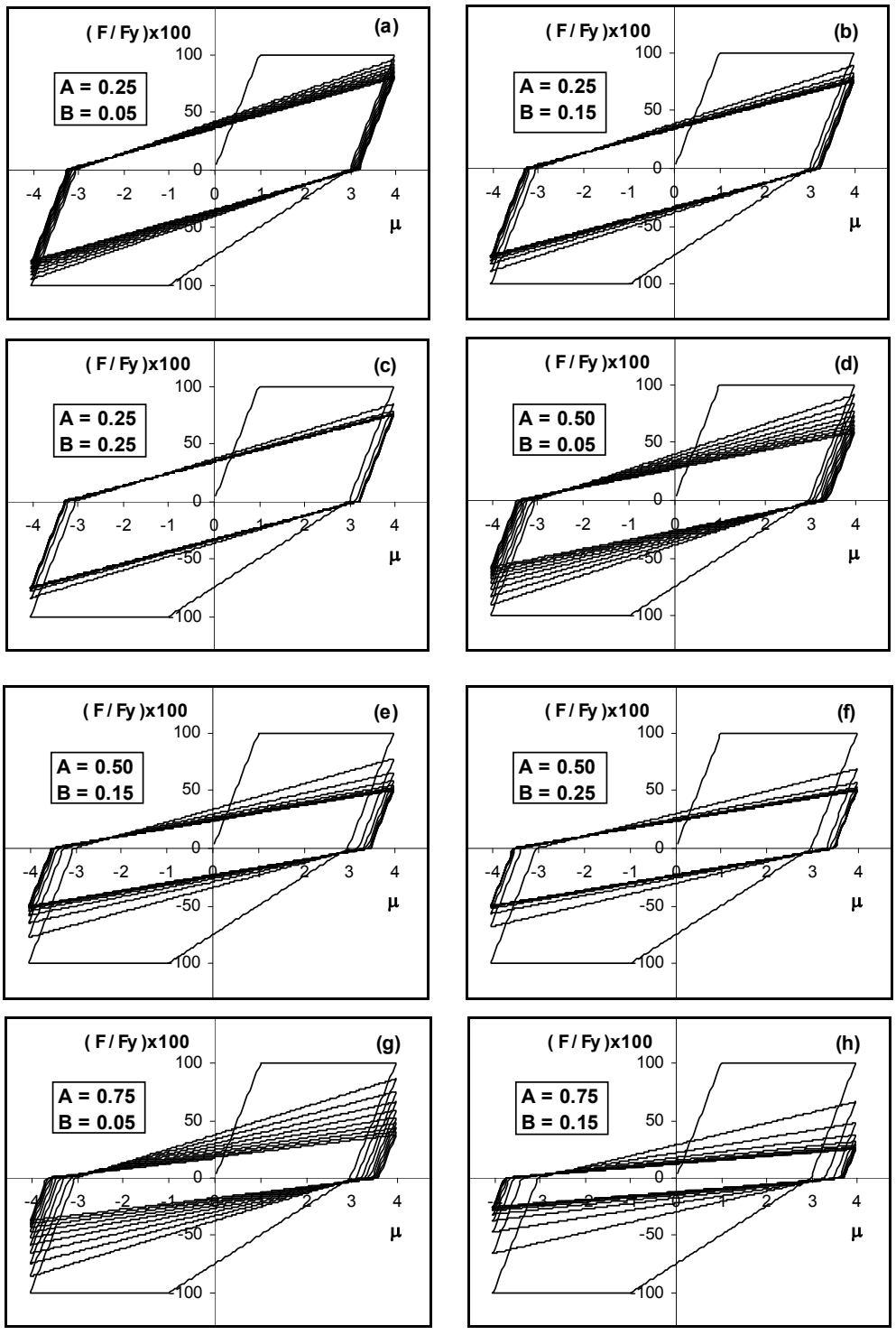


**Figure 4.6** Hysteresis models for exponential cyclic strength degradation (severe-to-gradual type)

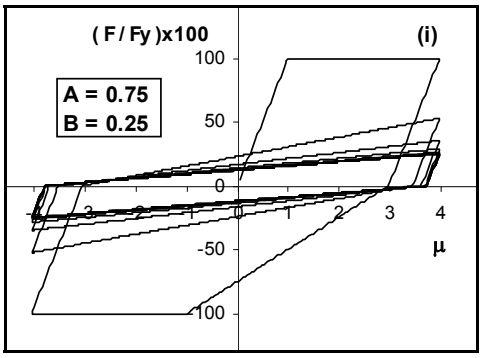


**Figure 4.6** (cont'd)

The dissipated energy per half-cycle and cumulative dissipated energy values for linear and exponential cyclic strength degradation cases are presented in Tables 4.3 and 4.4, respectively. It is clearly observed that, strength loss of the structural members under cyclic loading significantly reduces the energy dissipation capacities.

Figures 4.7 and 4.8 illustrate the dissipated energy values normalized by the dissipated energy values of the non-degrading model for each half-cycle in the positive direction of loading. For the linear cyclic strength degradation case, the energy dissipation capacity decreases uniformly with increasing number of cycles confirming with the relationship between the strength loss and energy dissipation capacity. For the exponential cyclic strength degradation case, it can be observed that, if the value of parameter '*B*' is large, energy dissipation capacity decreases more rapidly in the first few cycles. On the other hand, for cases in which *B*=0.05, energy dissipation capacity decreases more uniformly.

Cumulative dissipated energy values per half-cycle normalized by the total dissipated energy of non-degrading model in the positive direction of loading versus number of half-cycles relationship is presented in Figures 4.9 and 4.10. In the linear strength degradation case, with *C*=0.0200, energy dissipation capacity is

70 % of the corresponding capacity of the non-degrading model. This ratio is almost the same with the exponential degradation case of $A$=0.75 and $B$=0.05.

**Table 4.1** Strength capacity and deviation from initial capacity for linear strength degradation

| Cycle number | $C$ = 0.0050 | | $C$ = 0.0075 | | $C$ = 0.0100 | | $C$ = 0.0125 | | $C$ = 0.0150 | | $C$ = 0.0175 | | $C$ = 0.0200 | |
|---|---|---|---|---|---|---|---|---|---|---|---|---|---|---|
| | Cap. | Dev. | Cap. | Dev. | Cap. | Dev. | Cap. | Dev. | Cap. | Dev. | Cap. | Dev. | Cap. | Dev. |
| 1 | 100 | 0% | 100 | 0% | 100 | 0% | 100 | 0% | 100 | 0% | 100 | 0% | 100 | 0% |
| 2 | 98 | 2% | 97 | 3% | 96 | 4% | 95 | 5% | 94 | 6% | 93 | 7% | 92 | 8% |
| 3 | 96 | 4% | 94 | 6% | 92 | 8% | 90 | 10% | 88 | 12% | 86 | 14% | 84 | 16% |
| 4 | 94 | 6% | 91 | 9% | 88 | 12% | 85 | 15% | 82 | 18% | 79 | 21% | 76 | 24% |
| 5 | 92 | 8% | 88 | 12% | 84 | 16% | 80 | 20% | 76 | 24% | 72 | 28% | 68 | 32% |
| 6 | 90 | 10% | 85 | 15% | 80 | 20% | 75 | 25% | 70 | 30% | 65 | 35% | 60 | 40% |
| 7 | 88 | 12% | 82 | 18% | 76 | 24% | 70 | 30% | 64 | 36% | 58 | 42% | 52 | 48% |
| 8 | 86 | 14% | 79 | 21% | 72 | 28% | 65 | 35% | 58 | 42% | 51 | 49% | 44 | 56% |
| 9 | 84 | 16% | 76 | 24% | 68 | 32% | 60 | 40% | 52 | 48% | 44 | 56% | 36 | 64% |
| 10 | 82 | 18% | 73 | 27% | 64 | 36% | 55 | 45% | 46 | 54% | 37 | 63% | 28 | 72% |

**Table 4.2** Strength capacity and deviation from initial capacity for exponential strength degradation

| Cycle number | *A*=0.25 *B*=0.05 | | *A*=0.25 *B*=0.15 | | *A*=0.25 *B*=0.25 | | *A*=0.50 *B*=0.05 | | *A*=0.50 *B*=0.15 | | *A*=0.50 *B*=0.25 | | *A*=0.75 *B*=0.05 | | *A*=0.75 *B*=0.15 | | *A*=0.75 *B*=0.25 | |
|---|---|---|---|---|---|---|---|---|---|---|---|---|---|---|---|---|---|---|
| | Cap. | Dev. | Cap. | Dev. | Cap. | Dev. | Cap. | Dev. | Cap. | Dev. | Cap. | Dev. | Cap. | Dev. | Cap. | Dev. | Cap. | Dev. |
| 1 | 100 | 0% | 100 | 0% | 100 | 0% | 100 | 0% | 100 | 0% | 100 | 0% | 100 | 0% | 100 | 0% | 100 | 0% |
| 2 | 95 | 5% | 89 | 11% | 84 | 16% | 91 | 9% | 77 | 23% | 68 | 32% | 86 | 14% | 66 | 34% | 52 | 48% |
| 3 | 92 | 8% | 82 | 18% | 78 | 22% | 83 | 17% | 65 | 35% | 57 | 43% | 75 | 25% | 47 | 53% | 35 | 65% |
| 4 | 89 | 11% | 79 | 21% | 76 | 24% | 77 | 23% | 58 | 42% | 52 | 48% | 66 | 34% | 37 | 63% | 29 | 71% |
| 5 | 86 | 14% | 77 | 23% | 75 | 25% | 72 | 28% | 54 | 46% | 51 | 49% | 58 | 42% | 32 | 68% | 26 | 74% |
| 6 | 84 | 16% | 76 | 24% | 75 | 25% | 68 | 32% | 52 | 48% | 50 | 50% | 52 | 48% | 29 | 71% | 26 | 74% |
| 7 | 82 | 18% | 76 | 24% | 75 | 25% | 65 | 35% | 51 | 49% | 50 | 50% | 47 | 53% | 27 | 73% | 25 | 75% |
| 8 | 81 | 19% | 75 | 25% | 75 | 25% | 62 | 38% | 51 | 49% | 50 | 50% | 43 | 57% | 26 | 74% | 25 | 75% |
| 9 | 80 | 20% | 75 | 25% | 75 | 25% | 60 | 40% | 50 | 50% | 50 | 50% | 40 | 60% | 26 | 75% | 25 | 75% |
| 10 | 79 | 21% | 75 | 25% | 75 | 25% | 58 | 42% | 50 | 50% | 50 | 50% | 37 | 63% | 25 | 75% | 25 | 75% |

**Table 4.3** Dissipated energy per half-cycle and cumulative dissipated energy values for linear cyclic strength degradation

| Half cycle # | Dissipated energy per half-cycle | | | | | | | |
|---|---|---|---|---|---|---|---|---|
| | **No degr.** | ***C*=0.0050** | ***C*=0.0075** | ***C*=0.0100** | ***C*=0.0125** | ***C*=0.0150** | ***C*=0.0175** | ***C*=0.0200** |
| **1** | 300 | 300 | 300 | 300 | 300 | 300 | 300 | 300 |
| **2** | 450 | 450 | 450 | 450 | 450 | 450 | 450 | 450 |
| **3** | 300 | 295 | 293 | 290 | 288 | 285 | 283 | 280 |
| **4** | 300 | 296 | 294 | 292 | 290 | 288 | 285 | 283 |
| **5** | 300 | 291 | 286 | 282 | 277 | 272 | 267 | 263 |
| **6** | 300 | 292 | 288 | 283 | 279 | 274 | 270 | 265 |
| **7** | 300 | 287 | 280 | 273 | 266 | 259 | 252 | 244 |
| **8** | 300 | 288 | 281 | 274 | 267 | 260 | 253 | 246 |
| **9** | 300 | 283 | 274 | 264 | 255 | 245 | 235 | 224 |
| **10** | 300 | 283 | 274 | 265 | 255 | 246 | 235 | 225 |
| **11** | 300 | 278 | 267 | 255 | 243 | 230 | 217 | 203 |
| **12** | 300 | 279 | 267 | 255 | 243 | 230 | 217 | 203 |
| **13** | 300 | 274 | 260 | 245 | 230 | 214 | 198 | 180 |
| **14** | 300 | 274 | 260 | 246 | 230 | 214 | 197 | 179 |
| **15** | 300 | 270 | 253 | 236 | 217 | 198 | 178 | 157 |
| **16** | 300 | 270 | 253 | 235 | 217 | 197 | 176 | 155 |
| **17** | 300 | 265 | 246 | 225 | 204 | 181 | 157 | 132 |
| **18** | 300 | 265 | 246 | 225 | 203 | 179 | 155 | 129 |
| **19** | 300 | 261 | 238 | 215 | 190 | 163 | 135 | 105 |
| **20** | 300 | 260 | 238 | 214 | 188 | 161 | 132 | 101 |
| **Cum. diss. energy** | **6150** | **5761** | **5548** | **5324** | **5092** | **4846** | **4592** | **4324** |

**Table 4.4** Dissipated energy per half-cycle and cumulative dissipated energy values for exponential cyclic strength degradation

| Half cycle # | Dissipated energy per half-cycle | | | | | | | | | |
|---|---|---|---|---|---|---|---|---|---|---|
| | **No degr.** | ***A*=0.25 *B*=0.05** | ***A*=0.25 *B*=0.15** | ***A*=0.50 *B*=0.25** | ***A*=0.50 *B*=0.05** | ***A*=0.50 *B*=0.15** | ***A*=0.50 *B*=0.25** | ***A*=0.75 *B*=0.05** | ***A*=0.75 *B*=0.15** | ***A*=0.75 *B*=0.15** |
| **1** | 300 | 300 | 300 | 300 | 300 | 300 | 300 | 300 | 300 | 300 |
| **2** | 450 | 450 | 450 | 450 | 450 | 450 | 450 | 450 | 450 | 450 |
| **3** | 300 | 289 | 271 | 260 | 277 | 242 | 217 | 265 | 210 | 171 |
| **4** | 300 | 291 | 276 | 266 | 281 | 249 | 226 | 271 | 220 | 182 |
| **5** | 300 | 281 | 260 | 250 | 262 | 214 | 192 | 241 | 164 | 126 |
| **6** | 300 | 283 | 262 | 252 | 264 | 217 | 194 | 244 | 167 | 127 |
| **7** | 300 | 275 | 253 | 246 | 248 | 198 | 182 | 219 | 134 | 106 |
| **8** | 300 | 276 | 254 | 247 | 249 | 199 | 182 | 220 | 135 | 106 |
| **9** | 300 | 270 | 249 | 245 | 236 | 188 | 178 | 199 | 117 | 98 |
| **10** | 300 | 270 | 249 | 245 | 237 | 188 | 178 | 199 | 117 | 98 |
| **11** | 300 | 265 | 247 | 244 | 226 | 182 | 176 | 182 | 107 | 96 |
| **12** | 300 | 266 | 247 | 244 | 226 | 182 | 176 | 182 | 106 | 95 |
| **13** | 300 | 262 | 245 | 244 | 217 | 179 | 175 | 167 | 101 | 94 |
| **14** | 300 | 262 | 245 | 244 | 217 | 179 | 175 | 167 | 101 | 94 |
| **15** | 300 | 259 | 245 | 244 | 210 | 177 | 175 | 155 | 98 | 94 |
| **16** | 300 | 259 | 245 | 244 | 210 | 177 | 175 | 154 | 98 | 94 |
| **17** | 300 | 256 | 244 | 244 | 204 | 176 | 175 | 145 | 96 | 94 |
| **18** | 300 | 256 | 244 | 244 | 204 | 176 | 175 | 144 | 96 | 94 |
| **19** | 300 | 254 | 244 | 244 | 199 | 176 | 175 | 136 | 95 | 94 |
| **20** | 300 | 254 | 244 | 244 | 199 | 176 | 175 | 135 | 95 | 94 |
| **Cum. diss. energy** | **6150** | **5578** | **5274** | **5201** | **4916** | **4225** | **4051** | **4175** | **3007** | **2707** |

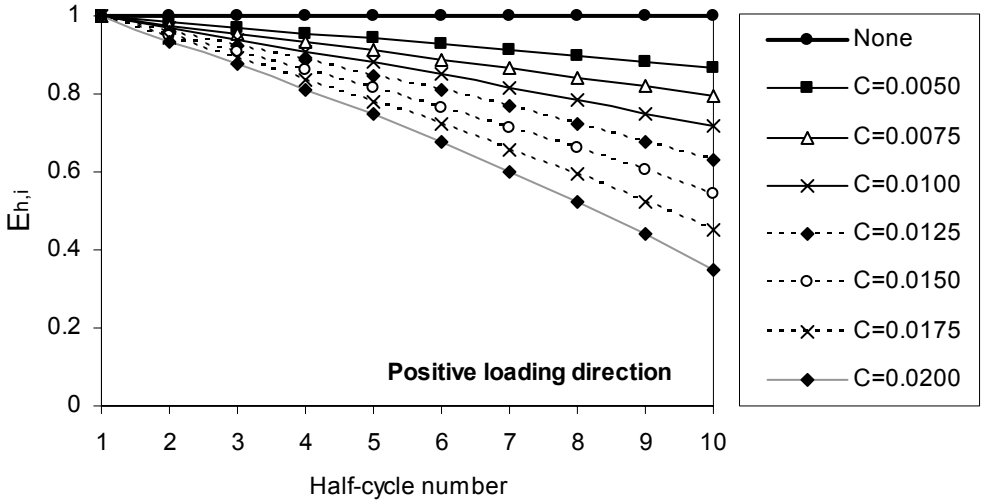


**Figure 4.7** Comparison of dissipated energy per half-cycle vs. number of half-cycles for linear cyclic strength degradation case

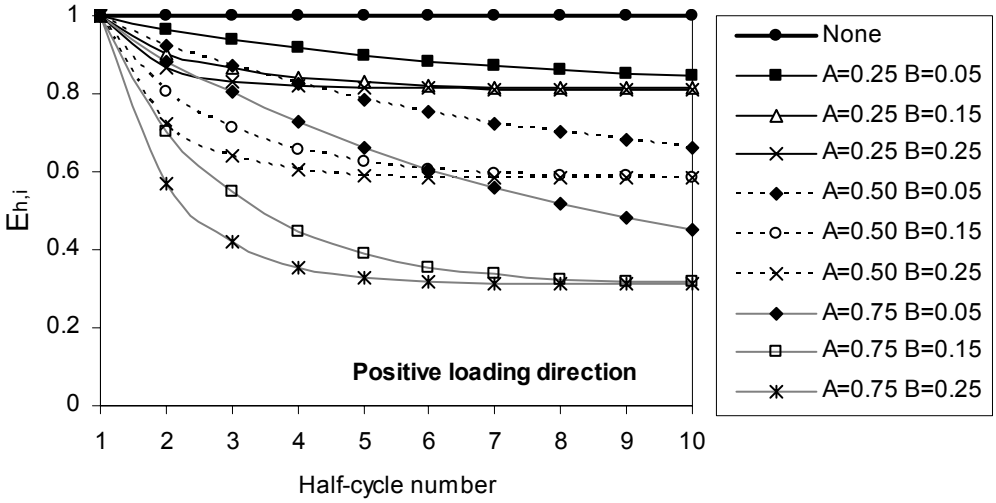


**Figure 4.8** Comparison of dissipated energy per half-cycle vs. number of half-cycles for exponential cyclic strength degradation case

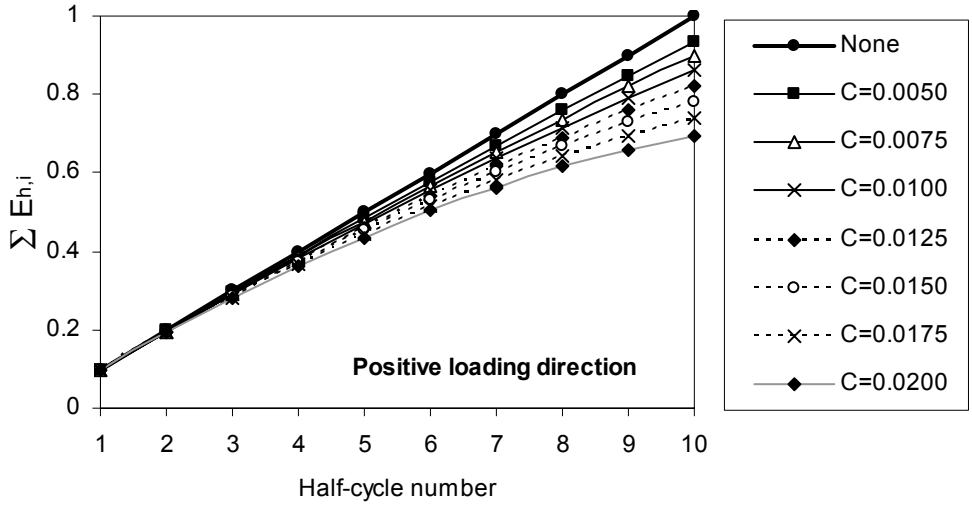


**Figure 4.9** Comparison of cumulative dissipated energy per half-cycle vs. number of half-cycles for linear cyclic strength degradation case

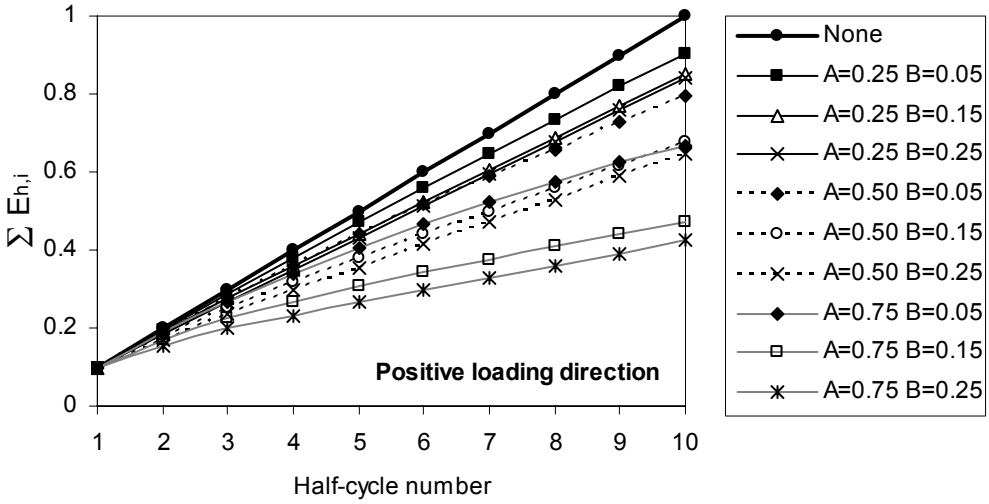


**Figure 4.10** Comparison of cumulative dissipated energy per half-cycle vs. number of half-cycles for exponential cyclic strength degradation case

### 4.2.2 In-cycle Strength Degradation

In-cycle strength degradation occurs as the deformations increase monotonically. Therefore, this degradation type is related with the shape of the monotonic force-displacement envelope (backbone curve) for hysteresis curves. Figure 4.11 presents an example plot for in-cycle strength degradation.

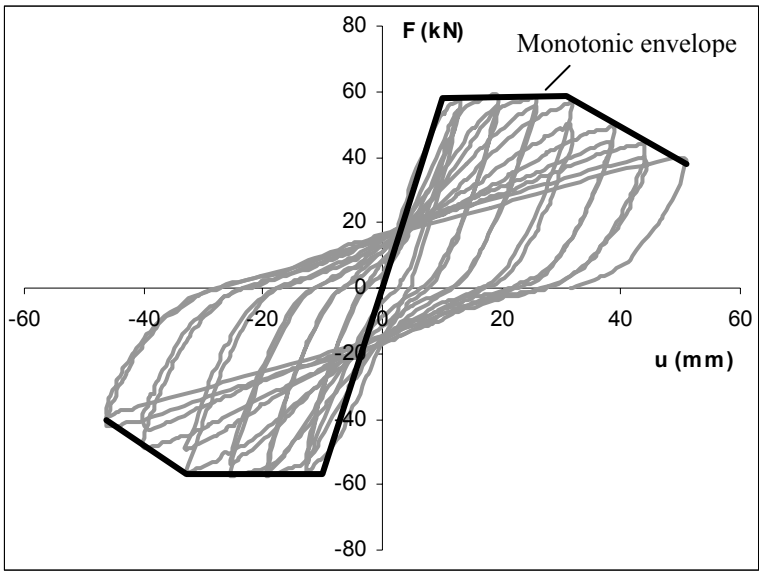


**Figure 4.11** Example plot for in-cycle strength degradation (Specimen C5-00N, Matamoros 1999)

The parameters of concern are shown in Figure 4.12. $F_y$ and $u_y$ are the yield force and yield displacement respectively, and $u_c$ is the displacement level of the capping point where the strength deteriorates rapidly beyond this point. $F_r$ is the residual strength and $u_r$ is displacement value for this point. $\alpha_1 K_o$ and $\alpha_2 K_o$ are the stiffness values of post-yield and post-capping branches, respectively. Monotonic test results of RC columns usually show that strength is "capped" and is followed

by a negative stiffness branch (Ibarra, 2003). The initial, post-yield and post-capping stiffness branches are investigated for the selected cyclic column tests in PEER database. In the selected column tests, the parameters $\alpha_1$ and $\alpha_2$, and the ratios $u_c/u_y$ and $F_r/F_y$ are determined for both directions of loading.

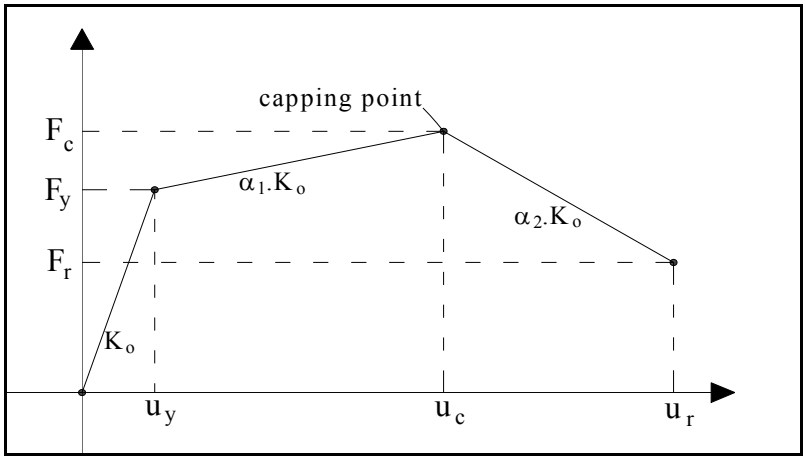


**Figure 4.12** Parametric definition of monotonic force-displacement envelope for in-cycle strength degradation

#### 4.2.2.1 Definition of Backbone Curve

The peaks of the hysteresis curves form an envelope curve which is also called as a backbone curve. Hysteresis models use a backbone curve based on the monotonic force-displacement relationship with additional rules to simulate the cyclic behavior of a structural member (Lehman and Moehle, 2000). There are mainly two types of backbone curves used for the construction of the hysteresis models for RC members in the literature: bilinear and trilinear backbone curves (Figure 4.13). As it can be observed from Figure 4.13.a, bilinear backbone curve is composed of two linear branches which are initial (elastic) stiffness branch and

post-yield stiffness branch. On the other hand, trilinear backbone curve considers the initial stiffness branch in two separate branches introducing cracking point of RC member. Sample cyclic column tests selected from the PEER database having bilinear and trilinear backbone curves can be seen in Figure 4.14. The monotonic force-displacement envelope used for the determination of the in-cycle strength degradation characteristics is a bilinear backbone curve with the addition of post-capping stiffness branch.

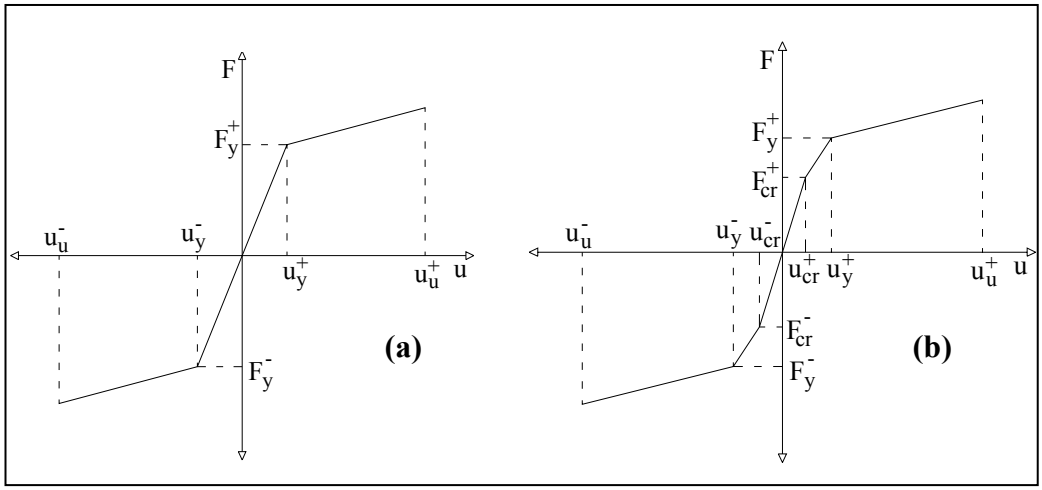


**Figure 4.13** Backbone curves a) Bilinear b) Trilinear

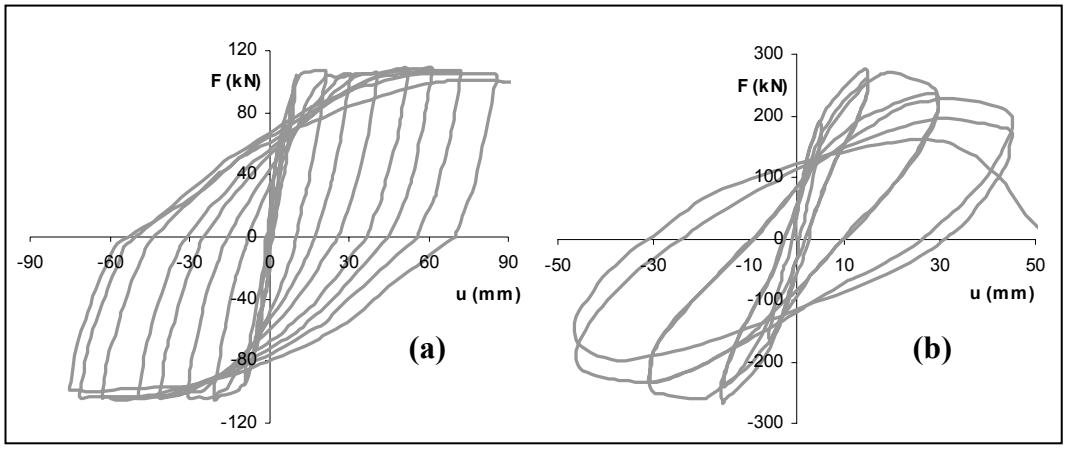


**Figure 4.14** Hysteresis curves with a) Bilinear backbone b) Trilinear backbone

## 4.3 The Calibration of Strength Degradation Parameters Using Cyclic Test Data

The analyses for the determination of strength degradation parameters are explained in this section. First, the criterion used for the selection of the test data is explained. Then one example for each case is explained in detail and the results and statistics for all tests are presented at the end.

### 4.3.1 Selection of Cyclic Test Data

The selection of cyclic test data in order to calibrate the strength degradation parameters is mainly based on the loading history and the presence of strength degradation. In other words, different number of test specimens are taken from Groups A-C based on the aforementioned criteria in order to quantify the strength degradation parameters that are considered in this study.

Specimens tested under constant amplitude (CA) loading are suitable for the cyclic strength degradation type. There are 31 constant amplitude cyclic tests among 196 column tests in PEER database. 16 of them exhibit severe strength degradation (strength degradation is 25% of maximum strength or higher) and 7 of them exhibit moderate strength degradation (degradation is between 15% and 25%). A total number of 20 tests are selected for the study of cyclic strength degradation in which 3 of them are from member Group B and 17 of them are from member Group C. The excluded tests are due to the irregularities in the shape of hysteresis loops. The selected cyclic tests are presented in Table 4.5 together with their member group names and observed levels of strength degradation.

As mentioned before, in-cycle strength losses occur due to the component damage as deformations increase monotonically. Therefore, standard (increasing) amplitude (SA) cyclic tests are suitable for this purpose. A total number of 55 cyclic column tests are used for the determination of in-cycle strength degradation

**Table 4.5** Selected column tests for cyclic strength degradation study

| No. | Test ID | Group | Level of strength degradation |
|---|---|---|---|
| **1** | Wight and Sozen, No. 40.092e | B | moderate |
| **2** | Wight and Sozen , No. 40.033ae | B | severe |
| **3** | Pujol 2002, No. 20-3-3S | B | severe |
| **4** | Pujol 2002, No. 10-3-2.25N | C | severe |
| **5** | Galeota et al. 1996, BA4 | C | severe |
| **6** | Pujol 2002, No. 10-3-3N | C | severe |
| **7** | Pujol 2002, No. 10-3-2.25S | C | moderate |
| **8** | Wight and Sozen, No. 25.033e | C | severe |
| **9** | Galeota et al. 1996, BA1 | C | severe |
| **10** | Erberik and Sucuoglu , CAH-1 | C | severe |
| **11** | Erberik and Sucuoglu , CAH-2 | C | severe |
| **12** | Galeota et al. 1996, AA4 | C | severe |
| **13** | Erberik and Sucuoglu , CAL-10 | C | moderate |
| **14** | Erberik and Sucuoglu , CAH-5 | C | moderate |
| **15** | Erberik and Sucuoglu CAL-9 | C | severe |
| **16** | Erberik and Sucuoglu , CAL-8 | C | severe |
| **17** | Erberik and Sucuoglu , CAH-6 | C | severe |
| **18** | Erberik and Sucuoglu , CAH-4 | C | severe |
| **19** | Erberik and Sucuoglu , CAH-3 | C | severe |
| **20** | Erberik and Sucuoglu , CALU-11 | C | moderate |

properties. The distribution of selected test specimens regarding member Groups A-C are as follows: 7 specimens from Group A (2 moderate, 5 severe degradation), 28 specimens from Group B (9 moderate, 19 severe degradation) and 20 specimens from Group C (1 moderate, 19 severe degradation). The selected cyclic column tests together with their member group names and observed levels of strength degradation are presented in Table 4.6. It is not surprising to observe that there are only a few specimens from Group A for both types of strength degradation, because by definition, the specimens in this group exhibit stable behavior with no or slight deterioration. In addition, it is more important to quantify the strength degradation parameter in cases of cyclic behavior with moderate-to-severe degradation. That is why most of the selected specimens are from Groups B and C.

**Table 4.6** Selected column tests for in-cycle strength degradation study

| No. | Test ID | Group | Level of strength degradation |
|---|---|---|---|
| **1** | Thomsen and Wallace 1994, B2 | A | severe |
| **2** | Thomsen and Wallace 1994, C2 | A | severe |
| **3** | Atalay and Penzien 1975, No. 11 | A | severe |
| **4** | Thomsen and Wallace 1994, D3 | A | severe |
| **5** | Thomsen and Wallace 1994, D1 | A | severe |
| **6** | Sugano 1996, UC15H | A | moderate |
| **7** | Watson and Park 1989, No. 5 | A | moderate |
| **8** | Ohno and Nishioka 1984, L3 | B | severe |
| **9** | Tanaka and Park 1990, No. 2 | B | severe |
| **10** | Ang et al. 1981, No. 3 | B | moderate |
| **11** | Wehbe et al. 1998, B1 | B | severe |
| **12** | Saatcioglu and Grira 1999, BG-10 | B | moderate |
| **13** | Atalay and Penzien 1975, No. 9 | B | severe |
| **14** | Xiao. HC4-8L19-T10-0.1P | B | severe |
| **15** | Saatcioglu and Grira 1999, BG-2 | B | severe |
| **16** | Azizinamini et al. 1988, NC-2 | B | moderate |
| **17** | Saatcioglu and Grira 1999, BG-3 | B | moderate |
| **18** | Saatcioglu and Grira 1999, BG-4 | B | severe |
| **19** | Soesianawati et al. 1986, No. 2 | B | severe |
| **20** | Zahn et al. 1986, No. 7 | B | moderate |
| **21** | Mo and Wang 2000,C3-2 | B | severe |
| **22** | Thomsen and Wallace 1994, C3 | B | severe |
| **23** | Paultre and Legeron, No. 1006015 | B | moderate |
| **24** | Bechtoula., 2002, D1N30 | B | moderate |
| **25** | Sugano 1996, UC20H | B | severe |
| **26** | Paultre et al., 2001, No. 1006052 | B | severe |
| **27** | Mo and Wang 2000,C1-2 | B | severe |
| **28** | Galeota et al. 1996, CA2 | B | severe |
| **29** | Bayrak and Sheikh 1996, AS-4HT | B | severe |
| **30** | Kanda et al. 1988, 85STC-1 | B | severe |
| **31** | Kanda et al. 1988, 85STC-2 | B | severe |
| **32** | Bayrak and Sheikh 1996, AS-3HT | B | severe |
| **33** | Saatcioglu and Grira 1999, BG-9 | B | moderate |
| **34** | Muguruma et al. 1989, BL-1 | B | moderate |
| **35** | Paultre and Legeron, No. 10013015 | B | severe |
| **36** | Bayrak and Sheikh 1996, AS-2HT | C | severe |
| **37** | Bayrak and Sheikh 1996, AS-6HT | C | severe |
| **38** | Matamoros et al. 1999,C5-00N | C | severe |
| **39** | Matamoros et al. 1999,C10-05S | C | severe |
| **40** | Mo and Wang 2000,C2-2 | C | severe |
| **41** | Paultre et al., 2001, No. 1008040 | C | severe |
| **42** | Paultre and Legeron, No. 1006025 | C | severe |
| **43** | Muguruma et al. 1989, BH-2 | C | moderate |
| **44** | Paultre and Legeron, , No. 1006040 | C | severe |
| **45** | Galeota et al. 1996, CA1 | C | severe |
| **46** | Pujol 2002, No. 10-2-3N | C | severe |
| **47** | Bayrak and Sheikh 1996, AS-5HT | C | severe |
| **48** | Mo and Wang 2000,C1-3 | C | severe |
| **49** | Mo and Wang 2000,C2-3 | C | severe |
| **50** | Matamoros et al. 1999,C10-20N | C | severe |
| **51** | Matamoros et al. 1999,C5-20N | C | severe |
| **52** | Sugano 1996, UC15L | C | severe |
| **53** | Paultre and Legeron, No. 10013025 | C | severe |
| **54** | Sugano 1996, UC20L | C | severe |
| **55** | Takemura., 1997, Test 1 (JSCE-4) | C | severe |

### 4.3.2 Cyclic Strength Degradation Case

Cyclic strength degradation parameters for the linear and exponential degradation cases are calculated according to the following procedure. Determination of "gradual-to-severe" type of exponential degradation parameters (*S* and *K*) is similar to the determination of "severe-to-gradual" type of exponential degradation parameters (*A* and *B*) and therefore, the exponential strength degradation example presented in this section is only considers "severe-to-gradual" type of exponential degradation. The example test for the determination of cyclic strength degradation parameters (*A*, *B* and *C*) is "Erberik and Sucuoglu 2001-CAH-1" (Figure 4.15). As it can be observed from the positive loading direction of the force-displacement relationship in Figure 4.15, most of the strength degradation takes place after the first cycle. On the other hand, strength degradation is observed to be uniform in the negative loading direction. The strength capacities at each positive and negative half-cycles and the corresponding strength losses are presented in Table 4.7 for the constant amplitude cyclic test under consideration.

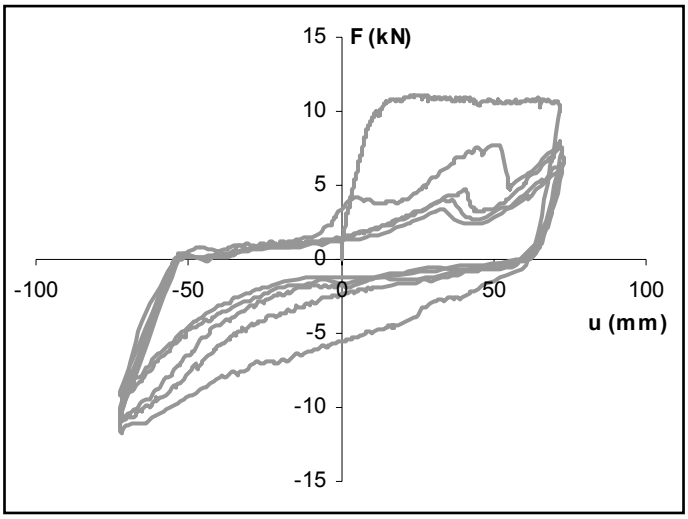


**Figure 4.15** Force-displacement relationship for Erberik and Sucuoglu 2001, CAH-1 cyclic column test

**Table 4.7** Strength and strength degradation values for Erberik and Sucuoglu 2001-CAH-1 column test

| **Strength degradation in positive (+) direction** | | | **Strength degradation in negative (-) direction** | | |
|---|---|---|---|---|---|
| ***N*** | ***F<sub>i</sub>* (kN)** | **$\Delta F_i$ (kN)** | ***N*** | ***F<sub>i</sub>* (kN)** | **$\Delta F_i$ (kN)** |
| 0 | 11.1 | 0 | 0 | -11.7 | 0 |
| 1 | 7.7 | 3.4 | 1 | -10.8 | 0.9 |
| 2 | 7.5 | 3.6 | 2 | -10.6 | 1.1 |
| 3 | 6.5 | 4.6 | 3 | -9.3 | 2.4 |
| 4 | 5.9 | 5.2 | 4 | -8.9 | 2.8 |

Next step is to determine the linear and exponential strength degradation parameters. Since $F_y$ and $u_m/u_y$ components of the Equations 4.1 and 4.2 are constant, the degradation formulas can be expressed in a simpler form.

Exponential formulation becomes

$$\Delta F(N) = p\left(1 - e^{-r.N}\right) \tag{4.4}$$

where

$$p = A F_y \tag{4.5}$$

$$r = B\left(u_m / u_y\right) \tag{4.6}$$

and linear formulation becomes

$$\Delta F(N) = q N \tag{4.7}$$

where

$$q = C\left(u_m / u_y\right) F_y \tag{4.8}$$

$N$ vs. $\Delta F$ data is used for the linear and nonlinear curve fitting calculations. The nonlinear fit for exponential case is performed by Mathcad 2000 (MathSoft, Inc.). The program gives the constants '$p$' and 'r' by minimizing the error in the curve fitting process. Linear fit is performed by using the spreadsheet program. The results for the sample cyclic test are presented in Table 4.8 and the fitted curves can be seen in Figures 4.16 and 4.17.

**Table 4.8** Calculated cyclic strength degradation parameters for the sample test

| **Erberik and Sucuoglu CAH-1 test / Cyclic strength degradation parameters** | | | |
|---|---|---|---|
| | | ***Positive direction*** | ***Negative direction*** |
| Exponential formulation constants | $p$ | 5.027 | 69.55 |
| | $r$ | 0.893 | 0.0105 |
| | ***A*** | **0.453** | **5.944** |
| | ***B*** | **0.176** | **0.002** |
| Linear formulation constants | $q$ | 1.5067 | 0.7167 |
| | ***C*** | **0.0268** | **0.0121** |

As it can be observed from the Figures 4.16 and 4.17, exponential fit is more appropriate for the positive loading direction whereas both linear and exponential fits yield satisfactory results for the negative loading direction. The coefficient of determination ($R^2$) of the exponential fit is 0.961 for the positive case and 0.960 for the negative case indicating good representation of cyclic strength degradation behavior. Linear formulation seems to be inappropriate for the positive side with a coefficient of determination of 0.72. On the other hand, linear formulation gives better results in the negative direction with a $R^2$ value of 0.96. The advantage of linear formulation over the exponential formulation in the case of negative direction is that the linear formulation has only one parameter ($C$) whereas exponential formulation has two parameters ($A$ & $B$) to be determined.

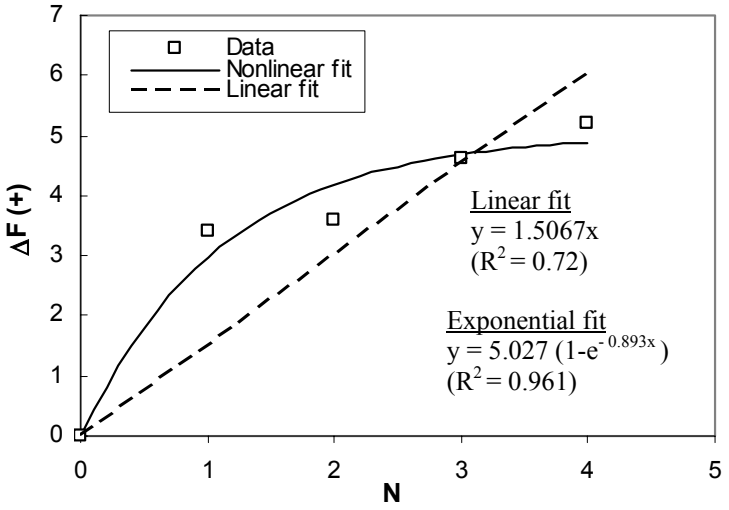


**Figure 4.16** Number of cycles vs. strength degradation plot for Erberik and Sucuoglu 2001-CAH-1 test in positive direction

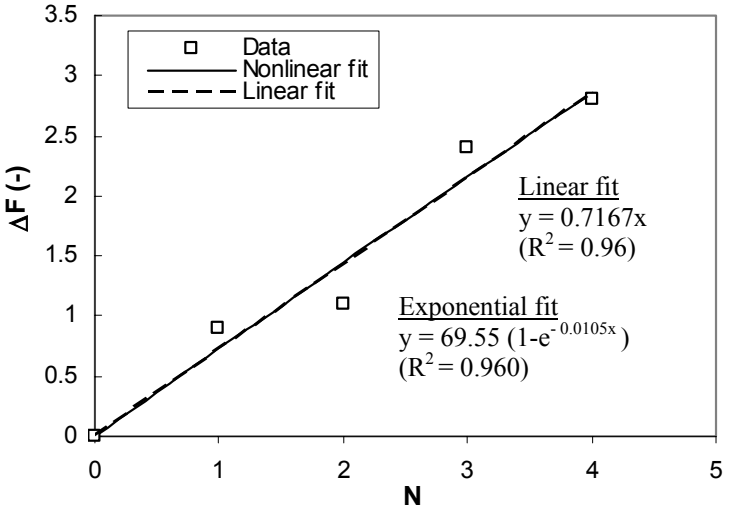


**Figure 4.17** Number of cycles vs. strength degradation plot for Erberik and Sucuoglu 2001-CAH-1 test in negative direction

The process explained above is repeated for the selected 20 column tests which have constant amplitude cyclic loading histories and the calculated parameters are presented in Tables 4.9 and 4.10 separately for positive and negative loading directions. For each cyclic test, the values obtained for exponential degradation function (severe-to-gradual or gradual-to-severe) and linear degradation function are listed. The values in bold character represent the better match (with higher $R^2$ value) with the observed (experimental) behavior. The abbreviation "N/A" stands for the cases where it is not possible to obtain a physically meaningful value for the parameter under consideration.

**Table 4.9** Result list for cyclic strength degradation parameters in positive dir.

| | | | | **Positive direction** | | | | |
|---|---|---|---|---|---|---|---|---|
| **Test #** | **Test ID** | **Group** | **Degradation level** | **Exponential** | | | | **Linear** |
| | | | | ***A*** | ***B*** | ***S*** | ***K*** | ***C*** |
| **1** | Erberik, CAH-1 | C | severe | **0.453** | **0.176** | N/A | N/A | 0.027 |
| **2** | Erberik, CAH-2 | C | severe | **0.719** | **0.306** | N/A | N/A | 0.041 |
| **3** | Erberik, CAH-3 | C | severe | **0.576** | **0.138** | N/A | N/A | 0.014 |
| **4** | Erberik, CAH-4 | C | severe | **0.780** | **0.111** | N/A | N/A | 0.026 |
| **5** | Erberik, CAH-5 | C | moderate | **0.272** | **0.104** | N/A | N/A | 0.009 |
| **6** | Erberik, CAH-6 | C | severe | **0.563** | **0.124** | N/A | N/A | 0.021 |
| **7** | Erberik, CAL-8 | C | severe | **0.466** | **0.147** | N/A | N/A | 0.027 |
| **8** | Erberik, CAL-9 | C | severe | **0.683** | **0.160** | N/A | N/A | 0.034 |
| **9** | Erberik, CAL-10 | C | moderate | **0.270** | **0.223** | N/A | N/A | 0.014 |
| **10** | Erberik, CALU-11 | C | moderate | **0.342** | **0.122** | N/A | N/A | 0.015 |
| **11** | Galeota, AA4 | C | severe | **0.510** | **0.075** | N/A | N/A | 0.022 |
| **12** | Galeota, BA1 | C | severe | **0.513** | **0.086** | N/A | N/A | 0.027 |
| **13** | Galeota, BA4 | C | severe | 0.850 | 0.042 | N/A | N/A | **0.028** |
| **14** | Pujol, 20-3-3S | B | severe | N/A | N/A | **0.004** | **0.126** | 0.010 |
| **15** | Pujol, 10-3-2.25N | C | severe | N/A | N/A | **0.065** | **0.031** | 0.005 |
| **16** | Pujol, 10-3-2.25S | C | moderate | 6.964 | 0.001 | N/A | N/A | **0.004** |
| **17** | Pujol, 10-3-3N | C | severe | N/A | N/A | **0.116** | **0.058** | 0.015 |
| **18** | Wight&Sozen,40.092E | B | moderate | N/A | N/A | **0.013** | **0.204** | 0.013 |
| **19** | Wight&Sozen,25.033E | C | severe | 10.638 | 0.002 | N/A | N/A | **0.025** |
| **20** | Wight&Sozen,40.033AE | B | severe | 12.958 | 0.005 | N/A | N/A | **0.060** |

**Table 4.10** Result list for cyclic strength degradation parameters in negative dir.

| Test # | Test ID | Group | Degradation level | Negative direction | | | | |
|---|---|---|---|---|---|---|---|---|
| | | | | Exponential | | | | Linear |
| | | | | ***A*** | ***B*** | ***S*** | ***K*** | ***C*** |
| **1** | Erberik, CAH-1 | C | severe | 5.944 | 0.002 | N/A | N/A | **0.012** |
| **2** | Erberik, CAH-2 | C | severe | **0.554** | **0.066** | N/A | N/A | 0.019 |
| **3** | Erberik, CAH-3 | C | severe | **0.386** | **0.131** | N/A | N/A | 0.009 |
| **4** | Erberik, CAH-4 | C | severe | **0.671** | **0.127** | N/A | N/A | 0.023 |
| **5** | Erberik, CAH-5 | C | moderate | **0.440** | **0.049** | N/A | N/A | 0.011 |
| **6** | Erberik, CAH-6 | C | severe | **0.605** | **0.103** | N/A | N/A | 0.022 |
| **7** | Erberik, CAL-8 | C | severe | **0.387** | **0.160** | N/A | N/A | 0.023 |
| **8** | Erberik, CAL-9 | C | severe | **0.368** | **0.046** | N/A | N/A | 0.011 |
| **9** | Erberik, CAL-10 | C | moderate | **0.288** | **0.121** | N/A | N/A | 0.013 |
| **10** | Erberik, CALU-11 | C | moderate | **0.395** | **0.463** | N/A | N/A | 0.020 |
| **11** | Galeota, AA4 | C | severe | **0.324** | **0.092** | N/A | N/A | 0.019 |
| **12** | Galeota, BA1 | C | severe | 0.950 | 0.030 | N/A | N/A | **0.024** |
| **13** | Galeota, BA4 | C | severe | 2.087 | 0.010 | N/A | N/A | **0.020** |
| **14** | Pujol, 20-3-3S | B | severe | N/A | N/A | **0.002** | **0.147** | 0.010 |
| **15** | Pujol, 10-3-2.25N | C | severe | N/A | N/A | **0.012** | **0.056** | 0.004 |
| **16** | Pujol, 10-3-2.25S | C | moderate | N/A | N/A | **0.085** | **0.023** | 0.003 |
| **17** | Pujol, 10-3-3N | C | severe | N/A | N/A | **0.010** | **0.135** | 0.012 |
| **18** | Wight&Sozen,40.092E | B | moderate | N/A | N/A | **0.017** | **0.183** | 0.012 |
| **19** | Wight&Sozen,25.033E | C | severe | 4.888 | 0.003 | N/A | N/A | **0.015** |
| **20** | Wight&Sozen,40.033AE | B | severe | 19.566 | 0.005 | N/A | N/A | **0.093** |

During the analysis, type of strength degradation (gradual-to-severe exponential, severe-to-gradual exponential or linear) in a specific loading direction of a cyclic test is chosen as the one with the largest $R^2$ value from the curve fit process. Therefore it is possible to encounter cases where the most appropriate strength degradation type differs in each loading direction of a single cyclic test. For instance for the cyclic test CAH-1, severe-to-gradual exponential strength degradation is more suitable for positive loading direction whereas linear strength degradation model is a better candidate to simulate the cyclic behavior in negative loading direction. This indicates that the cyclic degradation characteristics of a structural member with symmetrical cross-section can differ with respect to the loading direction even if it is subjected to the same amplitude of loading. This can

be attributed to the fact that the propagation of cracks, and in turn damage, in the loading direction where the first yield occurs is different from the other loading direction.

Since the number of constant amplitude cyclic tests of RC members is rather limited, it is not possible to make general comments about the resulting values of the strength degradation parameters. For instance, only two test program (Erberik & Sucuoglu and Galeota) seems to be suitable for the calibration of exponential degradation of severe-to-gradual type. Among these cyclic tests, three of them are classified as moderately degrading in terms of strength (Table 4.9 and 4.10). Considering both loading directions, the mean values of parameters *A* and *B* for these cyclic tests are 0.33 and 0.18, respectively. The variation in parameter *A* is small (COV=0.21) whereas there is a considerable variation in parameter *B* (COV=0.83). The number of cyclic tests which are classified as severely degrading in terms of strength is nine (Table 4.9 and 4.10). The mean values of parameters *A* and *B* for this group of cyclic tests are 0.53 and 0.13 with COV values of 0.25 and 0.47, respectively. The results indicate that parameter *B* that represents rate of strength degradation is rather an unstable parameter. The high value of parameter *B* in moderate degradation case is due to insufficient number of data and the unreasonably high value (*B*=0.463) obtained from the data of the cyclic test CALU-11. If the value obtained from this test is ignored, the value of parameter is immediately reduced to 0.10-0.12. Parameter *A* seems to be more consistent with reasonable COV values in this sense.

There exist five cyclic tests from two test programs (Pujol and Wight & Sozen) of gradual-to-severe type seems to yield a better match with the experimental data. Among these tests, two of them are classified as moderately degrading and the values of parameters *S* and *K* are in the range of 0.02-0.09 and 0.02-0.20, respectively. For severely degrading specimens, these values are in the range of 0.002-0.12 and 0.03-0.15, respectively. However it should be mentioned that it is not possible to conclude on the results obtained since much more experimental

data is required for the quantification of degradation parameters in such a special type of strength degradation model where the last few cycles are not stable at the onset of failure.

It is not possible to encounter many cyclic test data with moderate strength degradation for which linear type is more suitable (only one test of Pujol, 10-3-2.25S, with $C$=0.004). But accepting low $R^2$ values, the mean value of parameter $C$ for the aforementioned five tests can be obtained as 0.011 (COV=0.44). For severe degradation case of linear type, there exist more data from four different test programs (Table 4.9 and 4.10). The mean value of parameter $C$ is then obtained as 0.02 (COV=0.22) excluding the cyclic test 40.033AE (Wight & Sozen) which yields unreasonable values in both loading directions. It should be noted that, the variables $A$, $B$ and $C$ are not random variables and COV values are calculated just for the sake of comparison and to give a general idea of dispersion.

### 4.3.3 In-Cycle Strength Degradation Case

In-cycle strength degradation properties of the selected column tests are determined according to the process explained below. The column test C5-00N of Matamoros (1999) is used as example (Figure 4.11).

The trilinear force-displacement envelope is shown in Figure 4.12 with all the parameters involved in its construction. In order to calibrate the parameters that define the envelope by using experimental data, least squares method is employed separately for each linear segment, considering the peak values of each cycle from the selected cyclic tests. Hence the points ($u_y$, $F_y$), ($u_c$, $F_r$) and ($u_r$, $F_r$) are obtained for each considered cyclic test. The calculated parameters for the example test C5-00N by using the least squares method are presented in Table 4.11.

**Table 4.11** In-cycle strength degradation parameters for Matamoros (1999) C5-00N column test

| **In-cycle strength degradation parameters** | | | | |
|---|---|---|---|---|
| **Positive direction** | | | **Negative direction** | |
| $K_0$ (kN/mm)= | 5.78 | | $K_0$ (kN/mm)= | 5.69 |
| $\alpha_1 K_0$ (kN/mm)= | 0.03 | | $\alpha_1 K_0$ (kN/mm)= | -0.02 |
| $\alpha_2 K_0$ (kN/mm)= | -1.04 | | $\alpha_2 K_0$ (kN/mm)= | -1.20 |
| $\alpha_1$ = | 0.01 | | $\alpha_1$ = | 0.00 |
| $\alpha_2$ = | -0.18 | | $\alpha_2$ = | -0.21 |
| $u_c / u_y$ = | 3.10 | | $u_c / u_y$ = | 3.30 |
| $F_r / F_y$ = | 0.65 | | $F_r / F_y$ = | 0.71 |
| $u_r / u_y$ = | 5.10 | | $u_r / u_y$ = | 4.63 |

As it can be observed from Table 4.11, the post-yield stiffness is almost zero for this case. Capping point ductility level is 3.10 for the positive region and 3.30 for the negative region. The post-capping stiffness is 18 % of the initial stiffness for the positive side and 21 % for the negative side. The residual strength is 65 % of the yield strength for the positive side and 71 % for the negative case.

This process is repeated for the selected 55 cyclic column tests which have increasing amplitude loading histories in PEER database and the results are presented in Tables 4.12 and 4.13. The average values of the parameters for 55 cyclic tests can be seen in Tables 4.14.

The results reveal that, the in-cycle strength degradation behavior in both directions of loading is quite similar on the average. In positive direction of loading, the mean value of hardening slope in the post-yield branch is 3 % whereas the same mean value is 1 % in the negative direction of loading. The mean value of post-capping stiffness has a reduction of 80 % with respect to the initial stiffness for both loading directions. The mean residual-to-yield strength ratio is 60 %. The capping point and residual strength point ductility levels are almost the same for both directions with values of 3.30 and 7.40, respectively.

**Table 4.12** Result list for in-cycle strength degradation parameters (positive dir.)

| No. | Test ID | Group | $\alpha_1$ | $\alpha_2$ | $u_c / u_y$ | $F_r / F_y$ | $u_r / u_y$ |
|---|---|---|---|---|---|---|---|
| **1** | Thomsen and Wallace 1994, B2 | A | 0.14 | -0.13 | 2.00 | 0.82 | 4.44 |
| **2** | Thomsen and Wallace 1994, C2 | A | 0.02 | -0.06 | 2.60 | 0.69 | 8.00 |
| **3** | Atalay and Penzien 1975, No. 11 | A | 0.09 | -0.20 | 1.92 | 0.64 | 4.17 |
| **4** | Thomsen and Wallace 1994, D3 | A | 0.08 | -0.14 | 1.82 | 0.19 | 8.04 |
| **5** | Thomsen and Wallace 1994, D1 | A | 0.01 | -0.09 | 2.25 | 0.35 | 9.50 |
| **6** | Sugano 1996, UC15H | A | 0.04 | -0.24 | 3.15 | 0.86 | 4.08 |
| **7** | Watson and Park 1989, No. 5 | A | -0.01 | -0.20 | 3.25 | 0.66 | 4.88 |
| **8** | Ohno and Nishioka 1984, L3 | B | 0.01 | -0.10 | 6.25 | 0.73 | 9.38 |
| **9** | Tanaka and Park 1990, No. 2 | B | 0.00 | -0.04 | 2.70 | 0.76 | 8.60 |
| **10** | Ang et al. 1981, No. 3 | B | 0.17 | -0.08 | 2.05 | 0.93 | 5.10 |
| **11** | Wehbe et al. 1998, B1 | B | 0.07 | -0.40 | 3.93 | 0.66 | 5.26 |
| **12** | Saatcioglu and Grira 1999, BG-10 | B | 0.00 | -0.03 | 6.61 | 0.79 | 11.80 |
| **13** | Atalay and Penzien 1975, No. 9 | B | 0.39 | -0.25 | 1.62 | 0.68 | 3.85 |
| **14** | Xiao. HC4-8L19-T10-0.1P | B | 0.01 | -0.06 | 5.85 | 0.90 | 8.00 |
| **15** | Saatcioglu and Grira 1999, BG-2 | B | -0.01 | -0.04 | 3.31 | 0.78 | 8.31 |
| **16** | Azizinamini et al. 1988, NC-2 | B | 0.04 | -0.06 | 2.13 | 0.84 | 5.54 |
| **17** | Saatcioglu and Grira 1999, BG-3 | B | 0.09 | -0.03 | 2.76 | 0.95 | 9.68 |
| **18** | Saatcioglu and Grira 1999, BG-4 | B | 0.07 | -0.07 | 3.00 | 0.75 | 8.31 |
| **19** | Soesianawati et al. 1986, No. 2 | B | 0.14 | -0.09 | 2.04 | 0.42 | 10.53 |
| **20** | Zahn et al. 1986, No. 7 | B | -0.01 | -0.14 | 6.29 | 0.71 | 8.08 |
| **21** | Mo and Wang 2000,C3-2 | B | -0.02 | -0.92 | 5.25 | 0.53 | 5.65 |
| **22** | Thomsen and Wallace 1994, C3 | B | 0.08 | -0.10 | 2.10 | 0.31 | 10.25 |
| **23** | Paultre and Legeron, No. 1006015 | B | -0.02 | -0.05 | 4.68 | 0.64 | 10.60 |
| **24** | Bechtoula., 2002, D1N30 | B | 0.01 | -0.15 | 4.75 | 0.82 | 6.25 |
| **25** | Sugano 1996, UC20H | B | 0.02 | -0.07 | 3.10 | 0.52 | 10.25 |
| **26** | Paultre et al., 2001, No. 1006052 | B | -0.04 | -0.20 | 3.64 | 0.62 | 5.06 |
| **27** | Mo and Wang 2000,C1-2 | B | -0.03 | -0.64 | 5.00 | 0.33 | 5.84 |
| **28** | Galeota et al. 1996, CA2 | B | 0.00 | -0.17 | 2.10 | 0.52 | 4.90 |
| **29** | Bayrak and Sheikh 1996, AS-4HT | B | -0.03 | -0.18 | 3.57 | 0.26 | 7.18 |
| **30** | Kanda et al. 1988, 85STC-1 | B | -0.02 | -0.06 | 5.20 | 0.74 | 8.70 |
| **31** | Kanda et al. 1988, 85STC-2 | B | -0.02 | -0.05 | 3.50 | 0.70 | 8.66 |
| **32** | Bayrak and Sheikh 1996, AS-3HT | B | -0.01 | -0.09 | 4.00 | 0.53 | 9.10 |
| **33** | Saatcioglu and Grira 1999, BG-9 | B | 0.06 | -0.04 | 2.76 | 0.84 | 9.83 |
| **34** | Muguruma et al. 1989, BL-1 | B | 0.02 | -0.04 | 2.75 | 0.85 | 8.00 |
| **35** | Paultre and Legeron, No. 10013015 | B | -0.09 | -0.07 | 2.30 | 0.63 | 6.10 |
| **36** | Bayrak and Sheikh 1996, AS-2HT | C | -0.02 | -0.07 | 4.50 | 0.51 | 10.36 |
| **37** | Bayrak and Sheikh 1996, AS-6HT | C | -0.06 | -0.10 | 2.86 | 0.17 | 10.14 |
| **38** | Matamoros et al. 1999,C5-00N | C | 0.01 | -0.18 | 3.10 | 0.65 | 5.10 |
| **39** | Matamoros et al. 1999,C10-05S | C | 0.17 | -0.09 | 1.41 | 0.73 | 5.29 |
| **40** | Mo and Wang 2000,C2-2 | C | -0.01 | -0.73 | 5.94 | 0.24 | 6.91 |
| **41** | Paultre et al., 2001, No. 1008040 | C | 0.26 | -0.11 | 1.61 | 0.67 | 5.97 |
| **42** | Paultre and Legeron, No. 1006025 | C | -0.06 | -0.07 | 2.68 | 0.50 | 8.73 |
| **43** | Muguruma et al. 1989, BH-2 | C | 0.00 | -0.04 | 4.29 | 0.79 | 8.86 |
| **44** | Paultre and Legeron, , No. 1006040 | C | -0.26 | -0.13 | 1.28 | 0.36 | 5.64 |
| **45** | Galeota et al. 1996, CA1 | C | 0.19 | -0.16 | 2.00 | 0.30 | 7.75 |
| **46** | Pujol 2002, No. 10-2-3N | C | 0.01 | -2.96 | 3.33 | 0.53 | 3.50 |
| **47** | Bayrak and Sheikh 1996, AS-5HT | C | 0.18 | -0.12 | 1.45 | 0.33 | 7.50 |
| **48** | Mo and Wang 2000,C1-3 | C | 0.03 | -0.11 | 2.28 | 0.63 | 6.17 |
| **49** | Mo and Wang 2000,C2-3 | C | -0.07 | -0.96 | 5.77 | 0.19 | 6.29 |
| **50** | Matamoros et al. 1999,C10-20N | C | 0.02 | -0.12 | 2.56 | 0.73 | 5.09 |
| **51** | Matamoros et al. 1999,C5-20N | C | -0.03 | -0.18 | 2.44 | 0.54 | 4.78 |
| **52** | Sugano 1996, UC15L | C | 0.02 | -0.06 | 3.10 | 0.64 | 10.25 |
| **53** | Paultre and Legeron, No. 10013025 | C | 0.24 | -0.18 | 1.81 | 0.48 | 5.81 |
| **54** | Sugano 1996, UC20L | C | 0.00 | -0.05 | 4.10 | 0.71 | 10.25 |
| **55** | Takemura., 1997, Test 1 (JSCE-4) | C | -0.01 | -0.17 | 4.70 | 0.21 | 9.00 |

**Table 4.13** Result list for in-cycle strength degradation parameters (negative dir.)

| No. | Test ID | Group | $\alpha_1$ | $\alpha_2$ | $u_c / u_y$ | $F_r / F_y$ | $u_r / u_y$ |
|---|---|---|---|---|---|---|---|
| **1** | Thomsen and Wallace 1994, B2 | A | 0.05 | -0.07 | 2.00 | 0.66 | 7.6 |
| **2** | Thomsen and Wallace 1994, C2 | A | 0.00 | -0.08 | 3.00 | 0.61 | 8.06 |
| **3** | Atalay and Penzien 1975, No. 11 | A | 0.18 | -0.24 | 2.09 | 0.64 | 4.45 |
| **4** | Thomsen and Wallace 1994, D3 | A | -0.07 | -0.11 | 1.70 | 0.25 | 7.90 |
| **5** | Thomsen and Wallace 1994, D1 | A | 0.08 | -0.09 | 2.00 | 0.40 | 9.75 |
| **6** | Sugano 1996, UC15H | A | -0.03 | -0.33 | 3.13 | 0.61 | 4.13 |
| **7** | Watson and Park 1989, No. 5 | A | 0.00 | -0.10 | 2.38 | 0.74 | 4.79 |
| **8** | Ohno and Nishioka 1984, L3 | B | 0.01 | -0.12 | 6.31 | 0.70 | 9.25 |
| **9** | Tanaka and Park 1990, No. 2 | B | -0.01 | -0.04 | 2.03 | 0.73 | 8.65 |
| **10** | Ang et al. 1981, No. 3 | B | 0.17 | -0.08 | 1.80 | 0.89 | 5.00 |
| **11** | Wehbe et al. 1998, B1 | B | 0.06 | -0.83 | 3.91 | 0.63 | 4.57 |
| **12** | Saatcioglu and Grira 1999, BG-10 | B | -0.01 | -0.20 | 9.96 | 0.55 | 11.61 |
| **13** | Atalay and Penzien 1975, No. 9 | B | 0.02 | -0.25 | 2.38 | 0.69 | 3.77 |
| **14** | Xiao. HC4-8L19-T10-0.1P | B | -0.01 | -0.12 | 6.00 | 0.71 | 8.00 |
| **15** | Saatcioglu and Grira 1999, BG-2 | B | -0.01 | -0.05 | 3.31 | 0.72 | 8.31 |
| **16** | Azizinamini et al. 1988, NC-2 | B | 0.05 | -0.05 | 2.05 | 0.87 | 5.60 |
| **17** | Saatcioglu and Grira 1999, BG-3 | B | 0.05 | -0.01 | 2.75 | 0.98 | 9.68 |
| **18** | Saatcioglu and Grira 1999, BG-4 | B | -0.04 | -0.05 | 2.40 | 0.65 | 8.31 |
| **19** | Soesianawati et al. 1986, No. 2 | B | 0.00 | -0.07 | 4.13 | 0.70 | 8.53 |
| **20** | Zahn et al. 1986, No. 7 | B | 0.00 | -0.16 | 7.71 | 0.69 | 9.86 |
| **21** | Mo and Wang 2000,C3-2 | B | -0.04 | -0.39 | 4.75 | 0.56 | 5.50 |
| **22** | Thomsen and Wallace 1994, C3 | B | 0.15 | -0.12 | 1.89 | 0.13 | 10.25 |
| **23** | Paultre and Legeron, No. 1006015 | B | -0.03 | -0.03 | 4.40 | 0.74 | 9.15 |
| **24** | Bechtoula., 2002, D1N30 | B | 0.11 | -0.10 | 2.38 | 0.77 | 6.25 |
| **25** | Sugano 1996, UC20H | B | 0.01 | -0.09 | 3.10 | 0.41 | 10.30 |
| **26** | Paultre et al., 2001, No. 1006052 | B | -0.03 | -0.09 | 4.85 | 0.73 | 6.62 |
| **27** | Mo and Wang 2000,C1-2 | B | -0.02 | -0.43 | 4.61 | 0.42 | 5.84 |
| **28** | Galeota et al. 1996, CA2 | B | 0.08 | -0.20 | 1.70 | 0.31 | 5.50 |
| **29** | Bayrak and Sheikh 1996, AS-4HT | B | 0.07 | -0.13 | 2.13 | 0.30 | 8.11 |
| **30** | Kanda et al. 1988, 85STC-1 | B | -0.02 | -0.08 | 5.20 | 0.64 | 8.70 |
| **31** | Kanda et al. 1988, 85STC-2 | B | -0.01 | -0.05 | 3.50 | 0.71 | 8.80 |
| **32** | Bayrak and Sheikh 1996, AS-3HT | B | -0.04 | -0.08 | 3.80 | 0.43 | 9.40 |
| **33** | Saatcioglu and Grira 1999, BG-9 | B | -0.03 | -0.04 | 4.18 | 0.71 | 9.75 |
| **34** | Muguruma et al. 1989, BL-1 | B | -0.02 | -0.03 | 2.25 | 0.75 | 9.25 |
| **35** | Paultre and Legeron, No. 10013015 | B | -0.10 | -0.07 | 2.30 | 0.59 | 6.10 |
| **36** | Bayrak and Sheikh 1996, AS-2HT | C | -0.08 | -0.07 | 2.86 | 0.35 | 10.46 |
| **37** | Bayrak and Sheikh 1996, AS-6HT | C | -0.03 | -0.12 | 3.14 | 0.35 | 8.14 |
| **38** | Matamoros et al. 1999,C5-00N | C | 0.00 | -0.21 | 3.30 | 0.71 | 4.63 |
| **39** | Matamoros et al. 1999,C10-05S | C | 0.05 | -0.08 | 1.48 | 0.71 | 5.29 |
| **40** | Mo and Wang 2000,C2-2 | C | -0.04 | -0.50 | 6.09 | 0.10 | 7.50 |
| **41** | Paultre et al., 2001, No. 1008040 | C | -0.04 | -0.10 | 1.33 | 0.56 | 5.62 |
| **42** | Paultre and Legeron, No. 1006025 | C | -0.03 | -0.07 | 2.63 | 0.53 | 8.65 |
| **43** | Muguruma et al. 1989, BH-2 | C | 0.03 | -0.04 | 2.89 | 0.79 | 8.91 |
| **44** | Paultre and Legeron, , No. 1006040 | C | 0.01 | -0.11 | 1.25 | 0.47 | 6.31 |
| **45** | Galeota et al. 1996, CA1 | C | -0.18 | -0.20 | 1.43 | 0.22 | 5.00 |
| **46** | Pujol 2002, No. 10-2-3N | C | 0.02 | -2.23 | 3.42 | 0.49 | 3.67 |
| **47** | Bayrak and Sheikh 1996, AS-5HT | C | 0.22 | -0.13 | 1.40 | 0.46 | 6.25 |
| **48** | Mo and Wang 2000,C1-3 | C | -0.02 | -0.30 | 5.00 | 0.59 | 6.17 |
| **49** | Mo and Wang 2000,C2-3 | C | -0.01 | -0.52 | 6.25 | 0.46 | 7.19 |
| **50** | Matamoros et al. 1999,C10-20N | C | -0.01 | -0.12 | 2.44 | 0.70 | 4.81 |
| **51** | Matamoros et al. 1999,C5-20N | C | 0.03 | -0.15 | 1.50 | 0.52 | 4.94 |
| **52** | Sugano 1996, UC15L | C | 0.01 | -0.06 | 3.10 | 0.60 | 10.25 |
| **53** | Paultre and Legeron, No. 10013025 | C | 0.13 | -0.17 | 1.83 | 0.41 | 6.00 |
| **54** | Sugano 1996, UC20L | C | 0.01 | -0.04 | 3.10 | 0.72 | 10.25 |
| **55** | Takemura., 1997, Test 1 (JSCE-4) | C | -0.01 | -0.14 | 4.50 | 0.25 | 9.56 |

**Table 4.14** Means of in-cycle strength degradation parameters for 55 cyclic tests

| **In-cycle strength degradation parameters** | | | | |
|---|---|---|---|---|
| **Positive direction** | | | **Negative direction** | |
| $\alpha_1$ = | 0.03 | | $\alpha_1$ = | 0.01 |
| $\alpha_2$ = | -0.22 | | $\alpha_2$ = | -0.19 |
| $u_c$ / $u_y$ = | 3.30 | | $u_c$ / $u_y$ = | 3.29 |
| $F_r$ / $F_y$ = | 0.60 | | $F_r$ / $F_y$ = | 0.57 |
| $u_r$ / $u_y$ = | 7.37 | | $u_r$ / $u_y$ = | 7.40 |

# CHAPTER 5

# PINCHING

## 5.1 General

RC structural members under repeated cyclic loads can exhibit degradation in strength and stiffness as discussed in the previous chapters. Another type of degradation but yet as important as the aforementioned degradation types is "pinching". Pinching can be defined as the narrowing of the hysteresis loops mainly due to the bond deterioration at the reinforcing steel and concrete interface. The formation of cracks in concrete due to the high shear forces and in turn, large amount of decrease in the stiffness of the member can also cause the pinching behavior. The energy dissipation capacity of the member decreases due to the narrowing of the hysteresis loops. Decreased energy dissipation capacity leads higher levels of damage for the structural members under strong cyclic loads that cause inelastic behavior.

Pinching takes place during reloading phase of cyclic behavior of a RC member and stiffness deteriorates significantly until the crack closure point which the member regains its stiffness after that point forming an S-shaped force-displacement curve (Figure 5.1). Thus, the pinching behavior is modeled by several researchers by introducing two different slopes for the construction of reloading branch.

In this chapter, the cyclic column tests of PEER database which exhibit pinching are used to calibrate and verify the two well-known and widely used pinching rules in the literature. These are; Roufaiel & Meyer (1987) pinching rule based on the

shear span to depth ratio and Park et al. (1987) pinching rule implemented in the structural analysis program IDARC. First, the pinching rules are introduced in detail. Then a parametric study is conducted to examine the effect of pinching rules on the cyclic behavior structural members within a broad range of values. The final part of this chapter is devoted to the verification of the first pinching model proposed by Roufaiel & Meyer and calibration of the second pinching model proposed by Park et al. by using the experimental data from PEER database.

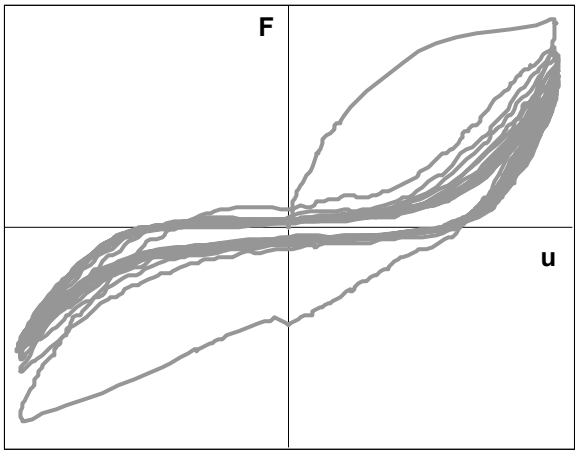


**Figure 5.1** Example force-displacement plot for pinching behavior

## 5.2 Definition of Pinching Rules

Hysteresis models proposed by several researchers for the simulation of the cyclic behavior of RC structural elements with degradation characteristics generally include stiffness and strength degradation. The drawback of these models is the absence of pinching because pinching type of degradation can be very vital for estimating the performance of the structural element since pinching is very much related with the energy dissipation characteristics of the member. There are several

hysteresis models for RC structural members in the literature that incorporates pinching. In this chapter, the focus is on the two of these models which are; Roufaiel and Meyer's model and Park et al.'s model. Only the pinching rules of the considered hysteresis models are investigated in this study.

In 1987, Roufaiel and Meyer proposed an enhanced mathematical model for RC frame members and verified the accuracy of their models by simulating various laboratory experiments present in the literature. According to their study, the proposed hysteresis model is capable of simulating the complete behavior of RC frame members under strong cyclic loads up to advanced states of degradation, even under the presence of high shear and axial forces. By evaluating test data of several researchers, Roufaiel and Meyer observed that the reloading branch gives hysteresis loops the characteristic pinched shape (S-shape) associated with diagonal shear cracks and the degree of pinching is related with the magnitude of shear force. As a result, the authors proposed an empirical pinching rule as a function of shear span-to-depth ratio ($a/d$):

$$F_p = \alpha_p F_n \qquad ; \qquad u_p = \alpha_p u_n \tag{5.1}$$

where

$$\begin{aligned} &\alpha_p = 0 && \text{for } a/d < 1.5 \\ &\alpha_p = 0.4\,(a/d) - 0.6 && \text{for } 1.5 < a/d < 4.0 \\ &\alpha_p = 1.0 && \text{for } a/d > 4.0 \end{aligned} \tag{5.2}$$

The reloading curve of the model is composed of two different branches (see Figure 5.2); first branch aims at point C ($u_p$, $F_p$) which is determined by Eq. 5.1 and 5.2. The point B ($u_n$, $F_n$) which is on the initial elastic branch is called "point of no pinching". The second branch of reloading then aims at the target point A. The worst extreme pinching occurs if the pinching parameter $\alpha_p$=0 ($a/d$ < 1.5). Then the reloading curve passes through the origin. According to this

rule, if *a/d* ratio is greater than 4.0, then no pinching is expected because of the low shear effect and reloading passes thorough the point B (point of no pinching). It should be noted that the original formulation of Roufaiel and Meyer is based on moment-curvature relationship. However, these can be replaced by any other work-conjugate pair and in this case, it is replaced by force-displacement pair in order to maintain consistency.

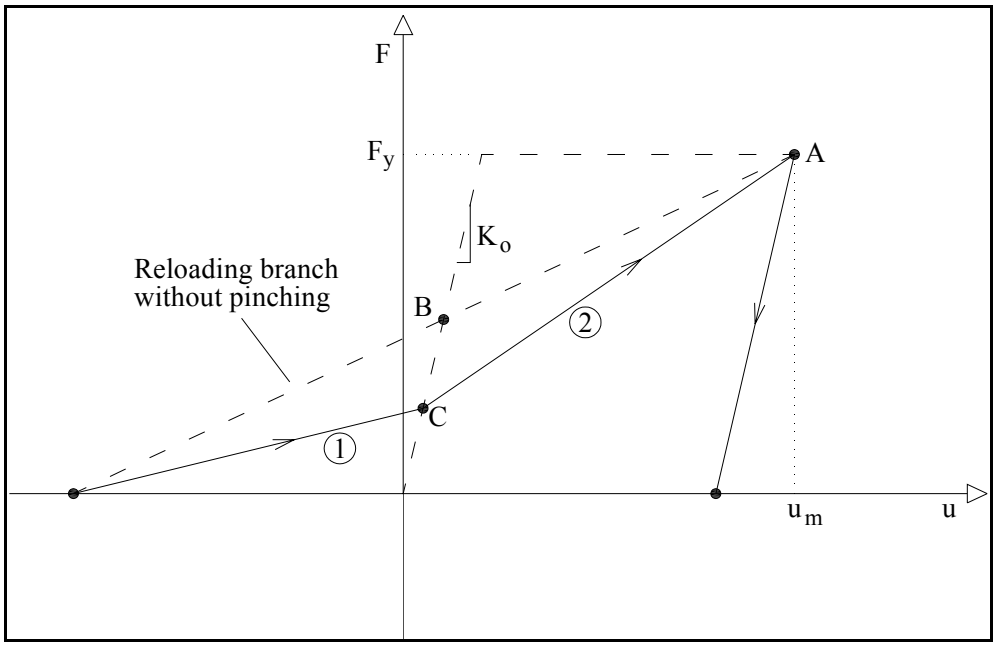


**Figure 5.2** Roufaiel and Meyer's pinching rule definition

The main parameter in Roufaiel and Meyer's pinching formulation is the *a/d* ratio which is shear span-to-depth ratio (*a/d*). Shear span (*a*) is the distance from the load to reaction. In 1950's researchers have observed that the dimensionless *a/d* ratio influenced the behavior and strength of RC members significantly. Ersoy et al. (2004) have discussed the effect of *a/d* ratio on RC beams and stated that the behavior is dominated by flexure when *a/d* ratio is large (greater than 7.0 or 8.0).

The authors stated that beams with $7 > a/d > 3$ fail by the formation of diagonal cracks at loads lower than the ones corresponding to flexural capacity. If the shear span further decreases ($1.5 < a/d < 3.0$), the type of failure is called "shear-compression failure". The member continues to carry the increasing load despite fully developed diagonal cracks until crushing of concrete in the compression zone. The formation of diagonal cracks due to the decreasing *a/d* ratio results in redistribution and the stress in longitudinal steel increases significantly. As a result, the possibility of slip of reinforcing steel increases and in turn, pinching can occur. Therefore, the *a/d* ratio used for the formulation of pinching behavior is a reasonable parameter.

The second pinching rule to be investigated is proposed by Park et al. (1987) for the hysteresis model which is developed for the computer program IDARC (Inelastic Damage Analysis of Reinforced Concrete Frame-Shear Wall Structures). IDARC is a structural analysis program developed for use as a research tool at the State University of New York at Buffalo. Park et al. investigated several hysteresis models available in the literature and found that most of them have specifically focused on a particular type of component such as beams, columns or shear walls. Then, the authors proposed a three-parameter hysteresis model that can be used to simulate all types of structural components. Stiffness, strength and pinching type of degradations are described using one parameter each. The parameter '$\gamma$' is used for the determination of pinching behavior.

Pinching behavior is modeled by introducing two different slopes for the reloading curve similar to Roufaiel and Meyer's pinching rule. First line of reloading aims at point B (see Figure 5.3) on the previous unloading branch which has a strength level of $\gamma F_y$. When the reloading reaches the displacement level of $u_s$ which is the crack closure point (point C in Figure 5.3) reloading aims the initial target point (point A in Figure 5.3). The recommended value for the parameter '$\gamma$' by IDARC is 0.5.

The main idea behind aforementioned pinching rules is to reduce the area of the hysteresis loop and implement the stiffness regain after the crack closure point to obtain the S-shaped force-displacement relationship observed from the experiments. The deformation level at which the reloading stiffness changes is the major difference between these two hysteresis models. The pinching rule proposed by Park et al. was later modified by Sivaselvan and Reinhorn (1999), by altering the crack closure point on the reloading branch. The authors proposed a weighted average of the yield and ultimate deformations for the crack closure point as a part of the study to enhance the hysteresis models to be used in computer programs IDARC2D and NSPECTRA.

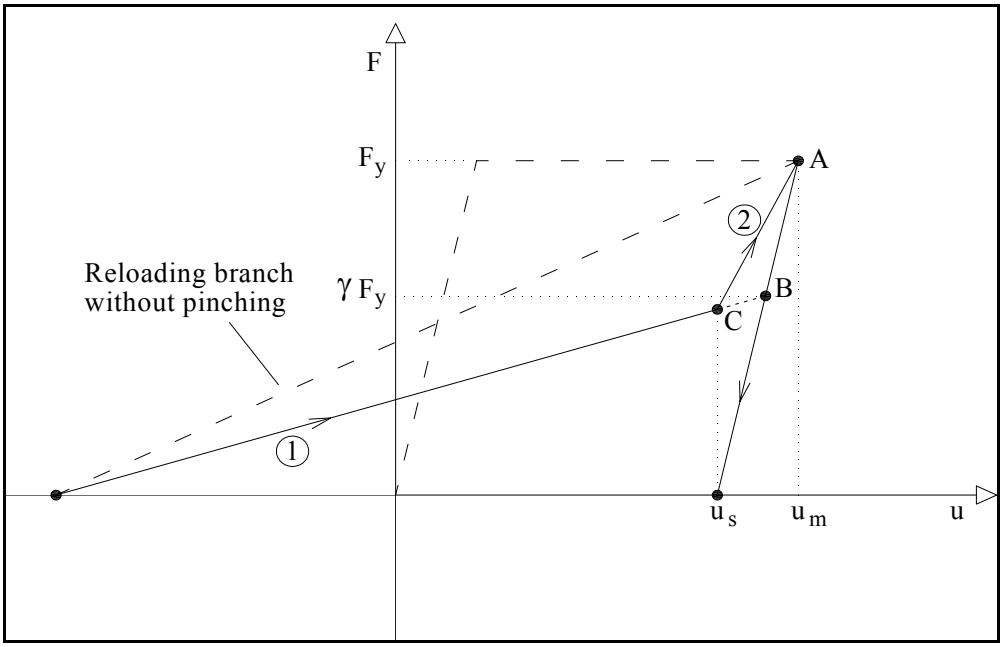


**Figure 5.3** Park et al. pinching rule definition

## 5.3 Parametric Study for Pinching Rules

In this section, a parametric study is conducted. The considered parameters are; '*a/d*' ratio for Roufaiel and Meyer's pinching rule and '$\gamma$' for Park et al.'s pinching rule. The purpose of this study is to observe the influence of the pinching parameters on the behavior and energy dissipation capacity of the structural members under cyclic loading. RC members that exhibit pinching behavior lose significant amount of their energy dissipation capacity. The degree of degradation is very much related to the selected pinching parameters. In this parametric study, a range of parameters for each pinching rule is selected and corresponding force-displacement relationships are plotted using INSPEC (Erberik, 2001) and the comparisons are made in terms of energy dissipation capacity.

Constant amplitude cyclic displacement loading history that has been employed in the parametric study of Chapter 4 is used again in this chapter for the generation of force-displacement relationships (see Figure 4.3). There exist 10 cycles in the loading history with an amplitude of 4.0 in terms of ductility ratio.

The selected *a/d* ratios for the Roufaiel and Meyer pinching case are 2.0, 2.5, 3.0, 3.5 and 4.0. '*a/d*' ratios greater than 4.0 will give the same result with the case *a/d*=4.0 according to Eq. 5.2. Also, '*a/d*' ratios equal or less than 1.5 will give extreme case of pinching where $\alpha_p$=0 meaning that the reloading passes from the origin. Therefore, *a/d* ratios greater than 4.0 and equal or less than 1.5 are not included in this parametric study.

The selected '$\gamma$' parameters for the Park et al. pinching case are 0.2, 0.3, 0.4, 0.5, 0.6, 0.7 and 0.8. Parameter $\gamma$=0.8 is selected as the upper bound because this case is very close to no-pinching situation and $\gamma$=0.2 is selected as the lower bound because below this level there are extreme pinching cases which are unlikely to occur in real structural elements.

In Figure 5.4, the force-displacement relationship generated for the no-pinching case can be seen. This is the hysteresis model proposed by Clough and Johnston (1966) which there is no strength and unloading stiffness degradation and reloading aims at the previous maximum response point. The generated force-displacement relationships for Roufaiel & Meyer and Park et al. pinching rules are presented in Figures 5.5 and 5.6, respectively.

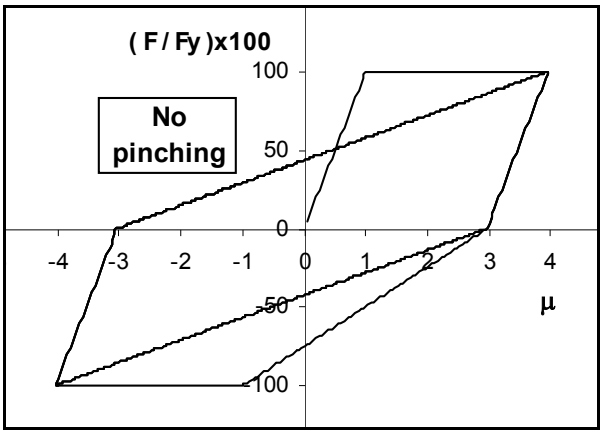


**Figure 5.4** Hysteresis model for no-pinching case

It can be observed from Figure 5.5 that, as the *a/d* ratio gets smaller, the area enclosed by the hysteresis loops gets narrower. Thus, the energy dissipation capacity decreases. When *a/d* ratio is equal to 2.0, the slope of reloading branch before the point of crack closure is nearly 25 % of the reloading slope of the no-pinching case in Figure 5.4. The case with *a/d* ratio is equal to 4.0 (Figure 5.5.a) is exactly the same with no-pinching case because the $\alpha_p$ factor in Eq. 5.2 is equal to 1.0, indicating that the reloading aims at the "point of no-pinching" (Point B in Figure 5.2).

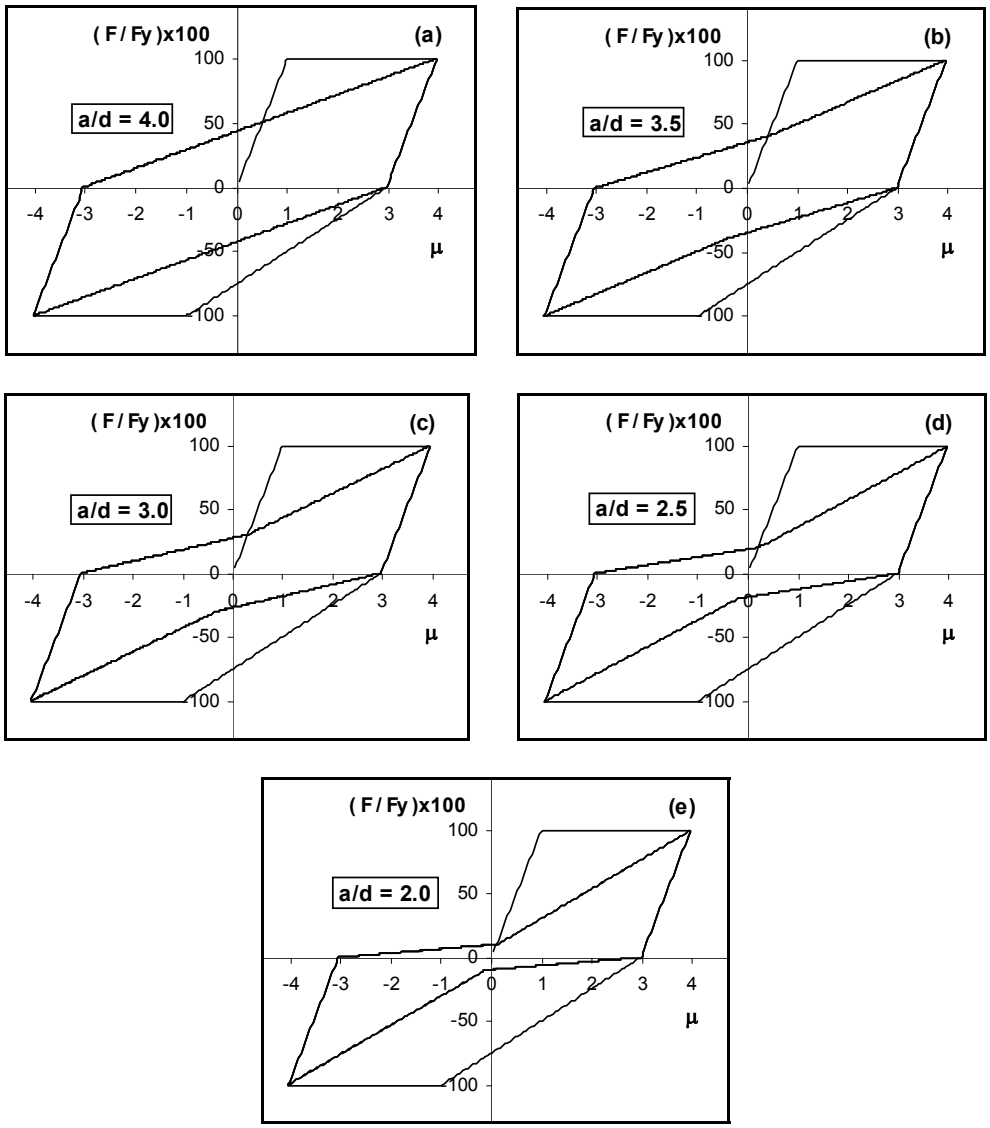


**Figure 5.5** Hysteresis models for Roufaiel&Meyer pinching case

As the pinching parameter '$\gamma$' of Park et al. rule decreases, the slope of the first reloading branch decreases and in turn, the energy dissipation capacity decreases significantly (Figure 5.6). When the first reloading aims at a strength level of 80 % of the yield strength, the reloading curve is almost linear and pinched shape of the hysteresis loops can barely be seen (Figure 5.6.a). When $\gamma$=0.2, the pinching is very severe and the slope of the first reloading branch is nearly 27 % of the reloading slope of the no-pinching case.

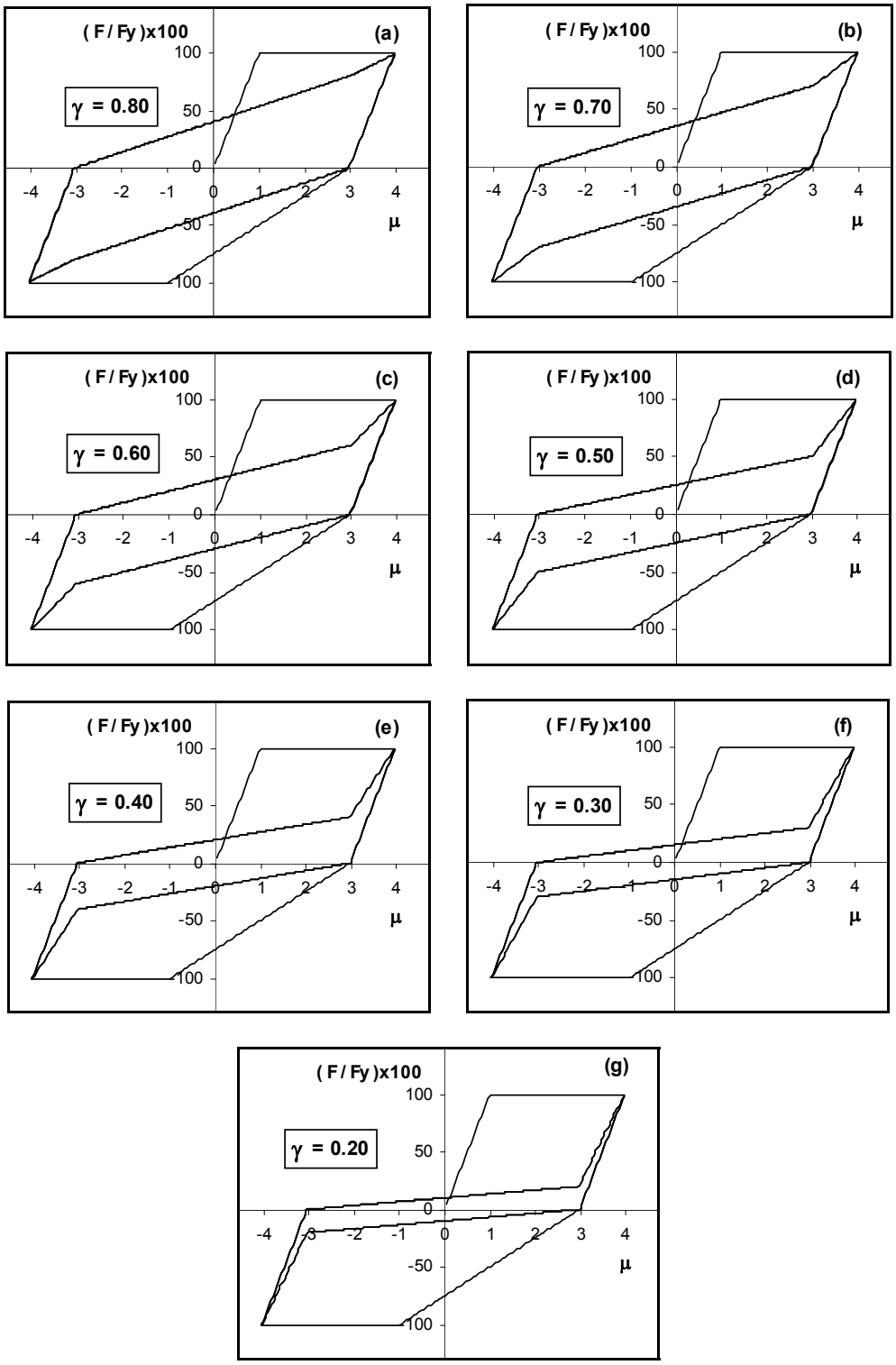


**Figure 5.6** Hysteresis models for Park et al. pinching case

Another important result can be deducted from Figures 5.5 and 5.6 in terms of rate of change of the energy dissipation capacities. Reloading curve stiffens when it reaches to the crack closure point. Park et al. pinching rule defines the location of the crack closure point at a location which is larger than Roufaiel & Meyer's pinching rule. As a result, the change in the value of parameter '$\gamma$' influences a larger area whereas the change of the *a/d* ratio and in turn $\alpha_p$ value influences a smaller area compared to Park et al. model. The dissipated energy values per half-cycle (unitless) are presented in Tables 5.1 and 5.2.

**Table 5.1** Dissipated energy per half-cycle and cumulative dissipated energy values for Roufaiel & Meyer's pinching rule

| **Half cycle #** | **Dissipated energy per half-cycle** | | | | | |
|---|---|---|---|---|---|---|
| | **No pinching** | ***a/d*=4.0** | ***a/d*=3.5** | ***a/d*=3.0** | ***a/d*=2.5** | ***a/d*=2.0** |
| **1** | 300 | 300 | 300 | 300 | 300 | 300 |
| **2** | 450 | 450 | 450 | 450 | 450 | 450 |
| **3** | 300 | 300 | 270 | 239 | 210 | 179 |
| **4** | 300 | 300 | 270 | 239 | 210 | 179 |
| **5** | 300 | 300 | 270 | 239 | 210 | 179 |
| **6** | 300 | 300 | 270 | 239 | 210 | 179 |
| ⋮ | ⋮ | ⋮ | ⋮ | ⋮ | ⋮ | ⋮ |
| **20** | 300 | 300 | 270 | 239 | 210 | 179 |
| **Cum. diss. energy** | **6150** | **6150** | **5610** | **5052** | **4530** | **3972** |

The normalized cumulative dissipated energy values with respect to no-pinching case are listed in Table 5.3. It can be observed that the energy dissipation capacities decrease with decreasing *a/d* ratio and $\gamma$ values.

**Table 5.2** Dissipated energy per half-cycle and cumulative dissipated energy values for Park et al. pinching rule

| Half cycle # | Dissipated energy per half-cycle | | | | | | | |
|---|---|---|---|---|---|---|---|---|
| | **No pinching** | **γ=0.8** | **γ=0.7** | **γ=0.6** | **γ=0.5** | **γ=0.4** | **γ=0.3** | **γ=0.2** |
| **1** | 300 | 300 | 300 | 300 | 300 | 300 | 300 | 300 |
| **2** | 450 | 450 | 450 | 450 | 450 | 450 | 450 | 450 |
| **3** | 300 | 280 | 245 | 210 | 175 | 140 | 105 | 70 |
| **4** | 300 | 280 | 245 | 210 | 175 | 140 | 105 | 70 |
| **5** | 300 | 280 | 245 | 210 | 175 | 140 | 105 | 70 |
| **6** | 300 | 280 | 245 | 210 | 175 | 140 | 105 | 70 |
| ⋮ | ⋮ | ⋮ | ⋮ | ⋮ | ⋮ | ⋮ | ⋮ | ⋮ |
| **20** | 300 | 280 | 245 | 210 | 175 | 140 | 105 | 70 |
| **Cum. diss. energy** | **6150** | **5790** | **5160** | **4530** | **3900** | **3270** | **2640** | **2010** |

**Table 5.3** Comparison of the normalized cumulative dissipated energy of the hysteresis models

| **Pinching Rule** | | **Normalized Cumulative Dissipated Energy** |
|---|---|---|
| No-pinching | | **100** |
| Roufaiel & Meyer | $a/d$ = 4.0 | 100 |
| Roufaiel & Meyer | $a/d$ = 3.5 | 91 |
| Roufaiel & Meyer | $a/d$ = 3.0 | 82 |
| Roufaiel & Meyer | $a/d$ = 2.5 | 74 |
| Roufaiel & Meyer | $a/d$ = 2.0 | 65 |
| Park et al. | $\gamma$ = 0.8 | 94 |
| Park et al. | $\gamma$ = 0.7 | 84 |
| Park et al. | $\gamma$ = 0.6 | 74 |
| Park et al. | $\gamma$ = 0.5 | 63 |
| Park et al. | $\gamma$ = 0.4 | 53 |
| Park et al. | $\gamma$ = 0.3 | 43 |
| Park et al. | $\gamma$ = 0.2 | 33 |

Figures 5.7 and 5.8 illustrate the dissipated energy values normalized by the dissipated energy values of the no-pinching model for each half-cycle in the positive direction of loading. In Figure 5.7, it is observed that the models with *a/d*=4.0 and 3.5 shows no pinching and slight pinching, respectively. The model with *a/d*=3.5 loses only 10 % of its energy dissipation capacity per half-cycle whereas this amount is more than 40 % in the model with *a/d*=2.0. It is observed from the Figure 5.8 that for the Park et al. pinching rule with $\gamma = 0.2$, the energy dissipation capacity of the half-cycles after initial half-cycle is nearly 20 % of the corresponding half-cycles of no-pinching case.

Cumulative dissipated energy values per half-cycle normalized by the total dissipated energy by the no-pinching model in the positive direction of loading versus number of half-cycles relation can be seen in Figures 5.9 and 5.10. These figures confirm that the energy dissipation capacity loses with respect to the pinching parameters is very important. The selection of parameter '$\gamma$' is crucial because of the fact that, the effect of '$\gamma$' on the energy dissipation capacity is more significant.

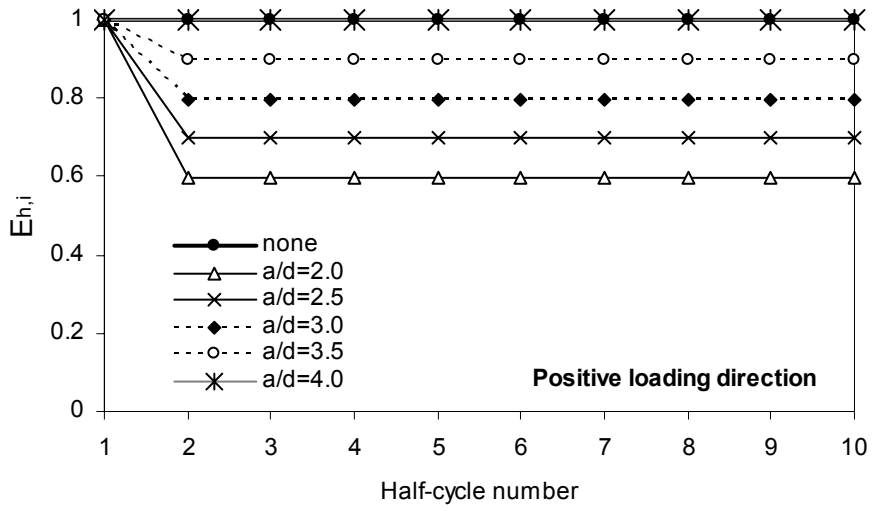


**Figure 5.7** Comparison of dissipated energy per half-cycle vs. number of half-cycles for Roufaiel&Meyer pinching case

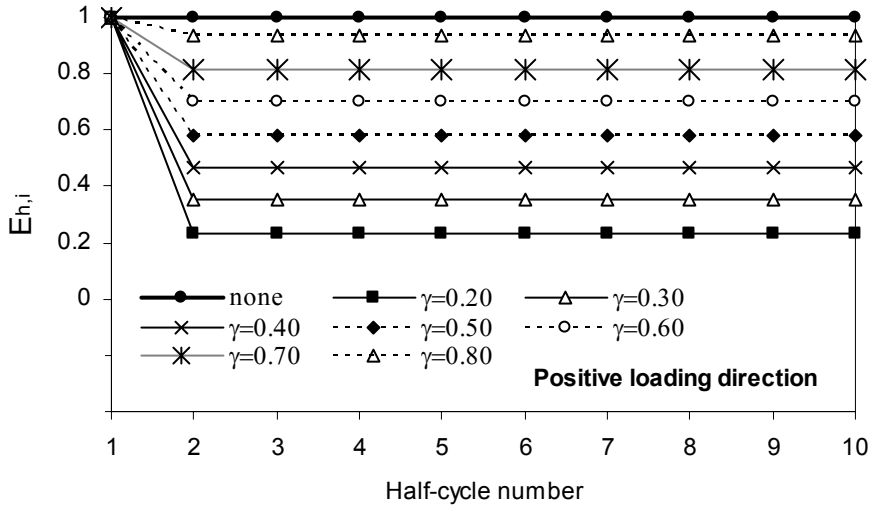


**Figure 5.8** Comparison of dissipated energy per half-cycle vs. number of half-cycles for Park et al. pinching case

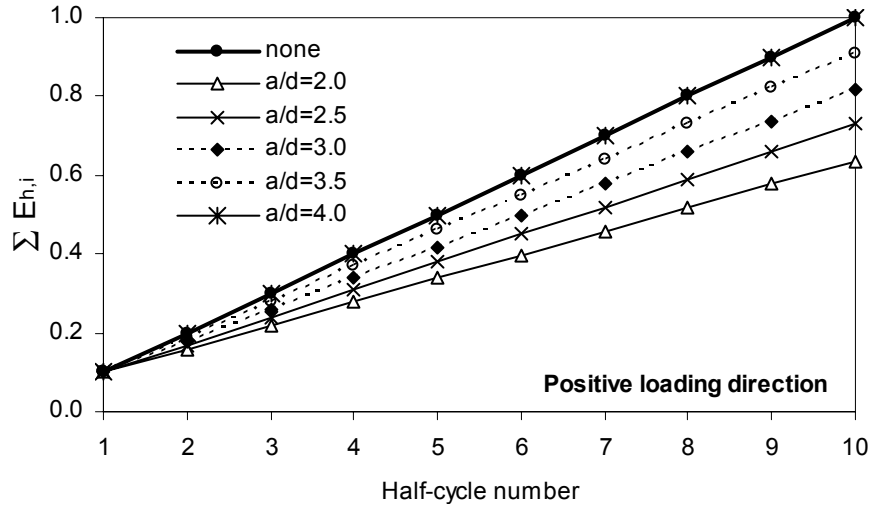


**Figure 5.9** Comparison of cumulative dissipated energy per half-cycle vs. number of half-cycles for Roufaiel&Meyer pinching case

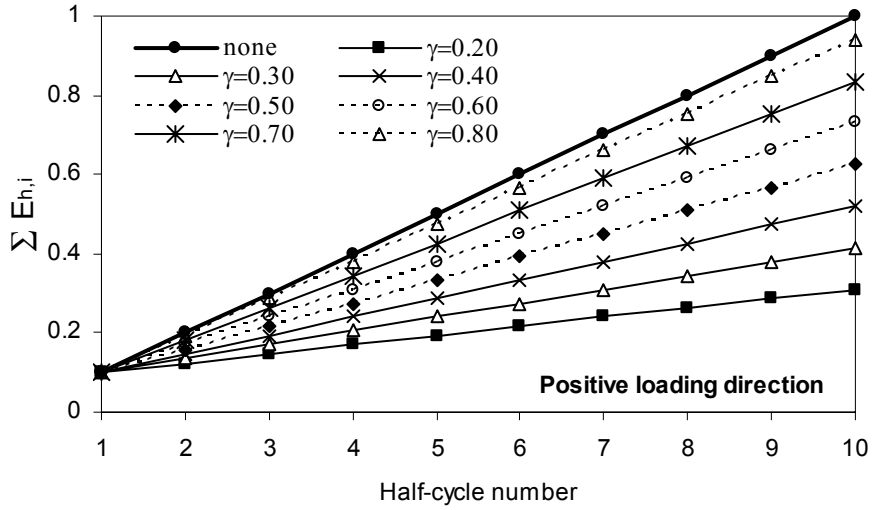


**Figure 5.10** Comparison of cumulative dissipated energy per half-cycle vs. number of half-cycles for Park et al. pinching case

## 5.4 Selection of Test Data

25 cyclic column tests which have pinched shaped half-cycles are selected from the PEER database for this study. The pinching behavior is not frequently observed in the columns of PEER database, as a result the number of tests is restrained at a number of 25. The half-cycles which have pinching behavior are extracted from the whole force-displacement relationship and investigated in terms of the parameters of the two aforementioned pinching rules.

The selected column tests are listed in Table 5.4 along with the group letters which were discussed in Chapter 2 and with the selected material and structural properties such as concrete strength, longitudinal reinforcement ratio, volumetric transverse reinforcement ratio, axial load ratio and shear ratio. The definition of these properties is done in Chapter 2.

**Table 5.4** Selected cyclic column tests from column database for pinching study

| No. | Test ID | Group | $f_c$ (Mpa) | $\rho_l$ | $\rho_t$ | Axial load ratio | Shear ratio |
|---|---|---|---|---|---|---|---|
| **1** | Atalay and Penzien 1975, No. 1S1 | B | 29.1 | 0.0163 | 0.015 | 0.10 | 0.138 |
| **2** | Atalay and Penzien 1975, No. 2S1 | B | 30.7 | 0.0163 | 0.009 | 0.09 | 0.132 |
| **3** | Atalay and Penzien 1975, No. 3S1 | B | 29.2 | 0.0163 | 0.015 | 0.10 | 0.127 |
| **4** | Atalay and Penzien 1975, No. 4S1 | A | 27.6 | 0.0163 | 0.009 | 0.10 | 0.112 |
| **5** | Atalay and Penzien 1975, No. 6S1 | C | 31.8 | 0.0163 | 0.009 | 0.18 | 0.160 |
| **6** | Erberik and Sucuoglu 2001, CAH-3 | C | 20.6 | 0.0134 | 0.013 | 0.00 | 0.187 |
| **7** | Erberik and Sucuoglu 2001, CAH-4 | C | 20.6 | 0.0134 | 0.013 | 0.00 | 0.186 |
| **8** | Erberik and Sucuoglu 2001, CAH-5 | C | 21.2 | 0.0134 | 0.013 | 0.00 | 0.176 |
| **9** | Erberik and Sucuoglu 2001, CAH-6 | C | 20.6 | 0.0134 | 0.013 | 0.00 | 0.183 |
| **10** | Erberik and Sucuoglu 2001, CAL-9 | C | 13 | 0.0134 | 0.013 | 0.00 | 0.213 |
| **11** | Erberik and Sucuoglu 2001, CALU-11 | C | 13 | 0.0134 | 0.013 | 0.00 | 0.217 |
| **12** | Pujol 2002, No. 10-1-2.25S | C | 36.5 | 0.0245 | 0.015 | 0.08 | 0.457 |
| **13** | Pujol 2002, No. 10-2-2.25N | C | 34.9 | 0.0245 | 0.015 | 0.08 | 0.464 |
| **14** | Pujol 2002, No. 10-2-2.25S | C | 34.9 | 0.0245 | 0.015 | 0.08 | 0.464 |
| **15** | Pujol 2002, No. 10-2-3N | C | 33.7 | 0.0245 | 0.011 | 0.08 | 0.457 |
| **16** | Pujol 2002, No. 10-3-1.5S | B | 32.1 | 0.0245 | 0.022 | 0.09 | 0.467 |
| **17** | Pujol 2002, No. 10-3-2.25N | C | 27.4 | 0.0245 | 0.015 | 0.10 | 0.514 |
| **18** | Pujol 2002, No. 10-3-3N | C | 29.9 | 0.0245 | 0.011 | 0.10 | 0.484 |
| **19** | Wehbe et al. 1998, A1 | B | 27.2 | 0.0222 | 0.005 | 0.10 | 0.292 |
| **20** | Wehbe et al. 1998, A2 | C | 27.2 | 0.0222 | 0.005 | 0.24 | 0.315 |
| **21** | Wehbe et al. 1998, B1 | B | 28.1 | 0.0222 | 0.006 | 0.09 | 0.294 |
| **22** | Wehbe et al. 1998, B2 | B | 28.1 | 0.0222 | 0.006 | 0.23 | 0.316 |
| **23** | Wight and Sozen 1973, No. 25.033E | C | 33.6 | 0.0245 | 0.007 | 0.07 | 0.349 |
| **24** | Wight and Sozen 1973, No. 25.033W | C | 33.6 | 0.0245 | 0.007 | 0.07 | 0.374 |
| **25** | Wight and Sozen 1973, No. 40.033E | B | 33.6 | 0.0245 | 0.007 | 0.11 | 0.374 |

There are 16 column tests among the selected tests which are included in Group C. Group C columns have energy-based index $I_{SD}$ less than 0.7 indicating that the energy dissipation capacities are low. Pinching behavior is the main factor for this and it should be expected that most of the column tests that experienced pinching are Group C columns. There are also eight Group B columns and one Group A column in the selected tests for pinching.

## 5.5 The Validity of Pinching Rules Regarding Cyclic Test Data

The purpose of this part of the study is to verify and compare the two pinching rules with the actual test data and to observe the improvement in terms of

modeling of the RC members with the implementation of pinching rules in the hysteresis models. Also, the factors affecting pinching type of degradation are discussed.

Dissipated energy value of the half-cycle that experienced pinching is the main quantity that enables us to compare the pinching rules. For this purpose, the experimental dissipated energy values are compared with the dissipated energy values of analytical half-cycles which are generated by considering the pinching rules. The sketch showing the experimental and analytical half-cycles for the comparison of pinching rules can be seen in Figure 5.11. In this figure, the thin solid curve represents the actual half-cycle with pinching behavior. The thick solid line represents the analytical half-cycle generated by using pinching rules. The location of crack closure point ($u_s$) in this figure is only for illustration. The analytical half-cycle shown with dashed lines is the half-cycle of none-degrading model. Dissipated energy per half-cycle value of non-degrading model is also calculated since it is used to assess the degree of pinching by comparing it with the actual dissipated energy per half-cycle value. In Figure 5.11 $F_i$ and $u_m$ represent the strength capacity and maximum displacement value of the half-cycle of interest, respectively.

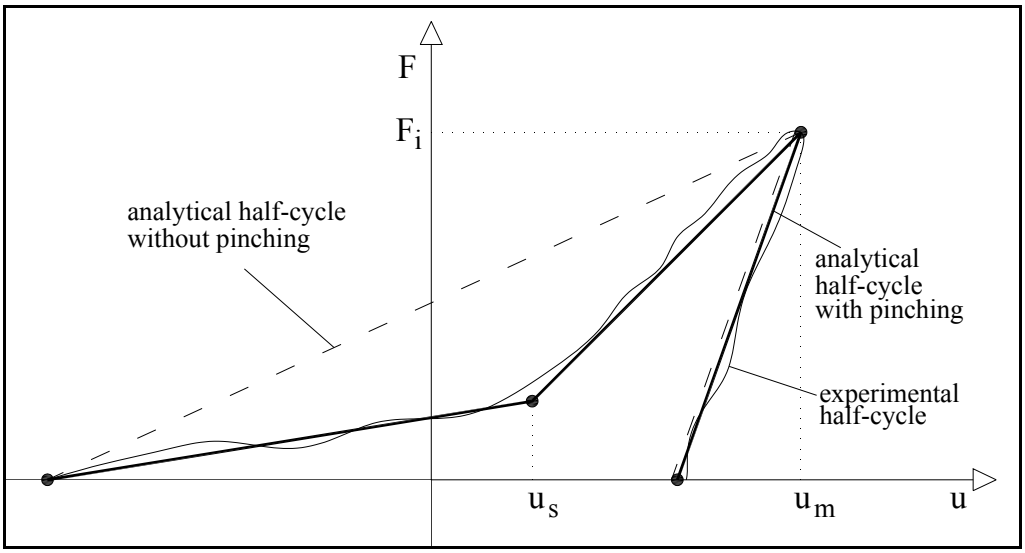


**Figure 5.11** Sketch for the calculation of the dissipated energy values

The experimental dissipated energy per half-cycle values are calculated from the available digitized force-displacement data as explained in Chapter 2. Also, observed strength capacities ($F_i$) at each half-cycle are recorded for the calculation of analytical dissipated energy values in order to isolate the effect of pinching behavior from the effects of strength and stiffness degradation behaviors. The analytical half-cycles for the Roufaiel & Meyer's pinching rule and Park et al. pinching rule are determined from the geometrical relations using the strength capacity of the actual half-cycle ($F_i$), maximum displacement value ($u_m$), initial elastic stiffness ($K_0$) and pinching parameters ($\alpha_p$ for Roufaiel & Meyer's pinching rule and $\gamma$ for Park et al. pinching rule). Initial elastic stiffness ($K_0$) is needed because unloading branch of the analytical half-cycle is assumed to be equal to initial stiffness meaning that there is no unloading stiffness degradation. Also, for the determination of the crack closure point for Roufaiel & Meyer's pinching (point C in Figure 5.2) which is on the initial elastic branch, the $K_0$ value should be known.

The formulations for the determination of energy dissipation capacities ($E_{h,i}$) for the analytical half-cycles of Roufaiel & Meyer's and Park et al.'s pinching rule are given in Equations 5.3 and 5.4, respectively.

$$E_{h,i} = 0.5 F_i \left(\alpha_p + 1\right)\left(u_m - \frac{F_i}{K_0}\right) \tag{5.3}$$

$$E_{h,i} = \gamma F_i \left[\frac{2\left(u_m - F_i/K_0\right)}{2\left(u_m - F_i/K_0\right) + \gamma\left(F_i/K_0\right)}\right]\left[u_m - 0.5\left(F_i/K_0\right)\right] \tag{5.4}$$

For the calculation of the energy dissipation value of non-degrading model, Eq. 5.3 is used with $\alpha_p$=1.0. Non-degrading model is exactly the same as Roufaiel & Meyer's model when $\alpha_p$=1.0, because the reloading aims at the "point of no pinching" (point B in Figure 5.2) in that case. Energy value of analytical half-cycle for Roufaiel & Meyer's pinching model is calculated using the available *a/d* ratio (*a/d* ratio is used for determining $\alpha_p$, Eq. 5.2) obtained from the PEER database. Park et al. recommended the value of 0.5 for the parameter $\gamma$. Thus, the energy dissipation value for Park et al. rule is determined by employing Eq. 5.4 with $\gamma$=0.5.

In order to assess the pinching rules in terms of dissipated energy in a more convenient basis, "energy ratio" is introduced. Energy ratio is defined as the ratio of the dissipated energy of analytical half-cycle determined from Equations 5.3 and 5.4 to the experimental dissipated energy of corresponding half-cycle. If this ratio is equal to 1.0, then the analytical half-cycle dissipates exactly the same amount of energy and it is a perfect match. If energy ratio is larger than 1.0, then the energy dissipation capacity determined from analytical pinching model is larger than the actual energy value obtained from the experiment. In other words, analytical model overestimates the energy dissipation capacity for that half-cycle. If energy ratio is less than 1.0, then the energy dissipation capacity is underestimated by the analytical model. In either case, the deviation in the estimation of energy dissipation capacity may lead to serious error in the assessment of the performance of RC members under strong cyclic loading.

The calibration of the parameter '$\gamma$' of Park et al. pinching rule is another subject of interest. Park et al. hysteresis model used in the structural analysis program IDARC recommends a value of 0.5 for '$\gamma$' as a default value for the analysis of RC members having pinching behavior. The selected column tests are investigated in terms of parameter $\gamma$ and the actual values of $\gamma$ are calculated using energy equivalent analytical half-cycles. Eq. 5.4 is employed with a range of $\gamma$ values and the value of $\gamma$ which gives the best estimation with a minimum error in the

dissipated energy is identified as '$\gamma_{actual}$' . Then the actual $\gamma$ values are compared with the default value of 0.5 by observing the results obtained from selected 25 cyclic column tests.

The procedure described above is illustrated over an example column test which is conducted by Erberik & Sucuoglu (2001) (specimen CAH-6). The force-displacement relationship is plotted in Figure 5.12. As it can be seen in Figure 5.12, after the initial half-cycle, pinching behavior is present for all remaining half-cycles in both positive and negative directions of loading.

Table 5.5 summarizes the results obtained for the half-cycles (except for the first half-cycle) in the positive direction of loading. In the first two columns of the table, the experimental dissipated energy and strength values at each half-cycle are listed. In columns 3 & 4, there exist the analytical dissipated energy values and energy ratios obtained from the non-degrading model. As it can be observed from the energy ratios; energy dissipation capacities are highly overestimated by non-degrading model. Calculated energy dissipation capacity of non-degrading model considering all pinched half-cycles is nearly 2.5 times (average of the energy ratios) of actual energy dissipation capacity. In the Roufaiel & Meyer pinching model section, $\alpha_p$ value computed from Eq. 5.2 as 0.73 ($a/d$=3.33) and it is listed along with the energy values of analytical model and energy ratios. By investigating the energy ratios, a slight improvement over the non-degrading model can be observed. Experimental energy dissipation is nearly 50 % of the capacity obtained from Roufaiel and Meyer's pinching model. However, a better estimation is achieved by Park et al. pinching rule with the default value of 0.5 for parameter $\gamma$. In this case, average of the energy ratios is 1.31 meaning that estimated energy dissipation capacity from analytical model is 31 % higher than the actual energy dissipation capacity. On the other hand, if the $\gamma$ parameters obtained from energy equivalent analytical half-cycles ($\gamma_{actual}$) are investigated; $\gamma_{actual}$ values are smaller than the default value of 0.5. The average of $\gamma_{actual}$ values is 0.4 and if this value is used for the pinching parameter, much better estimation in energy dissipation capacity will be achieved.

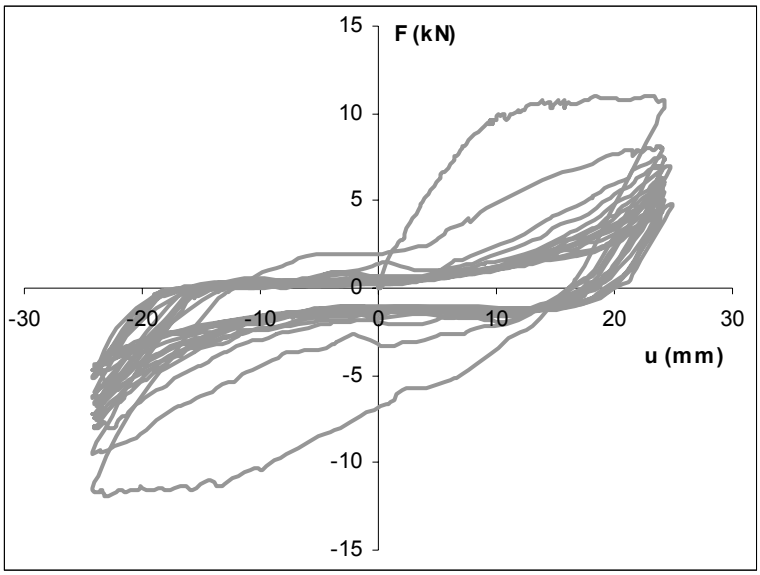


**Figure 5.12** Force-displacement plot for Erberik&Sucuoglu 2001, CAH-6 specimen

**Table 5.5** Energy ratio calculations for Erberik&Sucuoglu 2001, CAH-6 specimen (positive direction only)

| | **Experimental Data** | | **Non-degrading Model** | | **Roufaiel&Meyer Pinching Model** | | | **Park et al. Pinching Model** | | | |
|---|---|---|---|---|---|---|---|---|---|---|---|
| **no** | $E_{h,i}$ ***(Nm)*** | $F_i$ ***(kN)*** | $E_{h,i}$ ***(Nm)*** | **Energy ratio** | $\alpha_p$ | $E_{h,i}$ ***(Nm)*** | **Energy ratio** | $\gamma_{actual}$ | $\gamma_{default}$ | $E_{h,i}$ ***(Nm)*** | **Energy ratio** |
| **1** | 116.76 | 8.2 | 135.73 | 1.16 | 0.73 | 117.54 | 1.01 | 0.80 | 0.50 | 74.73 | 0.64 |
| **2** | 69.17 | 7.5 | 128.91 | 1.86 | 0.73 | 111.64 | 1.61 | 0.49 | 0.50 | 70.27 | 1.02 |
| **3** | 56.25 | 6.9 | 122.36 | 2.18 | 0.73 | 105.96 | 1.88 | 0.42 | 0.50 | 66.15 | 1.18 |
| **4** | 51.23 | 6.9 | 122.36 | 2.39 | 0.73 | 105.96 | 2.07 | 0.38 | 0.50 | 66.15 | 1.29 |
| **5** | 42.33 | 6.3 | 115.15 | 2.72 | 0.73 | 99.72 | 2.36 | 0.33 | 0.50 | 61.75 | 1.46 |
| **6** | 40.10 | 5.9 | 109.98 | 2.74 | 0.73 | 95.25 | 2.38 | 0.33 | 0.50 | 58.68 | 1.46 |
| **7** | 37.69 | 5.7 | 107.29 | 2.85 | 0.73 | 92.91 | 2.46 | 0.32 | 0.50 | 57.10 | 1.51 |
| **8** | 35.37 | 5.6 | 105.92 | 2.99 | 0.73 | 91.72 | 2.59 | 0.31 | 0.50 | 56.29 | 1.59 |
| **9** | 36.39 | 5.5 | 104.53 | 2.87 | 0.73 | 90.52 | 2.49 | 0.32 | 0.50 | 55.49 | 1.52 |
| **10** | 38.47 | 5.1 | 98.78 | 2.57 | 0.73 | 85.54 | 2.22 | 0.36 | 0.50 | 52.17 | 1.36 |
| **11** | 36.34 | 4.7 | 92.74 | 2.55 | 0.73 | 80.31 | 2.21 | 0.37 | 0.50 | 48.75 | 1.34 |
| **12** | 33.61 | 4.4 | 88.02 | 2.62 | 0.73 | 76.22 | 2.27 | 0.36 | 0.50 | 46.10 | 1.37 |
| **13** | 35.77 | 4.4 | 88.02 | 2.46 | 0.73 | 76.22 | 2.13 | 0.38 | 0.50 | 46.10 | 1.29 |
| **14** | 35.78 | 4.6 | 91.18 | 2.55 | 0.73 | 78.96 | 2.21 | 0.37 | 0.50 | 47.87 | 1.34 |
| | | | **Average** | **2.47** | | | **2.13** | **0.40** | | | **1.31** |

The procedure explained above, is repeated for 397 pinched half-cycles extracted from the selected 25 cyclic column tests. The results are listed in Table 5.6. In the first two columns of the table, shear span-to-depth (*a/d*) ratios of the test specimens and calculated $\gamma_{actual}$ values are listed. $\gamma_{actual}$ values listed for each tests are obtained from the average values for each half-cycle of that test for positive and negative direction together. The next three columns list the average values of energy ratios for each test in terms of non-degrading model (no pinching), Roufaiel & Meyer pinching model and Park et al. pinching model.

**Table 5.6** Result list for the pinching calculations

| | | | | **Non-deg. Model** | **Rou.&Meyer Model** | **Park Model** |
|---|---|---|---|---|---|---|
| | | | **Actual γ** | **Energy ratio** | **Energy ratio** | **Energy ratio** |
| **No.** | **Specimen Name** | ***a/d*** | **(average)** | **(average)** | **(average)** | **(average)** |
| **1** | Atalay and Penzien 1975, No. 1S1 | 5.5 | 0.73 | 1.30 | 1.30 | 0.72 |
| **2** | Atalay and Penzien 1975, No. 2S1 | 5.5 | 0.80 | 1.15 | 1.15 | 0.62 |
| **3** | Atalay and Penzien 1975, No. 3S1 | 5.5 | 0.80 | 1.15 | 1.15 | 0.62 |
| **4** | Atalay and Penzien 1975, No. 4S1 | 5.5 | 0.73 | 1.27 | 1.27 | 0.70 |
| **5** | Atalay and Penzien 1975, No. 6S1 | 5.5 | 0.74 | 1.31 | 1.31 | 0.71 |
| **6** | Erberik and Sucuoglu 2001, CAH-3 | 3.33 | 0.42 | 2.38 | 2.06 | 1.23 |
| **7** | Erberik and Sucuoglu 2001, CAH-4 | 3.33 | 0.60 | 1.68 | 1.46 | 0.86 |
| **8** | Erberik and Sucuoglu 2001, CAH-5 | 3.33 | 0.42 | 2.22 | 1.92 | 1.18 |
| **9** | Erberik and Sucuoglu 2001, CAH-6 | 3.33 | 0.49 | 2.06 | 1.78 | 1.10 |
| **10** | Erberik and Sucuoglu 2001, CAL-9 | 3.33 | 0.42 | 2.24 | 1.94 | 1.20 |
| **11** | Erberik and Sucuoglu 2001, CALU-11 | 3.33 | 0.26 | 3.49 | 3.02 | 1.93 |
| **12** | Pujol 2002, No. 10-1-2.25S | 2.25 | 0.67 | 1.44 | 0.93 | 0.77 |
| **13** | Pujol 2002, No. 10-2-2.25N | 2.25 | 0.60 | 1.61 | 1.05 | 0.85 |
| **14** | Pujol 2002, No. 10-2-2.25S | 2.25 | 0.61 | 1.59 | 1.04 | 0.85 |
| **15** | Pujol 2002, No. 10-2-3N | 2.25 | 0.63 | 1.54 | 1.00 | 0.83 |
| **16** | Pujol 2002, No. 10-3-1.5S | 2.25 | 0.80 | 1.10 | 0.72 | 0.59 |
| **17** | Pujol 2002, No. 10-3-2.25N | 2.25 | 0.64 | 1.48 | 0.96 | 0.80 |
| **18** | Pujol 2002, No. 10-3-3N | 2.25 | 0.64 | 1.52 | 0.99 | 0.81 |
| **19** | Wehbe et al. 1998, A1 | 3.83 | 0.79 | 1.17 | 1.13 | 0.63 |
| **20** | Wehbe et al. 1998, A2 | 3.83 | 0.79 | 1.21 | 1.16 | 0.63 |
| **21** | Wehbe et al. 1998, B1 | 3.83 | 0.79 | 1.13 | 1.09 | 0.59 |
| **22** | Wehbe et al. 1998, B2 | 3.83 | 0.79 | 1.15 | 1.11 | 0.62 |
| **23** | Wight and Sozen 1973, No. 25.033(E) | 2.87 | 0.55 | 1.71 | 1.32 | 0.95 |
| **24** | Wight and Sozen 1973, No. 25.033(W) | 2.87 | 0.55 | 1.67 | 1.29 | 0.93 |
| **25** | Wight and Sozen 1973, No. 40.033(E) | 2.87 | 0.62 | 1.53 | 1.18 | 0.82 |
| | **Average** | **3.49** | **0.64** | **1.60** | **1.33** | **0.86** |

By investigating Table 5.6, following observations can be made:

- Non-degrading model energy ratio average is calculated as 1.60 indicating that the non-degrading model which does not include pinching overestimates the actual energy dissipation capacity of the specimen by 60 %. This is not acceptable for a precise calculation of the performance of the structural member. Therefore, using a hysteresis model which does not include pinching can lead to serious misjudgments of the performance level of a structural member which likely to exhibit pinching behavior.
- Roufaiel & Meyer pinching rule's energy ratio average is 1.33. There is a 27 % improvement over the non-degrading model for the estimation of dissipated energy. The agreement with the actual pinching behavior is better but it should be noted that the energy ratio value of 1.33 means that the Roufaiel & Meyer's pinching rule overestimates the actual energy dissipation capacity which is on the unsafe side for the analysis of the performance.
- Park et al. pinching rule's energy ratio average is 0.86 meaning that this rule underestimates the energy dissipation capacity. However, if a value about 0.64 for the parameter $\gamma$ is employed in the calculation of the dissipated energy instead of 0.50 (which is the recommended value), a much better estimation will be achieved because increasing $\gamma$ also increases the area of the analytical half cycle and in turn, energy dissipation capacity.
- Non-degrading model's energy ratio can be considered as an indicator for the degree of pinching. If the non-degrading energy ratio is close to 1.0 then, the narrowing of the loops is small and the member can dissipate energy almost as much as the non-degrading model. Larger the non-degrading energy ratio indicates more severe pinching degradation. Roufaiel & Meyer's pinching rule gives better estimation for Atalay and Penzien (1975), Pujol (2002) and Wehbe et al. (1998) tests which have a non-degrading model energy ratio average of 1.32. On the other hand, Park et al. pinching rule (with default $\gamma$) gives better estimation for Erberik & Sucuoglu (2001) and Wight & Sozen (1973) tests which have a non-degrading model energy ratio average of 2.11. As a general observation, the

Park et al. pinching rule gives better results when there is severe pincing behavior whereas Roufaiel & Meyer's pinching rule is better for moderate or slight pinching degrees.

Phan et al. (1993) investigated experimental results of fifty five RC frame specimens to develop empirical expressions for predicting the three parameters of IDARC hysteresis model (Park et al. model). Empirical expressions for the hysteresis parameters are formulated by correlating the estimated parameters identified from the test data with a set of material and geometrical properties of the specimens. Then these results are used for the analysis of two frame structures with IDARC. The results show that the predicted hysteresis parameters give better results than the results obtained using default parameters. This confirms with the results seen in Table 5.6 that default value of parameter $\gamma$ does not always give good estimations and should be used with caution.

Among the selected 25 tests, the tests of Erberik & Sucuoglu (2001) show the most pinching degradation with an average non-degrading model energy ratio of 2.35. Test specimens have plain longitudinal reinforcing bars which can easily lose its contact with concrete and slip. This phenemonen is mentioned before to be the main reason for pinching behavior.

Several reseachers reveal the fact that the axial load level and the energy dissipation capacity is related with each other. Erberik and Acun (2005) stated that the presence of axial load on a RC column enhances the energy dissipation capacity in the sense that it closes the cracks and results in fatter cycles. Atalay and Penzien (1975) concluded that considerable effect of pinching deformations becomes noticable when the applied axial load is relatively low. To observe this relation, the axial load ratios of the 25 column tests versus non-degrading model energy ratios (measure of pinching) is plotted in Figure 5.13. The relation confirms with the above discussion that when the axial load level is increased, energy dissipation capacity is increased also and pinching effect decreases.

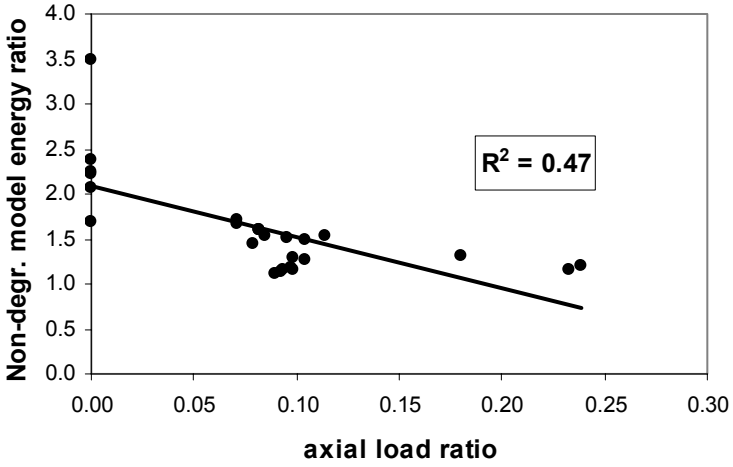


**Figure 5.13** Correlation between axial load ratio and non-degrading model energy ratio

The relationship between the *a/d* ratio and pinching is discussed in the Section 5.2. In 1989, Chung et al. also stated that one of the variables affecting the energy dissipation capacity of a RC member is shear span. The shear span-to-depth ratios (*a/d*) versus non-degrading model energy ratios of the 19 column tests are plotted in Figure 5.14. The test result of Erberik & Sucuoglu (2001) are not included because of the plain bars used for longitudinal reinforcement. It can be observed from Figure 5.14 that, when *a/d* ratio gets smaller pinching effect increases due to increase in the shear demand of the column. Considering the limited data, it can be further stated that specimens with larger *a/d* ratio experience less pinching.

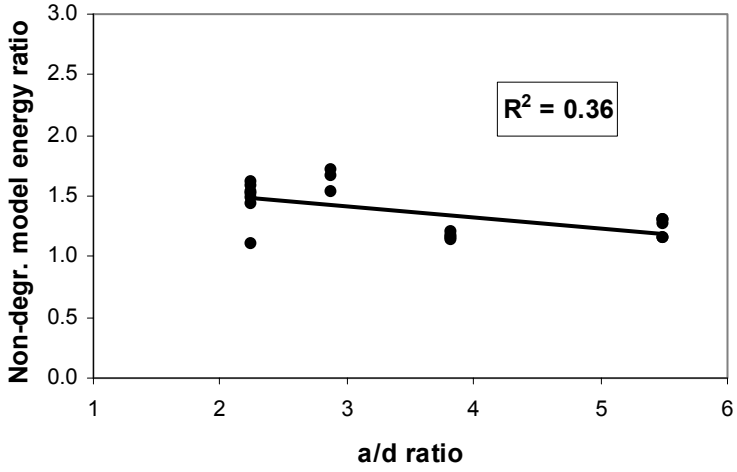


**Figure 5.14** Correlation between *a/d* ratio and non-degrading model energy ratio (Erberik & Sucuoglu test data is excluded)

# CHAPTER 6

# EFFECT OF DEGRADATION PARAMETERS ON THE SEISMIC BEHAVIOR OF SDOF SYSTEMS

## 6.1 General

The effect of degrading model parameters on behavior of simple structural systems subjected to experimentally generated loading patterns have been discussed in the previous chapters. In this chapter, the response of SDOF systems with various degradation characteristics is investigated using a set of seismic excitations recorded during some major earthquakes. The computer program that is employed to obtain response statistics of SDOF systems is INSPEC (Erberik, 2001).

The study conducted in this chapter can be considered as a complementary section to the whole study in this thesis and may be a prologue to a future research activity. Hence, the number of ground motions and the range of structural properties are limited in this study.

The effect of degradation parameters on the seismic response is investigated by employing SDOF systems having fundamental periods ($T$) of 0.5 s and 1.0 s, strength levels ($\eta$) of 0.1, 0.2 and 0.3 and a damping ratio ($\xi$) of 0.05. For the unloading degradation case with ductility-based rule, three different values of parameter '$a$' are used which are 0.0, 0.4 and 0.80 (from none-to-severe degradation levels). The values of 20, 4.0 and 0.5 are employed for the focus-based unloading parameter '$\alpha$', again representing none (or slight) to severe stiffness degradation levels. Three sets of parameters for each linear and exponential type of cyclic strength degradation are investigated. Parameters

$C$=0.005, 0.01 and 0.02 are used for linear strength degradation and parameters ($A$=0.2, $B$=0.05), ($A$=0.4, $B$=0.1) and ($A$=0.6, $B$=0.15) are used for exponential strength degradation. For pinching, Park et al. model with $\gamma$ parameters of 0.75, 0.6 and 0.40 are used to represent slight pinching to severe pinching cases. Finally, the combined degradation models are compared with the non-degrading model. For this purpose, two combined degradation models (moderate and severe) are constructed by using the set of parameters defined above. For moderate degradation model, unloading degradation parameter $a$=0.4, strength degradation parameter ($A$=0.4, $B$=0.1) and pinching parameter $\gamma$=0.6 are employed. For severe degradation model, unloading degradation parameter $\alpha$=0.5, strength degradation parameter $C$=0.02 and pinching parameter $\gamma$=0.4 are employed.

Comparison is performed by plotting displacement histories and force-displacement relationships of SDOF systems under specific ground motion data.

Three sets of ground motion data recorded during earthquakes are employed in this study. More detailed information about the selected ground motions is given in Section 6.2. As mentioned before, the obtained results and conclusions are based on these three ground motion data only and should be interpreted by considering this fact.

## 6.2 Ground Motions

Ground motion records used in this chapter are the east-west component from Erzincan earthquake (1992), the north-south component of Yarimca from Marmara earthquake (17 August 1999) and east-west component from Düzce earthquake (12 November1999). Throughout this chapter the ground motions are abbreviated as ERZ, MAR and DZC, respectively. The acceleration histories are presented in Figure 6.1. The intensity parameters such as magnitude ($M_w$), peak ground acceleration (PGA), peak ground velocity (PGV) and energy intensity (EI) of the considered earthquake records are listed in Table 6.1.

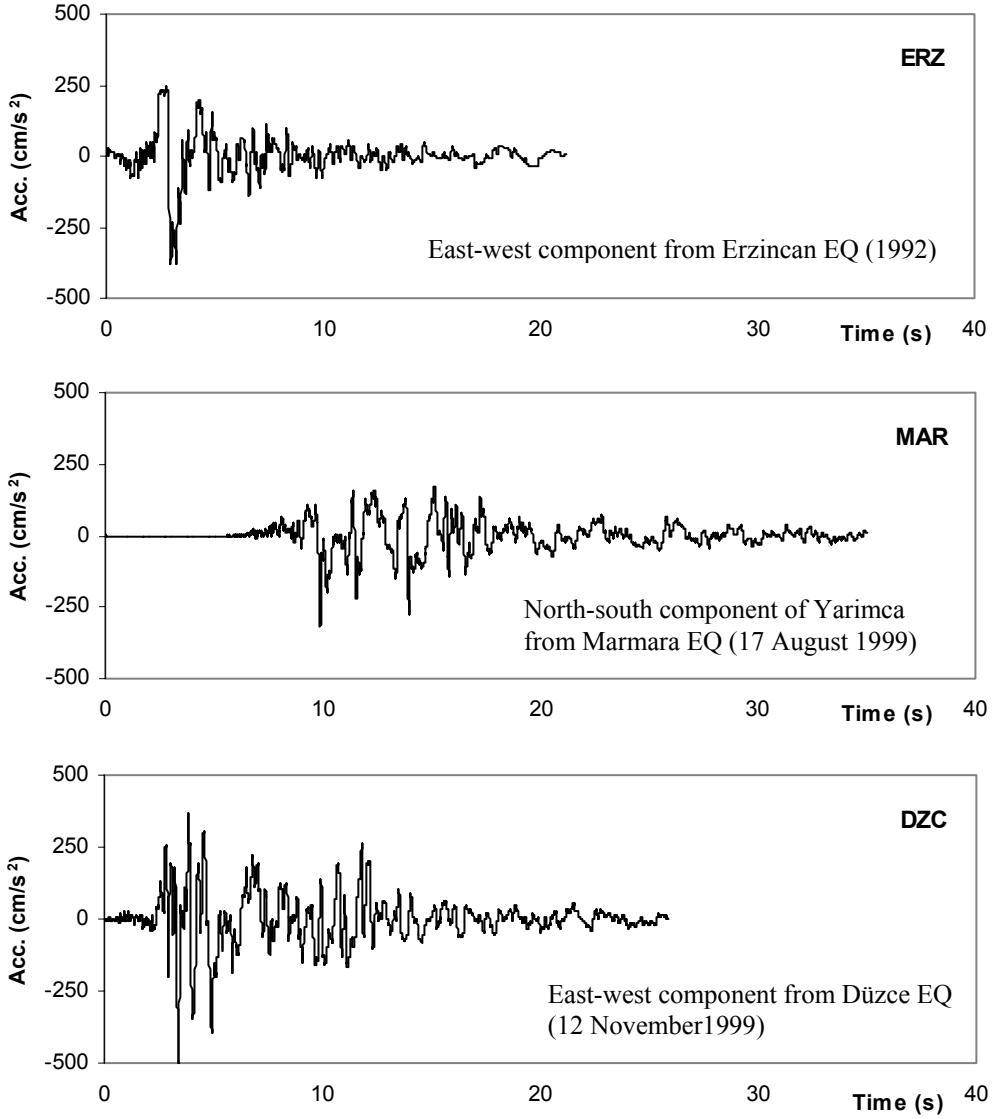


**Figure 6.1** Ground motions considered in this chapter from a) Erzincan 1992 b) Marmara 1999 c) Düzce 1999 earthquakes

**Table 6.1** Ground Motion Intensity Parameters

| Ground Motion | $M_w$ | PGA (cm/s$^2$) | PGV (cm/s) | EI |
|---|---|---|---|---|
| ERZ | 7.1 | 381.6 | 101.8 | 183.3 |
| MAR | 7.4 | 315.6 | 79.6 | 158.4 |
| DZC | 7.1 | 503.2 | 86.1 | 173.6 |

The main reason for the selection of these ground motion records is their high damaging potential. This reflected in Table 6.1 with high energy intensity (EI) values since EI is a direct measure of the average energy imparted by the earthquake into a structure throughout its entire duration (Sucuoglu et al., 1999). Higher energy possession of a ground motion leads many yield events and thus degradation behavior.

## 6.3 Influence of Unloading Stiffness Degradation Parameters on Seismic Response

First, the ductility-based unloading rule is investigated by employing a SDOF system with $T$=0.5 s, $\eta$=0.2 and $\xi$=0.05 which is subjected to ERZ. Three values of parameter '$a$' are considered: 0.0, 0.4 and 0.8. Calculated displacement responses are plotted in Figure 6.2 and force-displacement relationships are shown in Figure 6.3 for each case. Then, same SDOF system with focus-based unloading stiffness degradation is subjected to MAR with three different $\alpha$ parameters (20, 4.0 and 0.5). Displacement histories and force-displacement relationships are illustrated in Figures 6.4 and 6.5, respectively.

As it can be observed from Figure 6.2, maximum displacement values are not very different from each other (22.2 cm for $a$=0.0, 24.6 cm for $a$=0.4 and 28.6 cm for $a$=0.8). Same observation holds true for focus-based unloading degradation case (Figure 6.4). In this case maximum displacement values are 7.1 cm for $\alpha$=20, 7.1 cm for $\alpha$=4 and 8.7 cm for $\alpha$=0.5. So, it can be stated that the effect of unloading stiffness degradation on the maximum displacement response is not very pronounced but it only yields a slight increase for the structural parameters and ground motion records under interest. Another observation is that, the residual (offset) displacement values tend to decrease as the degradation in unloading stiffness increases. In ductility-based case, the offset displacement values are 7.6 cm, 5.9 cm and 2.91 for $a$=0.0, 0.4 and 0.8, respectively. Similarly in focus-based case, the offset displacement values are 2.0 cm, 1.2 cm and 0.2 for $\alpha$=20, 4 and

0.5, respectively. This is probably because of the fact that with the decrease in the slope of unloading branches shifts the offset point to the origin. This may not be the case in SDOF systems subjected to other different ground motion records. But briefly it can be stated that, either beneficial or detrimental, unloading stiffness characteristics have an influence on the offset (residual) displacement of SDOF systems.

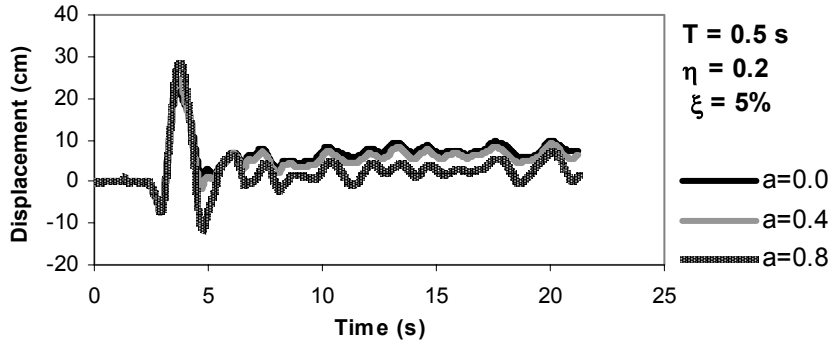


**Figure 6.2** Displacement responses of SDOF systems with unloading stiffness degradation (Ductility-based rule) subjected to ERZ

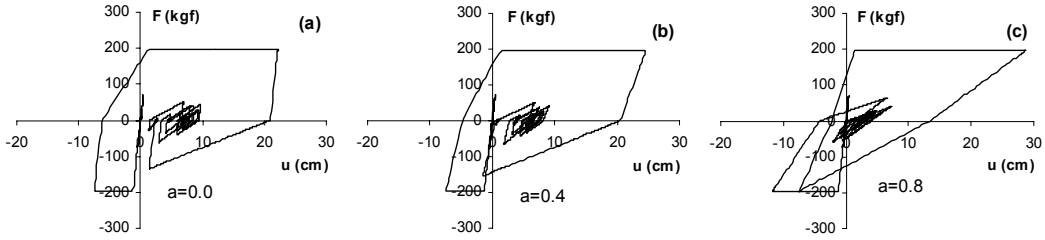


**Figure 6.3** Force-displacement relationships of SDOF systems with unloading stiffness degradation (Ductility-based rule) subjected to ERZ
($T$=0.5s,η=0.2,ξ=5%)

Also it is observed from the force-displacement plots in Figures 6.3 and 6.5 that unloading stiffness degradation causes the hysteresis loops to become narrower in terms of area and in turn, decreases energy dissipation capacity. In other words, hysteretic energy dissipation capacity of a RC member under seismic action decreases with increasing deterioration in unloading stiffness.

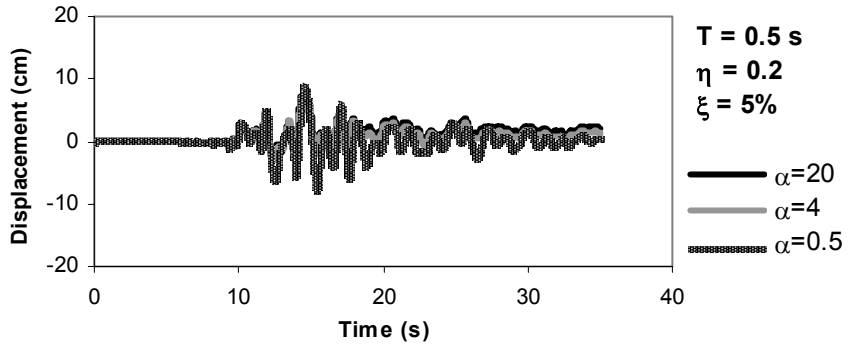


**Figure 6.4** Displacement responses of SDOF systems with unloading stiffness degradation (Focus-based rule) subjected to MAR

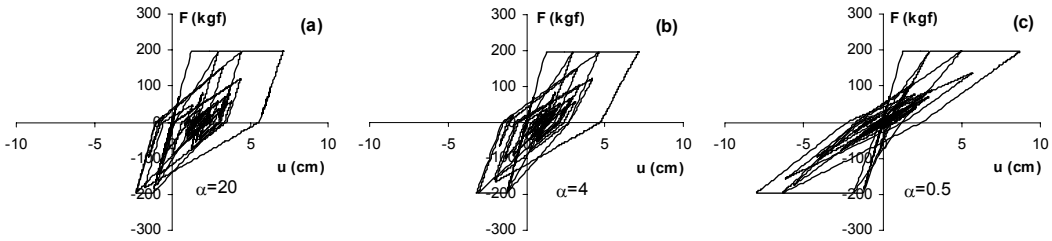


**Figure 6.5** Force-displacement relationships of SDOF systems with unloading stiffness degradation (Focus-based rule) subjected to MAR
($T$=0.5s,η=0.2,ξ=5%)

## 6.4 Influence of Strength Degradation Parameters on Seismic Response

First, linear strength degradation rule is investigated by employing three different SDOF systems with $T$=0.5 s, $\eta$=0.1, 0.2, 0.3 and $\xi$=0.05 which are subjected to DZC ground motion. Three values of parameter '$C$' are considered: 0.005, 0.01 and 0.02. Calculated displacement responses are plotted in Figure 6.6 and force-displacement relationships are shown in Figures 6.7-6.9 for each case. It should be noted that the specific case of linear degradation with $T$=0.5s, $\eta$=0.1 and $\xi$=0.05, shows no response when the strength degradation parameter $C$=0.02 because of the failure of the system. Then, another SDOF system with $T$=1.0s, $\eta$=0.2 and $\xi$=0.05 is employed for exponential type of strength degradation behavior. Exponential strength degradation parameters of ($A$=0.2, $B$=0.05), ($A$=0.4, $B$=0.1) and ($A$=0.6, $B$=0.15) are considered. MAR is selected for exponential strength degradation cases. Displacement responses are plotted in Figure 6.10 and force-displacement relationships are plotted in Figures 6.11.

As it can be observed from Figures 6.6-6.9 and Table 6.2, the maximum displacement and residual displacement values increase with increasing value of parameter '$C$' for a SDOF system having same structural properties. Same trend can be observed from Figures 6.10-6.11 that, increasing deterioration in strength increases the maximum displacement response.

It is found that, the dissipated energy capacities decrease with increasing level of strength degradation. But it is observed that, the deterioration in the energy dissipation capacity is not very significant for these cases. It is probably because of the fact that most of the energy is dissipated in the first few cycles and the contribution of other cycles is small.

**Table 6.2** Maximum displacement values for linear strength degradation case

| | $C$=0.005 | $C$=0.01 | $C$=0.02 |
|---|---|---|---|
| $T$=0.5s, η=0.1, ξ=0.05 | 23.98 cm | 34.59 cm | - |
| $T$=0.5s, η=0.2, ξ=0.05 | 17.29 cm | 19.01 cm | 46.25 cm |
| $T$=0.5s, η=0.3, ξ=0.05 | 14.62 cm | 15.10 cm | 18.24 cm |

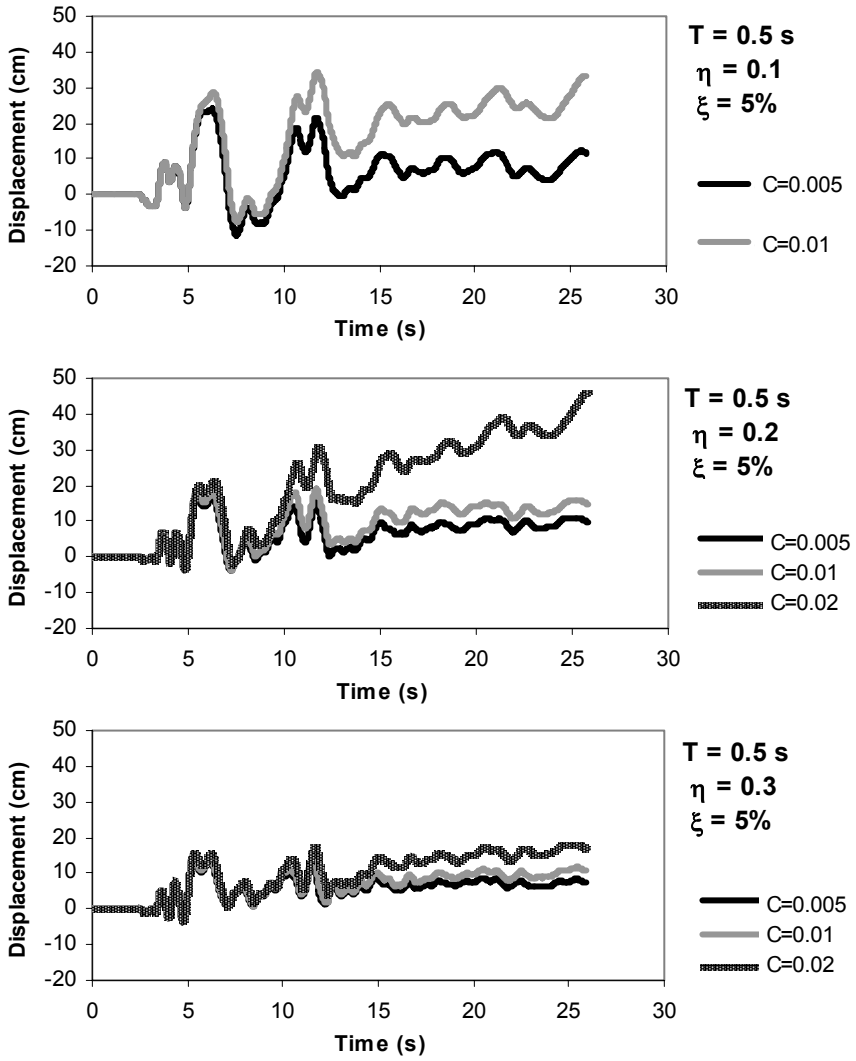


**Figure 6.6** Displacement responses of SDOF systems with strength degradation (linear type) subjected to DZC

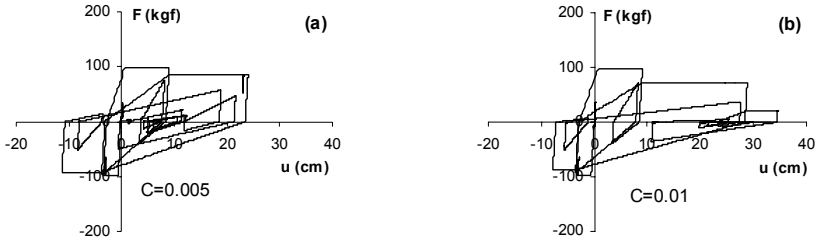


**Figure 6.7** Force-displacement relationships of SDOF systems with strength degradation (linear type) subjected to DZC
($T$=0.5s,η=0.1,ξ=5%)

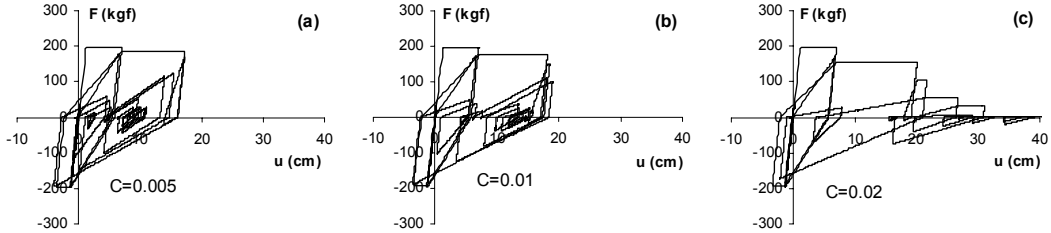


**Figure 6.8** Force-displacement relationships of SDOF systems with strength degradation (linear type) subjected to DZC
($T$=0.5s,η=0.2,ξ=5%)

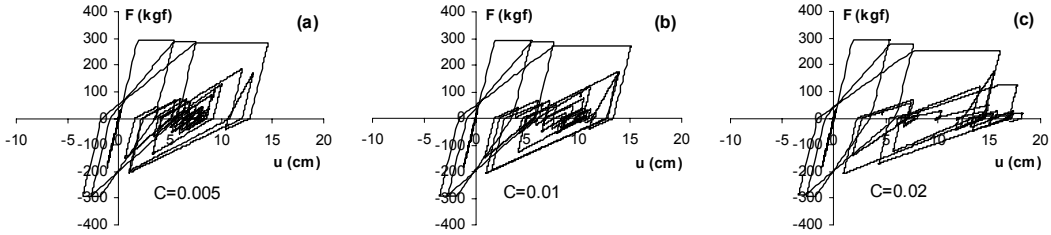


**Figure 6.9** Force-displacement relationships of SDOF systems with strength degradation (linear type) subjected to DZC
($T$=0.5s,η=0.3,ξ=5%)

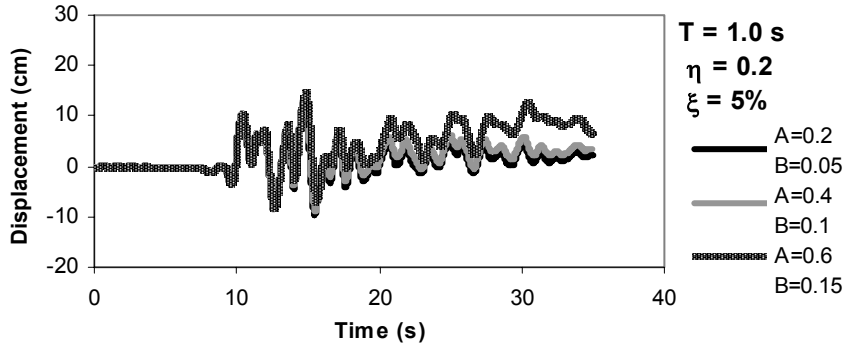


**Figure 6.10** Displacement responses of SDOF systems with strength degradation (exponential type) subjected to MAR

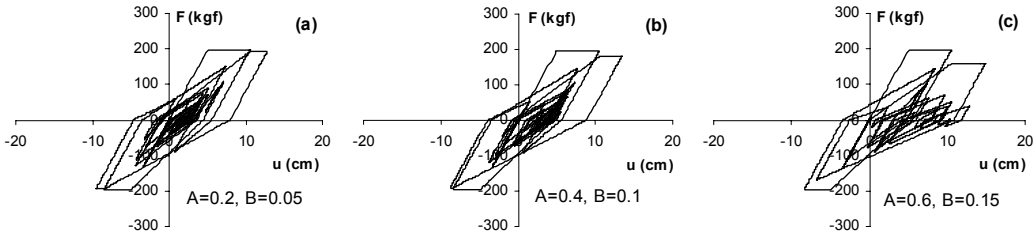


**Figure 6.11** Force-displacement relationships of SDOF systems with strength degradation (exponential type) subjected to MAR
($T$=1.0s,η=0.2,ξ=5%)

## 6.5 Influence of Pinching Parameters on Seismic Response

Pinching behavior is investigated by employing three different SDOF systems with $T$=0.5 s, η=0.1, 0.2, 0.3 and ξ=0.05 which are subjected to ERZ and MAR. Three values of parameter '$\gamma$' are considered: 0.75, 0.60 and 0.40. Calculated displacement responses are plotted in Figure 6.12 and Figure 6.16 for ERZ and MAR, respectively. Force-displacement relationships are shown in Figures 6.13-6.15 for ERZ and Figures 6.17-6.19 for MAR.

As it can be observed from Figures 6.12 and 6.16, displacement histories of the same structural system with different levels pinching are nearly same with each other for this set of ground motions. For example, maximum displacement values of the SDOF system ($T$=0.5s, $\eta$=0.1, $\xi$=5%) (which is subjected to MAR) are 18.9 cm for $\gamma$=0.75, 19.9 cm for $\gamma$=0.6 and 21.5 cm for $\gamma$=0.4. Maximum displacement values decrease with increasing strength level ($\eta$).

.

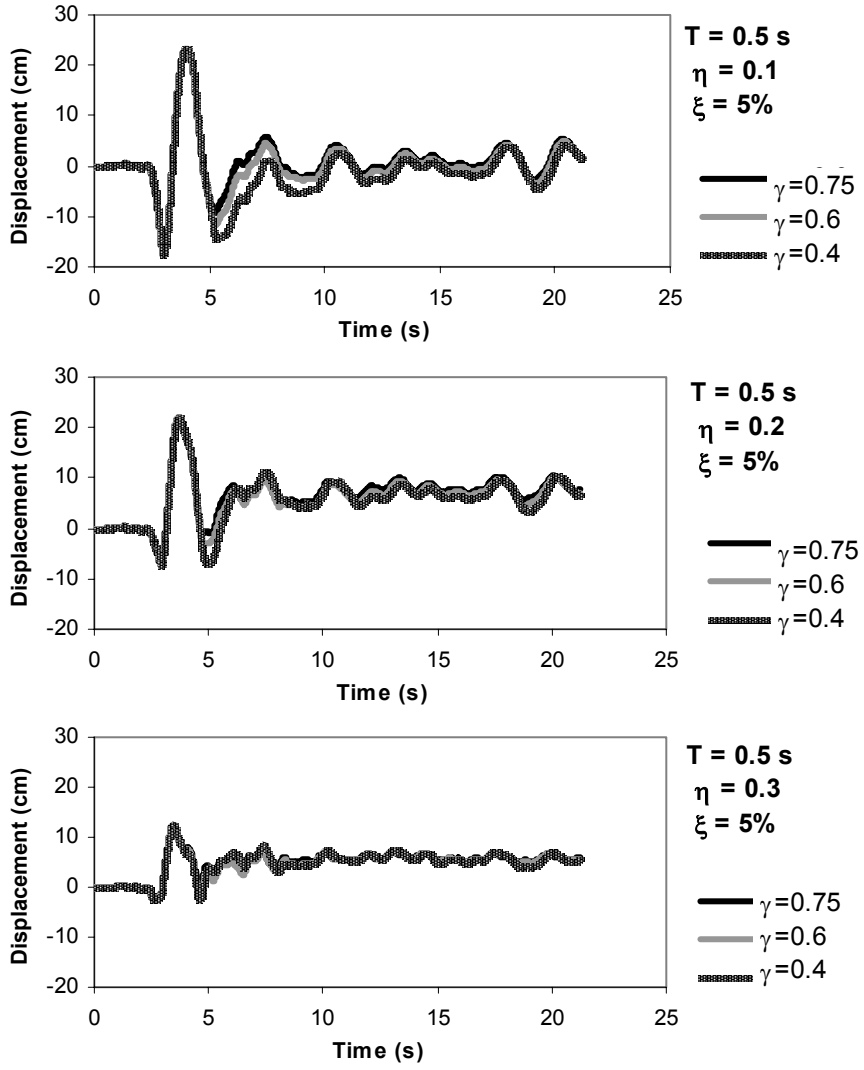


**Figure 6.12** Displacement responses of SDOF systems with pinching behavior (Park et al. rule) subjected to ERZ

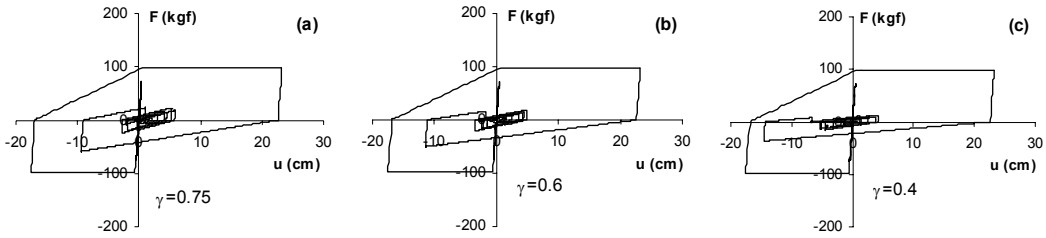


**Figure 6.13** Force-displacement relationships of SDOF systems with pinching behavior (Park et al. rule) subjected to ERZ
($T$=0.5s,η=0.1,ξ=5%)

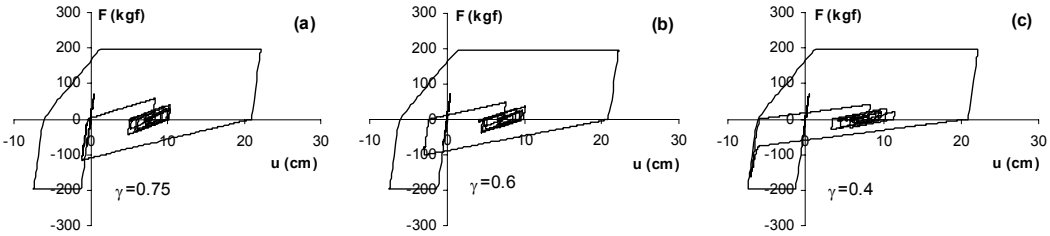


**Figure 6.14** Force-displacement relationships of SDOF systems with pinching behavior (Park et al. rule) subjected to ERZ
($T$=0.5s,η=0.2,ξ=5%)

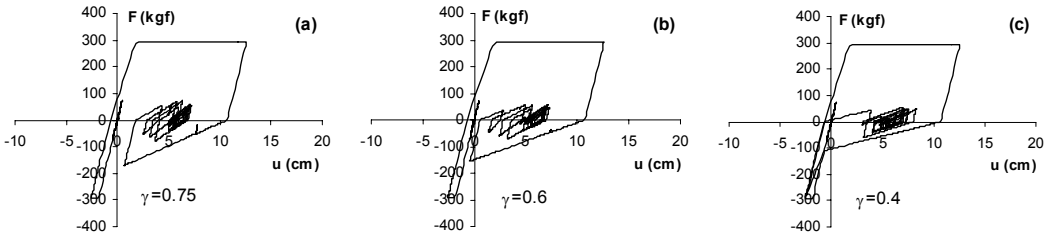


**Figure 6.15** Force-displacement relationships of SDOF systems with pinching behavior (Park et al. rule) subjected to ERZ
($T$=0.5s,η=0.3,ξ=5%)

It can also be stated that the effect of pinching behavior on the energy dissipation capacity of the SDOF systems is dependent on the ground motion characteristics. Most of the input energy from seismic loading is dissipated in the first few cycles for SDOF systems which are subjected to ERZ and pinched cycles do not contribute much to the overall dissipated energy (see Figures 6.13-.15). On the other hand, pinching effect is more clearly observed from the systems subjected to MAR (see Figures 6.17-6.19). As a result, the degree of adverse effect of pinching behavior on the dissipated energy can be different for each ground motion.

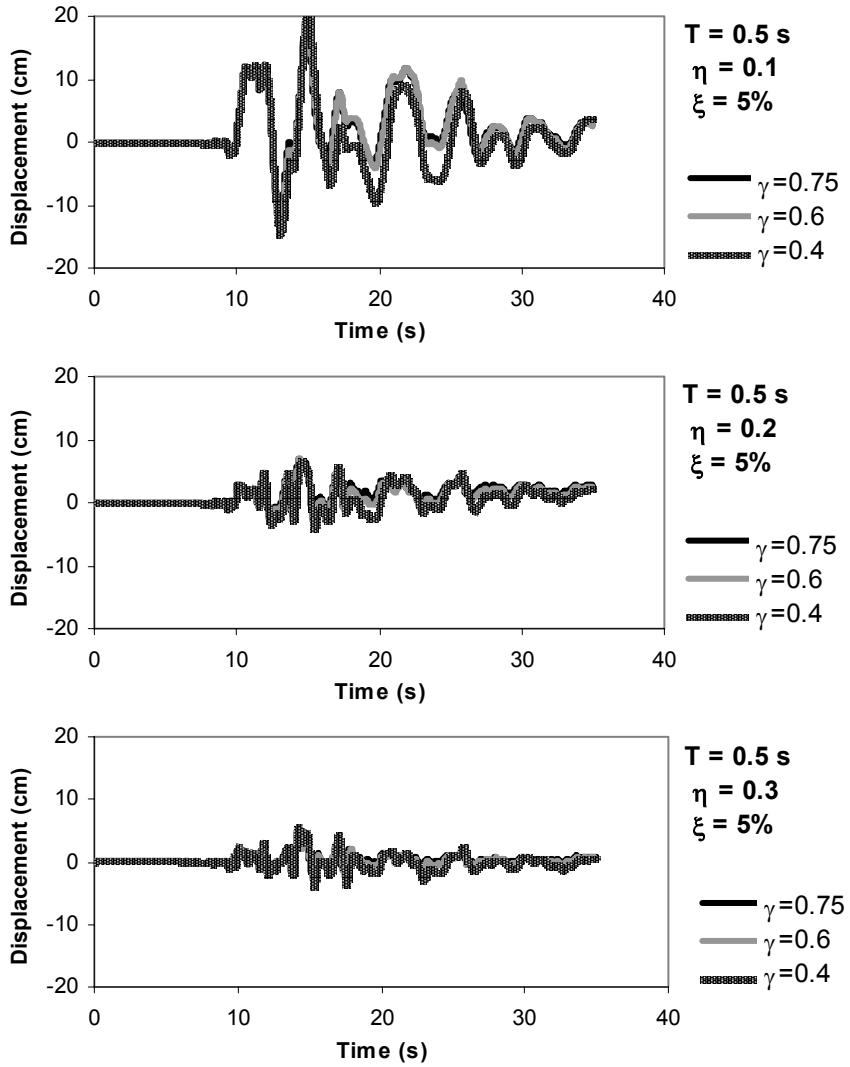


**Figure 6.16** Displacement responses of SDOF systems with pinching behavior (Park et al. rule) subjected to MAR

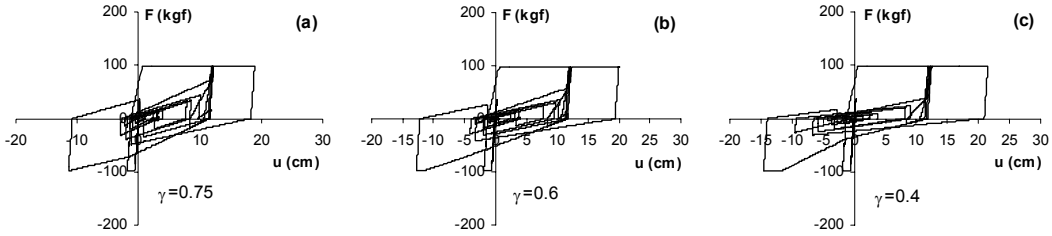


**Figure 6.17** Force-displacement relationships of SDOF systems with pinching behavior (Park et al. rule) subjected to MAR
($T$=0.5s,η=0.1,ξ=5%)

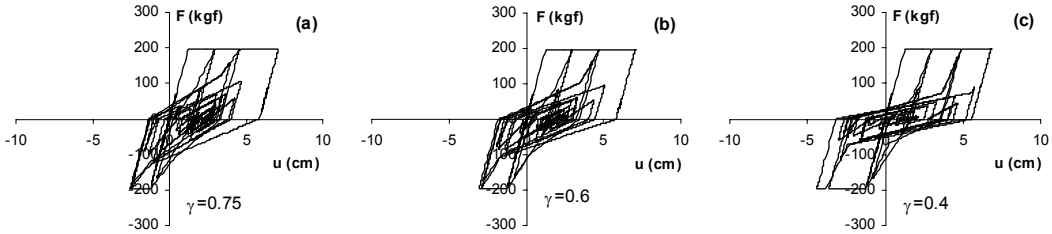


**Figure 6.18** Force-displacement relationships of SDOF systems with pinching behavior (Park et al. rule) subjected to MAR
($T$=0.5s,η=0.2,ξ=5%)

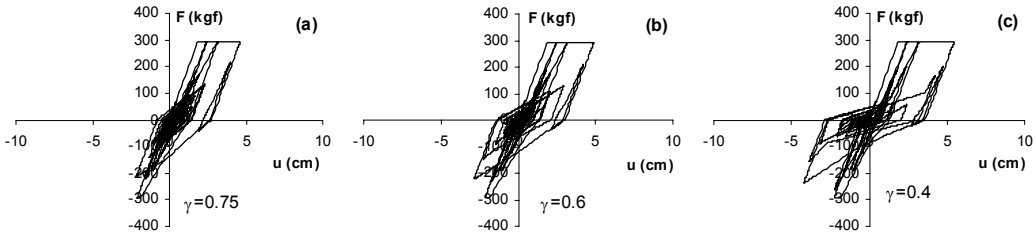


**Figure 6.19** Force-displacement relationships of SDOF systems with pinching behavior (Park et al. rule) subjected to MAR
($T$=0.5s,η=0.3,ξ=5%)

## 6.6 Comparison of the Seismic Response of None, Moderate and Severe Degrading SDOF systems

In this section, SDOF systems with combined stiffness, strength and pinching degrading characteristics subjected to seismic excitations are compared with the non-degrading systems. For this purpose, two levels of degradation are considered: moderate and severe. For moderate degrading systems, stiffness degradation rule is selected as ductility-based with parameter $a$=0.4, strength degradation is selected as exponential with parameters ($A$=0.4, $B$=0.1) and Park et al. pinching rule is employed with parameter $\gamma$=0.6. For severe degrading systems, unloading degradation (focus-based) parameter is selected as $\alpha$=0.5, strength degradation (linear) parameter is selected as $C$=0.02. Pinching parameter $\gamma$=0.4 is employed for severe model. Reference model is selected as stiffness degrading model (Clough and Johnston, 1966).

For moderate case, two SDOF systems with $T$=0.5-1.0 s, $\eta$=0.2 and $\xi$=5% are investigated under ERZ and MAR, respectively. Displacement histories are presented in Figures 6.20 and 6.22 and the maximum displacement values are listed in Table 6.3. The force-displacement relationships are plotted in Figures 6.21 and 6.23. By observing Figures 6.20-23 and Table 6.3, it can be stated that, maximum displacement values of moderately degrading systems are larger than the values of non-degrading systems. The residual displacement values are close to each other for this set of ground motions.

**Table 6.3** Maximum displacement values for non-degrading vs moderately degrading case

| | **None degrading** | **Moderate degrading** |
|---|---|---|
| **$T$=0.5s, $\eta$=0.2, $\xi$=0.05** | 22.1 cm | 24.5 cm |
| **$T$=1.0s, $\eta$=0.2, $\xi$=0.05** | 12.4 cm | 14.1 cm |

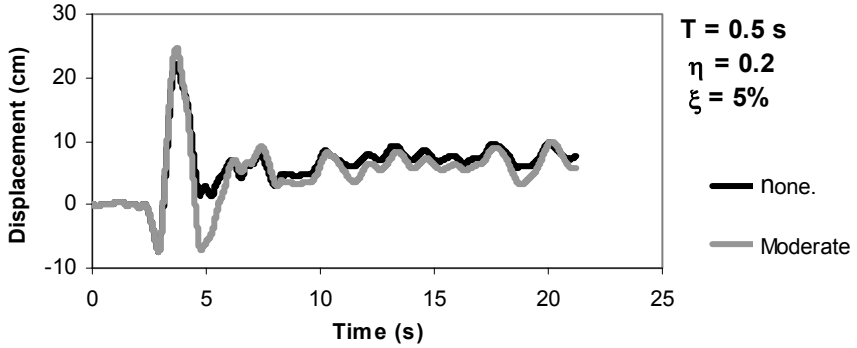


**Figure 6.20** Displacement responses of SDOF systems with none & moderate degradation subjected to ERZ

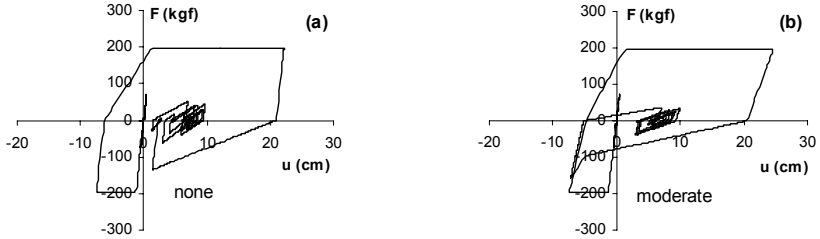


**Figure 6.21** Force-displacement relationships of SDOF systems with none & moderate-degradation subjected to ERZ
($T$=0.5s,η=0.2,ξ=5%)

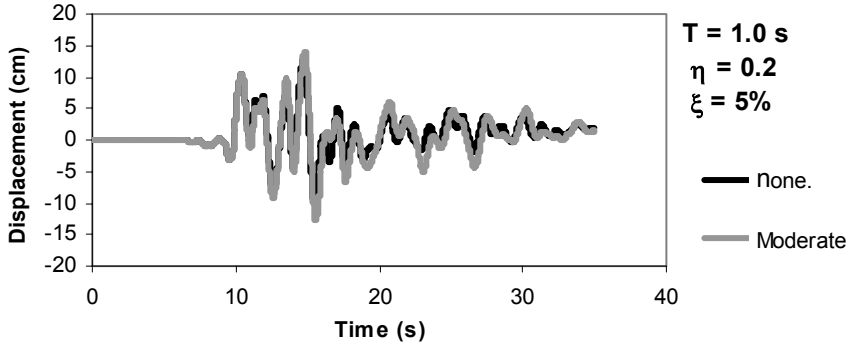


**Figure 6.22** Displacement responses of SDOF systems with none & moderate degradation subjected to MAR

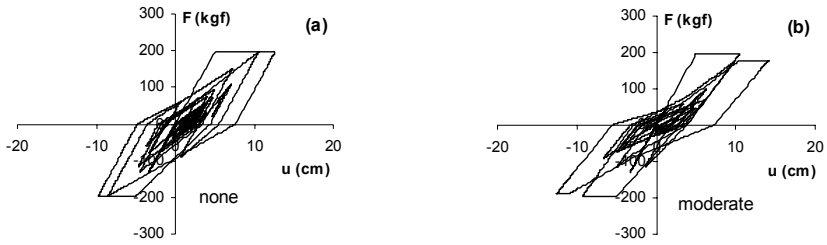


**Figure 6.23** Force-displacement relationships of SDOF systems with none & moderate-degradation subjected to MAR
($T$=1.0s,η=0.2,ξ=5%)

For severe degrading case, a SDOF system with $T$=0.5 s, η=0.2 and ξ=5% which is subjected to two different ground motions (MAR and DZC) are investigated. The related response histories are illustrated in Figures 6.24-6.27 and the maximum displacement values are listed in Table 6.4. As a general observation based on these two set of ground motions and structural properties, severely degrading systems exhibit nearly 1.2-1.5 times larger maximum displacement values. The narrowing of cycles are more pronounced in severely degrading systems as it can be observed from Figures 6.25 and 6.27.

**Table 6.4** Maximum displacement values for non-degrading vs severly degrading case

| | **None degrading** | **Moderate degrading** |
|---|---|---|
| ***T*=0.5s, η=0.2, ξ=0.05 (MAR)** | 7.1 cm | 10.8 cm |
| ***T*=0.5, η=0.2, ξ=0.05 (DZC)** | 16.4 cm | 20.0 cm |

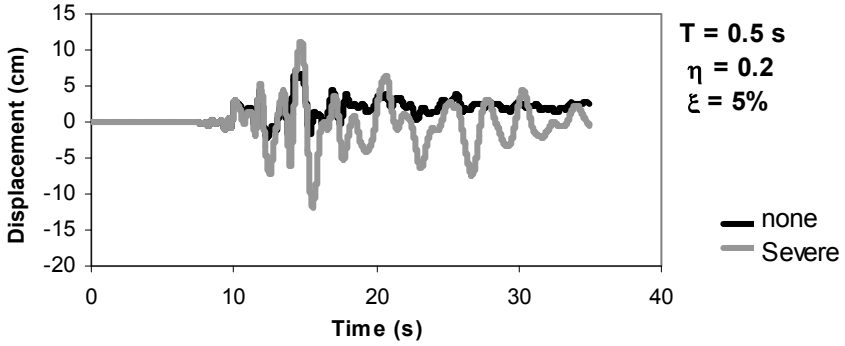


**Figure 6.24** Displacement responses of SDOF systems with none & severe degradation subjected to MAR

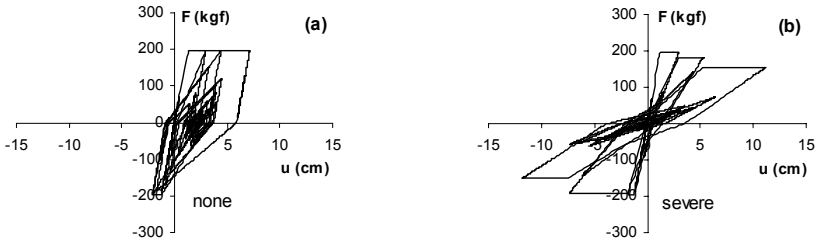


**Figure 6.25** Force-displacement relationships of SDOF systems with none & severe-degradation subjected to MAR
($T$=0.5s,η=0.2,ξ=5%)

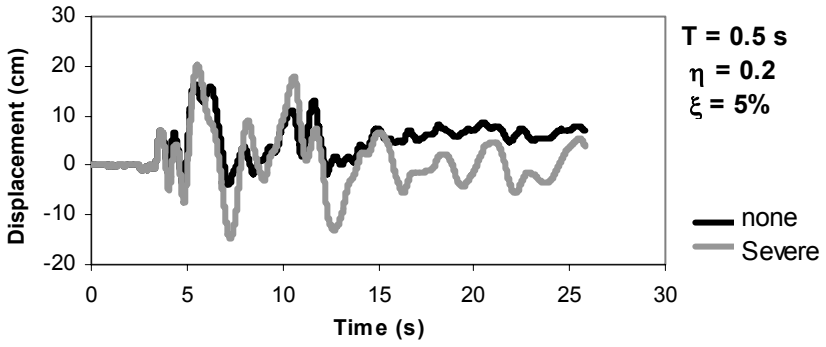


**Figure 6.26** Displacement responses of SDOF systems with none & severe degradation subjected to DZC

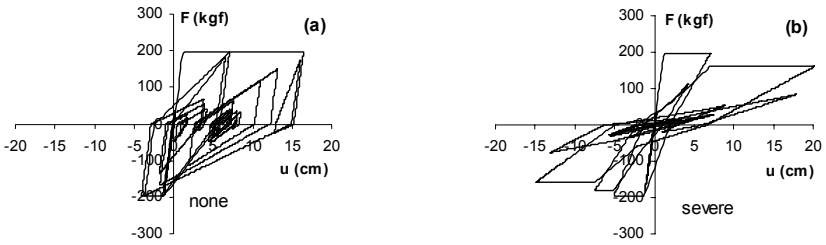


**Figure 6.27** Force-displacement relationships of SDOF systems with none & severe-degradation subjected to DZC
($T$=0.5s,η=0.2,ξ=5%)

The results indicate that when all the degradation components (unloading stiffness degradation, strength degradation and pinching) are combined in a structural system, the effect of degradation on response values (maximum displacement, residual displacement, hysteretic energy dissipation, etc.) becomes much more pronounced. However it should be again noted that the trends are obtained from a very small population of ground motion and structural input data which has no or very little statistical significance. Hence the results are not adequate to draw any general conclusions.

# CHAPTER 7

# SUMMARY AND CONCLUSIONS

## 7.1 Summary

RC structural members subjected to repeated cyclic loads usually exhibit degradation in strength and stiffness. Pinching behavior can also be observed when there exists high shear forces and the bond between reinforcing bars and concrete is poor. Most of the hysteresis models in the literature implement these degradation behaviors and define different degradation rules based on the experimental studies. In performance based design, the reliability of the developed models for the estimation of the RC behavior is very important to obtain accurate results. Therefore, a study concerning the accuracy of the degradation rules of known hysteresis models is conducted.

The column database of PEER provides a large number of cyclic load test data. The available data was used to calibrate the degradation parameters used for the hysteresis models which are widely used in literature. The database columns were classified into three groups according to their energy dissipation characteristics in order to investigate the degradation characteristics of the considered RC members more specifically rather than considering the complete database. Two energy-based indices ($I_{BL}$ and $I_{SD}$) were introduced for the classification of the test results.

A study concerning the unloading stiffness degradation parameters of two well-known rules (ductility-based and focus-based rules) was conducted. The test results from the PEER column database were used to calibrate the unloading

stiffness rule parameters available in the literature and then, the calculated values were compared with the recommended values. The correlations between unloading parameters were also examined.

Strength degradation behavior of RC members during hysteretic response was investigated in two parts: cyclic (cinematic) strength degradation and in-cycle (post-capping) strength degradation. PEER column database was employed for the investigation of the strength degradation properties of the RC members. First, the values of the parameters of two strength degradation formulas (linear and exponential) were obtained by using the selected cyclic test results in the database. Second, in-cycle strength degradation properties such as post-yield and post-capping lateral stiffness, deformation level of the capping point and residual strength ratio were investigated for the selected columns in PEER database.

Cyclic column tests of PEER database which exhibit pinching were used to calibrate and verify the two well-known and widely used pinching rules in the literature (Roufaiel & Meyer's rule and Park et al.'s rule). Experimental dissipated energy values were compared with the dissipated energy values of analytical half-cycles which were generated by considering the pinching rules. "Energy ratio" was introduced in order to assess the pinching rules in terms of dissipated energy.

In the last part of the study, effect of degradation parameters on the seismic behavior of SDOF systems is investigated. Three ground motion records from recent major earthquakes in Turkey are employed. Displacement histories, force deformation relationships, residual displacements and energy dissipation capacities of selected SDOF systems with varying periods and strength ratios are compared with each other for stiffness degradation, strength degradation and pinching cases separately.

## 7.2 Discussion of Results

In this section, summary of the results obtained from the calibration of degradation parameters are presented. Different values of degradation parameters have been obtained for each member group or degradation level by considering the dissipated hysteretic energy as the main factor. Also, actual behavior of two sample test specimens that experience unloading stiffness degradation, strength degradation and pinching are compared with the simulated degrading models which are constructed by using the calibrated degradation parameters to observe the improvement of degrading model over bilinear and stiffness degrading models (Figures 7.1-7.2).

The calibrated unloading stiffness degradation parameters for ductility-based rule are; $a$=0.55, 0.68 and 0.82 for member groups A, B and C, respectively. For focus-based rule, the calibrated parameters are; $\alpha$=2.80, 1.50 and 0.92 for member groups A, B and C, respectively.

For cyclic strength degradation, the degradation parameters are obtained as; $A$=0.33 / $B$=0.18 (severe-to-gradual type), $S$=0.02-0.09 / $K$=0.02-0.20 (gradual- to-severe type), $C$=0.011 (linear type) for moderate strength degradation level and $A$=0.53 / $B$=0.13 (severe-to-gradual type), $S$=0.002-0.12 / $K$=0.03-0.15 (gradual-to-severe type), $C$=0.020 (linear type) for severe strength degradation level.

The value of calibrated pinching parameter ($\gamma$) for Park et al. rule is 0.64. This value can be used for all member groups but it should be noted that most of the test specimens used for this calibration process are belong to Group C.

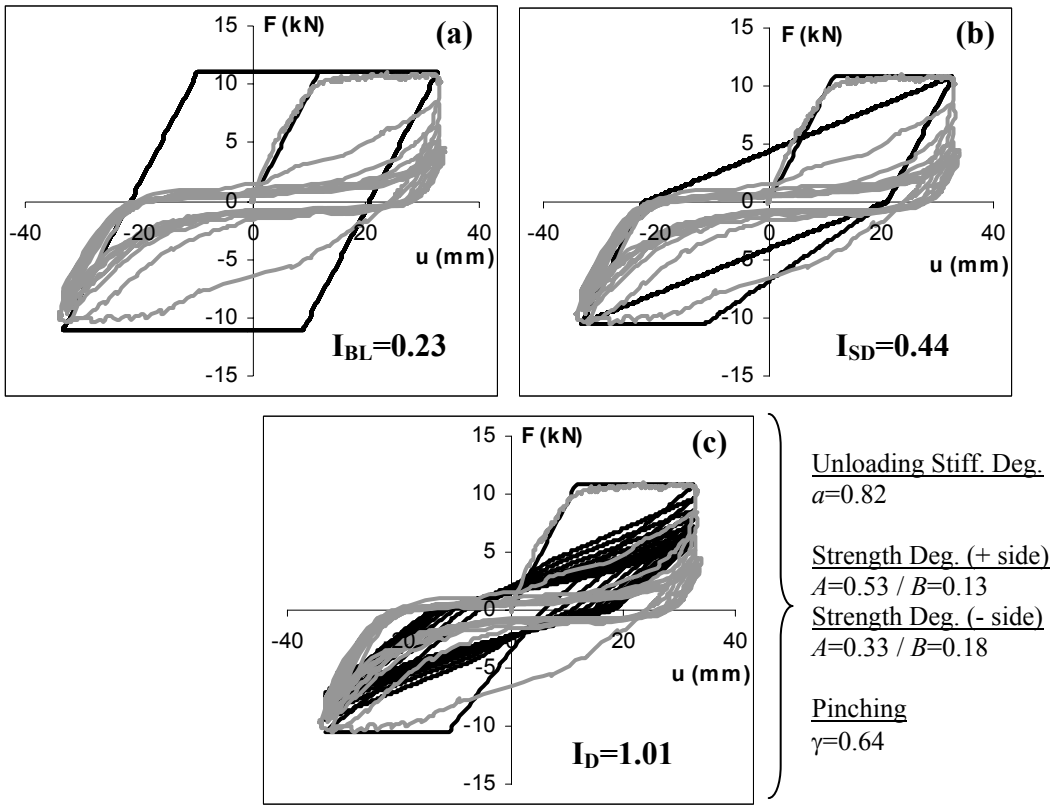


**Figure 7.1** Comparison of experimental force-displacement relationship with a) Bilinear model, b) Stiffness degrading model, c) Degrading model with calibrated degradation parameters for Erberik & Sucuoglu 2001-CAL-9 specimen

Test specimen CAL-9 (Erberik & Sucuoglu, 2001) is determined to be a Group C member since its energy-based index $I_{SD}$ is less than 0.7. As it can be observed from Figures 7.1.a and 7.1.b, both bilinear model and stiffness degrading models are far from estimating actual force-displacement relationship (gray curve). On the other hand, the degrading model with the calibrated parameters for Group C members (Figure 7.1.c) is much better in terms of force-displacement curve and estimated dissipated energy is exactly the same as the actual dissipated energy (energy-based index for degrading case $I_D$=1.01).

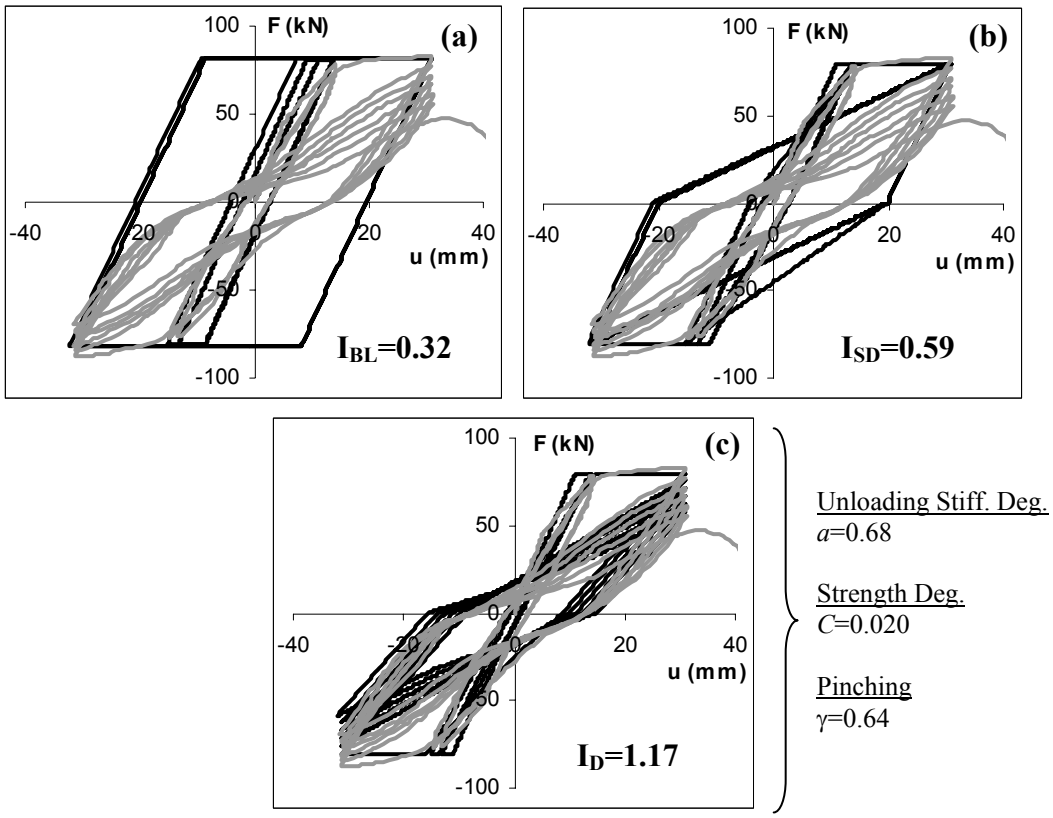


**Figure 7.2** Comparison of experimental force-displacement relationship with a) Bilinear model, b) Stiffness degrading model, c) Degrading model with calibrated degradation parameters for Wight & Sozen 1973-25033E specimen

Test specimen 25033E (Wight & Sozen, 1973) is determined to be a Group C member since its energy-based index $I_{SD}$ is less than 0.7. Again it can be observed from Figures 7.2.a and 7.2.b, both bilinear model and stiffness degrading models are far from estimating actual behavior. However, the degrading model is very similar with the actual force-displacement relationship. Also, energy-based index $I_D$ is equal to 1.17 indicating that energy dissipation capacity of the member is estimated by a reasonable accuracy. It should be noted that, the unloading stiffness parameter $a$=0.68 is used for this case, because the level of unloading stiffness degradation is not so high and $I_{SD}$ index is 0.59 indicating that employing a parameter which is determined for Group B does not cause serious errors in this case.

## 7.3 Conclusions

The following conclusions are drawn based on the results obtained from this study:

- Mean value of the energy-based index $I_{BL}$ indicates that actual energy dissipation capacity of a RC member is nearly 40 % of the energy dissipation capacity of the simulated bilinear model for that member. In other words, bilinear model highly overestimates the actual energy dissipation capacity. However, this percentage is about 75 % for the stiffness degrading model used for the calculation of $I_{SD}$. Hence, bilinear model is not a convenient model for the RC members subjected to cyclic loads that cause inelastic deformations.
- In general, a code confirming RC member can exhibit a force-displacement relationship very close to stiffness degrading model of Clough and Johnston (1966) which is simple to implement and practical to use in structural analysis procedures.
- It can be stated that ductility based rule is a better candidate to be used for analytical modeling of unloading stiffness degradation considering the COV values of parameters '$a$' and '$\alpha$' in Tables B.1 – B.60 (Appendix B). The COV values for parameter '$a$' are much smaller when compared to the COV values of parameter '$\alpha$' in most of the cyclic tests.
- The values of 0.4-0.5 for ductility-based unloading stiffness degradation parameter recommended in the literature are generally based on code confirming structural members and higher values of parameter '$a$' (0.7-0.8) should be used when considering RC members which exhibit moderate-to-severe degradation under cyclic loading.
- Recommended values for focus-based unloading parameters by IDARC are far from representing the actual behavior of RC columns under cyclic loading. While the recommended value for severe degradation is $\alpha$=4.0, the mean calculated value for RC column group with severe

degradation reduces to 0.92. Therefore, the recommended values for unloading stiffness degradation parameters in the literature are unable to represent the actual behavior and they should be used with great attention.

- It is observed from the results of column database that the degradation in unloading stiffness increases with increasing displacement ductility.
- Cyclic degradation characteristics of a structural member with symmetrical cross-section can differ with respect to the loading direction even if it is subjected to the same amplitude of loading.
- The mean values of parameters *A* and *B* for cyclic tests which are defined as moderately degrading in terms of strength are 0.33 and 0.18, respectively. The variation in parameter *A* is small (COV=0.21) whereas there is a considerable variation in parameter *B* (COV=0.83). The mean values of parameters *A* and *B* for severely degrading group of cyclic tests are 0.53 and 0.13 with COV values of 0.25 and 0.47, respectively. The results indicate that parameter *B* that represents rate of strength degradation is rather an unstable parameter.
- In-cycle strength degradation behavior in both directions of loading is quite similar on the average. In positive direction of loading, the mean value of hardening slope in the post-yield branch is 3 % whereas the same mean value is 1 % in the negative direction of loading.
- The mean value of post-capping stiffness has a reduction of 80 % with respect to the initial stiffness for both loading directions. The mean residual-to-yield strength ratio is 60 %. The capping point and residual strength point ductility levels are almost the same for both directions with values of 3.30 and 7.40, respectively.
- Roufaiel & Meyer pinching rule's energy ratio average is determined as 1.33. Although there is a 27 % improvement over the non-degrading model for the estimation of dissipated energy, it should be noted that the energy ratio value of 1.33 means that the Roufaiel & Meyer's

pinching rule overestimates the actual energy dissipation capacity which is on the unsafe side for the analysis of the performance.

- Park et al. pinching rule's energy ratio average is 0.86 meaning that this rule underestimates the energy dissipation capacity. However, if a value about 0.64 for the parameter $\gamma$ is employed in the calculation of the dissipated energy instead of 0.50 (which is the recommended value), it is possible to obtain a much better estimation.
- As a general observation, the Park et al. pinching rule gives better results when there is severe pinching behavior whereas Roufaiel & Meyer's pinching rule is better for moderate or slight pinching levels.
- Unloading stiffness degradation seems to influence the residual displacement in SDOF systems under seismic action.
- The effect of degradation (especially strength degradation and pinching) is closely related to the ground motion characteristics. For near fault records with a single significant pulse, generally this pulse governs the complete response and it is not possible to encounter the effect of degrading throughout the response. However for ground motion records with a considerable number of pulses that are able to induce inelastic behavior, the effect of degradation is much more pronounced.
- When all the degradation components (unloading stiffness degradation, strength degradation and pinching) are combined in a structural system, the effect of degradation on response values (maximum displacement, residual displacement, hysteretic energy dissipation, etc.) becomes much more pronounced. However it should be again noted that the trends are obtained from a very small population of ground motion and structural input data which has no or very little statistical significance.

## 7.4 Further Research Recommendations

The following recommendations are made for future research:

- Limited number of degrading model parameters is examined in this study. Actually there exist other parameters in the literature regarding unloading stiffness degradation, strength degradation and pinching. Hence a more comprehensive study can be conducted to obtain the range of values for all degrading model parameters which are currently in use.
- The study conducted in Chapter 6 can be considered as a complementary section to the whole study in this thesis and may be a prologue to a future research activity. Number of ground motion records and SDOF structural parameters considered in this study are rather limited and it is not possible to draw general conclusions regarding the influence of degradation on the seismic response of simple SDOF systems. Hence a more comprehensive study can be conducted by using considerable number of ground motion records with varying characteristics and a wider range of structural parameters in order to obtain the complete response surface.

## REFERENCES

American Concrete Institute (ACI 318-02), 2002. “Building Code Requirements for Structural Concrete”.

Ang, B.G., Priestley, M.J.N. and Park, R., 1981. "Ductility of Reinforced Bridge Piers Under Seismic Loading," Report 81-3, Department of Civil Engineering, University of Canterbury, Christchurch, New Zealand.

Arai, Y., Hakim, B., Kono, S., Watanabe, F., 2002. "Damage Assessment of Reinforced Concrete Columns Under High Axial Loading." Personal Contact.

Atalay, M.B., and Penzien, J., 1975. “The Seismic Behavior of Critical Regions of Reinforced Concrete Components as Influenced by Moment, Shear and Axial Force.” Report No. EERC 75-19, University of California, Berkeley, California.

Azizinamini, A., Johal, L. S., Hanson, N. W., Musser, D. W., and Corley, W. G., 1988. “Effects of Transverse Reinforcement on Seismic Performance of Columns, A Partial Parametric Investigation.” Project No. CR-9617, Construction Technology Laboratories, Skokie, Illinois.

Bayrak, O., and Sheikh, S., 1996. “Confinement Steel Requirements for High Strength Concrete Columns.” Proc. 11th World Conference on Earthquake Engineering, Aculpulco, Mexico, Paper No. 463.

Clough, R.W. and Johnston, S.B., 1966. “Effect of Stiffness Degradation on Earthquake Ductility Requirements”, Proceedings, Second Japan National Conference on Earthquake Engineering, pp.227-232.

Chung, Y.S., Meyer, C., and Shinozuka, M., 1989. “Modeling of Concrete Damage”, ACI Structural Journal, Vol.86, No.3. pp.259-271.

Erberik, M.A., 2001. “Energy Based Seismic Assessment of Degrading Systems”, PhD Thesis, Civil Engineering Department, METU.

Erberik, M.A., and Acun, B., 2005. “An Energy-based Softening Index for Seismic Performance Evaluation of Reinforced Concrete Column Members”, Earthquake Engineering Research Center, EE-21C, Topic 4.

Ersoy, U., Ozcebe, G., and Tankut, T., 2004. “Reinforced Concrete”, Department of Civil Engineering, Middle East Technical University.

FEMA440, 2005 “Improvement of Nonlinear Static Seismic Analysis Procedures”, Federal Emergency Management Agency, US Department of Homeland Security.

Galeota, D., Giammatteo, M.M., Marino, R., 1996. "Seismic Resistance of High Strength Concrete Columns." Proceedings of the Eleventh World Conference on Earthquake Engineering, Disc 3, Paper No. 1390.

Gill, W. D., Park, R., and Priestley, M.J.N., 1979. “Ductility of Rectangular Reinforced Concrete Columns with Axial Load.” Report 79-1, Department of Civil Engineering, University of Canterbury, Christchurch, New Zealand.

Ibarra, L.F., 2003. “Global Collapse of Frame Structures under Seismic Excitations”, PhD Thesis, Department of Civil and Environmental Engineering, Stanford University.

Kanda, M., Shirai, N., Adachi, H., and Sato, T., 1988. “Analytical Study on Elasto-Plastic Hysteretic Behaviors of Reinforced Concrete Members.” Transactions of the Japan Concrete Institute, 10.

Kawashima, K., MacRae, G.A., Hoshikuma, J. and Nagaya, K., 1998. “Residual Displacement Response Spectrum”, Journal of Structural Engineering ASCE, Vol.124 (5), pp.523-530.

Kent, D.C. and Park, R., 1971. “Flexural Members with Confined Concrete”, Journal of Structural Engineering ASCE, Vol.97 (7), pp.1969-1990.

Krawinkler, H., 1996. “Cyclic Loading Histories for Seismic Experimentation on Structural Components”, Earthquake Spectra, Vol.12, No.1, pp.1-12.

Lehman, D.E., and Moehle, J.P., 2000. “Seismic Performance of Well-Confined Concrete Bridge Columns”, Pacific Earthquake Engineering Research Center, PEER Report no.1998/01.

Legeron, F., and Paultre, P., 2000. “Behavior of High-Strength Concrete Columns under Cyclic Flexure and Constant Axial Load.” ACI Struct. J., 97(4), 591-601.

Mahin, S.A. and Bertero, V.V., 1976. “Nonlinear Seismic Response of a Coupled Wall System”, Journal of Structural Engineering ASCE, Vol.102 (ST9), pp.1759-1780.

Matamoros, A.B., 1999. “Study of Drift Limits for High-Strength Concrete Columns.” Department of Civil Engineering, University of Illinois at Urbana-Champaign.

Mo, Y.L., and Wang, S.J., 2000. “Seismic Behavior of RC Columns with Various Tie Configurations.” J. Struct. Eng., 126(10), 1122-1130.

Muguruma, H., Watanabe, F., and Komuro, T., 1989. “Applicability of High Strength Concrete to Reinforced Concrete Ductile Column.” Transactions of the Japan Concrete Institute, 11.

Nielsen, N.N. and Imbeault, F.A., 1970. “Validity of Various Hysteretic Systems”, Proceedings, Third Japan National Conference on Earthquake Engineering, pp.707-714.

Ohno, T., and Nishioka, T., 1984. “An Experimental Study on Energy Absorption Capacity of Columns in Reinforced Concrete Structures.” Proceedings of the JSCE, Structural Engineering/Earthquake Engineering, 1(2).

Pacific Earthquake Engineering Research Center (PEER) Structural Performance Database Website, 2003. “http://nisee.berkeley.edu/spd/index.html”.

Park, Y. J., Reinhorn, A. M. and Kunnath, S. K., 1987. “IDARC: Inelastic Damage Analysis of Reinforced Concrete Frame – Shear Wall Structures”, Technical Report NCEER-87-0008, State University of New York at Buffalo.

Park, R., and Paulay, T., 1990. “Use of Interlocking Spirals for Transverse Reinforcement in Bridge Columns.” Strength and Ductility of Concrete Substructures of Bridges, RRU (Road Research Unit) Bulletin 84, 1, 77-92.

Paultre, P., Legeron, F., and Mongeau, D., 2001. “Influence of Concrete Strength and Transverse Reinforcement Yield Strength on Behavior of High-Strength Concrete Columns.” ACI Struct. J., 98(4), 490-501.

Phan, L.T., Todd, D.R., and Lew, H.S., 1993. “Strengthening Methodology for Lightly Reinforced Concrete Frames-I”, NISTIR 5128,National Institute of Standards and Technology.

Pujol, S., 2002. "Drift Capacity of Reinforced Concrete Columns Subjected to Displacement Reversals." Thesis, Purdue University.

Roufaiel, M.S.L., and Meyer, C., 1987. “Analytical Modeling of Hysteretic Behavior of RC Frames”, Journal of Structural Engineering, ASCE, Vol.113, No.3, pp.429-444.

Saiidi,M. and Sozen, M.A., 1979. “Simple and Complex Models for Nonlinear Seismic Response of R/C Structures”, Structural Research Series 465, Civil Engineering Studies, University of Illinois, Urbana, IL.

Saatcioglu, M., and Grira, M., 1999. “Confinement of Reinforced Concrete Columns with Welded Reinforcement Grids.” ACI Struct. J., 96(1), 29-39.

Saatcioglu, M., and Ozcebe, G., 1989. “Response of Reinforced Concrete Columns to Simulated Seismic Loading.” ACI Struct. J., 86(1), 3-12.

Sakai, Y., Hibi, J., Otani, S., and Aoyama, H., 1990. “Experimental Study on Flexural Behavior of Reinforced Concrete Columns Using High-Strength Concrete.” Transactions of the Japan Concrete Institute, 12.

Sivaselvan, M.V., and Reinhorn, A.M., 1999. “Hysteretic Models for Cyclic Behavior of Deteriorating Inelastic Structures”, Technical Report MCEER-99-0018.

Soesianawati, M.T., Park, R., and Priestley, M.J.N., 1986. “Limited Ductility Design of Reinforced Concrete Columns.” Report 86-10, Department of Civil Engineering, University of Canterbury, Christchurch, New Zealand.

Stojadinovic, B., and Thewalt, C.R., 1996. “Energy Balanced Hysteresis Models”, Eleventh World Conference on Earthquake Engineering, paper no.1734.

Sucuoglu, H., Gulkan, P., Erberik, M.A., Akkar, D.S., 1999. “Measures of Ground Motion Intensity in Seismic Design”, Proceedings, Uğur Ersoy Symposium, July 1-2, METU Ankara, pp.105-119.

Sugano, S., 1996. “Seismic Behavior of Reinforced Concrete Columns Which used Ultra-High-Strength Concrete.” Eleventh World Conference on Earthquake Engineering, Paper No.1383.

Takeda,T., Sozen M. A. and Nielsen, N.N., 1970. “Reinforce Concrete Response to Simulated Earthquakes”, Journal of Structural Division, ASCE, Vol.96, No.ST-12, pp. 2557-2573.

Takemura, H. and Kawashima, K., 1997. "Effect of loading hysteresis on ductility capacity of bridge piers," Journal of Structural Engineering, Vol. 43A, pp. 849-858, Japan.

Tanaka, H., and Park, R., 1990. “Effect of Lateral Confining Reinforcement on the Ductile Behavior of Reinforced Concrete Columns.” Report 90-2, Department of Civil Engineering, University of Canterbury, Christchurch, New Zealand.

Taylor, A.W. et al., 1997. “A Summary of Cyclic Lateral Load Tests on Rectangular Reinforced Concrete Columns”, National Institute of Standards and Technology, Report NISTIR5984.

Taylor, A.W. et al., 1997. “Effect of Load Path on Damage to Concrete Bridge Piers”, National Institute of Standards and Technology.

Taylor, A.W. and Stone, W.C., 1993. “A Summary of Cyclic Lateral Load Tests of Spiral Reinforced Concrete Columns”, National Institute of Standards and Technology, Report NISTIR5285.

Thomsen, J., and Wallace, J., 1994. “Lateral Load Behavior of Reinforced Concrete Columns Constructed Using High-Strength Materials.” ACI Struct. J., 91(5), 605-615.

Tokdemir, F., 1995. “FORTRAN77”, Department of Computer Engineering, Middle East Technical University.

University of Washington Structral Performance Database Website, 2003. “http://www.ce.washington.edu/~peera1/main.htm”.

Watson, S., and Park, R., 1989. “Design of Reinforced Concrete Frames of Limited Ductility” Report 89-4, Department of Civil Engineering, University of Canterbury, Christchurch, New Zealand.

Wehbe, N., and Saiidi, M.S., and Sanders, D., 1998. “Confinement of Rectangular Bridge Columns for Moderate Seismic Areas.” National Center for Earthquake Engineering Research (NCEER) Bulletin, 12(1).

Wight, J.K., and Sozen, M.A., 1973. “Shear Strength Decay in Reinforced Concrete Columns Subjected to Large Deflection Reversals.” Structural Research Series No. 403, Civil Engineering Studies, University of Illinois, Urbana-Champaign.

Xiao, Y., and Martirossyan, A., 1998. “Seismic Performance of High-Strength Concrete Columns.” J. of Struct. Eng., 124(3), 241-251.

Zahn, F.A., Park, R., and Priestley, M.J.N., 1986. “Design of Reinforced Bridge Columns for Strength and Ductility.” Report 86-7, Department of Civil Engineering, University of Canterbury, Christchurch, New Zealand.

Zhou, X., Satoh, T., Jiang, W., Ono, A., and Shimizo, Y., 1987. “Behavior of Reinforced Concrete Short Column Under High Axial Load.” Transactions of the Japan Concrete Institute, 9.

# APPENDIX A

# PROPERTIES OF RC COLUMN TESTS IN PEER DATABASE

**Table A.1** Properties of RC column tests in PEER database

| No. | Test Specimen ID | $f_c$ (MPa) | $f_{yl}$ (MPa) | $\rho_l$ | $\rho_t$ | $\rho_w$ | Axial load Ratio | Slenderness Ratio | Shear Ratio | Shear span to depth Ratio | Confin. code | Loading History |
|---|---|---|---|---|---|---|---|---|---|---|---|---|
| **1** | Gill et al. 1979, No. 1 | 23.1 | 375 | 0.0179 | 0.016 | 0.007 | 0.26 | 15.10 | 0.487 | 2.18 | 7 | SA |
| **2** | Gill et al. 1979, No. 2 | 41.4 | 375 | 0.0179 | 0.025 | 0.011 | 0.21 | 15.10 | 0.422 | 2.18 | 7 | SA |
| **3** | Gill et al. 1979, No. 3 | 21.4 | 375 | 0.0179 | 0.017 | 0.008 | 0.42 | 15.10 | 0.495 | 2.18 | 4 | SA |
| **4** | Gill et al. 1979, No. 4 | 23.5 | 375 | 0.0179 | 0.030 | 0.013 | 0.60 | 15.10 | 0.511 | 2.18 | 4 | SA |
| **5** | Ang et al. 1981, No. 3 | 23.6 | 427 | 0.0151 | 0.025 | 0.011 | 0.38 | 27.68 | 0.263 | 4.00 | 4 | SA |
| **6** | Ang et al. 1981, No. 4 | 25 | 427 | 0.0151 | 0.019 | 0.009 | 0.21 | 27.68 | 0.224 | 4.00 | 4 | SA |
| **7** | Soesianawati et al. 1986, No. 1 | 46.5 | 446 | 0.0151 | 0.010 | 0.005 | 0.10 | 27.68 | 0.189 | 4.00 | 7 | SA |
| **8** | Soesianawati et al. 1986, No. 2 | 44 | 446 | 0.0151 | 0.013 | 0.006 | 0.30 | 27.68 | 0.272 | 4.00 | 7 | SA |
| **9** | Soesianawati et al. 1986, No. 3 | 44 | 446 | 0.0151 | 0.009 | 0.004 | 0.30 | 27.68 | 0.270 | 4.00 | 7 | SA |
| **10** | Soesianawati et al. 1986, No. 4 | 40 | 446 | 0.0151 | 0.006 | 0.003 | 0.30 | 27.68 | 0.271 | 4.00 | 7 | SA |
| **11** | Zahn et al. 1986, No. 7 | 28.3 | 440 | 0.0151 | 0.014 | 0.007 | 0.22 | 27.68 | 0.259 | 4.00 | 4 | SA |
| **12** | Zahn et al. 1986, No. 8 | 40.1 | 440 | 0.0151 | 0.018 | 0.009 | 0.39 | 27.68 | 0.274 | 4.00 | 4 | SA |
| **13** | Watson and Park 1989, No. 5 | 41 | 474 | 0.0151 | 0.013 | 0.006 | 0.50 | 27.68 | 0.295 | 4.00 | 7 | SA |
| **14** | Watson and Park 1989, No. 6 | 40 | 474 | 0.0151 | 0.006 | 0.003 | 0.50 | 27.68 | 0.301 | 4.00 | 7 | SA |
| **15** | Watson and Park 1989, No. 7 | 42 | 474 | 0.0151 | 0.024 | 0.012 | 0.70 | 27.68 | 0.292 | 4.00 | 7 | SA |
| **16** | Watson and Park 1989, No. 8 | 39 | 474 | 0.0151 | 0.014 | 0.007 | 0.70 | 27.68 | 0.305 | 4.00 | 7 | SA |
| **17** | Watson and Park 1989, No. 9 | 40 | 474 | 0.0151 | 0.045 | 0.022 | 0.70 | 27.68 | 0.317 | 4.00 | 7 | SA |
| **18** | Tanaka and Park 1990, No. 1 | 25.6 | 474 | 0.0157 | 0.026 | 0.011 | 0.20 | 27.68 | 0.229 | 4.00 | 6 | SA |
| **19** | Tanaka and Park 1990, No. 2 | 25.6 | 474 | 0.0157 | 0.026 | 0.011 | 0.20 | 27.68 | 0.231 | 4.00 | 6 | SA |
| **20** | Tanaka and Park 1990, No. 3 | 25.6 | 474 | 0.0157 | 0.026 | 0.011 | 0.20 | 27.68 | 0.240 | 4.00 | 9 | SA |
| **21** | Tanaka and Park 1990, No. 4 | 25.6 | 474 | 0.0157 | 0.026 | 0.011 | 0.20 | 27.68 | 0.233 | 4.00 | 6 | SA |
| **22** | Tanaka and Park 1990, No. 5 | 32 | 511 | 0.0125 | 0.017 | 0.007 | 0.10 | 20.76 | 0.243 | 3.00 | 6 | SA |
| **23** | Tanaka and Park 1990, No. 6 | 32 | 511 | 0.0125 | 0.017 | 0.007 | 0.10 | 20.76 | 0.258 | 3.00 | 8 | SA |
| **24** | Tanaka and Park 1990, No. 7 | 32.1 | 511 | 0.0125 | 0.021 | 0.009 | 0.30 | 20.76 | 0.370 | 3.00 | 6 | SA |
| **25** | Tanaka and Park 1990, No. 8 | 32.1 | 511 | 0.0125 | 0.021 | 0.009 | 0.30 | 20.76 | 0.389 | 3.00 | 8 | SA |

**Table A.1** (cont'd)

| No. | Test Specimen ID | $f_c$ (MPa) | $f_{yl}$ (MPa) | $\rho_l$ | $\rho_t$ | $\rho_w$ | Axial load Ratio | Slenderness Ratio | Shear Ratio | Shear span to depth Ratio | Confin. code | Loading History |
|---|---|---|---|---|---|---|---|---|---|---|---|---|
| **26** | Park and Paulay 1990, No. 9 | 26.9 | 432 | 0.0188 | 0.019 | 0.011 | 0.10 | 20.58 | 0.329 | 2.97 | 5 | SA |
| **27** | Ohno and Nishioka 1984, L2 | 24.8 | 362 | 0.0142 | 0.007 | 0.003 | 0.03 | 27.68 | 0.151 | 4.00 | 2 | SA |
| **28** | Ohno and Nishioka 1984, L3 | 24.8 | 362 | 0.0142 | 0.007 | 0.003 | 0.03 | 27.68 | 0.142 | 4.00 | 2 | SA |
| **29** | Zhou et al. 1987, No. 214-08 | 21.1 | 341 | 0.0222 | 0.014 | 0.006 | 0.80 | 13.84 | 0.544 | 2.00 | 2 | SA |
| **30** | Kanda et al. 1988, 85STC-1 | 27.9 | 374 | 0.0162 | 0.010 | 0.004 | 0.11 | 20.76 | 0.268 | 3.00 | 2 | SA |
| **31** | Kanda et al. 1988, 85STC-2 | 27.9 | 374 | 0.0162 | 0.010 | 0.004 | 0.11 | 20.76 | 0.282 | 3.00 | 2 | SA |
| **32** | Kanda et al. 1988, 85STC-3 | 27.9 | 374 | 0.0162 | 0.010 | 0.004 | 0.11 | 20.76 | 0.268 | 3.00 | 2 | SA |
| **33** | Muguruma et al. 1989, AH-1 | 85.7 | 399.6 | 0.038 | 0.034 | 0.016 | 0.40 | 17.30 | 0.690 | 2.50 | 4 | SA |
| **34** | Muguruma et al. 1989, AL-2 | 85.7 | 399.6 | 0.038 | 0.034 | 0.016 | 0.63 | 17.30 | 0.684 | 2.50 | 4 | SA |
| **35** | Mugumura et al. 1989, AH-2 | 85.7 | 399.6 | 0.038 | 0.034 | 0.016 | 0.63 | 17.30 | 0.698 | 2.50 | 4 | SA |
| **36** | Muguruma et al. 1989, BL-1 | 115.8 | 399.6 | 0.038 | 0.034 | 0.016 | 0.25 | 17.30 | 0.586 | 2.50 | 4 | SA |
| **37** | Muguruma et al. 1989, BH-1 | 115.8 | 399.6 | 0.038 | 0.034 | 0.016 | 0.25 | 17.30 | 0.598 | 2.50 | 4 | SA |
| **38** | Muguruma et al. 1989, BH-2 | 115.8 | 399.6 | 0.038 | 0.034 | 0.016 | 0.42 | 17.30 | 0.701 | 2.50 | 4 | SA |
| **39** | Sakai et al. 1990, B1 | 99.5 | 379 | 0.0243 | 0.013 | 0.005 | 0.35 | 13.84 | 0.664 | 2.00 | 4 | VA |
| **40** | Sakai et al. 1990, B2 | 99.5 | 379 | 0.0243 | 0.019 | 0.008 | 0.35 | 13.84 | 0.657 | 2.00 | 4 | VA |
| **41** | Sakai et al. 1990, B3 | 99.5 | 379 | 0.0243 | 0.015 | 0.006 | 0.35 | 13.84 | 0.719 | 2.00 | 4 | SA |
| **42** | Sakai et al. 1990, B4 | 99.5 | 379 | 0.0243 | 0.013 | 0.005 | 0.35 | 13.84 | 0.664 | 2.00 | 4 | VA |
| **43** | Atalay and Penzien 1975, No. 1S1 | 29.1 | 367 | 0.0163 | 0.015 | 0.006 | 0.10 | 38.03 | 0.138 | 5.50 | 2 | SA |
| **44** | Atalay and Penzien 1975, No. 2S1 | 30.7 | 367 | 0.0163 | 0.009 | 0.004 | 0.09 | 38.03 | 0.132 | 5.50 | 2 | SA |
| **45** | Atalay and Penzien 1975, No. 3S1 | 29.2 | 367 | 0.0163 | 0.015 | 0.006 | 0.10 | 38.03 | 0.127 | 5.50 | 2 | SA |
| **46** | Atalay and Penzien 1975, No. 4S1 | 27.6 | 429 | 0.0163 | 0.009 | 0.004 | 0.10 | 38.03 | 0.112 | 5.50 | 2 | SA |
| **47** | Atalay and Penzien 1975, No. 5S1 | 29.4 | 429 | 0.0163 | 0.015 | 0.006 | 0.20 | 38.03 | 0.164 | 5.50 | 2 | SA |
| **48** | Atalay and Penzien 1975, No. 6S1 | 31.8 | 429 | 0.0163 | 0.009 | 0.004 | 0.18 | 38.03 | 0.160 | 5.50 | 2 | SA |
| **49** | Atalay and Penzien 1975, No. 9 | 33.3 | 363 | 0.0163 | 0.015 | 0.006 | 0.26 | 38.03 | 0.164 | 5.50 | 2 | SA |
| **50** | Atalay and Penzien 1975, No. 10 | 32.4 | 363 | 0.0163 | 0.009 | 0.004 | 0.27 | 38.03 | 0.165 | 5.50 | 2 | SA |

**Table A.1** (cont'd)

| No. | Test Specimen ID | $f_c$ (MPa) | $f_{yl}$ (MPa) | $\rho_l$ | $\rho_t$ | $\rho_w$ | Axial load Ratio | Slenderness Ratio | Shear Ratio | Shear span to depth Ratio | Confin. code | Loading History |
|---|---|---|---|---|---|---|---|---|---|---|---|---|
| **51** | Atalay and Penzien 1975, No. 11 | 31 | 363 | 0.0163 | 0.015 | 0.006 | 0.28 | 38.03 | 0.166 | 5.50 | 2 | SA |
| **52** | Atalay and Penzien 1975, No. 12 | 31.8 | 363 | 0.0163 | 0.009 | 0.004 | 0.27 | 38.03 | 0.166 | 5.50 | 2 | SA |
| **53** | Azizinamini et al. 1988, NC-2 | 39.3 | 439 | 0.0194 | 0.021 | 0.009 | 0.21 | 20.78 | 0.369 | 3.00 | 3 | SA |
| **54** | Azizinamini et al. 1988, NC-4 | 39.8 | 439 | 0.0194 | 0.012 | 0.005 | 0.31 | 20.78 | 0.386 | 3.00 | 3 | SA |
| **55** | Saatcioglu and Ozcebe 1989, U1 | 43.6 | 430 | 0.0321 | 0.007 | 0.003 | 0.00 | 19.77 | 0.365 | 2.86 | 2 | VA |
| **56** | Saatcioglu and Ozcebe 1989, U3 | 34.8 | 430 | 0.0321 | 0.013 | 0.006 | 0.14 | 19.77 | 0.395 | 2.86 | 2 | VA |
| **57** | Saatcioglu and Ozcebe 1989, U4 | 32 | 438 | 0.0321 | 0.020 | 0.009 | 0.15 | 19.77 | 0.500 | 2.86 | 2 | VA |
| **58** | Saatcioglu and Ozcebe 1989, U6 | 37.3 | 437 | 0.0321 | 0.020 | 0.008 | 0.13 | 19.77 | 0.492 | 2.86 | 6 | VA |
| **59** | Saatcioglu and Ozcebe 1989, U7 | 39 | 437 | 0.0321 | 0.020 | 0.008 | 0.13 | 19.77 | 0.480 | 2.86 | 6 | VA |
| **60** | Galeota et al. 1996, AA4 | 80 | 430 | 0.0151 | 0.014 | 0.005 | 0.20 | 31.56 | 0.281 | 4.56 | 4 | CA |
| **61** | Galeota et al. 1996, BA1 | 80 | 430 | 0.0151 | 0.020 | 0.008 | 0.20 | 31.56 | 0.287 | 4.56 | 4 | CA |
| **62** | Galeota et al. 1996, BA4 | 80 | 430 | 0.0151 | 0.020 | 0.008 | 0.20 | 31.56 | 0.224 | 4.56 | 4 | CA |
| **63** | Galeota et al. 1996, CA1 | 80 | 430 | 0.0151 | 0.041 | 0.016 | 0.20 | 31.56 | 0.205 | 4.56 | 4 | SA |
| **64** | Galeota et al. 1996, CA2 | 80 | 430 | 0.0151 | 0.041 | 0.016 | 0.30 | 31.56 | 0.256 | 4.56 | 4 | SA |
| **65** | Galeota et al. 1996, CA3 | 80 | 430 | 0.0151 | 0.041 | 0.016 | 0.20 | 31.56 | 0.268 | 4.56 | 4 | SA |
| **66** | Galeota et al. 1996, CA4 | 80 | 430 | 0.0151 | 0.041 | 0.016 | 0.30 | 31.56 | 0.274 | 4.56 | 4 | SA |
| **67** | Galeota et al. 1996, BB | 80 | 430 | 0.0603 | 0.020 | 0.008 | 0.20 | 31.56 | 0.321 | 4.56 | 4 | SA |
| **68** | Galeota et al. 1996, BB1 | 80 | 430 | 0.0603 | 0.020 | 0.008 | 0.20 | 31.56 | 0.396 | 4.56 | 4 | SA |
| **69** | Galeota et al. 1996, BB4 | 80 | 430 | 0.0603 | 0.020 | 0.008 | 0.30 | 31.56 | 0.356 | 4.56 | 4 | SA |
| **70** | Galeota et al. 1996, BB4B | 80 | 430 | 0.0603 | 0.020 | 0.008 | 0.30 | 31.56 | 0.348 | 4.56 | 4 | SA |
| **71** | Galeota et al. 1996, CB1 | 80 | 430 | 0.0603 | 0.041 | 0.016 | 0.20 | 31.56 | 0.350 | 4.56 | 4 | SA |
| **72** | Galeota et al. 1996, CB2 | 80 | 430 | 0.0603 | 0.041 | 0.016 | 0.20 | 31.56 | 0.339 | 4.56 | 4 | SA |
| **73** | Galeota et al. 1996, CB3 | 80 | 430 | 0.0603 | 0.041 | 0.016 | 0.30 | 31.56 | 0.346 | 4.56 | 4 | SA |
| **74** | Galeota et al. 1996, CB4 | 80 | 430 | 0.0603 | 0.041 | 0.016 | 0.30 | 31.56 | 0.350 | 4.56 | 4 | SA |
| **75** | Wehbe et al. 1998, A1 | 27.2 | 448 | 0.0222 | 0.005 | 0.003 | 0.10 | 26.49 | 0.292 | 3.83 | 6 | SA |

**Table A.1** (cont'd)

| No. | Test Specimen ID | $f_c$ (MPa) | $f_{yl}$ (MPa) | $\rho_l$ | $\rho_t$ | $\rho_w$ | Axial load Ratio | Slenderness Ratio | Shear Ratio | Shear span to depth Ratio | Confin. code | Loading History |
|---|---|---|---|---|---|---|---|---|---|---|---|---|
| **76** | Wehbe et al. 1998, A2 | 27.2 | 448 | 0.0222 | 0.005 | 0.003 | 0.24 | 26.49 | 0.315 | 3.83 | 6 | SA |
| **77** | Wehbe et al. 1998, B1 | 28.1 | 448 | 0.0222 | 0.006 | 0.004 | 0.09 | 26.49 | 0.294 | 3.83 | 6 | SA |
| **78** | Wehbe et al. 1998, B2 | 28.1 | 448 | 0.0222 | 0.006 | 0.004 | 0.23 | 26.49 | 0.316 | 3.83 | 6 | SA |
| **79** | Xiao and Martirossyan 1998, HC4-8L19-T10-0.1P | 76 | 510 | 0.0355 | 0.034 | 0.016 | 0.10 | 13.84 | 0.607 | 2.00 | 6 | SA |
| **80** | Xiao and Martirossyan 1998, HC4-8L19-T10-0.2P | 76 | 510 | 0.0355 | 0.034 | 0.016 | 0.20 | 13.84 | 0.708 | 2.00 | 6 | SA |
| **81** | Xiao and Martirossyan 1998, HC4-8L16-T10-0.1P | 86 | 510 | 0.0246 | 0.034 | 0.016 | 0.10 | 13.84 | 0.486 | 2.00 | 6 | SA |
| **82** | Xiao and Martirossyan 1998, HC4-8L16-T10-0.2P | 86 | 510 | 0.0246 | 0.034 | 0.016 | 0.19 | 13.84 | 0.562 | 2.00 | 6 | SA |
| **83** | Sugano 1996, UC10H | 118 | 393 | 0.0186 | 0.017 | 0.008 | 0.60 | 13.84 | 0.639 | 2.00 | 4 | SA |
| **84** | Sugano 1996, UC15H | 118 | 393 | 0.0186 | 0.027 | 0.013 | 0.60 | 13.84 | 0.698 | 2.00 | 4 | SA |
| **85** | Sugano 1996, UC20H | 118 | 393 | 0.0186 | 0.035 | 0.016 | 0.60 | 13.84 | 0.750 | 2.00 | 4 | SA |
| **86** | Sugano 1996, UC15L | 118 | 393 | 0.0186 | 0.027 | 0.013 | 0.35 | 13.84 | 0.695 | 2.00 | 4 | SA |
| **87** | Sugano 1996, UC20L | 118 | 393 | 0.0186 | 0.035 | 0.016 | 0.35 | 13.84 | 0.708 | 2.00 | 4 | SA |
| **88** | Bayrak and Sheikh 1996, ES-1HT | 72.1 | 454 | 0.0258 | 0.028 | 0.014 | 0.50 | 41.79 | 0.163 | 6.04 | 2 | SA |
| **89** | Bayrak and Sheikh 1996, AS-2HT | 71.7 | 454 | 0.0258 | 0.026 | 0.012 | 0.36 | 41.79 | 0.186 | 6.04 | 3 | SA |
| **90** | Bayrak and Sheikh 1996, AS-3HT | 71.8 | 454 | 0.0258 | 0.026 | 0.012 | 0.50 | 41.79 | 0.180 | 6.04 | 3 | SA |
| **91** | Bayrak and Sheikh 1996, AS-4HT | 71.9 | 454 | 0.0258 | 0.046 | 0.022 | 0.50 | 41.79 | 0.167 | 6.04 | 3 | SA |
| **92** | Bayrak and Sheikh 1996, AS-5HT | 101.8 | 454 | 0.0258 | 0.051 | 0.025 | 0.45 | 41.79 | 0.192 | 6.04 | 3 | SA |
| **93** | Bayrak and Sheikh 1996, AS-6HT | 101.9 | 454 | 0.0258 | 0.060 | 0.029 | 0.46 | 41.79 | 0.170 | 6.04 | 3 | SA |
| **94** | Bayrak and Sheikh 1996, AS-7HT | 102 | 454 | 0.0258 | 0.025 | 0.012 | 0.45 | 41.79 | 0.161 | 6.04 | 3 | SA |
| **95** | Bayrak and Sheikh 1996, ES-8HT | 102.2 | 454 | 0.0258 | 0.038 | 0.019 | 0.47 | 41.79 | 0.183 | 6.04 | 2 | SA |
| **96** | Saatcioglu and Grira 1999, BG-1 | 34 | 455.6 | 0.0195 | 0.009 | 0.004 | 0.43 | 32.52 | 0.258 | 4.70 | 4 | SA |
| **97** | Saatcioglu and Grira 1999, BG-2 | 34 | 455.6 | 0.0195 | 0.019 | 0.008 | 0.43 | 32.52 | 0.252 | 4.70 | 4 | SA |
| **98** | Saatcioglu and Grira 1999, BG-3 | 34 | 455.6 | 0.0195 | 0.019 | 0.008 | 0.20 | 32.52 | 0.226 | 4.70 | 4 | SA |
| **99** | Saatcioglu and Grira 1999, BG-4 | 34 | 455.6 | 0.0293 | 0.012 | 0.005 | 0.46 | 32.52 | 0.261 | 4.70 | 4 | SA |
| **100** | Saatcioglu and Grira 1999, BG-5 | 34 | 455.6 | 0.0293 | 0.025 | 0.011 | 0.46 | 32.52 | 0.264 | 4.70 | 4 | SA |

**Table A.1** (cont'd)

| No. | Test Specimen ID | $f_c$ (MPa) | $f_{yl}$ (MPa) | $\rho_l$ | $\rho_t$ | $\rho_w$ | Axial load Ratio | Slenderness Ratio | Shear Ratio | Shear span to depth Ratio | Confin. code | Loading History |
|---|---|---|---|---|---|---|---|---|---|---|---|---|
| **101** | Saatcioglu and Grira 1999, BG-6 | 34 | 477.8 | 0.0229 | 0.025 | 0.011 | 0.46 | 32.52 | 0.287 | 4.70 | 4 | SA |
| **102** | Saatcioglu and Grira 1999, BG-7 | 34 | 455.6 | 0.0293 | 0.012 | 0.005 | 0.46 | 32.52 | 0.272 | 4.70 | 4 | SA |
| **103** | Saatcioglu and Grira 1999, BG-8 | 34 | 455.6 | 0.0293 | 0.012 | 0.005 | 0.23 | 32.52 | 0.275 | 4.70 | 4 | SA |
| **104** | Saatcioglu and Grira 1999, BG-9 | 34 | 427.8 | 0.0328 | 0.012 | 0.005 | 0.46 | 32.52 | 0.282 | 4.70 | 4 | SA |
| **105** | Saatcioglu and Grira 1999, BG-10 | 34 | 427.8 | 0.0328 | 0.025 | 0.011 | 0.46 | 32.52 | 0.270 | 4.70 | 4 | SA |
| **106** | Matamoros et al. 1999,C10-05N | 69.6 | 586.1 | 0.0193 | 0.026 | 0.009 | 0.05 | 20.79 | 0.248 | 3.00 | 2 | SA |
| **107** | Matamoros et al. 1999,C10-05S | 69.6 | 586.1 | 0.0193 | 0.027 | 0.009 | 0.05 | 20.79 | 0.242 | 3.00 | 2 | SA |
| **108** | Matamoros et al. 1999,C10-10N | 67.8 | 572.3 | 0.0193 | 0.022 | 0.009 | 0.10 | 20.79 | 0.317 | 3.00 | 2 | SA |
| **109** | Matamoros et al. 1999,C10-10S | 67.8 | 573.3 | 0.0193 | 0.021 | 0.009 | 0.10 | 20.79 | 0.305 | 3.00 | 2 | SA |
| **110** | Matamoros et al. 1999,C10-20N | 65.5 | 572.3 | 0.0193 | 0.021 | 0.009 | 0.21 | 20.79 | 0.356 | 3.00 | 2 | SA |
| **111** | Matamoros et al. 1999,C10-20S | 65.5 | 573.3 | 0.0193 | 0.021 | 0.009 | 0.21 | 20.79 | 0.338 | 3.00 | 2 | SA |
| **112** | Matamoros et al. 1999,C5-00N | 37.9 | 572.3 | 0.0193 | 0.021 | 0.009 | 0.00 | 20.79 | 0.257 | 3.00 | 2 | SA |
| **113** | Matamoros et al. 1999,C5-00S | 37.9 | 573.3 | 0.0193 | 0.021 | 0.009 | 0.00 | 20.79 | 0.254 | 3.00 | 2 | SA |
| **114** | Matamoros et al. 1999,C5-20N | 48.3 | 586.1 | 0.0193 | 0.026 | 0.009 | 0.14 | 20.79 | 0.300 | 3.00 | 2 | SA |
| **115** | Matamoros et al. 1999,C5-20S | 48.3 | 587.1 | 0.0193 | 0.026 | 0.009 | 0.14 | 20.79 | 0.294 | 3.00 | 2 | SA |
| **116** | Matamoros et al. 1999,C5-40N | 38.1 | 572.3 | 0.0193 | 0.021 | 0.009 | 0.36 | 20.79 | 0.369 | 3.00 | 2 | SA |
| **117** | Matamoros et al. 1999,C5-40S | 38.1 | 573.3 | 0.0193 | 0.021 | 0.009 | 0.36 | 20.79 | 0.372 | 3.00 | 2 | SA |
| **118** | Mo and Wang 2000,C1-1 | 24.9 | 497 | 0.0214 | 0.015 | 0.006 | 0.11 | 24.22 | 0.333 | 3.50 | 6 | SA |
| **119** | Mo and Wang 2000,C1-2 | 26.7 | 497 | 0.0214 | 0.015 | 0.006 | 0.16 | 24.22 | 0.341 | 3.50 | 6 | SA |
| **120** | Mo and Wang 2000,C1-3 | 26.1 | 497 | 0.0214 | 0.015 | 0.006 | 0.22 | 24.22 | 0.389 | 3.50 | 6 | SA |
| **121** | Mo and Wang 2000,C2-1 | 25.3 | 497 | 0.0214 | 0.014 | 0.006 | 0.11 | 24.22 | 0.327 | 3.50 | 4 | SA |
| **122** | Mo and Wang 2000,C2-2 | 27.1 | 497 | 0.0214 | 0.014 | 0.006 | 0.16 | 24.22 | 0.328 | 3.50 | 4 | SA |
| **123** | Mo and Wang 2000,C2-3 | 26.8 | 497 | 0.0214 | 0.014 | 0.006 | 0.21 | 24.22 | 0.388 | 3.50 | 4 | SA |
| **124** | Mo and Wang 2000,C3-1 | 26.4 | 497 | 0.0214 | 0.014 | 0.006 | 0.11 | 24.22 | 0.303 | 3.50 | 4 | SA |
| **125** | Mo and Wang 2000,C3-2 | 27.5 | 497 | 0.0214 | 0.014 | 0.006 | 0.15 | 24.22 | 0.323 | 3.50 | 4 | SA |

**Table A.1** (cont'd)

| No. | Test Specimen ID | $f_c$ (MPa) | $f_{yl}$ (MPa) | $\rho_l$ | $\rho_t$ | $\rho_w$ | Axial load Ratio | Slenderness Ratio | Shear Ratio | Shear span to depth Ratio | Confin. code | Loading History |
|---|---|---|---|---|---|---|---|---|---|---|---|---|
| **126** | Mo and Wang 2000,C3-3 | 26.9 | 497 | 0.0214 | 0.014 | 0.006 | 0.21 | 24.22 | 0.377 | 3.50 | 4 | SA |
| **127** | Thomsen and Wallace 1994, A1 | 102.7 | 517.1 | 0.0245 | 0.014 | 0.006 | 0.00 | 27.10 | 0.202 | 3.92 | 6 | SA |
| **128** | Thomsen and Wallace 1994, A3 | 86.3 | 517.1 | 0.0245 | 0.014 | 0.006 | 0.20 | 27.10 | 0.335 | 3.92 | 6 | SA |
| **129** | Thomsen and Wallace 1994, B1 | 87.5 | 455.1 | 0.0245 | 0.016 | 0.007 | 0.00 | 27.10 | 0.159 | 3.92 | 3 | SA |
| **130** | Thomsen and Wallace 1994, B2 | 83.4 | 455.1 | 0.0245 | 0.016 | 0.007 | 0.10 | 27.10 | 0.244 | 3.92 | 3 | SA |
| **131** | Thomsen and Wallace 1994, B3 | 90 | 455.1 | 0.0245 | 0.016 | 0.007 | 0.20 | 27.10 | 0.284 | 3.92 | 3 | SA |
| **132** | Thomsen and Wallace 1994, C1 | 67.5 | 475.8 | 0.0245 | 0.016 | 0.007 | 0.00 | 27.10 | 0.209 | 3.92 | 3 | SA |
| **133** | Thomsen and Wallace 1994, C2 | 74.6 | 475.8 | 0.0245 | 0.016 | 0.007 | 0.10 | 27.10 | 0.237 | 3.92 | 3 | SA |
| **134** | Thomsen and Wallace 1994, C3 | 81.8 | 475.8 | 0.0245 | 0.016 | 0.007 | 0.20 | 27.10 | 0.257 | 3.92 | 3 | SA |
| **135** | Thomsen and Wallace 1994, D1 | 75.8 | 475.8 | 0.0245 | 0.013 | 0.006 | 0.20 | 27.10 | 0.277 | 3.92 | 3 | SA |
| **136** | Thomsen and Wallace 1994, D2 | 87 | 475.8 | 0.0245 | 0.011 | 0.005 | 0.20 | 27.10 | 0.274 | 3.92 | 3 | SA |
| **137** | Thomsen and Wallace 1994, D3 | 71.2 | 475.8 | 0.0245 | 0.009 | 0.004 | 0.20 | 27.10 | 0.264 | 3.92 | 3 | SA |
| **138** | Paultre and Legeron, 2000, No. 1006015 | 92.4 | 451 | 0.0215 | 0.041 | 0.019 | 0.14 | 45.38 | 0.119 | 6.56 | 3 | SA |
| **139** | Paultre and Legeron, 2000, No. 1006025 | 93.3 | 430 | 0.0215 | 0.041 | 0.019 | 0.28 | 45.38 | 0.154 | 6.56 | 3 | SA |
| **140** | Paultre and Legeron, 2000, No. 1006040 | 98.2 | 451 | 0.0215 | 0.041 | 0.019 | 0.39 | 45.38 | 0.142 | 6.56 | 3 | SA |
| **141** | Paultre and Legeron, 2000, No. 10013015 | 94.8 | 451 | 0.0215 | 0.019 | 0.009 | 0.14 | 45.38 | 0.106 | 6.56 | 3 | SA |
| **142** | Paultre and Legeron, 2000, No. 10013025 | 97.7 | 430 | 0.0215 | 0.019 | 0.009 | 0.26 | 45.38 | 0.162 | 6.56 | 3 | SA |
| **143** | Paultre and Legeron, 2000, No. 10013040 | 104.3 | 451 | 0.0215 | 0.019 | 0.009 | 0.37 | 45.38 | 0.168 | 6.56 | 3 | SA |
| **144** | Paultre et al., 2001, No. 806040 | 78.7 | 446 | 0.0215 | 0.041 | 0.019 | 0.40 | 45.38 | 0.168 | 6.56 | 3 | SA |
| **145** | Paultre et al., 2001, No. 1206040 | 109.2 | 446 | 0.0215 | 0.041 | 0.019 | 0.41 | 45.38 | 0.171 | 6.56 | 3 | SA |
| **146** | Paultre et al., 2001, No. 1005540 | 109.5 | 446 | 0.0215 | 0.044 | 0.020 | 0.41 | 45.38 | 0.157 | 6.56 | 3 | SA |
| **147** | Paultre et al., 2001, No. 1008040 | 104.2 | 446 | 0.0215 | 0.031 | 0.014 | 0.37 | 45.38 | 0.153 | 6.56 | 3 | SA |
| **148** | Paultre et al., 2001, No. 1005552 | 104.5 | 446 | 0.0215 | 0.044 | 0.020 | 0.53 | 45.38 | 0.168 | 6.56 | 3 | SA |
| **149** | Paultre et al., 2001, No. 1006052 | 109.4 | 446 | 0.0215 | 0.041 | 0.019 | 0.51 | 45.38 | 0.164 | 6.56 | 3 | SA |
| **150** | Pujol 2002, No. 10-2-3N | 33.7 | 453 | 0.0245 | 0.011 | 0.005 | 0.08 | 15.57 | 0.457 | 2.25 | 2 | SA |

**Table A.1** (cont'd)

| No. | Test Specimen ID | $f_c$ (MPa) | $f_{yl}$ (MPa) | $\rho_l$ | $\rho_t$ | $\rho_w$ | Axial load Ratio | Slenderness Ratio | Shear Ratio | Shear span to depth Ratio | Confin. code | Loading History |
|---|---|---|---|---|---|---|---|---|---|---|---|---|
| **151** | Pujol 2002, No. 10-2-3S | 33.7 | 453 | 0.0245 | 0.011 | 0.005 | 0.08 | 15.57 | 0.457 | 2.25 | 2 | SA |
| **152** | Pujol 2002, No. 10-3-1.5N | 32.1 | 453 | 0.0245 | 0.022 | 0.011 | 0.09 | 15.57 | 0.467 | 2.25 | 2 | SA |
| **153** | Pujol 2002, No. 10-3-1.5S | 32.1 | 453 | 0.0245 | 0.022 | 0.011 | 0.09 | 15.57 | 0.467 | 2.25 | 2 | SA |
| **154** | Pujol 2002, No. 10-3-3N | 29.9 | 453 | 0.0245 | 0.011 | 0.005 | 0.10 | 15.57 | 0.484 | 2.25 | 2 | CA |
| **155** | Pujol 2002, No. 10-3-3S | 29.9 | 453 | 0.0245 | 0.011 | 0.005 | 0.10 | 15.57 | 0.484 | 2.25 | 2 | SA |
| **156** | Pujol 2002, No. 10-3-2.25N | 27.4 | 453 | 0.0245 | 0.015 | 0.007 | 0.10 | 15.57 | 0.514 | 2.25 | 2 | CA |
| **157** | Pujol 2002, No. 10-3-2.25S | 27.4 | 453 | 0.0245 | 0.015 | 0.007 | 0.10 | 15.57 | 0.514 | 2.25 | 2 | CA |
| **158** | Pujol 2002, No. 20-3-3N | 36.4 | 453 | 0.0245 | 0.011 | 0.005 | 0.16 | 15.57 | 0.509 | 2.25 | 2 | CA |
| **159** | Pujol 2002, No. 20-3-3S | 36.4 | 453 | 0.0245 | 0.011 | 0.005 | 0.16 | 15.57 | 0.509 | 2.25 | 2 | CA |
| **160** | Pujol 2002, No. 10-2-2.25N | 34.9 | 453 | 0.0245 | 0.015 | 0.007 | 0.08 | 15.57 | 0.464 | 2.25 | 2 | SA |
| **161** | Pujol 2002, No. 10-2-2.25S | 34.9 | 453 | 0.0245 | 0.015 | 0.007 | 0.08 | 15.57 | 0.464 | 2.25 | 2 | SA |
| **162** | Pujol 2002, No. 10-1-2.25N | 36.5 | 453 | 0.0245 | 0.015 | 0.007 | 0.08 | 15.57 | 0.457 | 2.25 | 2 | SA |
| **163** | Pujol 2002, No. 10-1-2.25S | 36.5 | 453 | 0.0245 | 0.015 | 0.007 | 0.08 | 15.57 | 0.457 | 2.25 | 2 | SA |
| **164** | Bechtoula et al, 2002, D1N30 | 37.6 | 461 | 0.0243 | 0.012 | 0.005 | 0.30 | 17.30 | 0.566 | 2.50 | 8 | SA |
| **165** | Bechtoula et al, 2002, D1N60 | 37.6 | 461 | 0.0243 | 0.012 | 0.005 | 0.60 | 17.30 | 0.524 | 2.50 | 8 | SA |
| **166** | Bechtoula et al, 2002, L1N60 | 39.2 | 388 | 0.0169 | 0.019 | 0.008 | 0.57 | 13.84 | 0.642 | 2.00 | 8 | SA |
| **167** | Bechtoula et al, 2002, L1N6B | 32.2 | 388 | 0.0194 | 0.019 | 0.009 | 0.59 | 14.83 | 0.706 | 2.14 | 8 | SA |
| **168** | Takemura and Kawashima, 1997, Test 1 (JSCE-4) | 35.9 | 363 | 0.0158 | 0.005 | 0.002 | 0.03 | 21.54 | 0.168 | 3.11 | 2 | SA |
| **169** | Takemura and Kawashima, 1997, Test 2 (JSCE-5) | 35.7 | 363 | 0.0158 | 0.005 | 0.002 | 0.03 | 21.54 | 0.164 | 3.11 | 2 | SA |
| **170** | Takemura and Kawashima, 1997, Test 3 (JSCE-6) | 34.3 | 363 | 0.0158 | 0.005 | 0.002 | 0.03 | 21.54 | 0.171 | 3.11 | 2 | SA |
| **171** | Takemura and Kawashima, 1997, Test 4 (JSCE-7) | 33.2 | 363 | 0.0158 | 0.005 | 0.002 | 0.03 | 21.54 | 0.179 | 3.11 | 2 | VA |
| **172** | Wight and Sozen 1973, No. 40.033a(East) | 34.7 | 496 | 0.0245 | 0.007 | 0.003 | 0.12 | 19.88 | 0.380 | 2.87 | 2 | CA |
| **173** | Wight and Sozen 1973, No. 40.033a(West) | 34.7 | 496 | 0.0245 | 0.007 | 0.003 | 0.12 | 19.88 | 0.396 | 2.87 | 2 | CA |
| **174** | Wight and Sozen 1973, No. 40.048(East) | 26.1 | 496 | 0.0245 | 0.010 | 0.005 | 0.15 | 19.88 | 0.471 | 2.87 | 2 | SA |
| **175** | Wight and Sozen 1973, No. 40.048(West) | 26.1 | 496 | 0.0245 | 0.010 | 0.005 | 0.15 | 19.88 | 0.443 | 2.87 | 2 | SA |

**Table A.1** (cont'd)

| No. | Test Specimen ID | $f_c$ (MPa) | $f_{yl}$ (MPa) | $\rho_l$ | $\rho_t$ | $\rho_w$ | Axial load Ratio | Slenderness Ratio | Shear Ratio | Shear span to depth Ratio | Confin. code | Loading History |
|---|---|---|---|---|---|---|---|---|---|---|---|---|
| **176** | Wight and Sozen 1973, No. 40.033(East) | 33.6 | 496 | 0.0245 | 0.007 | 0.003 | 0.11 | 19.88 | 0.374 | 2.87 | 2 | CA |
| **177** | Wight and Sozen 1973, No. 40.033(West) | 33.6 | 496 | 0.0245 | 0.007 | 0.003 | 0.11 | 19.88 | 0.415 | 2.87 | 2 | CA |
| **178** | Wight and Sozen 1973, No. 25.033(East) | 33.6 | 496 | 0.0245 | 0.007 | 0.003 | 0.07 | 19.88 | 0.349 | 2.87 | 2 | CA |
| **179** | Wight and Sozen 1973, No. 25.033(West) | 33.6 | 496 | 0.0245 | 0.007 | 0.003 | 0.07 | 19.88 | 0.374 | 2.87 | 2 | CA |
| **180** | Wight and Sozen 1973, No. 40.067(East) | 33.4 | 496 | 0.0245 | 0.014 | 0.006 | 0.11 | 19.88 | 0.354 | 2.87 | 2 | CA |
| **181** | Wight and Sozen 1973, No. 40.067(West) | 33.4 | 496 | 0.0245 | 0.014 | 0.006 | 0.11 | 19.88 | 0.379 | 2.87 | 2 | CA |
| **182** | Wight and Sozen 1973, No. 40.147(East) | 33.5 | 496 | 0.0245 | 0.031 | 0.015 | 0.11 | 19.88 | 0.461 | 2.87 | 2 | CA |
| **183** | Wight and Sozen 1973, No. 40.147(West) | 33.5 | 496 | 0.0245 | 0.031 | 0.015 | 0.11 | 19.88 | 0.436 | 2.87 | 2 | CA |
| **184** | Wight and Sozen 1973, No. 40.092(East) | 33.5 | 496 | 0.0245 | 0.019 | 0.009 | 0.11 | 19.88 | 0.444 | 2.87 | 2 | CA |
| **185** | Wight and Sozen 1973, No. 40.092(West) | 33.5 | 496 | 0.0245 | 0.019 | 0.009 | 0.11 | 19.88 | 0.465 | 2.87 | 2 | CA |
| **186** | Erberik and Sucuoglu 2001, CAH-1 | 20.6 | 330 | 0.0134 | 0.013 | 0.007 | 0.00 | 23.07 | 0.180 | 3.33 | 2 | CA |
| **187** | Erberik and Sucuoglu 2001, CAH-2 | 20.6 | 330 | 0.0134 | 0.013 | 0.007 | 0.00 | 23.07 | 0.178 | 3.33 | 2 | CA |
| **188** | Erberik and Sucuoglu 2001, CAH-3 | 20.6 | 330 | 0.0134 | 0.013 | 0.007 | 0.00 | 23.07 | 0.187 | 3.33 | 2 | CA |
| **189** | Erberik and Sucuoglu 2001, CAH-4 | 20.6 | 330 | 0.0134 | 0.013 | 0.007 | 0.00 | 23.07 | 0.186 | 3.33 | 2 | CA |
| **190** | Erberik and Sucuoglu 2001, CAH-5 | 21.2 | 330 | 0.0134 | 0.013 | 0.007 | 0.00 | 23.07 | 0.176 | 3.33 | 2 | CA |
| **191** | Erberik and Sucuoglu 2001, CAH-6 | 20.6 | 330 | 0.0134 | 0.013 | 0.007 | 0.00 | 23.07 | 0.183 | 3.33 | 2 | CA |
| **192** | Erberik and Sucuoglu 2001, CAL-8 | 13 | 330 | 0.0134 | 0.013 | 0.007 | 0.00 | 23.07 | 0.219 | 3.33 | 2 | CA |
| **193** | Erberik and Sucuoglu 2001, CAL-9 | 13 | 330 | 0.0134 | 0.013 | 0.007 | 0.00 | 23.07 | 0.213 | 3.33 | 2 | CA |
| **194** | Erberik and Sucuoglu 2001, CAL-10 | 13 | 330 | 0.0134 | 0.013 | 0.007 | 0.00 | 23.07 | 0.196 | 3.33 | 2 | CA |
| **195** | Erberik and Sucuoglu 2001, CALU-11 | 13 | 330 | 0.0134 | 0.013 | 0.007 | 0.00 | 23.07 | 0.217 | 3.33 | 2 | CA |
| **196** | Erberik and Sucuoglu 2001, CAL-12 | 13 | 330 | 0.0134 | 0.013 | 0.007 | 0.00 | 23.07 | 0.181 | 3.33 | 2 | CA |

# APPENDIX B

## UNLOADING STIFFNESS PROPERTIES OF THE CYCLIC TESTS

**Table B.1** Unloading stiffness properties of the cyclic test # 1 (Group-A)

| Test ID: Saatcioglu and Ozcebe 1989, Spec. U6 | | | number of occurrence | Ductility based: Parameter 'a' | Focus based: Parameter 'α' | Deviation from initial stiffness (%) |
|---|---|---|---|---|---|---|
| Initial | $K_o$ = | 16.5 | - | - | - | - |
| Unloading | $K_{un,1}$= | 15.71 | 3 | 0.13 | 8.0 | 4.8 |
| | $K_{un,2}$= | 14.45 | 3 | 0.15 | 9.2 | 12.4 |
| | $K_{un,3}$= | 13.83 | 3 | 0.14 | 12.2 | 16.2 |
| | $K_{un,4}$= | 14.67 | 3 | 0.08 | 27.6 | 11.1 |
| K values are in kN/mm. | | | **μ =** | **0.13** | **14.2** | **11.1** |
| | | | **σ =** | 0.03 | 8.2 | 4.3 |
| | | | **cov =** | 0.23 | 0.6 | 0.4 |

**Table B.2** Unloading stiffness properties of the cyclic test # 2 (Group-A)

| Test ID: Ohno and Nishioka 1984, Specimen L2 | | | number of occurrence | Ductility based: Parameter 'a' | Focus based: Parameter 'α' | Deviation from initial stiffness (%) |
|---|---|---|---|---|---|---|
| Initial | $K_o$ = | 11.67 | - | - | - | - |
| Unl. | $K_{un,1}$= | 8.75 | 1 | 0.31 | 3.7 | 25.0 |
| | $K_{un,2}$= | 7.00 | 1 | 0.40 | 2.8 | 40.0 |
| | $K_{un,3}$= | 6.56 | 1 | 0.37 | 3.7 | 43.8 |
| | $K_{un,4}$= | 5.83 | 1 | 0.39 | 4.0 | 50.0 |
| | $K_{un,5}$= | 5.53 | 1 | 0.38 | 4.5 | 52.6 |
| | $K_{un,6}$= | 5.83 | 1 | 0.33 | 6.2 | 50.0 |
| | $K_{un,7}$= | 6.18 | 1 | 0.28 | 8.8 | 47.1 |
| K values are in kN/mm. | | | **μ =** | **0.35** | **4.8** | **44.1** |
| | | | **σ =** | 0.05 | 2.0 | 9.4 |
| | | | **cov =** | 0.13 | 0.4 | 0.2 |

**Table B.3** Unloading stiffness properties of the cyclic test # 3 (Group-A)

| Test ID: Galeota 1996 Specimen BB1 | | | number of occurrence | Ductility based: Parameter 'a' | Focus based: Parameter 'α' | Deviation from initial stiffness (%) |
|---|---|---|---|---|---|---|
| Initial | $K_o$ = | 11.92 | - | - | - | - |
| Unl | $K_{un,1}$= | 8.16 | 1 | 0.72 | 0.5 | 31.6 |
| | $K_{un,2}$= | 5.74 | 4 | 0.54 | 1.6 | 51.9 |
| K values are in kN/mm. | | | **μ =** | **0.58** | **1.4** | **47.8** |
| | | | **σ =** | 0.08 | 0.5 | 9.1 |
| | | | **cov =** | 0.14 | 0.4 | 0.2 |

**Table B.4** Unloading stiffness properties of the cyclic test # 4 (Group-A)

| Test ID: Gill et al. 1979 Specimen 3 | | | number of occurrence | Ductility based: Parameter 'a' | Focus based: Parameter 'α' | Deviation from initial stiffness (%) |
|---|---|---|---|---|---|---|
| Initial | $K_o$ = | 91.18 | - | - | - | - |
| Unl | $K_{un,1}$= | 47.84 | 2 | 0.82 | 0.8 | 47.5 |
| | $K_{un,2}$= | 44.64 | 3 | 0.63 | 1.4 | 51.0 |
| K values are in kN/mm. | | | **μ =** | **0.71** | **1.2** | **49.6** |
| | | | **σ =** | 0.10 | 0.3 | 1.9 |
| | | | **cov =** | 0.14 | 0.3 | 0.0 |

**Table B.5** Unloading stiffness properties of the cyclic test # 5 (Group-A)

| Test ID: Galeota 1996 Specimen CB3 | | | number of occurrence | Ductility based: Parameter 'a' | Focus based: Parameter 'α' | Deviation from initial stiffness (%) |
|---|---|---|---|---|---|---|
| Initial | $K_o$ = | 15.00 | - | - | - | - |
| Unl. | $K_{un,1}$= | 7.50 | 1 | 0.77 | 0.5 | 50.0 |
| | $K_{un,2}$= | 5.89 | 4 | 0.53 | 2.2 | 60.7 |
| | $K_{un,3}$= | 6.60 | 2 | 0.37 | 5.5 | 56.0 |
| K values are in kN/mm. | | | **μ =** | **0.52** | **2.9** | **57.8** |
| | | | **σ =** | 0.13 | 1.9 | 4.1 |
| | | | **cov =** | 0.26 | 0.7 | 0.1 |

**Table B.6** Unloading stiffness properties of the cyclic test # 6 (Group-A)

| Test ID: Galeota 1996 Specimen BB4 | | | number of occurrence | Ductility based: Parameter 'a' | Focus based: Parameter 'α' | Deviation from initial stiffness (%) |
|---|---|---|---|---|---|---|
| Initial | $K_o$ = | 15.00 | - | - | - | - |
| Unl. | $K_{un,1}$= | 10.31 | 1 | 0.69 | 0.6 | 31.3 |
| | $K_{un,2}$= | 6.88 | 4 | 0.56 | 1.5 | 54.2 |
| | $K_{un,3}$= | 6.88 | 1 | 0.42 | 3.5 | 54.2 |
| K values are in kN/mm. | | | **μ =** | **0.56** | **1.7** | **50.3** |
| | | | **σ =** | 0.08 | 1.0 | 9.4 |
| | | | **cov =** | 0.15 | 0.6 | 0.2 |

**Table B.7** Unloading stiffness properties of the cyclic test # 7 (Group-A)

| Test ID: Hakim_Kono 2002 Column L1N6B | | | number of occurrence | Ductility based Parameter 'a' | Focus based Parameter 'α' | Deviation from initial stiffness (%) |
|---|---|---|---|---|---|---|
| Initial | $K_o$ = | 236.00 | - | - | - | - |
| Unl. | $K_{un,1}$= | 148.24 | 2 | 0.79 | 0.7 | 37.2 |
| | $K_{un,2}$= | 107.89 | 2 | 0.89 | 0.5 | 54.3 |
| | $K_{un,3}$= | 73.57 | 2 | 0.72 | 1.0 | 68.8 |
| K values are in kN/mm. | | | **μ =** | **0.80** | **0.7** | **53.4** |
| | | | **σ =** | 0.08 | 0.2 | 14.2 |
| | | | **cov =** | 0.10 | 0.3 | 0.3 |

**Table B.8** Unloading stiffness properties of the cyclic test # 8 (Group-A)

| Test ID: Galeota 1996 Specimen CB1 | | | number of occurrence | Ductility based Parameter 'a' | Focus based Parameter 'α' | Deviation from initial stiffness (%) |
|---|---|---|---|---|---|---|
| Initial | $K_o$ = | 12.69 | - | - | - | - |
| Unl. | $K_{un,1}$= | 9.71 | 1 | 0.62 | 0.7 | 23.5 |
| | $K_{un,2}$= | 6.88 | 4 | 0.48 | 2.1 | 45.8 |
| | $K_{un,3}$= | 6.88 | 1 | 0.32 | 5.8 | 45.8 |
| K values are in kN/mm. | | | **μ =** | **0.48** | **2.5** | **42.1** |
| | | | **σ =** | 0.10 | 1.7 | 9.1 |
| | | | **cov =** | 0.20 | 0.7 | 0.2 |

**Table B.9** Unloading stiffness properties of the cyclic test # 9 (Group-A)

| Test ID: "Thompson and Wallace, 1994, B1" | | | number of occurrence | Ductility based Parameter 'a' | Focus based Parameter 'α' | Deviation from initial stiffness (%) |
|---|---|---|---|---|---|---|
| Initial | $K_o$ = | 5.33 | - | - | - | - |
| Unl. | $K_{un,1}$= | 4.89 | 2 | 0.19 | 9.2 | 8.3 |
| | $K_{un,2}$= | 4.80 | 2 | 0.15 | 10.5 | 10.0 |
| | $K_{un,3}$= | 4.17 | 2 | 0.21 | 7.7 | 21.9 |
| | $K_{un,4}$= | 3.50 | 1 | 0.28 | 6.0 | 34.4 |
| K values are in kN/mm. | | | **μ =** | **0.20** | **8.7** | **16.4** |
| | | | **σ =** | 0.04 | 1.6 | 10.0 |
| | | | **cov =** | 0.22 | 0.2 | 0.6 |

**Table B.10** Unloading stiffness properties of the cyclic test # 10 (Group-A)

| Test ID: Galeota 1996 Specimen CB4 | | | number of occurrence | Ductility based: Parameter 'a' | Focus based: Parameter 'α' | Deviation from initial stiffness (%) |
|---|---|---|---|---|---|---|
| Initial | $K_o$ = | 15.45 | - | - | - | - |
| Unl. | $K_{un,1}$= | 8.95 | 1 | 0.79 | 0.4 | 42.1 |
| | $K_{un,2}$= | 7.08 | 4 | 0.60 | 1.2 | 54.2 |
| | $K_{un,3}$= | 7.73 | 1 | 0.38 | 4.1 | 50.0 |
| K values are in kN/mm. | | | **μ =** | **0.60** | **1.6** | **51.5** |
| | | | **σ =** | 0.13 | 1.3 | 4.9 |
| | | | **cov =** | 0.21 | 0.8 | 0.1 |

**Table B.11** Unloading stiffness properties of the cyclic test # 11 (Group-A)

| Test ID: Tanaka 90, Specimen 9 | | | number of occurrence | Ductility based: Parameter 'a' | Focus based: Parameter 'α' | Deviation from initial stiffness (%) |
|---|---|---|---|---|---|---|
| Initial | $K_o$ = | 31.67 | - | - | - | - |
| Unl. | $K_{un,1}$= | 20.00 | 2 | 0.66 | 0.7 | 36.8 |
| | $K_{un,2}$= | 19.00 | 2 | 0.39 | 3.0 | 40.0 |
| | $K_{un,3}$= | 15.20 | 2 | 0.43 | 3.2 | 52.0 |
| | $K_{un,4}$= | 14.62 | 2 | 0.39 | 4.4 | 53.8 |
| K values are in kN/mm. | | | **μ =** | **0.47** | **2.8** | **45.7** |
| | | | **σ =** | 0.12 | 1.4 | 7.9 |
| | | | **cov =** | 0.26 | 0.5 | 0.2 |

**Table B.12** Unloading stiffness properties of the cyclic test # 12 (Group-A)

| Test ID: Atalay and Penzien, 1975, Spec. 4 | | | number of occurrence | Ductility based: Parameter 'a' | Focus based: Parameter 'α' | Deviation from initial stiffness (%) |
|---|---|---|---|---|---|---|
| Initial | $K_o$ = | 3.69 | - | - | - | - |
| Unl. | $K_{un,1}$= | 3.00 | 4 | 0.43 | 1.7 | 18.8 |
| | $K_{un,2}$= | 2.67 | 4 | 0.36 | 2.8 | 27.8 |
| | $K_{un,3}$= | 2.67 | 2 | 0.28 | 4.8 | 27.8 |
| K values are in kN/mm. | | | **μ =** | **0.37** | **2.7** | **24.2** |
| | | | **σ =** | 0.06 | 1.2 | 4.7 |
| | | | **cov =** | 0.16 | 0.4 | 0.2 |

**Table B.13** Unloading stiffness properties of the cyclic test # 13 (Group-A)

| Test ID: Hakim_Kono 2002 Column L1N60 | | | number of occurrence | Ductility based: Parameter 'a' | Focus based: Parameter 'α' | Deviation from initial stiffness (%) |
|---|---|---|---|---|---|---|
| Initial | $K_o$ = | 325.00 | - | - | - | - |
| Unl. | $K_{un,1}$= | 216.67 | 2 | 0.72 | 0.5 | 33.3 |
| | $K_{un,2}$= | 162.50 | 2 | 0.76 | 0.5 | 50.0 |
| | $K_{un,3}$= | 130.00 | 2 | 0.78 | 0.5 | 60.0 |
| | $K_{un,4}$= | 86.67 | 2 | 0.69 | 1.1 | 73.3 |
| K values are in kN/mm. | | | **μ =** | **0.74** | **0.6** | **54.2** |
| | | | **σ =** | 0.03 | 0.3 | 15.6 |
| | | | **cov =** | 0.05 | 0.4 | 0.3 |

**Table B.14** Unloading stiffness properties of the cyclic test # 14 (Group-A)

| Test ID: Galeota 1996 Specimen BB4B | | | number of occurrence | Ductility based: Parameter 'a' | Focus based: Parameter 'α' | Deviation from initial stiffness (%) |
|---|---|---|---|---|---|---|
| Initial | $K_o$ = | 14.55 | - | - | - | - |
| Unl. | $K_{un,1}$= | 10.32 | 1 | 0.70 | 0.6 | 29.0 |
| | $K_{un,2}$= | 6.96 | 4 | 0.58 | 1.3 | 52.2 |
| | $K_{un,3}$= | 6.87 | 2 | 0.50 | 2.8 | 52.8 |
| K values are in kN/mm. | | | **μ =** | **0.57** | **1.7** | **49.0** |
| | | | **σ =** | 0.07 | 0.9 | 8.8 |
| | | | **cov =** | 0.12 | 0.5 | 0.2 |

**Table B.15** Unloading stiffness properties of the cyclic test # 15 (Group-A)

| Test ID: Sugano 1996, No.UC15H | | | number of occurrence | Ductility based: Parameter 'a' | Focus based: Parameter 'α' | Deviation from initial stiffness (%) |
|---|---|---|---|---|---|---|
| Initial | $K_o$ = | 180.00 | - | - | - | - |
| Unl. | $K_{un,1}$= | 144.00 | 1 | 0.47 | 1.4 | 20.0 |
| | $K_{un,2}$= | 105.88 | 2 | 0.69 | 0.6 | 41.2 |
| | $K_{un,3}$= | 83.72 | 2 | 0.65 | 1.0 | 53.5 |
| | $K_{un,4}$= | 64.44 | 2 | 0.71 | 1.1 | 64.2 |
| K values are in kN/mm. | | | **μ =** | **0.65** | **1.0** | **48.2** |
| | | | **σ =** | 0.08 | 0.3 | 15.6 |
| | | | **cov =** | 0.13 | 0.3 | 0.3 |

**Table B.16** Unloading stiffness properties of the cyclic test # 16 (Group-A)

| Test ID: Galeota 1996 Specimen CB2 | | | number of occurrence | Ductility based: Parameter 'a' | Focus based: Parameter 'α' | Deviation from initial stiffness (%) |
|---|---|---|---|---|---|---|
| Initial | $K_o$ = | 14.55 | - | - | - | - |
| Unl. | $K_{un,1}$= | 9.14 | 1 | 0.72 | 0.5 | 37.1 |
| | $K_{un,2}$= | 6.67 | 4 | 0.54 | 1.8 | 54.2 |
| | $K_{un,3}$= | 6.96 | 1 | 0.38 | 4.3 | 52.2 |
| K values are in kN/mm. | | | **μ =** | **0.54** | **2.0** | **51.0** |
| | | | **σ =** | 0.11 | 1.2 | 6.8 |
| | | | **cov =** | 0.20 | 0.6 | 0.1 |

**Table B.17** Unloading stiffness properties of the cyclic test # 17 (Group-A)

| Test ID: Soesianawati et al. 86, Specimen 1 | | | number of occurrence | Ductility based: Parameter 'a' | Focus based: Parameter 'α' | Deviation from initial stiffness (%) |
|---|---|---|---|---|---|---|
| Initial | $K_o$ = | 19.00 | - | - | - | - |
| Unl. | $K_{un,1}$= | 10.86 | 2 | 0.81 | 0.3 | 42.9 |
| | $K_{un,2}$= | 7.31 | 2 | 0.66 | 1.1 | 61.5 |
| | $K_{un,3}$= | 7.04 | 2 | 0.54 | 2.1 | 63.0 |
| | $K_{un,4}$= | 6.79 | 2 | 0.49 | 3.1 | 64.3 |
| | $K_{un,5}$= | 7.04 | 2 | 0.43 | 4.5 | 63.0 |
| K values are in kN/mm. | | | **μ =** | **0.58** | **2.2** | **58.9** |
| | | | **σ =** | 0.14 | 1.5 | 8.5 |
| | | | **cov =** | 0.24 | 0.7 | 0.1 |

**Table B.18** Unloading stiffness properties of the cyclic test # 18 (Group-A)

| Test ID: Sugano 1996, No.UC10H | | | number of occurrence | Ductility based: Parameter 'a' | Focus based: Parameter 'α' | Deviation from initial stiffness (%) |
|---|---|---|---|---|---|---|
| Initial | $K_o$ = | 220.00 | - | - | - | - |
| Unl. | $K_{un,1}$= | 183.33 | 1 | 0.43 | 1.7 | 16.7 |
| | $K_{un,2}$= | 143.48 | 1 | 0.59 | 1.0 | 34.8 |
| | $K_{un,3}$= | 110.00 | 1 | 0.66 | 1.0 | 50.0 |
| | $K_{un,4}$= | 89.47 | 1 | 0.82 | 0.8 | 59.3 |
| K values are in kN/mm. | | | **μ =** | **0.62** | **1.1** | **40.2** |
| | | | **σ =** | 0.16 | 0.4 | 18.7 |
| | | | **cov =** | 0.26 | 0.4 | 0.5 |

**Table B.19** Unloading stiffness properties of the cyclic test # 19 (Group-A)

| Test ID<br>**Tanaka 90 specimen 1** | | | number of occurrence | Ductility based<br>Parameter 'a' | Focus based<br>Parameter 'α' | Deviation from initial stiffness (%) |
|---|---|---|---|---|---|---|
| Initial | $K_o$ = | 14.55 | - | - | - | - |
| Unl. | $K_{un,1}$= | 9.41 | 2 | 0.63 | 0.8 | 35.3 |
| | $K_{un,2}$= | 5.04 | 2 | 0.74 | 0.9 | 65.4 |
| | $K_{un,3}$= | 5.04 | 2 | 0.58 | 2.0 | 65.4 |
| | $K_{un,4}$= | 4.42 | 2 | 0.57 | 2.5 | 69.6 |
| K values are in kN/mm. | | | **μ =** | **0.63** | **1.6** | **58.9** |
| | | | **σ =** | 0.07 | 0.8 | 14.7 |
| | | | **cov =** | 0.12 | 0.5 | 0.2 |

**Table B.20** Unloading stiffness properties of the cyclic test # 20 (Group-A)

| Test ID<br>**Watson and Park 89, Specimen 5** | | | number of occurrence | Ductility based<br>Parameter 'a' | Focus based<br>Parameter 'α' | Deviation from initial stiffness (%) |
|---|---|---|---|---|---|---|
| Initial | $K_o$ = | 35.00 | - | - | - | - |
| Unl. | $K_{un,1}$= | 19.40 | 2 | 1.46 | 0.3 | 44.6 |
| | $K_{un,2}$= | 15.00 | 2 | 0.98 | 0.4 | 57.1 |
| | $K_{un,3}$= | 11.55 | 2 | 0.91 | 0.5 | 67.0 |
| | $K_{un,4}$= | 9.32 | 2 | 0.88 | 0.6 | 73.4 |
| | $K_{un,5}$= | 10.47 | 1 | 0.76 | 1.2 | 70.1 |
| | $K_{un,6}$= | 10.67 | 1 | 0.74 | 1.5 | 69.5 |
| K values are in kN/mm. | | | **μ =** | **1.00** | **0.6** | **62.4** |
| | | | **σ =** | 0.25 | 0.4 | 11.0 |
| | | | **cov =** | 0.26 | 0.6 | 0.2 |

**Table B.21** Unloading stiffness properties of the cyclic test # 21 (Group-B)

| Test ID: Ohno and Nishioka 1984, Specimen L3 | | | number of occurrence | Ductility based: Parameter 'a' | Focus based: Parameter 'α' | Deviation from initial stiffness (%) |
|---|---|---|---|---|---|---|
| Initial | $K_o$ = | 12.5 | - | - | - | - |
| Unl. | $K_{un,1}$= | 8.33 | 5 | 0.44 | 2.0 | 33.3 |
| | $K_{un,2}$= | 6.93 | 5 | 0.44 | 2.6 | 44.6 |
| | $K_{un,3}$= | 6.19 | 5 | 0.43 | 3.1 | 50.5 |
| | $K_{un,4}$= | 5.50 | 3 | 0.44 | 3.2 | 56.0 |
| | $K_{un,5}$= | 5.81 | 2 | 0.40 | 4.1 | 53.5 |
| | $K_{un,6}$= | 5.31 | 1 | 0.38 | 5.4 | 57.5 |
| | $K_{un,7}$= | 4.31 | 1 | 0.48 | 4.1 | 65.5 |
| K values are in kN/mm. | | | **μ =** | **0.43** | **3.0** | **47.3** |
| | | | **σ =** | 0.02 | 0.8 | 9.3 |
| | | | **cov =** | 0.04 | 0.3 | 0.2 |

**Table B.22** Unloading stiffness properties of the cyclic test # 22 (Group-B)

| Test ID: Tanaka 90 Specimen 2 | | | number of occurrence | Ductility based: Parameter 'a' | Focus based: Parameter 'α' | Deviation from initial stiffness (%) |
|---|---|---|---|---|---|---|
| Initial | $K_o$ = | 16.30 | - | - | - | - |
| Unl. | $K_{un,1}$= | 9.41 | 2 | 0.70 | 0.7 | 42.3 |
| | $K_{un,2}$= | 5.04 | 2 | 0.77 | 0.8 | 69.1 |
| | $K_{un,3}$= | 5.04 | 2 | 0.61 | 1.8 | 69.1 |
| | $K_{un,4}$= | 4.11 | 2 | 0.62 | 2.2 | 74.8 |
| K values are in kN/mm. | | | **μ =** | **0.67** | **1.4** | **63.8** |
| | | | **σ =** | 0.07 | 0.7 | 13.5 |
| | | | **cov =** | 0.10 | 0.5 | 0.2 |

**Table B.23** Unloading stiffness properties of the cyclic test # 23 (Group-B)

| Test ID: Atalay and Penzien, 1975, Spec. 9 | | | number of occurrence | Ductility based: Parameter 'a' | Focus based: Parameter 'α' | Deviation from initial stiffness (%) |
|---|---|---|---|---|---|---|
| Initial | $K_o$ = | 5.38 | - | - | - | - |
| Unl. | $K_{un,1}$= | 2.59 | 4 | 0.84 | 0.6 | 51.9 |
| | $K_{un,2}$= | 2.08 | 4 | 0.78 | 0.9 | 61.4 |
| | $K_{un,3}$= | 3.00 | 4 | 0.43 | 3.6 | 44.3 |
| K values are in kN/mm. | | | **μ =** | **0.69** | **1.7** | **52.5** |
| | | | **σ =** | 0.19 | 1.4 | 7.3 |
| | | | **cov =** | 0.27 | 0.8 | 0.1 |

**Table B.24** Unloading stiffness properties of the cyclic test # 24 (Group-B)

| Test ID<br>**Wight and Sozen, 1973, Spec. WS147W** | | | number of occurrence | Ductility based<br>Parameter 'a' | Focus based<br>Parameter '$\alpha$' | Deviation from initial stiffness (%) |
|---|---|---|---|---|---|---|
| Initial | $K_o$ = | 9.17 | - | - | - | - |
| Unl. | $K_{un,1}$= | 4.39 | 6 | 0.48 | 2.5 | 52.1 |
| K values are in kN/mm. | | | **$\mu$ =** | **0.48** | **2.5** | **52.1** |
| | | | **$\sigma$ =** | 0.00 | 0.0 | 0.0 |
| | | | **cov =** | 0.00 | 0.0 | 0.0 |

**Table B.25** Unloading stiffness properties of the cyclic test # 25 (Group-B)

| Test ID<br>**Ang et al. 1981 Specimen 4** | | | number of occurrence | Ductility based<br>Parameter 'a' | Focus based<br>Parameter '$\alpha$' | Deviation from initial stiffness (%) |
|---|---|---|---|---|---|---|
| Initial | $K_o$ = | 17.00 | - | - | - | - |
| Unl. | $K_{un,1}$= | 9.67 | 2 | 0.88 | 0.5 | 43.1 |
| | $K_{un,2}$= | 6.09 | 2 | 0.74 | 0.9 | 64.2 |
| | $K_{un,3}$= | 5.67 | 3 | 0.61 | 1.8 | 66.7 |
| K values are in kN/mm. | | | **$\mu$ =** | **0.73** | **1.2** | **59.2** |
| | | | **$\sigma$ =** | 0.12 | 0.6 | 11.1 |
| | | | **cov =** | 0.16 | 0.5 | 0.2 |

**Table B.26** Unloading stiffness properties of the cyclic test # 26 (Group-B)

| Test ID<br>**Tanaka 90, Specimen 6** | | | number of occurrence | Ductility based<br>Parameter 'a' | Focus based<br>Parameter '$\alpha$' | Deviation from initial stiffness (%) |
|---|---|---|---|---|---|---|
| Initial | $K_o$ = | 35.91 | - | - | - | - |
| Unl. | $K_{un,1}$= | 20.54 | 2 | 0.72 | 0.7 | 42.8 |
| | $K_{un,2}$= | 13.82 | 2 | 0.64 | 1.2 | 61.5 |
| | $K_{un,3}$= | 13.70 | 2 | 0.52 | 2.4 | 61.8 |
| | $K_{un,4}$= | 11.59 | 2 | 0.53 | 2.8 | 67.7 |
| K values are in kN/mm. | | | **$\mu$ =** | **0.60** | **1.8** | **58.5** |
| | | | **$\sigma$ =** | 0.09 | 0.9 | 10.0 |
| | | | **cov =** | 0.14 | 0.5 | 0.2 |

**Table B.27** Unloading stiffness properties of the cyclic test # 27 (Group-B)

| Test ID: Pujol 2002, No. 10-3-1.5S | | | number of occurrence | Ductility based: Parameter 'a' | Focus based: Parameter 'α' | Deviation from initial stiffness (%) |
|---|---|---|---|---|---|---|
| Initial | $K_o$ = | 18.33 | - | - | - | - |
| Unl. | $K_{un,1}$= | 10.00 | 7 | 0.48 | 2.2 | 45.5 |
| | $K_{un,2}$= | 9.80 | 10 | 0.42 | 3.3 | 46.5 |
| | $K_{un,3}$= | 6.67 | 1 | 0.62 | 2.1 | 63.6 |
| K values are in kN/mm. | | | **μ =** | **0.45** | **2.8** | **47.1** |
| | | | **σ =** | 0.05 | 0.5 | 4.2 |
| | | | **cov =** | 0.12 | 0.2 | 0.1 |

**Table B.28** Unloading stiffness properties of the cyclic test # 28 (Group-B)

| Test ID: Wehbe et al. 1998,Specimen B2 | | | number of occurrence | Ductility based: Parameter 'a' | Focus based: Parameter 'α' | Deviation from initial stiffness (%) |
|---|---|---|---|---|---|---|
| Initial | $K_o$ = | 13.67 | - | - | - | - |
| Unl. | $K_{un,1}$= | 8.16 | 2 | 1.79 | 0.4 | 40.3 |
| | $K_{un,2}$= | 7.34 | 2 | 0.88 | 0.8 | 46.3 |
| | $K_{un,3}$= | 6.69 | 2 | 0.67 | 1.1 | 51.0 |
| | $K_{un,4}$= | 6.18 | 2 | 0.62 | 1.4 | 54.8 |
| | $K_{un,5}$= | 5.94 | 3 | 0.59 | 1.8 | 56.5 |
| K values are in kN/mm. | | | **μ =** | **0.88** | **1.2** | **50.4** |
| | | | **σ =** | 0.46 | 0.5 | 6.2 |
| | | | **cov =** | 0.53 | 0.4 | 0.1 |

**Table B.29** Unloading stiffness properties of the cyclic test # 29 (Group-B)

| Test ID: Azizinamini et al., 1988, Spec. NC-2 | | | number of occurrence | Ductility based: Parameter 'a' | Focus based: Parameter 'α' | Deviation from initial stiffness (%) |
|---|---|---|---|---|---|---|
| Initial | $K_o$ = | 37.50 | - | - | - | - |
| Unl. | $K_{un,1}$= | 20.29 | 2 | 0.84 | 0.4 | 45.9 |
| | $K_{un,2}$= | 16.13 | 2 | 0.83 | 0.6 | 57.0 |
| | $K_{un,3}$= | 16.96 | 2 | 0.63 | 1.3 | 54.8 |
| | $K_{un,4}$= | 18.95 | 2 | 0.47 | 2.6 | 49.5 |
| | $K_{un,5}$= | 16.00 | 2 | 0.53 | 2.4 | 57.3 |
| | $K_{un,6}$= | 17.05 | 2 | 0.45 | 3.4 | 54.5 |
| K values are in kN/mm. | | | **μ =** | **0.63** | **1.8** | **53.2** |
| | | | **σ =** | 0.17 | 1.1 | 4.3 |
| | | | **cov =** | 0.26 | 0.6 | 0.1 |

**Table B.30** Unloading stiffness properties of the cyclic test # 30 (Group-B)

| Test ID: Xiao 98,Specimen nr. HC4-8L19-T10-0.2P | | | number of occurrence | Ductility based Parameter 'a' | Focus based Parameter 'α' | Deviation from initial stiffness (%) |
|---|---|---|---|---|---|---|
| Initial | $K_o$ = | 63.33 | - | - | - | - |
| Unl. | $K_{un,1}$= | 27.80 | 3 | 0.97 | 0.5 | 56.1 |
| | $K_{un,2}$= | 26.91 | 3 | 0.74 | 1.0 | 57.5 |
| | $K_{un,3}$= | 21.79 | 3 | 0.66 | 1.4 | 65.6 |
| | $K_{un,4}$= | 21.43 | 2 | 0.56 | 2.3 | 66.2 |
| K values are in kN/mm. | | | **μ =** | **0.75** | **1.2** | **60.9** |
| | | | **σ =** | 0.15 | 0.6 | 4.7 |
| | | | **cov =** | 0.21 | 0.5 | 0.1 |

**Table B.31** Unloading stiffness properties of the cyclic test # 31 (Group-B)

| Test ID: Atalay and Penzien, 1975, Spec. 3 | | | number of occurrence | Ductility based Parameter 'a' | Focus based Parameter 'α' | Deviation from initial stiffness (%) |
|---|---|---|---|---|---|---|
| Initial | $K_o$ = | 4.38 | - | - | - | - |
| Unl. | $K_{un,1}$= | 2.80 | 4 | 0.85 | 0.3 | 36.1 |
| | $K_{un,2}$= | 2.25 | 4 | 0.71 | 0.7 | 48.6 |
| | $K_{un,3}$= | 1.79 | 4 | 0.72 | 0.9 | 59.1 |
| | $K_{un,4}$= | 1.79 | 4 | 0.63 | 1.3 | 59.1 |
| K values are in kN/mm. | | | **μ =** | **0.73** | **0.8** | **50.7** |
| | | | **σ =** | 0.08 | 0.4 | 9.8 |
| | | | **cov =** | 0.11 | 0.5 | 0.2 |

**Table B.32** Unloading stiffness properties of the cyclic test # 32 (Group-B)

| Test ID: Zahn et al. 86, Specimen 7 | | | number of occurrence | Ductility based Parameter 'a' | Focus based Parameter 'α' | Deviation from initial stiffness (%) |
|---|---|---|---|---|---|---|
| Initial | $K_o$ = | 17.08 | - | - | - | - |
| Unl. | $K_{un,1}$= | 5.03 | 2 | 0.90 | 0.5 | 70.6 |
| | $K_{un,2}$= | 4.31 | 1 | 0.75 | 1.1 | 74.7 |
| | $K_{un,3}$= | 4.50 | 1 | 0.69 | 1.5 | 73.7 |
| | $K_{un,4}$= | 3.85 | 1 | 0.72 | 1.6 | 77.5 |
| K values are in kN/mm. | | | **μ =** | **0.79** | **1.0** | **73.4** |
| | | | **σ =** | 0.10 | 0.5 | 2.9 |
| | | | **cov =** | 0.12 | 0.5 | 0.0 |

**Table B.33** Unloading stiffness properties of the cyclic test # 33 (Group-B)

| Test ID: "Matamoros et. al 1999 Specimen c10-10 South" | | | number of occurrence | Ductility based Parameter 'a' | Focus based Parameter 'α' | Deviation from initial stiffness (%) |
|---|---|---|---|---|---|---|
| Initial | $K_o$ = | 11.50 | - | - | - | - |
| Unl. | $K_{un,1}$= | 5.10 | 2 | 0.94 | 0.4 | 55.7 |
| | $K_{un,2}$= | 4.21 | 2 | 0.80 | 0.6 | 63.4 |
| | $K_{un,3}$= | 4.06 | 2 | 0.75 | 1.0 | 64.7 |
| | $K_{un,4}$= | 3.89 | 2 | 0.67 | 1.4 | 66.2 |
| | $K_{un,5}$= | 4.31 | 2 | 0.56 | 2.3 | 62.5 |
| K values are in kN/mm. | | | **μ =** | **0.75** | **1.1** | **62.5** |
| | | | **σ =** | 0.13 | 0.7 | 3.8 |
| | | | **cov =** | 0.18 | 0.6 | 0.1 |

**Table B.34** Unloading stiffness properties of the cyclic test # 34 (Group-B)

| Test ID: Paultre, Legeron, July-August 2000 test 1006015 | | | number of occurrence | Ductility based Parameter 'a' | Focus based Parameter 'α' | Deviation from initial stiffness (%) |
|---|---|---|---|---|---|---|
| Initial | $K_o$ = | 5.50 | - | - | - | - |
| Unl. | $K_{un,1}$= | 1.94 | 2 | 0.89 | 0.3 | 64.7 |
| | $K_{un,2}$= | 1.66 | 2 | 0.72 | 0.9 | 69.9 |
| | $K_{un,3}$= | 1.66 | 2 | 0.65 | 1.5 | 69.9 |
| | $K_{un,4}$= | 1.69 | 2 | 0.58 | 2.2 | 69.4 |
| | $K_{un,5}$= | 1.77 | 2 | 0.52 | 3.2 | 67.9 |
| | $K_{un,6}$= | 1.31 | 1 | 0.61 | 2.6 | 76.1 |
| K values are in kN/mm. | | | **μ =** | **0.67** | **1.7** | **69.1** |
| | | | **σ =** | 0.13 | 1.0 | 3.1 |
| | | | **cov =** | 0.20 | 0.6 | 0.0 |

**Table B.35** Unloading stiffness properties of the cyclic test # 35 (Group-B)

| Test ID: Atalay and Penzien, 1975, Spec. 2 | | | number of occurrence | Ductility based Parameter 'a' | Focus based Parameter 'α' | Deviation from initial stiffness (%) |
|---|---|---|---|---|---|---|
| Initial | $K_o$ = | 4.29 | - | - | - | - |
| Unl. | $K_{un,1}$= | 3.01 | 5 | 0.88 | 0.5 | 29.9 |
| | $K_{un,2}$= | 2.42 | 4 | 0.65 | 0.9 | 43.6 |
| | $K_{un,3}$= | 2.19 | 4 | 0.57 | 1.4 | 48.8 |
| | $K_{un,4}$= | 2.28 | 4 | 0.47 | 2.4 | 46.8 |
| K values are in kN/mm. | | | **μ =** | **0.65** | **1.2** | **41.6** |
| | | | **σ =** | 0.16 | 0.7 | 8.0 |
| | | | **cov =** | 0.24 | 0.6 | 0.2 |

**Table B.36** Unloading stiffness properties of the cyclic test # 36 (Group-B)

| Test ID: Watson and Park 89, Specimen 6 | | | number of occurrence | Ductility based: Parameter 'a' | Focus based: Parameter 'α' | Deviation from initial stiffness (%) |
|---|---|---|---|---|---|---|
| Initial | $K_o$ = | 40.00 | - | - | - | - |
| Unl. | $K_{un,1}$= | 21.50 | 2 | 0.90 | 0.3 | 46.3 |
| | $K_{un,2}$= | 18.85 | 2 | 0.80 | 0.6 | 52.9 |
| | $K_{un,3}$= | 11.90 | 2 | 0.90 | 0.5 | 70.2 |
| K values are in kN/mm. | | | **μ =** | **0.86** | **0.5** | **56.5** |
| | | | **σ =** | 0.05 | 0.1 | 11.1 |
| | | | **cov =** | 0.06 | 0.3 | 0.2 |

**Table B.37** Unloading stiffness properties of the cyclic test # 37 (Group-B)

| Test ID: Galeota 1996 Specimen CA2 | | | number of occurrence | Ductility based: Parameter 'a' | Focus based: Parameter 'α' | Deviation from initial stiffness (%) |
|---|---|---|---|---|---|---|
| Initial | $K_o$ = | 15.63 | - | - | - | - |
| Unl. | $K_{un,1}$= | 5.67 | 4 | 0.83 | 0.6 | 63.7 |
| | $K_{un,2}$= | 5.29 | 1 | 0.64 | 1.9 | 66.2 |
| | $K_{un,3}$= | 5.67 | 2 | 0.56 | 2.8 | 63.7 |
| K values are in kN/mm. | | | **μ =** | **0.73** | **1.5** | **64.1** |
| | | | **σ =** | 0.14 | 1.1 | 0.9 |
| | | | **cov =** | 0.19 | 0.7 | 0.0 |

**Table B.38** Unloading stiffness properties of the cyclic test # 38 (Group-B)

| Test ID: Kanda et al. 1988, Spec. STC1 | | | number of occurrence | Ductility based: Parameter 'a' | Focus based: Parameter 'α' | Deviation from initial stiffness (%) |
|---|---|---|---|---|---|---|
| Initial | $K_o$ = | 15.00 | - | - | - | - |
| Unl. | $K_{un,1}$= | 7.20 | 3 | 0.71 | 0.7 | 52.0 |
| | $K_{un,2}$= | 6.55 | 3 | 0.62 | 1.2 | 56.4 |
| | $K_{un,3}$= | 5.15 | 3 | 0.62 | 1.6 | 65.6 |
| | $K_{un,4}$= | 4.67 | 3 | 0.59 | 2.2 | 68.9 |
| | $K_{un,5}$= | 4.18 | 1 | 0.59 | 2.6 | 72.1 |
| K values are in kN/mm. | | | **μ =** | **0.63** | **1.5** | **61.6** |
| | | | **σ =** | 0.05 | 0.6 | 7.5 |
| | | | **cov =** | 0.08 | 0.4 | 0.1 |

**Table B.39** Unloading stiffness properties of the cyclic test # 39 (Group-B)

| Test ID: Pujol 2002, No. 20-3-3N | | | number of occurrence | Ductility based: Parameter 'a' | Focus based: Parameter 'α' | Deviation from initial stiffness (%) |
|---|---|---|---|---|---|---|
| Initial | $K_o$ = | 25.00 | - | - | - | - |
| Unl. | $K_{un,1}$= | 9.76 | 1 | 1.36 | 0.2 | 61.0 |
| | $K_{un,2}$= | 9.26 | 1 | 0.81 | 0.7 | 63.0 |
| | $K_{un,3}$= | 10.29 | 6 | 0.64 | 1.3 | 58.9 |
| K values are in kN/mm. | | | **μ =** | **0.75** | **1.1** | **59.6** |
| | | | **σ =** | 0.25 | 0.4 | 1.5 |
| | | | **cov =** | 0.34 | 0.4 | 0.0 |

**Table B.40** Unloading stiffness properties of the cyclic test # 40 (Group-B)

| Test ID: Atalay and Penzien, 1975, Spec. 1 | | | number of occurrence | Ductility based: Parameter 'a' | Focus based: Parameter 'α' | Deviation from initial stiffness (%) |
|---|---|---|---|---|---|---|
| Initial | $K_o$ = | 4.29 | - | - | - | - |
| Unl. | $K_{un,1}$= | 3.05 | 4 | 0.84 | 0.4 | 28.8 |
| | $K_{un,2}$= | 2.68 | 4 | 0.57 | 1.2 | 37.4 |
| | $K_{un,3}$= | 2.42 | 4 | 0.51 | 1.8 | 43.6 |
| K values are in kN/mm. | | | **μ =** | **0.64** | **1.1** | **36.6** |
| | | | **σ =** | 0.15 | 0.6 | 6.4 |
| | | | **cov =** | 0.23 | 0.5 | 0.2 |

**Table B.41** Unloading stiffness properties of the cyclic test # 41 (Group-C)

| Test ID: Bayrak and Sheikh 1996, AS2-HT | | | number of occurrence | Ductility based: Parameter 'a' | Focus based: Parameter 'α' | Deviation from initial stiffness (%) |
|---|---|---|---|---|---|---|
| Initial | $K_o$ = | 29 | - | - | - | - |
| Unl. | $K_{un,1}$= | 7.23 | 2 | 1.01 | 0.1 | 75.1 |
| | $K_{un,2}$= | 4.96 | 2 | 0.94 | 0.3 | 82.9 |
| | $K_{un,3}$= | 4.26 | 2 | 0.86 | 0.7 | 85.3 |
| | $K_{un,4}$= | 3.63 | 2 | 0.85 | 1.0 | 87.5 |
| | $K_{un,5}$= | 4.36 | 1 | 0.71 | 2.1 | 85.0 |
| K values are in kN/mm. | | | **μ =** | **0.89** | **0.7** | **82.9** |
| | | | **σ =** | 0.09 | 0.6 | 4.8 |
| | | | **cov =** | 0.10 | 0.9 | 0.1 |

**Table B.42** Unloading stiffness properties of the cyclic test # 42 (Group-C)

| Test ID: Bayrak and Sheikh 1996, AS6-HT | | | number of occurrence | Ductility based: Parameter 'a' | Focus based: Parameter 'α' | Deviation from initial stiffness (%) |
|---|---|---|---|---|---|---|
| Initial | $K_o$ = | 22.86 | - | - | - | - |
| Unl. | $K_{un,1}$= | 10.28 | 2 | 0.82 | 0.5 | 55.0 |
| | $K_{un,2}$= | 6.74 | 2 | 0.86 | 0.6 | 70.5 |
| | $K_{un,3}$= | 5.63 | 2 | 0.84 | 0.8 | 75.4 |
| | $K_{un,4}$= | 4.50 | 2 | 0.84 | 1.1 | 80.3 |
| | $K_{un,5}$= | 4.75 | 1 | 0.75 | 1.7 | 79.2 |
| K values are in kN/mm. | | | **μ =** | **0.83** | **0.9** | **71.3** |
| | | | **σ =** | 0.03 | 0.4 | 9.9 |
| | | | **cov =** | 0.04 | 0.4 | 0.1 |

**Table B.43** Unloading stiffness properties of the cyclic test # 43 (Group-C)

| Test ID: "Matamoros et. al 1999 Specimen c5-00 North" | | | number of occurrence | Ductility based: Parameter 'a' | Focus based: Parameter 'α' | Deviation from initial stiffness (%) |
|---|---|---|---|---|---|---|
| Initial | $K_o$ = | 5.80 | - | - | - | - |
| Unl. | $K_{un,1}$= | 4.67 | 2 | 0.31 | 3.3 | 19.5 |
| | $K_{un,2}$= | 4.00 | 2 | 0.39 | 2.9 | 31.0 |
| | $K_{un,3}$= | 4.00 | 2 | 0.30 | 4.4 | 31.0 |
| | $K_{un,4}$= | 3.07 | 2 | 0.46 | 2.9 | 47.0 |
| | $K_{un,5}$= | 2.47 | 2 | 0.56 | 2.3 | 57.5 |
| | $K_{un,6}$= | 2.40 | 1 | 0.54 | 2.6 | 58.6 |
| K values are in kN/mm. | | | **μ =** | **0.42** | **3.1** | **39.2** |
| | | | **σ =** | 0.10 | 0.7 | 14.9 |
| | | | **cov =** | 0.25 | 0.2 | 0.4 |

**Table B.44** Unloading stiffness properties of the cyclic test # 44 (Group-C)

| Test ID: "Matamoros et. al 1999 Specimen c10-05 South" | | | number of occurrence | Ductility based Parameter 'a' | Focus based Parameter 'α' | Deviation from initial stiffness (%) |
|---|---|---|---|---|---|---|
| Initial | $K_o$ = | 8.00 | - | - | - | - |
| Unl. | $K_{un,1}$= | 4.07 | 2 | 0.79 | 0.7 | 49.1 |
| | $K_{un,2}$= | 4.15 | 2 | 0.61 | 1.5 | 48.1 |
| | $K_{un,3}$= | 3.33 | 2 | 0.65 | 1.5 | 58.3 |
| | $K_{un,4}$= | 2.93 | 2 | 0.67 | 1.6 | 63.4 |
| | $K_{un,5}$= | 2.63 | 1 | 0.69 | 1.6 | 67.2 |
| | $K_{un,6}$= | 3.15 | 1 | 0.56 | 2.5 | 60.6 |
| K values are in kN/mm. | | | **μ =** | **0.67** | **1.5** | **56.6** |
| | | | **σ =** | 0.07 | 0.5 | 7.3 |
| | | | **cov =** | 0.11 | 0.3 | 0.1 |

**Table B.45** Unloading stiffness properties of the cyclic test # 45 (Group-C)

| Test ID: Paultre, Legeron, July-August 2000 test 1006025 | | | number of occurrence | Ductility based Parameter 'a' | Focus based Parameter 'α' | Deviation from initial stiffness (%) |
|---|---|---|---|---|---|---|
| Initial | $K_o$ = | 7.25 | - | - | - | - |
| Unl. | $K_{un,1}$= | 1.98 | 2 | 0.97 | 0.2 | 72.6 |
| | $K_{un,2}$= | 1.58 | 2 | 0.89 | 0.5 | 78.2 |
| | $K_{un,3}$= | 1.64 | 2 | 0.75 | 1.3 | 77.3 |
| | $K_{un,4}$= | 2.42 | 2 | 0.50 | 3.7 | 66.6 |
| K values are in kN/mm. | | | **μ =** | **0.78** | **1.4** | **73.7** |
| | | | **σ =** | 0.19 | 1.5 | 4.9 |
| | | | **cov =** | 0.24 | 1.0 | 0.1 |

**Table B.46** Unloading stiffness properties of the cyclic test # 46 (Group-C)

| Test ID: Mugaruma et al. 1989, Spec. BH2 | | | number of occurrence | Ductility based Parameter 'a' | Focus based Parameter 'α' | Deviation from initial stiffness (%) |
|---|---|---|---|---|---|---|
| Initial | $K_o$ = | 80.00 | - | - | - | - |
| Unl. | $K_{un,1}$= | 33.50 | 2 | 0.83 | 0.4 | 58.1 |
| | $K_{un,2}$= | 24.27 | 2 | 0.78 | 0.6 | 69.7 |
| | $K_{un,3}$= | 18.92 | 2 | 0.80 | 0.8 | 76.4 |
| | $K_{un,4}$= | 17.92 | 1 | 0.73 | 1.2 | 77.6 |
| | $K_{un,5}$= | 16.69 | 1 | 0.71 | 1.4 | 79.1 |
| K values are in kN/mm. | | | **μ =** | **0.78** | **0.8** | **70.6** |
| | | | **σ =** | 0.04 | 0.4 | 8.5 |
| | | | **cov =** | 0.06 | 0.5 | 0.1 |

**Table B.47** Unloading stiffness properties of the cyclic test # 47 (Group-C)

| Test ID: Mugaruma et al. 1989, Spec. AH1 | | | number of occurrence | Ductility based: Parameter 'a' | Focus based: Parameter 'α' | Deviation from initial stiffness (%) |
|---|---|---|---|---|---|---|
| Initial | $K_o$ = | 80.00 | - | - | - | - |
| Unl. | $K_{un,1}$= | 30.68 | 2 | 0.80 | 0.6 | 61.6 |
| | $K_{un,2}$= | 20.73 | 2 | 0.81 | 0.6 | 74.1 |
| | $K_{un,3}$= | 15.64 | 2 | 0.82 | 0.6 | 80.4 |
| | $K_{un,4}$= | 13.69 | 1 | 0.79 | 0.8 | 82.9 |
| | $K_{un,5}$= | 14.13 | 1 | 0.73 | 1.2 | 82.3 |
| | $K_{un,6}$= | 12.69 | 1 | 0.73 | 1.4 | 84.1 |
| K values are in kN/mm. | | | **μ =** | **0.79** | **0.8** | **75.7** |
| | | | **σ =** | 0.04 | 0.3 | 8.7 |
| | | | **cov =** | 0.04 | 0.4 | 0.1 |

**Table B.48** Unloading stiffness properties of the cyclic test # 48 (Group-C)

| Test ID: Paultre, Legeron, July-August 2000 test 1006040 | | | number of occurrence | Ductility based: Parameter 'a' | Focus based: Parameter 'α' | Deviation from initial stiffness (%) |
|---|---|---|---|---|---|---|
| Initial | $K_o$ = | 7.75 | - | - | - | - |
| Unl. | $K_{un,1}$= | 3.10 | 2 | 0.85 | 0.6 | 60.1 |
| | $K_{un,2}$= | 2.00 | 2 | 0.89 | 0.6 | 74.2 |
| | $K_{un,3}$= | 2.19 | 2 | 0.69 | 1.9 | 71.7 |
| K values are in kN/mm. | | | **μ =** | **0.81** | **1.0** | **68.7** |
| | | | **σ =** | 0.10 | 0.7 | 6.7 |
| | | | **cov =** | 0.12 | 0.6 | 0.1 |

**Table B.49** Unloading stiffness properties of the cyclic test # 49 (Group-C)

| Test ID: Paultre, Legeron, Mongequ, July-August 2001 test 1005540 | | | number of occurrence | Ductility based: Parameter 'a' | Focus based: Parameter 'α' | Deviation from initial stiffness (%) |
|---|---|---|---|---|---|---|
| Initial | $K_o$ = | 9.50 | - | - | - | - |
| Unl. | $K_{un,1}$= | 3.37 | 2 | 0.92 | 0.4 | 64.6 |
| | $K_{un,2}$= | 2.73 | 2 | 0.80 | 0.9 | 71.3 |
| | $K_{un,3}$= | 2.38 | 2 | 0.72 | 1.3 | 74.9 |
| K values are in kN/mm. | | | **μ =** | **0.81** | **0.9** | **70.2** |
| | | | **σ =** | 0.09 | 0.4 | 4.7 |
| | | | **cov =** | 0.11 | 0.5 | 0.1 |

**Table B.50** Unloading stiffness properties of the cyclic test # 50 (Group-C)

| Test ID: Wehbe et al. 1998,Specimen A2 | | | number of occurrence | Ductility based Parameter 'a' | Focus based Parameter 'α' | Deviation from initial stiffness (%) |
|---|---|---|---|---|---|---|
| Initial | $K_o$ = | 19.50 | - | - | - | - |
| Unl. | $K_{un,1}$= | 9.79 | 2 | 1.47 | 0.4 | 49.8 |
| | $K_{un,2}$= | 7.46 | 2 | 0.93 | 0.5 | 61.7 |
| | $K_{un,3}$= | 6.30 | 2 | 0.85 | 0.8 | 67.7 |
| | $K_{un,4}$= | 6.06 | 3 | 0.73 | 1.2 | 68.9 |
| K values are in kN/mm. | | | **μ =** | **0.96** | **0.8** | **62.8** |
| | | | **σ =** | 0.30 | 0.3 | 7.9 |
| | | | **cov =** | 0.31 | 0.4 | 0.1 |

**Table B.51** Unloading stiffness properties of the cyclic test # 51 (Group-C)

| Test ID: Azizinamini et al., 1988, Spec. NC-4 | | | number of occurrence | Ductility based Parameter 'a' | Focus based Parameter 'α' | Deviation from initial stiffness (%) |
|---|---|---|---|---|---|---|
| Initial | $K_o$ = | 50.00 | - | - | - | - |
| Unl. | $K_{un,1}$= | 21.13 | 2 | 0.88 | 0.4 | 57.7 |
| | $K_{un,2}$= | 19.19 | 2 | 0.74 | 0.8 | 61.6 |
| | $K_{un,3}$= | 19.44 | 2 | 0.64 | 1.5 | 61.1 |
| K values are in kN/mm. | | | **μ =** | **0.75** | **0.9** | **60.2** |
| | | | **σ =** | 0.11 | 0.5 | 1.9 |
| | | | **cov =** | 0.14 | 0.6 | 0.0 |

**Table B.52** Unloading stiffness properties of the cyclic test # 52 (Group-C)

| Test ID: Mugaruma et al. 1989, Spec. BH1 | | | number of occurrence | Ductility based Parameter 'a' | Focus based Parameter 'α' | Deviation from initial stiffness (%) |
|---|---|---|---|---|---|---|
| Initial | $K_o$ = | 61.25 | - | - | - | - |
| Unl. | $K_{un,1}$= | 28.88 | 2 | 0.82 | 0.4 | 52.9 |
| | $K_{un,2}$= | 18.83 | 2 | 0.85 | 0.4 | 69.3 |
| | $K_{un,3}$= | 13.33 | 2 | 0.87 | 0.6 | 78.2 |
| | $K_{un,4}$= | 12.38 | 2 | 0.81 | 0.8 | 79.8 |
| | $K_{un,5}$= | 12.06 | 1 | 0.74 | 1.2 | 80.3 |
| K values are in kN/mm. | | | **μ =** | **0.83** | **0.6** | **71.2** |
| | | | **σ =** | 0.04 | 0.3 | 11.2 |
| | | | **cov =** | 0.05 | 0.4 | 0.2 |

**Table B.53** Unloading stiffness properties of the cyclic test # 53 (Group-C)

| Test ID: Paultre, Legeron, Mongequ, July-August 2001 test 806040 | | | number of occurrence | Ductility based: Parameter 'a' | Focus based: Parameter 'α' | Deviation from initial stiffness (%) |
|---|---|---|---|---|---|---|
| Initial | $K_o$ = | 10.67 | - | - | - | - |
| Unl. | $K_{un,1}$= | 2.86 | 2 | 2 | 0.85 | 0.4 |
| | $K_{un,2}$= | 2.14 | 2 | 2 | 0.83 | 0.6 |
| | $K_{un,3}$= | 1.76 | 2 | 2 | 0.81 | 0.9 |
| | $K_{un,4}$= | 1.83 | 3 | 2 | 0.72 | 1.4 |
| K values are in kN/mm. | | | **μ =** | **0.80** | **0.8** | **79.9** |
| | | | **σ =** | 0.05 | 0.4 | 4.4 |
| | | | **cov =** | 0.06 | 0.5 | 0.1 |

**Table B.54** Unloading stiffness properties of the cyclic test # 54 (Group-C)

| Test ID: Tanaka 90, Specimen 7 | | | number of occurrence | Ductility based: Parameter 'a' | Focus based: Parameter 'α' | Deviation from initial stiffness (%) |
|---|---|---|---|---|---|---|
| Initial | $K_o$ = | 48.75 | - | - | - | - |
| Unl. | $K_{un,1}$= | 15.53 | 2 | 0.87 | 0.4 | 68.1 |
| | $K_{un,2}$= | 12.15 | 2 | 0.82 | 0.7 | 75.1 |
| | $K_{un,3}$= | 11.18 | 2 | 0.74 | 1.2 | 77.1 |
| K values are in kN/mm. | | | **μ =** | **0.81** | **0.8** | **73.4** |
| | | | **σ =** | 0.05 | 0.3 | 4.2 |
| | | | **cov =** | 0.07 | 0.4 | 0.1 |

**Table B.55** Unloading stiffness properties of the cyclic test # 55 (Group-C)

| Test ID: Atalay and Penzien, 1975, Spec. 6 | | | number of occurrence | Ductility based: Parameter 'a' | Focus based: Parameter 'α' | Deviation from initial stiffness (%) |
|---|---|---|---|---|---|---|
| Initial | $K_o$ = | 4.80 | - | - | - | - |
| Unl. | $K_{un,1}$= | 2.48 | 4 | 0.87 | 0.4 | 48.3 |
| | $K_{un,2}$= | 2.10 | 4 | 0.79 | 0.6 | 56.3 |
| | $K_{un,3}$= | 1.68 | 4 | 0.90 | 0.7 | 65.0 |
| K values are in kN/mm. | | | **μ =** | **0.85** | **0.6** | **56.5** |
| | | | **σ =** | 0.05 | 0.2 | 7.1 |
| | | | **cov =** | 0.06 | 0.3 | 0.1 |

**Table B.56** Unloading stiffness properties of the cyclic test # 56 (Group-C)

| Test ID: "Matamoros et. al 1999 Specimen c5-40 North" | | | number of occurrence | Ductility based Parameter 'a' | Focus based Parameter 'α' | Deviation from initial stiffness (%) |
|---|---|---|---|---|---|---|
| Initial | $K_o$ = | 13.33 | - | - | - | - |
| Unl. | $K_{un,1}$= | 6.82 | 2 | 0.87 | 0.3 | 48.9 |
| | $K_{un,2}$= | 4.67 | 2 | 0.91 | 0.4 | 65.0 |
| | $K_{un,3}$= | 4.62 | 2 | 0.74 | 1.1 | 65.4 |
| K values are in kN/mm. | | | **μ =** | **0.84** | **0.6** | **59.7** |
| | | | **σ =** | 0.08 | 0.4 | 8.4 |
| | | | **cov =** | 0.09 | 0.6 | 0.1 |

**Table B.57** Unloading stiffness properties of the cyclic test # 57 (Group-C)

| Test ID: Bayrak and Sheikh 1996, AS5-HT | | | number of occurrence | Ductility based Parameter 'a' | Focus based Parameter 'α' | Deviation from initial stiffness (%) |
|---|---|---|---|---|---|---|
| Initial | $K_o$ = | 43.75 | - | - | - | - |
| Unl. | $K_{un,1}$= | 13.89 | 2 | 0.97 | 0.5 | 68.3 |
| | $K_{un,2}$= | 10.78 | 2 | 0.84 | 1.0 | 75.4 |
| | $K_{un,3}$= | 8.29 | 1 | 0.84 | 1.3 | 81.1 |
| K values are in kN/mm. | | | **μ =** | **0.90** | **0.8** | **73.7** |
| | | | **σ =** | 0.07 | 0.4 | 5.5 |
| | | | **cov =** | 0.08 | 0.4 | 0.1 |

**Table B.58** Unloading stiffness properties of the cyclic test # 58 (Group-C)

| Test ID: "Matamoros et. al 1999 Specimen c10-20 North" | | | number of occurrence | Ductility based Parameter 'a' | Focus based Parameter 'α' | Deviation from initial stiffness (%) |
|---|---|---|---|---|---|---|
| Initial | $K_o$ = | 14.00 | - | - | - | - |
| Unl. | $K_{un,1}$= | 6.19 | 2 | 1.00 | 0.1 | 55.8 |
| | $K_{un,2}$= | 4.00 | 2 | 1.04 | 0.1 | 71.4 |
| | $K_{un,3}$= | 3.06 | 2 | 1.03 | 0.3 | 78.2 |
| | $K_{un,4}$= | 3.14 | 2 | 0.91 | 0.7 | 77.6 |
| K values are in kN/mm. | | | **μ =** | **0.99** | **0.3** | **70.7** |
| | | | **σ =** | 0.06 | 0.2 | 9.6 |
| | | | **cov =** | 0.06 | 0.8 | 0.1 |

**Table B.59** Unloading stiffness properties of the cyclic test # 59 (Group-C)

| **Test ID** | | | **number of occurrence** | **Ductility based** | **Focus based** | **Deviation from initial stiffness (%)** |
|---|---|---|---|---|---|---|
| **Bayrak and Sheikh 1996, ES1-HT** | | | | **Parameter 'a'** | **Parameter 'α'** | |
| Initial | $K_o$ = | 27.00 | - | - | - | - |
| Unl. | $K_{un,1}$= | 9.93 | 2 | 0.82 | 0.4 | 63.2 |
| | $K_{un,2}$= | 6.70 | 2 | 0.84 | 0.6 | 75.2 |
| | $K_{un,3}$= | 5.78 | 1 | 0.78 | 1.2 | 78.6 |
| K values are in kN/mm. | | | **μ =** | **0.82** | **0.6** | **71.1** |
| | | | **σ =** | 0.03 | 0.3 | 7.3 |
| | | | **cov =** | 0.03 | 0.5 | 0.1 |

**Table B.60** Unloading stiffness properties of the cyclic test # 60 (Group-C)

| **Test ID** | | | **number of occurrence** | **Ductility based** | **Focus based** | **Deviation from initial stiffness (%)** |
|---|---|---|---|---|---|---|
| **Paultre, Legeron, July-August 2000 test 10013025** | | | | **Parameter 'a'** | **Parameter 'α'** | |
| Initial | $K_o$ = | 10.00 | - | - | - | - |
| Unl. | $K_{un,1}$= | 3.84 | 2 | 1.04 | 0.3 | 61.6 |
| | $K_{un,2}$= | 2.58 | 2 | 1.03 | 0.5 | 74.2 |
| | $K_{un,3}$= | 2.53 | 1 | 0.78 | 1.3 | 74.7 |
| K values are in kN/mm. | | | **μ =** | **0.98** | **0.6** | **69.2** |
| | | | **σ =** | 0.11 | 0.4 | 7.0 |
| | | | **cov =** | 0.11 | 0.7 | 0.1 |